Stratospheric Ozone Depletion by Halocarbons: Chemistry and Transport (1979)

Pages
250

Size
5 x 9

ISBN
0309333059

Panel on Stratospheric Chemistry and Transport;
Committee on Impacts of Stratospheric Change;
Assembly of Mathematical and Physical Sciences;
National Research Council

Stratospheric Ozone Depletion by Halocarbons: Chemistry and Transport

Panel on Stratospheric Chemistry and Transport
Committee on Impacts of Stratospheric Change
Assembly of Mathematical and Physical Sciences
National Research Council

NATIONAL ACADEMY OF SCIENCES
Washington, D.C. 1979

NOTICE: The project that is the subject of this report was approved by the Governing Board of the National Research Council, whose members are drawn from the Councils of the National Academy of Sciences, the National Academy of Engineering, and the Institute of Medicine. The members of the Committee responsible for the report were chosen for their special competences and with regard for appropriate balance.

This report has been reviewed by a group other than the authors according to procedures approved by a Report Review Committee consisting of members of the National Academy of Sciences, the National Academy of Engineering, and the Institute of Medicine.

Available from
Committee on Impacts of Stratospheric Change
2101 Constitution Avenue
Washington, D.C. 20418

PANEL ON STRATOSPHERIC CHEMISTRY AND TRANSPORT

Harold I. Schiff, York University, *Chairman*

Julius Chang, Lawrence Livermore Laboratory
Edwin F. Danielsen, Oregon State University†
Robert Dickinson, National Center for Atmospheric Research
*Dieter H. Ehhalt, Institut für Chemie, KFA, Jülich
Eldon E. Ferguson, Environmental Research Laboratories, NOAA
James P. Friend, Drexel University
David M. Golden, SRI International
Frederick Kaufman, University of Pittsburgh
Julius London, University of Colorado (member since March 1, 1979)
*Brian A. Thrush, Cambridge University
John W. Tukey, Bell Laboratories and Princeton University
Cheves Walling, University of Utah
Geoffrey Watson, Princeton University (member until April 10, 1979)

Consultants

Dixon Butler, Goddard Space Flight Center, NASA
Richard M. Stolarski, Goddard Space Flight Center, NASA

Milton W. Rosen, *Executive Secretary*

---

*Corresponsing Member
†Now at Ames Research Center, NASA

COMMITTEE ON IMPACTS OF STRATOSPHERIC CHANGE

John W. Tukey, Bell Laboratories and Princeton University,
Chairman

Martyn M. Caldwell, Utah State University
Thomas B. Fitzpatrick, Harvard University
James P. Friend, Drexel University
Maureen Henderson, University of Washington
Francis S. Johnson, University of Texas at Dallas
Frederick Kaufman, University of Pittsburgh
Allen Latham, Jr., Haemonetics Corporation
J. Murray Mitchell, Jr., Environmental Data Service, NOAA
Hans A. Panofsky, Pennsylvania State University
C. Stan Rupert, University of Texas at Dallas
Harold I. Schiff, York University

Milton W. Rosen, *Executive Secretary*

PREFACE

The dependence of life on the earth's surface on the very small amount of ozone in the stratosphere has been known for some time. Only recently, however, have scientists realized that the quantity of stratospheric ozone is controlled by trace amounts of other substances whose concentrations are thousands of times smaller than that of ozone itself. It is this fact that has led to concern about excessive depletion of the ozone layer, since it is likely that human activities can add these trace substances to the atmosphere, appreciably altering their concentrations and thereby affecting the balance of life-supporting ozone.

During the past decade, several technologies have been identified as possible contributors to ozone depletion--supersonic aircraft (SST's) that release nitrogen oxides and aerosol spray cans, refrigerators, and air conditioners that release halocarbons. Previous reports of the National Academy of Sciences have dealt with the projected effects of these technologies.

The best current data suggest that the potential effects of SST's are smaller than previously predicted but that those of halocarbon releases are greater. The present report updates earlier findings on the halocarbon problem.

Predictions of ozone depletion are based on mathematical computer models that contain large numbers of equations representing the chemical reactions going on in the atmosphere, as well as the air motions that move atmospheric constituents around. Since neither of these factors can be represented with absolute accuracy, the cumulative uncertainties are appreciable.

However, the international scientific community has worked diligently during recent years to improve the data for the computers and to do the atmospheric measurements required to check the validity of the models. Unfortunately, given the complexity of the ozone problem, absolute answers cannot be offered, nor even promised for the future.

This report like the ones before it, describes the state of knowledge at the time of writing. It represents an effort to provide political leaders with the best available data and to assess the uncertainty limits of the predictions based on those data. We hope it will assist governments in the United States and elsewhere in taking appropriate action.

Harold I. Schiff, *Chairman*
Panel on Stratospheric Chemistry
and Transport

CONTENTS

PRINCIPAL FINDINGS

- There is agreement with previous reports that continued release of halocarbons into the atmosphere will result in a decrease in stratospheric ozone.
- New values for some of the chemical rate coefficients have increased the predicted ozone reduction resulting from continued release of chlorofluoromethanes (CFMs).
- The most probable value calculated for the eventual ozone depletion due to continued release of CFMs at the 1977 level is 16.5 percent. This value is obtained from the value of 18.6 percent calculated from the computer model by allowing for possible tropospheric sinks for CFMs and for the effects on stratospheric chemistry of the CFM greenhouse effect.
- There have been considerable improvements in the computer models and in the laboratory and atmospheric measurements, which have reduced the uncertainty range.
- Although there are a few exceptions, the comparison between the models and measurements of substances in the present stratosphere is considered to be satisfactory within the uncertainties of the measurements. We therefore believe that the projections for ozone depletion are valid within the stated uncertainty ranges.
- The uncertainties in the chemical rate coefficients, in atmospheric transport, and in the use of one-dimensional models have been combined to give an overall uncertainty range of a factor of 6 within a 95 percent confidence level.
- The uncertainty range means that for the case of continued release of CFMs at the 1977 level there is 1 chance in 40 that the ozone depletion will be less than 5 percent and 1 chance in 40 that it will be greater than 28 percent.
- Even allowing for the best professional judgment of the possibility that some important chemical reaction has

been overlooked or that there remain large errors in the measured chemical rate coefficients, we believe that there is a 3 out of 4 chance that continued release of CFMs at the 1977 level will result in an ozone depletion that lies in the range of 9 to 24 percent.

- If the rapidly increasing use of F-22 (CHF_2Cl) and methyl chloroform (CH_3CCl_3) continues unabated, the release rates and atmospheric behavior of these compounds will require careful attention. However, since chemical reactions remove appreciable fractions of these compounds before they reach the stratosphere, substitution of F-22 for F-11 ($CFCl_3$) and F-12 (CF_2Cl_2) would be beneficial.
- It is unlikely that direct measurements of the average global ozone amount would permit detection of a decrease of less than 5 percent attributable to human activity. Total cessation of CFM release at the time of detection would result in a decrease of ozone of about 7 percent some 15 years later.

1 SUMMARY: PROJECTED CHANGES IN STRATOSPHERIC OZONE

REITERATION OF THE PROBLEM

The importance of the relatively small amount of ozone in the earth's atmosphere lies mainly in its ability to absorb the biologically harmful ultraviolet radiation from the sun and to prevent most of it from reaching the surface. In addition, ozone plays an important role in determining the climate of this planet.

Most of the ozone is located in the stratosphere, a region of the atmosphere located between 10 and 50 km above the surface. Its concentration is determined by a balance between photochemical processes that produce it and others that destroy it and never reaches more than a few ten-thousandths of a percent. The natural processes that destroy ozone are believed to involve substances that are normally present in trace amounts, thousands of times less than that of ozone itself. These include chemical compounds that contain hydrogen (HO_x), nitrogen (NO_x), and chlorine (ClO_x). These compounds enter into catalytic chain reactions in which one molecule can destroy many ozone molecules before being removed by some competing process. The concern is that human activities can appreciably alter the amounts of these catalytic substances in the stratosphere.

A number of such activities have been identified, including the use of high-flying aircraft, halocarbons, nuclear weapons, and nitrogen fertilizers. There may be others not yet identified. The "Clean Air Amendment of 1977" requires that all possibilities be evaluated. However, since the release of halocarbons appears to be the greatest and most immediate threat, the present report confines itself to evaluating the possible effects on stratospheric ozone of continued release of halocarbons.

PREVIOUS EVALUATIONS

The National Academy of Sciences (NAS) released a report in September 1976 entitled *Halocarbons: Effects on Stratospheric Ozone*.* The study focused attention on chlorofluoromethanes (CFMs). Two of these, $CFCl_3$ (F-11) and CF_2Cl_2 (F-12), were of greatest concern. They were being produced and released in large and increasing quantities. They were not removed, to our knowledge, in the troposphere (the region between the surface and the stratosphere), and so the same large quantities could enter the stratosphere. Here they could be dissociated by ultraviolet radiation into ClO_x fragments capable of destroying ozone. The main conclusion of that report was that "their continued release at the 1973 production rates would cause the ozone to decrease steadily until a probable reduction of about 6 to 7.5 percent is reached, with an uncertainty range of at least 2 to 20 percent using what are believed to be roughly 95 percent confidence limits. The time required for the reduction to attain half of this steady-state value (3 to 3.75 percent) would be 40 to 50 years."

The uncertainty range is determined by uncertainties in the rates at which these substances are released into the atmosphere, by uncertainties in the rate constants that determine the speeds of seven of the most important chemical reactions, and by the use of one-dimensional computer models to represent the distribution and transport of chemical species. Uncertainties in the rate constants made the largest contributions to the overall uncertainty. The 6 to 7.5 percent range for the most probable reduction allowed for the possibility of some CFM removal in the troposphere.

In August 1977, the National Aeronautics and Space Administration (NASA) released a report entitled *Chlorofluoromethanes and the Stratosphere*.† Eight modeling groups evaluated the ultimate ozone reduction resulting from continued release of these two substances at the 1975 rates. Their predictions of the most likely value ranged from 10.8 to 16.5 percent. This spread in most likely values is due to differences between the eight models and should not be confused with the uncertainty range given above for the NAS report. It will be noted that the most probable values predicted for ozone reduction in the NASA,

---

*Subsequently referred to as the NAS, 1976 report.

†Subsequently referred to as the NASA, 1977 report.

1977 report are close to a factor of 2 larger than, although still within the uncertainty range of, that of the NAS, 1976 report. The reason is that, in the period between these two reports, the rate constant for an important chemical reaction ($NO + HO_2$) had been remeasured, using improved techniques, and found to be substantially different from the value used in the earlier report.

PRESENT FINDINGS

Chlorofluoromethanes

Since the release of these two reports, there have been continuing improvements in the computer models and in the measurements used as inputs to these models. There has also been a considerable increase in the number and the quality of atmospheric measurements that can be used to check the validity of the models. These activities have not altered the principal conclusion reached in the previous reports that continued release of halocarbons into the atmosphere will result in a significant decrease in the amount of stratospheric ozone. For comparison purposes with the previous reports, the present study estimates an eventual decrease of 18.6 percent in the total amount of ozone for continued release of F-11 and F-12 at the 1977* rates, which we call Case A.

Other considerations, to be discussed below, but not included in the previous reports, have led us to reduce the "best estimate" for the eventual ozone decrease to a value of 16.5 percent. Our estimate of uncertainty is such that there is a 95 percent probability that the true value of the ozone reduction lies between 5 percent and 28 percent, i.e., a range of a factor of 6. Ozone reduction to half the eventual value, to about 8 percent if the eventual value were 16.5 percent, would occur in about 30 years.

Although several countries have taken action to reduce the amount of CFMs that they are releasing into the atmosphere, release rates in other countries are increasing.

---

*The NAS, 1976 report used 1973 release rates; the NASA, 1977 report used 1975 release rates. These, and the 1977 release rates, are all within 5 percent of each other (cf. Chapter 2).

It is therefore not possible to anticipate future, global release rates with any high degree of confidence. We have therefore chosen three additional scenarios to span the likely range. In Case B we assume the 1977 release rate until 1983, followed by a 25 percent reduction at that time, and then continuation at that reduced level. Case C is similar to Case B, except that an additional reduction of 25 percent is assumed to occur in 1988 with constant release thereafter at half the 1977 level. Cases B and C both tacitly presume further regulation to limit release. Case D has been suggested to us by the National Research Council Committee on Alternatives for the Reduction of CFC Emissions to reflect the increasing release rate in other industrial countries. It assumes a constant release rate at the 1977 level until 1980, a 7 percent per annum growth rate until 2000, and a constant release rate at the year 2000 level beyond that date.

The projected steady-state values for Cases B and C are 13.2 percent and 9.4 percent, respectively, with the same sixfold uncertainty range at the 95 percent confidence level. Case D leads to an ozone reduction of 25 percent in the year 2025 and an eventual steady-state reduction of 56.7 percent. High reliance cannot be placed on the steady-state value since, at large levels of ozone reduction, changes in the dynamics and the temperature structure of the stratosphere are expected that would invalidate the model's treatment of transport. It is highly probable that the steady-state reduction for Case D would be at least 30 percent.

It is interesting to note that the model and error analysis also shows that a (2.1 ± 1.5) percent reduction in O_3 should have occurred and that by the year 2000 the reduction will be (5 ± 3.5) percent, almost independent of which of the four cases is considered. Although there is no likelihood of it happening, immediately stopping all release worldwide would still produce roughly one and a half times the present reduction in about 15 years, after which the ozone level could gradually recover.

Other Halocarbons

Although the production of F-11 and F-12 has not been increasing significantly during the past four years, there has been a dramatic increase in the production of two other halocarbons capable of affecting stratospheric ozone. The use of F-22 ($CHClF_2$), largely in refrigeration, has increased 25 percent in the past two years, and the production of methyl chloroform (CH_3CCl_3) is now doubling every five years. Atmospheric measurements indicate that methyl chloroform is now contributing between a quarter to half as many chlorine atoms to the stratosphere as either F-11 or F-12. If it gains increased usage, as a substitute for other solvents in degreasing and coating operations, it may well become the largest source of stratospheric chlorine.*

ESTIMATES OF UNCERTAINTIES

Uncertainties Due to Chemistry

To estimate the effect on stratospheric ozone of any scenario of halocarbon release rate, it is necessary to know the detailed chemistry of all substances that may be involved and the rates at which chemical species are transported into and out of the stratosphere.

In the model calculations, it is assumed that there are no processes that remove F-11 and F-12 in the troposphere and thereby prevent them from affecting stratospheric ozone. In our previous report we considered all such "inactive" removal processes that had been suggested and put upper limits on the degree to which each of them might reduce the predicted ozone depletion. Only three of these had upper limits that could have reduced the predictions by as much as 10 percent of the most probable value. The limits of two of these, removal by chemical reaction by gaseous ions and photodecomposition in the troposphere by sunlight, were based on the failure to observe these processes in laboratory experiments and an estimate of the detection limits in these experiments. Subsequent consideration has indicated that these processes are unlikely to be of any significance. The limit of the third process, removal by oceans, was based on very sparse measurements of the concentrations of F-11 in surface waters. Subsequent measurements have suggested that this process is also unimportant. One new removal process has been suggested,

---

*Once methyl chloroform reaches the *stratosphere*, its effectiveness in destroying ozone is not identical to that of CFMs because of differences in the chemistry of these compounds. But, to a first approximation, these differences may be ignored.

photodecomposition of the halocarbons when in contact with desert sand. This suggestion is based on laboratory studies that reveal that halocarbons, when in contact with sandlike materials, can be decomposed by light of wavelengths that do not otherwise decompose them. These studies are at present not definitive enough to permit a reliable estimate of how much change, if any, is likely to result from this process. Nevertheless we have reduced our estimate from 18.6 percent to 17.4 percent for the most likely ozone reduction for Case A to take into account this and other possible "inactive" removal processes.

A more direct way to determine whether such processes do, in fact, exist would be to compare the amount of fluorocarbons released into the atmosphere minus the amount that has been calculated to have been dissociated in the stratosphere, with the amount still remaining in the entire atmosphere. Any difference between these two quantities could then be ascribed to inactive removal in the troposphere. Our previous study indicated that the uncertainties in the calculations based on the total amount now present in the atmosphere were too large to reach meaningful conclusions. Despite considerable improvement in the number and quality of the measurements that situation still obtains. It has been suggested that a more definitive answer to the problem may be achieved by measuring the rate at which the amount of fluorocarbons in the atmosphere increases with time. An experiment to make such measurements has been initiated.

All other halocarbons that are being released into the atmosphere in appreciable quantities contain either hydrogen atoms or double bonds and therefore are removed, to some extent, in the troposphere by reaction with HO radicals. This removal is virtually complete for most of these substances, so that they do not pose a threat to stratospheric ozone. Tropospheric removal by reaction with HO is, however, not complete for three of these halocarbons, methyl chloride, methyl chloroform, and F-22, so that appreciable fractions of these substances do reach the stratosphere and contribute to ozone destruction. Methyl chloride is mainly produced by natural processes and is therefore present in the natural atmosphere in essentially unchanging amounts. By contrast, F-22, and, to a large extent, methyl chloroform, are man-made chemicals that are being produced in rapidly accelerating amounts. The fraction of these chemicals that reaches the stratosphere depends on the HO concentrations in the troposphere, which are only poorly known.

For these reasons we have not undertaken an estimate of the magnitude of the threat to stratospheric ozone posed by the increasing use of these chemicals, although there are sufficient grounds for concern. There is a need for increased measurements, in the troposphere, particularly of HO concentration. There is also a need for increased research efforts to improve our understanding of tropospheric chemistry.

Our understanding of stratospheric chemistry has improved considerably since our last report. Stratospheric measurements have supported the basic chemical postulates. Halocarbons do reach the stratosphere; they do photodissociate into fragments that can catalyze the destruction of ozone, and these fragments do, in fact, react with ozone. But there are still limitations to our knowledge of stratospheric chemistry that introduce uncertainties in our estimate of the magnitude of the expected ozone reduction.

There has been considerable improvement in the accuracy with which the rate constants are known for the chemical reactions that are believed to occur in the stratosphere. But since the number of these reactions is large, at least 125, the cumulative uncertainty is also large and is unlikely to show rapid improvement in the near future. Measurements of several reactions have been made by more reliable, direct methods and have led to large changes in their rate constants compared with the values (deduced by indirect methods) that were used in our earlier report. These new values, particularly that for the reaction of HO_2 with NO, have resulted in an increase in the predicted impact by halocarbons on ozone. In addition, they have forced us to recognize a much greater interaction among the various chemical families that affect stratospheric ozone; e.g., a change in the amount of NO_x or HO_x in the stratosphere has a marked affect on the ozone reduction caused by halocarbons. It is felt that large changes in the adopted values of rate constants are unlikely to occur in the future because direct methods are now generally used to measure these quantities. There is, however, a need to measure rate constants over the range of pressures that exist in the stratosphere, since there is reason to believe that some of them may be pressure-dependent. Moreover, many of the measurements have been made without confirming that the products of the reactions are the ones assumed. Efforts should be made to define all the products of each chemical reaction.

In any description of a chemical system there is always the possibility that an important process has been overlooked or dismissed as being unimportant. This happened just before the completion of the NAS, 1976 report when it was learned that chlorine nitrate ($ClONO_2$) was more stable than previously believed. The inclusion of the new information caused a reduction of the predicted ozone depletion by a factor of about 1.85. More recently, it has been suggested that hypochlorous acid, HOCl, might play a similar role. However, most of the laboratory studies on this compound indicate that it will be broken up relatively rapidly by sunlight and therefore will not provide a significant holding tank for stratospheric chlorine.

Two additional reactions that may affect the impact of halocarbons on stratospheric ozone have come to our attention too late to be incorporated into our model calculations. One of these, the reaction of Cl atoms with formaldehyde (CH_2O), has the effect of decreasing the ozone depletion by roughly 7 percent of the calculated value. The other reaction, between ClO and BrO, increases the impact of halocarbons on stratospheric ozone by approximately the same factor. Since the effects of these two reactions operate in opposite directions, are somewhat speculative, and are not large, we do not believe their omission in our model produces significant errors in our projections.

In assessing *the uncertainty in our prediction caused by the uncertainties in rate constants* we have used an error analysis similar to that used in the NASA, 1977 report, which we consider to be an improvement over the method used in our 1976 report. This analysis gives a cumulative uncertainty for the predicted ozone change of a range *of a factor of 4 at the 95 percent confidence limit.** This can be compared with the fivefold range of uncertainty in our 1976 report in which only seven key reactions were considered. The lower range we obtain using all (~125) reactions in the analysis is a measure of the improvement that has been achieved in the laboratory measurements.

---

*More specifically, for the most probable value of 16.5 percent for steady-state ozone reduction in Case A, there is 1 chance in 40 that, because of this particular error, it could be lower than 6.3 percent and 1 chance in 40 that it could be higher than 26 percent. The uncertainty range of a factor of 4 is equivalent to a ±60 percent uncertainty in the predicted value, i.e., (1 + 0.6)/(1 - 0.6) = 4.

Uncertainty Due to Transport

The predictions of this and previous reports have been made using the so-called one-dimensional (1-D) model. This type of model considers only vertical motions of chemical substances. But air, of course, moves in three dimensions. The justification for this approximation is that, when all the motions are summed over all latitudes and longitudes, the effects of horizontal motions of substances largely cancel and the vertical movements dominate. These models therefore represent some form of global average over both distance and time. The speed with which these substances enter or leave the stratosphere as a result of these vertical movements is characterized by an "eddy-diffusion" coefficient $K(z)$, the value of which depends on altitude. The values of $K(z)$ are usually determined by measuring the change with height of the concentration of some trace substances whose chemistry is believed to be well understood. Methane (CH_4) and nitrous oxide (N_2O) have often been used for this purpose.

The analysis of these data by the method used in the NAS, 1976 report indicates a somewhat wider possible variability than that given in our earlier report.

However, a second approach (described in Chapter 4), has, in fact, resulted in a decrease in our uncertainty estimate. This approach involves fitting simple analytic expressions to the vertical distributions of the concentrations of trace species. Data on three species were used, the measured N_2O data, global ozone data, and the distribution of an inert tracer generated by a three-dimensional model. This method showed remarkable self-consistency among the three tracers used and agreed with the results for N_2O in the first method. It is felt that the uncertainty in the eddy-diffusion coefficient at a given altitude is about a factor of 2, although it is admitted that this uncertainty estimate is somewhat subjective. Fortunately, the prediction of ozone depletion from halocarbon injection is not too sensitive to the choice of eddy-diffusion coefficient. Slower transport would permit a greater buildup of the chlorine compounds (ClO_x) that destroy ozone but would also increase the concentration of nitrogen compounds (NO_x). Because of chemical coupling processes, the increased NO_x would, in turn, decrease the effect of the chlorine compounds.

We estimate an uncertainty in the projections due to the use of the 1-D method of characterizing transport to *be a range of a factor of 2 within the 95 percent confidence level.* This can be compared with the threefold range of our earlier report.

Other Uncertainties Inherent in the 1-D Model

We have seen that the 1-D model represents the vertical distribution of different chemicals averaged over the entire globe and over all seasons. Thus chemical reactions are represented as occurring between the average concentrations of each chemical species at a given altitude. In the real world, the reactions occur between chemicals having their instantaneous, local concentration. The global average of the products of these concentrations, which determine the chemical rates, is not necessarily the same as the product of their averages, which is used in 1-D models.

Moreover, there are feedback effects involving temperature changes resulting from ozone changes. A decrease in ozone due to halocarbons would result in a decrease in the stratospheric temperature that affects the rates of many of the chemical reactions. This temperature feedback is calculated to lower the predicted ozone reduction by 1.8 percent, for Case A at steady state.

The amount of water vapor in the stratosphere is believed to be governed mainly by the temperature of the tropical tropopause, by the boundary between the tropical troposphere and the tropical stratosphere, and by stratospheric methane. Stratospheric temperature will probably decrease as a result of halocarbon injection. Tropospheric temperature, in contrast, will increase because of the enhanced greenhouse effect caused by the halocarbons. The net effect is believed to be an increase in tropopause temperature, which would permit more water to enter the stratosphere. Increased water content results in ozone decrease. This feedback effect is estimated to increase ozone depletion for Case A at steady state by 0.9 percent. Temperature changes will also affect the transport to some extent.

All these effects, the use of the 1-D approximation in treating the chemistry, and the temperature feedback effects just mentioned have their own uncertainties. We estimate that together they introduce an uncertainty in our projections of a range of a factor of 2.3 at the 95 percent confidence level.

VALIDATION OF THE 1-D MODELS

There has been considerable refinement in the 1-D models. All models include methods for treating the diurnal (day and night) changes in solar intensity. Some are also capable of calculating the temperature changes that occur if the composition of the atmosphere changes. The quality of the data used as inputs to the models has also improved as a result of more and better atmospheric measurements.

The validity of the models can be checked by comparing calculated concentrations of minor constituents against measurements, particularly the way these concentrations change with height. There are, however, severe limitations to these comparisons. The 1-D models can, of course, only provide globally averaged values of these height profiles for long-lived trace species. Although the number of measurements and their geographic coverage have both increased considerably, they are still far from providing true global averages. However, the comparison can be considered satisfactory for most substances within these limitations and the uncertainties of the measurements. There are, however, some notable exceptions. One of the ClO measurement experiments has given high values for the concentrations, which are totally inconsistent with the models and our understanding of the chlorine budget. There are also some other disturbing inconsistencies between models and measurements, such as the shapes of the vertical profiles of ClO, HCl, and HF. Some of these may be the result of horizontal transport, which is excluded in the concept of 1-D models. Some early calculations made with two-dimensional (2-D) models do appear to account for some of the discrepancies. Two-dimensional models are under active development by several groups and may well provide us with improved projections in the near future. One of the interesting results already achieved with these models is an indication that the ozone changes resulting from halocarbon releases will be greater at mid and high latitudes than in the tropics and that, at these higher latitudes, the changes are largest in late winter and smallest in late summer. Three-dimensional (3-D) models would, in principle, be the most realistic for making predictions, and attempts are being made to incorporate chemistry in existing 3-D, general circulation models. But the cost and complexity make it unlikely that 3-D models will provide useful projections of ozone depletion in the near future. They are, however, making useful contributions in examining some of the feedback processes, and their continued development should be encouraged.

In summary, 1-D models have probably reached their maximum potential. Despite their limitations, we believe that they provide projections for ozone depletion that have validity within the stated uncertainty ranges.

OTHER EFFECTS

We have become increasingly aware of the fact that the atmosphere is a closely coupled system. Changes in the tropospheric chemistry cause changes in the stratospheric chemistry. Changes in the amounts of HO_x and NO_x in the stratosphere will affect the impact of changing the amount of ClO_x. It is therefore difficult to project accurately the effect of increased halocarbon release when the release of other man-made pollutants may also be increasing in an undetermined way.

A moderate increase in stratospheric NO_x resulting, for example, from increased use of nitrogen fertilizers, would reduce the effect of halocarbons on ozone because of the coupling between ClO_x and NO_x chemistry and would increase the ozone amount at lower altitudes.

The amount of carbon dioxide (CO_2) in our atmosphere is increasing rapidly as a result of the increased use of fossil fuels. It is probably also increasing because of the continuing removal of tropical rain forests, which are believed to play an important role in determining the CO_2 balance. An increase in CO_2 would warm the troposphere but cool the stratosphere. A decrease in stratospheric temperature would result in an increase in stratospheric ozone, thus offsetting to a small degree the decrease caused by halocarbon release.

An even more complex set of reactions can occur as a result of increased anthropogenic release of carbon monoxide (CO). Increased CO decreases the amount of HO in the troposphere. A decrease in HO concentration would permit a larger fraction of certain halocarbons such as methyl chloride (from natural sources) and methyl chloroform and F-22 (from human sources) to reach the stratosphere and thereby decrease stratospheric ozone. At the same time, through a set of complex reactions, involving HO_x and NO_x, there is likely to be an increase in the amount of ozone in the troposphere so that the net change in total ozone due to changes in CO is uncertain.

Even if we had reasonable scenarios for the increase in these other pollutants, our knowledge of tropospheric chemistry is still too incomplete to allow meaningful predictions to be made on the net ozone change that they would produce. This is an additional reason for increased research efforts in tropospheric chemistry.

OZONE MONITORING AS AN EARLY WARNING SYSTEM

The uncertainties inherent in the use of atmospheric models have prompted the suggestion that monitoring the total amount of global ozone might provide a direct way of detecting whether ozone depletion due to human activity is indeed occurring and, if such change were detected, could provide the basis for implementing regulation against that activity.

We have seen that stopping halocarbon releases will not immediately result in ozone returning to its former level. There is a time delay between halocarbon release and ozone destruction; the maximum ozone decrease actually occurs some 15 years after all release has stopped. Therefore, to be effective, an *early warning system* must be capable of detecting changes due to human activity in time to prevent the eventual maximum ozone decrease being greater than acceptable levels.

Most of the ozone measurements are now made with Dobson instruments located at a number of ground-based stations. There are a number of problems involved in using the data from this Dobson network to provide total global ozone amounts and trends. There are short- and long-term natural variations in the amount of ozone above any given station due to seasonal and other factors, many of which are unknown. Our study shows that there is an inherent statistical error due to these variations, which would limit the detection of a trend caused by human activity to at least 1.5 percent almost independent of the number of stations used for the analysis. In addition to these statistical errors, other long-term (5- to 100-year) changes may occur, which could lead to misinterpretation. The Dobson instruments may have long-term calibration and drift errors. Most of the Dobson stations are located on land; changes in meteorological patterns could move relatively high ozone amounts from sea to land or vice versa. Long-term changes in atmospheric aerosols, clouds, and temperature could also lead to incorrect interpretation as ozone trends. Finally, there could be long-term changes in ozone due, for example, to changes in solar flux and changes in atmospheric substances resulting from natural or human causes not directly related to CFM releases. We therefore conclude that it is unlikely that a Dobson network would, within the next decade, be able to identify a reduction in global ozone attributable to CFM releases of less than 4 to 5 percent. The model predicts that such an ozone change will occur by about 1995. Total cessation of CFM release at that point would result in a decrease in ozone of about 7 percent some 15 years later.

Model calculations have shown that the decrease in ozone concentration due to CFM release is twice as great at 40 km as is the decrease in total ozone. There are also reasons for believing that natural variability is smaller at that altitude. Monitoring ozone concentrations at this altitude should therefore provide a more sensitive early warning system. This region of the stratosphere is best monitored by satellite. A number of satellites are currently measuring ozone by several techniques. The time period for which data are available is short, and some of the data still require verification. At the time of writing, the satellites do not provide a superior system for trend analysis to the Dobson network but should be able to do so in the near future.

CONCLUSIONS

Effects of CFM Releases

We find ourselves in agreement with the principal conclusion reached in our earlier report, viz.: that it is inevitable that CFMs released into the atmosphere do destroy ozone. In fact, the laboratory and atmospheric measurements, made in the interim between these two reports, have tended to strengthen this conclusion.

The value of the ozone depletion caused by continuing release of F-11 and F-12 at the 1977 (similar to 1973) rates obtained by our 1-D model calculations is 18.6 percent. This can be compared with the most probable value of 7.5 percent of our previous report. The difference between these values is mainly the result of new, more reliable, measurements of the rate constants of several key chemical reactions.

Destruction of ozone by halocarbons also changes the temperature profile in the stratosphere, which, in turn, changes the rates at which a number of chemical reactions occur. The temperature change in the stratosphere and the temperature change in the troposphere resulting from the increased greenhouse effect due to the halocarbons also alter the amount of water vapor that reaches the stratosphere. This, in turn, changes the amount of ozone destruction. *These feedbacks were not considered quantitatively in our previous report but are evaluated in the present report. They result in a reduction of the most probable value of ozone reduction to 17.7 percent.*

Although there is no compelling reason to believe that a "sink" exists that removes a significant portion of CFMs in the troposphere, we recognize that such a possibility exists. Removal by photodestruction in the presence of desert sand is one such possibility. *To make provision for possible tropospheric sinks we have, somewhat arbitrarily, reduced the most probable value to 16.5 percent.*

An improved error analysis has been used to estimate the uncertainty range due to uncertainties in all the rate constants. At the 95 percent confidence level, this source of uncertainty amounts to a range of a factor of 4, and remains the largest source of uncertainty.

Somewhat more subjectively, we estimate the uncertainty due to the approximation used to represent transport to be a range of a factor of 1.9.

The combination of these two sources of error gives a total uncertainty of a range of a factor of 5, which can be compared with the range of a factor of 10 estimated for these two sources of errors in the previous report. This improvement of the uncertainty range reflects the improvements in both laboratory and atmospheric measurements.

We have also estimated the error due to the feedback effects mentioned above and made an even more subjective estimate of the uncertainty resulting from the approximation inherent in treating rates of chemical reactions by the average concentrations of the 1-D models. These sources of uncertainties are estimated to amount to a range of a factor of 2.3.

Combination of all these sources of error amounts to a range of a factor of 6. Thus our best estimate is that for continued CFM values at 1977 levels there is 1 chance in 40 that ozone depletion will be less than 5 percent and 1 chance in 40 that it will be greater than 28 percent.

There are two possible sources of errors that, inherently, cannot be quantified. One is that some important chemical reaction has been overlooked. The other is that some systematic error exists in the chemistry, such as the existence of pressure dependence on the reaction rates, or that other product channels exist for some of the reactions. It is obviously impossible to estimate the unknown with any precision. Nevertheless, our experience of the past has prompted us to hazard a rough estimate of the probability. Inclusion of this subjective estimate obviously broadens the uncertainty limits. For example, with steady CFM release at the 1977 level, there is a 3 out of 4 chance that the ozone depletion will reach a steady-state value between 10 to 23 percent without including the uncertainty estimate due to these unknown effects; inclusion of this estimate extends the range to 9 to 24 percent.

Release of Other Halocarbons

We have not attempted to evaluate the ozone depletion due to halocarbons that contain hydrogen largely because our lack of knowledge of tropospheric chemistry introduces a large uncertainty in the fraction of these compounds that reach the stratosphere. However, if current trends in the rapidly increasing use of F-22 and methyl chloroform continue unabated, the release rates and atmospheric behavior of these compounds will require careful attention.

2 SOURCES OF STRATOSPHERIC CHLORINE

Large quantities of halocarbons and other volatile halogen sources are continually being produced by human activities and, to a less-well-understood extent, by natural processes. The amount of these that reach the stratosphere depends not only on the quantities produced but also on two other factors: the fraction released into the lower atmosphere and the fraction of this, in turn, that survives to reach the stratosphere. Obviously, for any material to have a significant effect on stratospheric ozone, these three quantities must all be large. The primary subjects of this chapter are production and release, while tropospheric survival is considered in the following chapter under sinks. However, we shall consider in detail only those halogen sources that are known to have relatively long tropospheric lifetimes, excluding, for example, HCl, which is released in significant quantities but, because of its water solubility, is rapidly "rained out" in the troposphere (as discussed in detail in our 1976 report) so that little reaches the stratosphere.

It should also be noted that materials of appreciable tropospheric lifetime (the only ones of concern to us) enter the stratosphere at a rate essentially proportional to their average tropospheric concentration. Thus direct measurement of this quantity provides a measure of their current contribution to ozone destruction. Further, to the extent that this concentration has reached a steady state, it is simply the rate of release (plus any diffusion back from the stratosphere) divided by the average tropospheric lifetime (determined by rates of destruction in the troposphere and diffusion into the stratosphere). Thus any of these quantities can be calculated if the others are known, and this approach at present provides the best way of estimating release from natural sources.

For halocarbons containing C—H bonds or unsaturation, rates of tropospheric destruction are rapid compared to diffusion into the stratosphere, and lifetimes are relatively short. Unfortunately, estimation of the actual lifetimes is still rather qualitative. The chief path of removal is by reaction with hydroxyl radicals, and while the rate constants for the reactions are quite accurately known, there remains a large uncertainty in the average tropospheric hydroxyl radical concentration (cf. Chapter 3).

CFMs

Data on production and end use of the principal CFMs, F-11 (CCl_3F), F-12 (CCl_2F_2), and F-22 ($CHClF_2$) have been collected from cooperating companies (accounting for about 95 percent of total world production) through the efforts of the Chemical Manufacturers Association (CMA) and collated and reported by Alexander Grant and Company (1977). From these, estimates of total world production and release have been prepared by E. I. du Pont de Nemours and Company (McCarthy *et al.*, 1977). Production figures are stated to be reliable to ±5% and release data to ±10%. These figures have recently been revised slightly (McCarthy, 1978) because of correction of data from one reporting company and revision downward of the estimate of production in Eastern Europe and China. An independent figure for F-11 and F-12 production in the Soviet Union has become available (Borisenkov and Kazakov, 1977). For 1975, the figures are 7.4×10^3 and 31.2×10^3 metric tons, respectively. In the revision, total Communist Bloc production has been taken as 1.15 times that reported for the Soviet Union. As a consequence, estimates of cumulative release of F-11 and F-12 have been reduced 2.7 and 0.2 percent, respectively. Figures for the past 10 years, based on these revised data, appear in Table 2.1. The results show clearly that the exponential growth in production of F-11 and F-12 that occurred until the early 1970's has ended at least temporarily, and present production is actually slightly lower than in 1973. On the other hand, production of F-22, used primarily as a refrigerant, continues to rise (a comparable amount of F-22, not included in the table, is produced and consumed as a chemical intermediate and not released to the atmosphere).

Since the CFM problem was first identified, there has also been a pronounced change in the use pattern of CFMs. Most uses have continued to rise slowly, but use of aerosol propellants has shown a significant drop, due almost

TABLE 2.1 Worldwide Production and Release of CFMs (10^3 metric tons)[a]

	F-11		F-12		F-22	
Year	Production	Release	Production	Release	Production	Release
Cumulative to 1967	894	760	1788	1463	180	51
1967	160	135	243	208	37	12
1968	185	155	279	238	46	16
1969	220	180	311	270	56	20
1970	241	205	337	296	59	23
1971	267	225	361	319	64	26
1972	311	254	402	348	70	31
1973	354	291	448	386	77	36
1974	378	321	473	420	88	42
1975	323	312	420	413	74	47
1976	350	304	450	396	93	56
1977	331	307	424	377	97	58
Cumulative (1967-1977)	4011	3448	5935	5135	941	418
1978	308	284	401	391	--	--

[a] Source: McCarthy (1977; 1978).

entirely to a decline in the United States, where sales for this purpose in 1977 were 61 percent of those in 1976, and, from the data in our 1976 report, about 46 percent of sales in 1973. In the rest of the world, sales for aerosol use appear to be almost exactly the same in 1973 and 1977 (MCA data, 1978, for reporting companies making up 95 percent of the total).

In contrast, MCA data on reporting companies shows that sales of F-11 and F-12 for refrigerants and for blowing agents for closed-cell foam have continued to rise (Table 2.2). The combined increase in the past 5 years amounts to about 44 percent. A more complete breakdown of U.S. sales for 1976 and 1977 is available (McCarthy, 1978) and gives the distribution shown in Table 2.3.

While these changes in use decrease the current release rates for CFMs, they considerably complicate their calculation and extrapolation into the future, particularly since, while essentially all CFMs manufactured are eventually released, the delay in release varies widely with use. The procedures used in estimating these delays are discussed by McCarthy *et al.* (1977).

TABLE 2.2 Worldwide Sales of F-11 and F-12 for Major Nonaerosol Uses[a,b] (10^3 metric tons)

	F-11			F-12		
Year	RH	RNH	BA	RH	RNH	BA
1970	0.6	12.7	34.2	25.5	55.1	5.0
1971	0.8	14.1	42.6	26.2	59.9	5.4
1972	1.0	15.9	51.8	29.6	66.9	7.3
1973	1.3	18.2	62.2	34.0	73.9	8.8
1974	1.5	19.0	63.0	33.2	77.6	9.9
1975	1.7	14.9	55.6	32.7	71.0	9.5
1976	5.2	21.7	52.2	58.3	69.8	6.5
1977	4.9	19.9	60.1	65.6	89.0	8.9
1978	5.4	21.8	60.5	57.6	99.8	16.7

[a] Source: MCA report, June 26, 1978.

[b] RH, Refrigeration, hermetically sealed; RNH, refrigeration, nonhermetically sealed; BA, blowing agent for closed-cell foams. Total aerosol sales for 1977: F-11, 165; F-12, 174.9, are offered for comparison.

TABLE 2.3 1977 Distribution (%) of U.S. Sales by Category for F-11 and F-12[a]

	F-11		F-12	
Use	1976	1977	1976	1977
Refrigeration (hermetically sealed)	3.3	3.5	18.7	21.0
Refrigeration (nonhermetically sealed)	6.3	5.6	25.6	38.0
Blowing agent, closed-cell foam	17.7	25.0	1.6	2.9
Blowing agent, open-cell foam	14.5	17.0	2.6	4.2
Aerosol propellant	52.4	40.7	44.7	29.7
All others	5.8	8.2	6.8	4.2
TOTAL SALES (10^3 metric tons)	115.5	93.8	174.0	154.8

[a] Source: McCarthy (1978).

TABLE 2.4 Distribution of Worldwide Sales of CFMs (F-11 and F-12) in 1977 (10^3 metric tons); Quantities in Parenthesis, Percentage of Total (%)

	Aerosols	Refrigerants	Other	Total
U.S.	84.2	99.9	64.5	248.6
	(12.0)	(14.3)	(9.2)	(35.5)
non-U.S.	255.7	79.5	116.1	451.0
	(36.5)	(11.4)	(16.6)	(64.5)
World[a]	339.9	179.4	180.6	699.6
	(48.6)	(25.6)	(25.8)	(100)

[a] From MCA data on reporting companies, approximately 95% of actual total.

In Table 2.4, sales data for F-11 and F-12 for 1977 (MCA data) are combined in a form to show the effect of various strategies on reducing CFM emissions and clearly illustrate the worldwide nature of the problem. Elimination of aerosol use in the United States would have reduced emissions by 12.0 percent, and restriction of CFMs to use as refrigerants would have added only another 9.2 percent. On the other hand, worldwide elimination of aerosol use would have reduced emissions by 48.6 percent; and restriction to refrigerants would leave only 25.6 percent of the 1977 total. Somewhere between these two figues, CFMs would no longer provide the major source of man-made halocarbons in the atmosphere (see below).

In contrast to these figures, if uses of CFMs abroad are not restricted, worldwide release of CFMs may well increase, regardless of what is done in the United States. Indeed, one study (Peters, 1979) has projected a worldwide increase of releases of 7 percent/year in 1980-2000, assuming no regulation abroad. The drastic consequences of such a scenario are discussed later in this report.

OTHER HALOCARBONS

While there appear to be only modest changes in patterns of production and release of most other halocarbons since our 1976 report, there is now much more information on their presence and distribution in the atmosphere. Table 2.5

TABLE 2.5 Worldwide 1976 Release Rates from Human Activities, Atmospheric Concentrations, and Chlorine Contributions of Principal Halocarbons

Compound	Release (10^3 metric tons)[a]	Conc. (PPT)[b]	Cl Contribution (%)[c]
CCl_3F	308	126	15.7
CCl_2F_2	380	220	18.3
$CHClF_2$	60	n.d.	--
CCl_4	57	120	20.0
CH_3CCl_3	439	94	11.7
CH_2ClCH_2Cl	489	n.d.	--
CH_2Cl_2	416	32	2.7
$CCl_2{=}CCl_2$	577	26	4.3
$CHCl{=}CCl_2$	453	8	1.0
$CH_2{=}CHCl$	373	n.d.	--
CH_3Cl	7	613	25.3
$CHCl_3$	15	8	1.0

[a] CCl_3F and CCl_2F_2 from Table 2.1; other halomethanes, Environmental Studies Board (1978); CH_3CCl_3, Table 2.6; balance Bauer (1978).
[b] Singh *et al*. (1978). Estimated worldwide average for 1978.
[c] % contribution to total tropospheric chlorine in halocarbon form.

summarizes data on halocarbons released in the largest quantities as a consequence of human activities, together with a recent summary of average world background concentrations. From this, their relative contributions to the chlorine burden (and accordingly the relative rates at which they might be expected to introduce chlorine into the stratosphere) has been calculated. (In such a calculation, e.g., a molecule of CCl_4 is considered to contribute four Cl's and CH_3Cl contributes one Cl.)

Most of the halocarbons released in largest amounts contain C—H bonds, unsaturation, or both. As discussed further in the next chapter, such structures are rapidly attacked by HO radicals in the atmosphere and are destroyed within a matter of weeks or months. As a consequence, their atmospheric concentrations are low, or undetectable, and to date have made little contribution to the ozone problem.

Some of the other halocarbons deserve further discussion. Methyl chloroform, CCl_3CH_3, is replacing trichloroethylene and perchloroethylene as a solvent and degreasing agent because of lower toxicity and because, on account of its greater stability, it makes less contribution to local atmospheric pollution. In such uses, virtually all of it escapes to the atmosphere. Production and release figures both have doubled approximately every five years since 1960 and have been reviewed by Neely and Plonka (1977). Data since 1970, together with projections through 1982, based largely on announced expansions in production facilities, are listed in Table 2.6. Methyl chloroform is now one of the major contributors to the halocarbon burden; and its tropospheric concentration appears to be increasing at a rate of 17%/year (Singh *et al.*, 1978). Further, recent estimates of its tropospheric life, five to ten years, are considerably larger than those given in our 1976 report, so a larger fraction should reach the stratosphere than had been thought previously.

From Table 2.6, methyl chloroform production may be expected to increase; and, in fact, the data suggest that it may be finding additional uses. In particular, the coatings industry employs enormous quantities of solvent, which largely escape to the atmosphere. Estimated emissions in the United States alone amount to 2.4×10^6 metric tons/year (EPA, 1978). Use of many solvents are at present restricted because of their effect in local atmospheric pollution; and, if they were to be replaced to a significant

TABLE 2.6 Worldwide Production Estimates for Methyl Chloroform (10^3 metric tons)

Year	Amount
1970	181
1971	192
1972	268
1973	351
1974	390
1975	375
1976	439
1977	(587)[a]
1979	(707)[a]
1982	(853)[a]

[a] Estimates from McConnell and Schiff (1978).

extent by methyl chloroform, its contribution to the atmospheric halogen burden could quickly exceed that of the CFMs.

The situation in regard to the halomethanes (other than the CFMs) has recently been reviewed by another NRC panel (Environmental Studies Board, 1978) amplifying the discussion in our last report. In the past, CCl_4 found extensive use as a solvent, but release is now chiefly adventitious loss during manufacture during conversion to F-11 and F-12 (its chief use) plus loss in its use as a grain fumigant in marine shipment. The Panel estimated that 7.3 percent of U.S. production was released by these paths in 1973 and gives U.S. production in 1976 as 388×10^3 metric tons. If world production is taken as double this, as in our previous report, and we apply the same factor for release, we obtain the 1976 release of 57×10^3 metric tons listed in Table 2.5. World release rates for other halomethanes were estimated in the same manner, as twice those given for the United States in the Environmental Studies Board (ESB) report cited above.

Methyl chloride, CH_3Cl, is the most abundant halocarbon in the atmosphere but, from its low release rate from anthropogenic sources and expected short life, must be predominently of natural origin. As noted in our previous report (NAS, 1976), much arises from biological processes occurring in the oceans, either directly or via the reaction of methyl iodide or methyl bromide with chloride ion in seawater. As noted in the ESB report, methyl chloride has been detected in cigarette smoke by several investigators; this source alone contributes the order of 10^4 metric tons/year to the atmosphere. It has also been detected in the pyrolysis and combustion of other organic material, so that such sources, e.g., slash-burn agriculture, the burning of agricultural wastes, and urban combustion processes presumably make a large, but unknown contribution.

Some of the chloroform, $CHCl_3$, detected at low levels in the atmosphere may also be of natural origins, since higher concentrations are reported in ocean air masses and in helium equilibrated with seawater. However, how much is due to pollution of coastal waters by human activities and how much $CHCl_3$ is produced adventitiously through the use of chlorine in, for example, water treatment and bleaching operations is also unknown.

From Table 2.5, it is clear that human activities now introduce a variety of halocarbons into the atmosphere in a quantity sufficient to contribute significantly to the halocarbon burden. All need to be taken into account in considering the total effect on the ozone layer. However, it should be noted here, and will be considered in greater detail in subsequent chapters, that atmospheric concentrations of most of the materials in Table 2.5 are near the steady state that would be reached if release continues at the present rate. On the other hand, the major CFMs, F-11 and F-12, because of their long lives and until recently exponential growth in production, are still far from any steady state, and the same appears to be true for F-22 and methyl chloroform. Concentrations of these have increased significantly during the time over which measurements have been made, and will continued to do so. Accordingly, their contribution to the flux of halogen into the stratosphere will increase as well, even if their rate of release is maintained at present levels. As noted earlier, the rate of release of methyl chloroform is actually expected to increase and may constitute a serious potential problem.

In addition to the halocarbons, a number of other compounds that play an important role in the ozone cycle, N_2O, CO, CO_2, and CH_4, are also produced in significant quantities by human activities and are discussed further in subsequent chapters.

REFERENCES

Bauer, E. 1978. "A Catalog of Perturbing Influences on Stratospheric Ozone," FAA-EQ-78-20.

Borisenkov, Y. P., and Y. Y. Kazakov. 1977. Manuscript.

Environmental Studies Board, National Research Council. 1978. *Chloroform, Carbon Tetrachloride, and Other Halomethanes: An Environmental Assessment*. National Academy of Sciences, Washington, D.C.

EPA-450/2-78-022. 1978. Control techniques for volatile organic emission from stationary sources, Table 2.4-1. May.

McCarthy, R. L. 1978. E. I. du Pont de Nemours and Company, personal communication.

McCarthy, R. L., F. A. Bower, and J. P. Jesson. 1977. The fluorocarbon-ozone theory--I, *Atmos. Environ. 11*, 491-497.

McCarthy, R. L. 1977. World production and release of chlorofluorocarbons 11 and 12 through 1976, manuscript.

McConnell, J. C., and H. I. Schiff. 1978. Methyl chloroform: impact on stratospheric ozone, *Science 199*, 175.

Neely, W. B., and J. H. Plonka. 1977. Dow Chemical Company, manuscript.

Peters, M. 1979. University of Colorado, personal communication.

Singh, H. B., L. Salas, H. Shigeishi, and E. Scriber. 1978. Global distribution of selected halocarbons, SF_6 and N_2O, EPA-600/2-78-100. December.

3 ATMOSPHERIC CHEMISTRY

INTRODUCTION

The present chapter differs somewhat in arrangement and sequence of topics from those in the earlier NAS, 1976 report. The gas-phase chemical and photochemical reactions, which are the heart of the transformations under consideration, are broken into two categories, broadly described as tropospheric and stratospheric. Such an organization facilitates the consideration of all halocarbons that may ultimately contribute to stratospheric ozone destruction by focusing attention first on the role of their tropospheric chemistry as a possible removal mechanism and second on the stratospheric chemistry as the ultimate center of catalytic action.

Although the experimental values of some of the rate constants for the chemical reactions have changed, their uncertainties have been reduced, and new potentially important processes have been introduced, our earlier picture of the overall chemical problem has remained essentially unchanged. In briefest summary, those halocarbon molecules that are resistant to chemical attack in the troposphere are slowly transported through the tropopause and lower stratosphere and decomposed in the mid to upper stratosphere, mainly by ultraviolet solar radiation. Cl atoms and ClO radicals are generated, and they bring about a rapid, catalytic removal of "odd" oxygen (O atoms and ozone), which is equivalent to, but concurrent with, the direct reaction

$$O + O_3 \rightarrow 2O_2$$

Chlorine-containing species are involved in some 30 to 35 reaction steps, about 10 of which affect the stratospheric ozone budget in a substantial way (Table 3.1).

TABLE 3.1 Important Chemical and Photochemical Processes[a]

(a)	ClO_x	$Cl + O_3 \rightarrow ClO + O_2$	(1)
		$ClO + O \rightarrow Cl + O_2$	(2)
		$ClO + NO \rightarrow Cl + NO_2$	(3)
		$Cl + CH_4 \rightarrow HCl + CH_3$	(4)
		$HCl + OH \rightarrow Cl + H_2O$	(5)
		$ClO + NO_2 + M \rightarrow ClONO_2 + M$	(6)
		$ClONO_2 + h\nu \rightarrow Cl + NO_3$, etc.	(7)
		$ClO + HO_2 \rightarrow HOCl + O_2$	(8)
		$HOCl + h\nu \rightarrow Cl + OH$, $ClO + H$	(9)
(b)	O_x	$O + O_2 + M \rightarrow O_3 + M$	(10)
		$O + O_3 \rightarrow O_2 + O_2$	(11)
		$O_3 + h\nu \rightarrow O_2^{(*)} + O^{(*)}$	(12)
		$O(^1D) + M \rightarrow O + M$	(13)
(c)	NO_x	$NO + O_3 \rightarrow NO_2 + O_2$	(14)
		$NO_2 + O \rightarrow NO + O_2$	(15)
		$NO_2 + h\nu \rightarrow NO + O$	(16)
		$N_2O + O(^1D) \rightarrow NO + NO$	(17)
		$N_2O + h\nu \rightarrow N_2 + O$	(18)
(d)	HO_x	$HO + O_3 \rightarrow HO_2 + O_2$	(19)
		$HO_2 + O_3 \rightarrow HO + O_2 + O_2$	(20)
		$H_2O + O(^1D) \rightarrow HO + HO$	(21)
		$OH + HO_2 \rightarrow H_2O + O_2$	(22)
		$NO + HO_2 \rightarrow NO_2 + HO$	(23)
		$HO + NO_2 + M \rightarrow HNO_3 + M$	(24)

[a] Rate constants for their reactions are included in Table D.1.

According to current knowledge, these reactions are a subset of the approximately 100-120 stratospheric reactions needed for a detailed description of stratospheric chemistry. Within the framework of this current knowledge, a quantitative understanding of stratospheric chemical transformations and of the effects of man-made perturbations requires accurate values of many reaction rate coefficients (usually denoted k_i) and of photolysis rate coefficients (J_i). Fortunately, only about 20 to 30 of these processes appear to have a major effect on the results of one-dimensional model calculations; their k's and J's must therefore be known with good accuracy.

In an evaluation of this type, several questions arise:

(a) How may the reactions be ordered according to their importance in the overall scheme?

(b) How accurately are the rate coefficients known now, and what further improvements are in sight?

(c) What assurance do we have that the present reaction scheme is reasonably complete, i.e., that no important species, reaction steps, or multiple pathways for current reactions have been omitted?

Question (a) is important in guiding laboratory studies toward those processes to which the quantitative assessment of the overall process is most sensitive. An analysis of this type will be discussed. Question (b) requires a paradigm for judging accuracy in such a manner that use is made of theoretical predictions as well as of experimental data. The impact of new experimental methods currently being developed, which may bring about the more direct, reliable determination of rate parameters, also needs to be explored. Question (c) is, in many ways, the most difficult to address. We essentially rely on the collective wisdom and experience of the chemical (kinetics) community to judge whether important species or steps have been omitted. Often rate parameters have been measured by monitoring only the disappearance of reactants in laboratory studies and by assuming the course of the reaction to be known; yet in some recent studies, product channels have turned out to be different from what had been expected.

The apportioning of the chemical ozone loss among the different catalytic "families," O_x, NO_x, HO_x, and ClO_x, is also discussed in this chapter. This approach is useful for comparison with direct measurements of catalytic species in the stratosphere, particularly when several key species can be determined simultaneously. It is not suited, however, to the prediction of future changes in ozone concentration on the basis of simple extrapolation, because of the intricate couplings of the different catalytic cycles.

TROPOSPHERIC HALOCARBON INTERCEPTION

Role of Tropospheric Chemistry

As discussed in the NAS, 1976 report, for the assessment of possible stratospheric ozone destruction due to halocarbons, the troposphere can be regarded as providing possible loss mechanisms for some halocarbons prior to their transport to the stratosphere. Only reactions of HO radicals with halocarbons are sufficiently fast to provide for such removal. Unsaturated halocarbons also react with ozone, but these reactions are too slow to be of importance. If the rate coefficient for reaction with HO and its concentration (mixing ratio) were known, the tropospheric lifetime could be calculated. The troposphere HO concentration is not yet well known, however, although direct measurements are being made.

HO production is dependent on local ozone photolysis, which partly results in the formation of $O(^1D)$, whose rapid reaction with H_2O generates HO. It is also tied to the multistep process of methane oxidation (see Figure 3.1) in the course of which HO_2 is produced and subsequently reacts with NO to form HO and NO_2. NO_2 is photolyzed at wavelengths between 300 and 400 nm to regenerate NO and to produce an oxygen atom, which rapidly forms ozone by three-body recombination. Although some of these steps are now reasonably well characterized, the detailed course of methane oxidation under tropospheric conditions is only

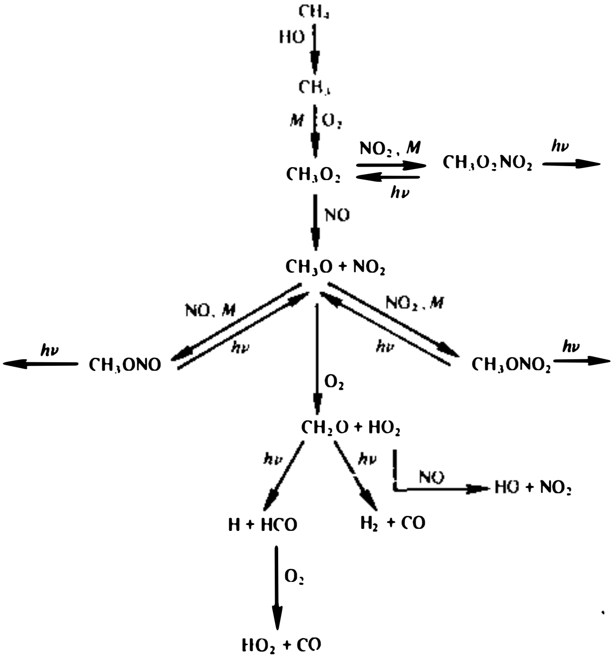

FIGURE 3.1 Tropospheric methane oxidation.

qualitatively and incompletely understood, and thus the reliable prediction of HO_x (HO and HO_2) concentration levels is still beyond our reach.

Specific difficulties with a quantitative understanding of HO concentrations in the troposphere include the uncertainty in the value of the branching ratio of formaldehyde photolysis under tropospheric conditions to produce either H_2 + CO or H + HCO (Moortgat *et al.*, 1978; Horowitz and Calvert, 1978). Further uncertainty is introduced by the effect of the increasing man-made source of CO, which reacts with HO in a manner that eventually affects the HO/HO_2 balance.

Tropospheric Gas-Phase Chemistry

Earlier data, which provided upper limits for the immeasurably slow rate of reaction of F-11 ($CFCl_3$) and F-12 (CF_2Cl_2) with OH, have been confirmed and extended. By finding no observable reaction in laboratory experiments up to 210°C, Chang and Kaufman (1977a) have been able to deduce a lower limit of about 10,000 years for the atmospheric removal time of F-11 and F-12 due to this process.

For hydrogen-containing paraffinic halocarbons such as F-22 (CHF_2Cl) and methyl chloroform (CH_3CCl_3) tropospheric reactions become important, and the corresponding removal times are much shorter, of the order of 20-30 and 5-10 years, respectively, based on laboratory measurement of rate coefficients for reaction with OH (Watson *et al.*, 1977; Chang and Kaufman, 1977b). These lifetimes are highly dependent on the tropospheric OH concentration, which is as yet poorly known (see page 125, Tropospheric HO). Two other compounds, CH_2ClCH_2Cl and CH_2Cl_2, which are released into the atmosphere in large quantities (Table 2.4) have been shown to react rapidly with OH (Howard and Evenson, 1976; Perry *et al.*, 1976; Davis *et al.*, 1976) and are thereby efficiently removed. Olefinic halocarbons such as $CH_2{=}CHCl$, $CHCl{=}CCl_2$, and $CCl_2{=}CCl_2$ (Table 2.4) react faster still (Perry *et al.*, 1977; Chang and Kaufman, 1977b) and therefore cannot accumulate in the troposphere. Laboratory measurements of rate constants for the reaction of halocarbons with OH radicals using the two principal experimental methods, flash photolysis and discharge flow, are simple and reliable. Precision of ±5-10 percent (single standard deviation) and accuracy of ±15 to 20 percent are normally attained.

Tropospheric Photolysis

In the NAS, 1976 report, it was shown that extrapolation of the far-ultraviolet absorptions of F-11 and F-12 to longer wavelengths would not give sufficient absorption intensity in the near ultraviolet (wavelengths greater than 290 nm) for these compounds to be decomposed significantly by direct photolysis in the troposphere. No evidence for such a process has been reported by the highly sensitive technique of optoacoustic spectroscopy, but the lower bound of about 100 years for their tropospheric lifetimes, which corresponds to this detection limit, is still too low to provide useful information, i.e., the technique is not sufficiently sensitive. There are, however, theoretical reasons that apparently exclude photolysis in that wavelength range. The question of the photolysis of halocarbons adsorbed on solid particles is taken up in Chapter 5.

STRATOSPHERIC CHEMISTRY

Stratospheric Gas-Phase Chemistry

Most of the potentially important stratospheric reactions are listed in Table 3.1 under the categories ClO_x, O_x, NO_x, and HO_x. The convenient division of these reactions into families as indicated is not without some ambiguities. Note that steps (3) and (6) involve NO_x as well as ClO_x, that (5) and (8) involve HO_x as well as ClO_x, and that steps (23) and (24) couple NO_x and HO_x.

These reactions are singled out as the result of a sensitivity analysis, which is discussed in some detail in the Appendix A. This sensitivity analysis introduces several quantities:

(1) The sensitivity parameter,

$$r_i = \left(\frac{R_i - R_o}{R_o}\right) \left(\frac{k_i - k_{oi}}{k_{oi}}\right) \approx \frac{\partial \ln R_i}{\partial \ln k_i}$$

where R_o is the calculated ozone depletion due to continuous halocarbon release at a prescribed rate using an accepted set of rate constants k_o. R_i is the equivalent estimate of ozone depletion calculated after varying the *i*th rate constant from k_{oi} to k_i, corresponding to the

95 percent confidence interval of its measured value. Since the R_O value is calculated for prescribed initial conditions, and for a specified man-made perturbation, the r_i's are dependent on these parameters and assumptions.

(2) The experimental uncertainty factor, f_i, which corresponds to changing a particular k_i or J_i by one single standard deviation (68 percent confidence level) of its measured value.

(3) The calculated error contribution factor, $u_i = 2r_i \ln f_i$, i.e., the combined effect of r_i and f_i on the calculated ozone depletion, where the factor 2 is introduced to increase the u_i's to the 2σ or 95 percent confidence level.

Table 3.2 lists some of the most important of the thermal rate processes as ranked by the magnitude of u_i.

Data for the uncertainties in the rate constants (given in Table D.2) are presented for 20 processes, omitting several of the listed ones whose u_i is small. The largest u_i values are near 0.25, and there are six above 0.14. The total chemical error factor, U (see below), is equal to a factor of 1.72 by which the calculated depletion of total ozone due to continuous halocarbon release should be multiplied or divided in order to be within the 95 percent confidence limit (a factor of 1.34 at the 1σ or 68 percent limit). This evaluation refers only to the effect of these 20 reactions and not, of course, to any uncertainties due to transport or model deficiencies or to different choices of other catalyst concentrations (NO_x, HO_x), or to different halocarbon release scenarios.

As discussed in Appendix A, this linear sensitivity analysis is qualitatively reasonable but highly oversimplified, i.e., the r_i's are not constant but depend on the details of the model calculation (see Table D.3), on the magnitude of $\Delta \ln k_i$, and also on the magnitude of k for other reactions and on other perturbations. The f_i's are chosen to take account of both random and systemic errors in the laboratory measurement of the particular rate constant, but the choice is often arbitrary, especially when there are conflicting experimental data. In this simple analysis, which assumes the errors to be linear, independent, and have a log-normal distribution, the overall multiplicative uncertainty of the ozone reduction at the $2\sigma_i$ (95 percent confidence) level is given by

$$U = \exp\left(\pm\{\Sigma u_i^{\,2}\}^{1/2}\right)$$

TABLE 3.2 Sensitivity Calculation for 20 Important Reactions[a],[b]

Reaction	Sensitivity Factor, r_i	Experimental Uncertainty Factor, f_i	Error Contribution Factor, $u_i = \partial r_i \ln f_i$
(22) $HO + HO_2 \rightarrow H_2O + O_2$	-0.18	2	-0.25
(17) $N_2O + O(^1D) \rightarrow NO + NO$	-0.43	1.3	-0.23
(2) $ClO + O \rightarrow Cl + O_2$	0.44	1.2	0.16
(21) $O_3 + h\nu = O_2 + O(^1D)$	-0.30	1.3	-0.16
(13) $O(^1D) + M \rightarrow O + M$	0.30	1.3	0.16
(19) $HO + O_3 \rightarrow HO_2 + O_2$	-0.32	1.25	-0.14
(24) $NO_2 + HO + M \rightarrow HNO_3 + M$	0.25	1.3	0.13
(18) $N_2O + h\nu \rightarrow N_2 + O(^1D)$	0.36	1.2	0.13
(16) $NO_2 + h\nu \rightarrow NO + O$	0.20	1.3	0.10
(6) $ClO + NO_2 + M \rightarrow ClONO_2 + M$	-0.17	1.3	-0.09
(23) $HO_2 + NO \rightarrow HO + NO_2$	0.18	1.2	0.07
(14) $NO + O_3 \rightarrow NO_2 + O_2$	-0.19	1.2	-0.07
(5) $HCl + HO \rightarrow Cl + H_2O$	0.26	1.15	0.07
(20) $HO_2 + O_3 \rightarrow HO + O_2 + O_2$	0.08	1.4	0.05
(3) $ClO + NO \rightarrow Cl + NO_2$	-0.11	1.25	-0.05
(1) $Cl + O_3 \rightarrow ClO + O_2$	0.17	1.15	0.05
(10) $O + O_2 + M \rightarrow O_3 + M$	-0.15	1.2	0.05
(21) $H_2O + O(^1D) \rightarrow HO + HO$	0.12	1.25	0.05
(15) $NO_2 + O \rightarrow NO + O_2$	-0.20	1.1	-0.04
(4) $Cl + CH_4 \rightarrow HCl + CH_3$	-0.11	1.15	-0.03

$$\left(\sum_{1}^{20} u_i{}^2\right)^{1/2} = 0.542,\ U_{20} = 1.72$$

$$\left(\sum_{i}^{6} u_i{}^2\right)^{1/2} = 0.460,\ U_6 = 1.58$$

---

[a] Reactions are ordered by decreasing magnitude of u_i.
[b] Provided by R. Stolarski and D. Butler, GSFC.

The entire analysis is only valid for "small" changes and breaks down in the event of gross errors or major omissions. Table 3.2 indicates that many of the reaction rate constants are fairly accurately known (f_i ~ 1.1 or 1.2). If only the six largest u_i values are included and the uncertainties due to the other 14 processes are neglected, the corresponding overall uncertainty, U', equals 1.58, i.e., not much smaller than the above $U = 1.72$. It is also clear that the narrowing of uncertainty for any one process, even letting the largest u_i go to zero, has a rather small effect on U, i.e., U would go from 1.72 to 1.62 if the f-value of the $HO + HO_2$ reaction were reduced to 1.0, i.e., its rate constant were known with perfect accuracy.

Because of the large uncertainties and arbitrariness in the r_i, f_i, and resulting u_i values, this sensitivity analysis should only be used as a rough guideline. No significance should be ascribed to the exact values of u_i, the meaningful point being whether a given u_i is large ($\gtrsim 0.2$), fairly large (~0.1 to 0.2), or small. A comparison with the limited sensitivity analysis of the NAS, 1976 report shows major changes of the r's and decrease of the f's.

There has been much progress in the experimental measurement of the rate parameters, and there have also been a few dramatic changes such as the large increase of k_{23} amounting to more than an order of magnitude (Howard and Evenson, 1977), which was quickly confirmed by other groups (Thrush, 1977; Reimann and Kaufman, 1978a; Margitan, 1978), so that its error contribution factor, u_{23}, is now thought to be small. There have also been new studies of reaction (22) (Burrows *et al.*, 1977; Chang and Kaufman, 1978) whose u value was thereby reduced but it is still among the largest contributors. The effect of water vapor (Hamilton and Lii, 1977) probably due to the formation of $HO_2 \cdot H_2O$ complexes needs further clarification, but it is most unlikely to be important in the stratosphere, where the H_2O volume mixing ratio (mole fraction) is only a few parts per million. The rates of reactions (1), (3), (4), (5), and (6) are all quite accurately known today and do not contribute very much to the overall uncertainty. Reaction (2) has also received further attention, but since its r value is among the largest, k_2 needs to be measured more accurately.

Our general feeling of optimism regarding the progress of rate measurements needs to be tempered by several cautionary notes: (1) Many of the experimental data refer to the rate of disappearance of one reactive species, and assumptions are often made regarding the stoichiometry of the process that neglect possible uncertainties in product branching ratios. (2) Some of the rate constants appear to have unexpected pressure dependence (Cox, 1978; Burrows *et al.*, 1978), which is not easily measured by the available experimental techniques. (3) Some of the measured rate constants are difficult to understand in the framework of our current theoretical understanding of chemical kinetics. For example, the most recent study of reaction (20) by the discharge-flow laser-magnetic-resonance methods (Zahniser and Howard, 1979) reports an pre-exponential factor of 1.05×10^{-14} cm^3 sec^{-1}, unusually small for a two-body reaction even with a highly restricted transition state. Furthermore, there are some apparently simple reactions, e.g., (3) and (23), whose rate constants have negative temperature coefficients that are not easily explained (Golden, 1979). The large magnitude of k_{22}, especially when compared with its symmetrical counterparts $OH + OH \rightarrow H_2O + O$ and $HO_2 + HO_2 \rightarrow H_2O_2 + O_2$, is unexpected. Inconsistencies exist in the thermal decomposition (Knauth, 1978) and recombination data for $ClONO_2$. Very large deviations from the predicted range for kinetic parameters may indicate erroneous experimental results, but the bounds within which theoretical predictions are expected to hold are still somewhat uncertain. The predictive power of reaction rate theory is in need of critical assessment. Recent realization that many of the reaction steps considered heretofore as direct chemical steps may, in fact, be complex processes that proceed by way of an energized bound intermediate complex may help us to rationalize some of the above inconsistencies (Golden, 1979).

Returning to the questions raised earlier, we see that we have answered question (a) with Table 3.2. We can answer question (b), the chances for narrowing of the uncertainties, by pointing out that if the r_i and f_i values of Table 3.2 are meaningful, small reductions will not change our picture very much. Thus, k_{22}, k_{17}, and k_2 continue to be among the major contributors, mainly because either their sensitivity parameter, r_i, or their f_i values are high. For k_2, no further experimental work is available since the NASA, 1977 report. For reaction (17), the formation of NO in the $O(^1D) + N_2O$ reaction, whose r_i is -0.43, no reduction in f_i is likely to occur soon.

Although important progress has been achieved in the measurement of k_{22}, it remains high on the list of reactions in need of further study. Reaction (22) is a major stratospheric sink of HO_x and thereby plays a large role in setting the level of stratospheric HO_x concentrations. In the NAS, 1976 report, the large uncertainty of k_{22} had contributed about half of the overall uncertainty due to reaction rate constants. That earlier analysis included only seven critical reactions and is not directly comparable with the error analysis presented in this report.

Question (c) of the Introduction deals with the problem of omission of important species or steps. This can never be answered definitively, but we believe that errors are more likely to arise from the misassignment of pathways for an already considered reaction, or possibly from lack of knowledge of its pressure and temperature dependence, than from outright omission of a process. The likelihood of another major change among sensitive rate constants (large r_i) would seem to be fairly small. Earlier, such upheavals have occurred when indirect methods had been used to measure rate constants as, for example, in the case of the NO + HO_2 reaction, (23). With the development of specific and highly sensitive detection methods for the reactive species, and with increased use of flow or flash techniques that allow the desired reactions to be examined directly, large errors have become less likely. All the reactions listed above, for example, have been or are being investigated by such modern experimental techniques.

In dismissing possible omissions we are mindful of the recent past. $ClONO_2$ had not been considered as part of the ClO_x scheme until shortly before the completion of the NAS, 1976 report. It was included when its rate of photolysis in the atmosphere was seen to be surprisingly small; laboratory measurements of the absorption coefficient, rate of formation, and rates of reaction followed within less than a year. Its effect on calculated ozone depletion due to ClO_x was substantial, and efforts to confirm its presence by atmospheric infrared absorption measurements are under way. A similar situation has developed more recently regarding the role of hypochlorous acid, HOCl. Ultraviolet absorption measurements in the 1930's had shown a strong band near 320 nm, which is now being ascribed to impurities by some investigators. The magnitude of its true absorption coefficient at wavelengths greater the 300 nm is still somewhat uncertain (Molina and Molina, 1978; Timmons, 1977; DeMore, 1976; Knauth *et al.*, 1979). If the solar photolysis of HOCl were to be sufficiently slow and if its source term by reaction (8) is as large as recent experiments indicate, HOCl might turn out to be another inactive ClO_x reservoir species like $ClONO_2$, and the catalytic ozone destruction by ClO_x may well be reduced. Birks (1978), Reimann and Kaufman (1978b), and Stimpfle *et al.* (1979) report that k_8 is fairly large (3×10^{-12} to 6×10^{-12} cm^3 sec^{-1} at 298 K). Although it now appears that photolysis is fast and HOCl relatively unimportant, it will need to be included in the model.

Two other reactions have recently been suggested as being of possible importance but have not yet been incorporated in our model calculations. The first involves the reaction of Cl with formaldehyde, which has been found to have a large rate coefficient (Michael *et al.*, 1979). Although the stratospheric concentration of formaldehyde has not been measured, model calculations by Stief *et al.* (1978) have suggested that the inclusion of this reaction may reduce the calculated ozone perturbation by about 7 percent of its numerical value (in their model, from a 20 to a 18.5 percent O_3 decrease).

The other reaction is between ClO and BrO. It provides an additional chain for O_3 destruction if the ClO + BrO reaction regenerates Cl and/or Br, i.e., if the O + ClO or BrO steps are short-circuited, and it also partially short-circuits the "null" cycle that regenerates O from ClO + NO via NO_2. Both of these effects result in an increase in the calculated ozone perturbation. Although the overall ClO + BrO rate constant is reasonably well known (Clyne and Watson, 1977), neither the detailed reaction channels nor the stratospheric BrO_x concentrations are well characterized at present. Since the additional chain process can operate without O-atom steps, it may be important in the lower stratosphere and needs to be carefully evaluated and then incorporated into the model.

A species that has not yet been considered in sufficient detail is the highly metastable excited $^1\Delta_g$ state of O_2, which is formed in the photolysis of O_3 and whose subsequent deactivation processes are mainly very slow. Its concentration is therefore quite large, and if a particular reaction channel exists whose rate is large, $O_2(^1\Delta_g)$ may have a substantial effect on the overall chemistry.

Very recently, studies of ClO reactions in two different laboratories have suggested, but not proved, the existence of minor reaction channels in which HCl might be formed directly either by $ClO + HO_2 \rightarrow HCl + O_3$ (Stimpfle *et al.*, 1979) or by $ClO + HO \rightarrow HCl + O_2$ (Leu and Lin, 1979). Neither reaction is mechanistically favored, but even a small fractional yield of HCl would decrease substantially the ClO_x catalysis and therefore requires further experimental work.

It is not feasible to incorporate each new set of proposed reactions into the large computer model unless (a) its effect is fairly substantial, and (b) the basis of its laboratory measurement is sound. Future reappraisals of this type or introduction of new and important species into the present chemical model of the stratosphere cannot, of course, be ruled out. Nevertheless, the continued attention that this problem has received over a period of several years makes it improbable that major omissions are still present.

Stratospheric Photochemistry

In the two years since the publication of the NAS, 1977 report, considerable efforts have been made to measure the absorption spectra, photolysis rates, and products of species of actual or potential stratospheric importance. It has been recognized that many of these spectra show small but definite changes in intensity distribution between ambient and stratospheric temperatures; this normally takes the expected form of narrowing of relatively broad absorption bands at lower temperatures. Many of the new data were tabulated in the NASA, 1977 report and will not be repeated here.

Ozone The absorption coefficient of O_3 is well established, and O_3 is known to decompose with unit quantum efficiency throughout the visible and ultraviolet regions of the spectrum. However, the form and temperature dependence of the threshold near 310 nm, where production of ground state $O(^3P)$ is superseded by $O(^1D)$, which reacts with N_2O to yield NO and with H_2O, CH_4, and H_2 to yield HO and H, is less well established. Moortgat and Kudszuz (1978) have recently given an analytical expression for the form of the quantum yield near threshold as a function of temperture that is sufficiently accurate for atmospheric modeling. However, these data may have to be scaled by as much as 10 percent in the light of the results of Fairchild *et al.* (1978), who report that photolysis of ozone between 270 and 310 nm yields some $O(^3P)$ directly, i.e., that the quantum yield of $O(^1D)$ may only be ~0.9. This is further supported by molecular-beam experiments of Y. T. Lee (University of California, Berkeley, personal communication, 1979). Although further work is still needed to resolve the details of the quantum yield of $O(^1D)$ formation from O_3 near its threshold of 313 nm, these details are unlikely to have a major effect on the relative change in ozone column due to added F-11 and F-12. [This is not true for F-22 or methyl chloroform since their mixing ratios depend on HO, which, in turn, depends on $O(^1D)$.]

Nitrogen Oxides Graham and Johnston (1978) have published their work on the absorption coefficients of NO_3 and N_2O_5 quoted in the NASA, 1978 report. For NO_3 the two processes

$$\begin{aligned} NO_3 + h\nu &= NO_2 + O \\ &= NO + O_2 \end{aligned}$$

give average quantum yields of $\phi_1 = 0.77$, $\phi_2 = 0.23$ between 470 and 610 nm, and $\phi_2 = 0.07$ between 610 and 700 nm. No new data on the mechanism of photolysis of N_2O_5 were obtained.

Chlorine-Nitrogen Compounds Clausen *et al.* (1978) have obtained absorption spectra of $ClONO_2$, ClONO, and $ClNO_2$ at temperatures between 223 and 293 K. Their absorption cross sections for $ClONO_2$ are consistently 10-30 percent lower than those of Rowland, Spencer, and Molina (1976) which are adopted here and were quoted in the NASA, 1977 report. For ClONO and $ClNO_2$, which are of minor atmospheric important, agreement with the work cited in the NASA, 1977 report is excellent.

There have been two recent studies of the photolysis of $ClONO_2$, both aimed at discerning its photochemical mechanism. In one study (Smith *et al.*, 1977), the conclusion is that the principal products of the primary photolytic act are O atoms and ClONO. In the other study (Chang *et al.*, 1979), evidence is presented for the products being Cl atoms and NO_3.

HOCl This species, which is a major product of the ClO + HO_2 reaction, is difficult to study in the laboratory because the equilibrium constant of the reaction

$$H_2O + Cl_2O = 2HOCl$$

is close to unity and shows little temperature dependence. Furthermore, the ultraviolet absorption spectra of Cl_2O and HOCl are hard to separate, being rather similar and somewhat featureless. Interest centers on the strength of absorption by HOCl at wavelengths greater than 300 nm, which would lead to rapid photolysis in the stratosphere. Experimental results of Knauth *et al.* (1979) and of Molina and Molina (1978) are in approximate agreement with the data of DeMore quoted in the NASA, 1977 report, although their absorption cross sections show less of a tail toward longer wavelengths, whereas results of Timmons (1977) show very little absorption above 300 nm. On balance, present results favor a short photochemical lifetime of approximately 30 minutes for HOCl in the stratosphere, the primary process being

$$HOCl + h\nu = HO + Cl$$

Such rapid photolysis would make HOCl an unimportant stratospheric species.

Pernitric Acid Graham *et al.* (1978) and Cox and Patrick (1979) have determined the ultraviolet absorption spectrum of HO_2NO_2 and measured its rate of formation from HO_2 and NO_2.

Apportioning of Odd-Oxygen Loss

In the absence of fast coupling reactions among the different catalyst families, the local O_x destruction rate due to a given family may be easily set down. For NO_x, for example, a steady-state calculation for reactions (14), (15), and (16) gives $2k_{15}[O][NO_2]$ as the simple answer. Similar considerations for ClO_x, reactions (1) and (2), give $2k_2[O][ClO]$. When a coupling reaction such as (3) is added, one can easily show that in the steady-state approximation, the odd-oxygen removal due to NO_x is reduced by $k_3[NO][ClO]$, but the removal due to ClO_x is increased by that same term, i.e., the total removal due to both NO_x and ClO_x remains unchanged. Johnston and Podolske (1978) have therefore proposed that the simplest representation of the complicated overall scheme leaves the apportioning unchanged and introduces the coupling steps only in order to calculate the fraction of a particular catalyst family that is in the molecular form that takes part in the rate-limiting step, for example, NO_2 for NO_x, ClO for ClO_x. This approach is particularly valuable for the comparison with local measurements of catalyst concentrations. If O_3, O, NO_2, ClO, HO_2, and HO could be measured simultaneously in the mid to upper stratosphere, one would be able to check the overall balance between production and loss terms of O_x and thereby verify the correctness of the reaction scheme.

However, this analysis does not permit the prediction of the effect on ozone concentration of adding more catalyst. When such information is required, as is the main task of this report, one must carry out the full model calculation, because the perturbation of increasing (or reducing) the total concentration level of a given catalyst family has an immediate effect on the distribution of all other catalyst families among their molecular forms, e.g., increasing NO_x reduces ClO and HO_2 by the fast coupling steps. This is the reason for the highly nonlinear behavior described in Chapter 9 (Table 9.1), where very large increases of NO_x (via N_2O additions) to the present model atmosphere produce minimal changes in the ozone column calculated for a standard halocarbon release scenario.

SUMMARY AND CONCLUSIONS

This chapter shows that much progress has been achieved in the laboratory measurement of stratospheric reaction and photolysis rate constants. If, for example, the seven reactions that had been singled out for uncertainty analysis in the NAS, 1977 report are taken as a subset of Table 3.2, and a U value is calculated using our present data, we obtain an uncertainty factor of 1.39 compared with 2.26 two years ago. The uncertainties are now more evenly distributed than before, and they are individually smaller in magnitude. This means that future progress will be more difficult, since it will require the whittling down of uncertainties for a fairly large number of reactions. In that context, the continued guidance by sensitivity calculations is of great importance. We need to understand in detail how well the sensitivity parameters, r_i, are known and how they depend on all major variables.

Setting aside questions of product ratios and pressure dependency, present laboratory techniques are certainly capable of reducing the f_i values of all the reactions listed in Table 3.2 to about 1.10 to 1.20. If the total uncertainty (95 percent) for the 20 reactions is recalculated using $f_i = 1.15$, U is found to be about 1.4, a value beyond which further improvement will be difficult to achieve.

Our understanding of stratospheric chemistry has grown substantially. Accurate laboratory measurements obviously lag somewhat behind this understanding, but the gap has been narrowed. Soon, our less-advanced knowledge of tropospheric processes may seriously limit further progress, since chlorine-containing substitutes for F-11 and F-12 for certain user applications will probably contain H atoms and be subject to strong tropospheric interception.

RECOMMENDATIONS FOR FUTURE RESEARCH

The problems in understanding atmospheric chemistry and photochemistry, which have been mentioned here, are not limited to the specific problem of ozone destruction due to anthropogenic chlorine release. The resolution of these problems requires continued advances in our abilities to make precise measurements of rate constants and J values over an extended range of pressure and temperature and by studying both reactant loss and product appearance. At the same time, advances in general theory need to be made so that rate processes can be understood within a general framework.

Specific tasks include measurement of the wavelength-dependent quantum yields and branching ratios of the stratospheric photolyses of species such as O_3, $ClONO_2$, HOCl, and NO_3. Stratospheric chemical processes that need investigation by alternative techniques from those already employed are those that are most difficult to understand in terms of modern theory, i.e., those with negative activation energies and incomprehensible *A* factors. Reactions of HO_2 species are a particular, but not the only, example of this need.

Because of the strong interactions between tropospheric and stratospheric processes, it has become clear that the complex chemistry of the troposphere is in need of further study. The mechanism of methane oxidation should be elucidated as a step toward the necessary understanding of HO_x chemistry. A very important process for which a good absolute measurement, as a function of temperature, is required is

$$CH_3O_2 + NO \rightarrow CH_3O + NO_2$$

Also needed are rate data at room temperature and lower for

$$CH_3O + O_2 \rightarrow CH_2O + HO_2$$

The recent report (Chang and Barker, 1979) that oxygen atoms add to formaldehyde as well as abstract, makes a product study of the reaction of OH with formaldehyde a high priority, since a branching here could have an effect on the HO/HO_2 and CO/CO_2 ratios.

REFERENCES

Birks, J. 1978. Chemistry Department, University of California, personal communication.

Burrows, J. P., G. W. Harris, and B. A. Thrush. 1977. *Nature 267*, 238.

Burrows, J. P., *et al*. 1978. Paper presented at WMO Symposium, Toronto, Canada, June 26-30.

Chang, J. S., and J. R. Barker. 1979. *J. Phys. Chem. 83*, in press.

Chang, J. S., and F. Kaufman. 1977a. *Geophys. Res. Lett. 4*, 192.

Chang, J. S., and F. Kaufman. 1977b. *J. Chem. Phys. 66*, 4989.

Chang, J. S., and F. Kaufman. 1978. *J. Phys. Chem. 82*, 1683.

Chang, J. S., J. R. Barker, J. E. Davenport, and D. M. Golden. 1979. *Chem. Phys. Lett. 60*, 385.

Clausen, H., H. D. Knauth, and R. Schindler. 1978. Institute of Physical Chemistry, University of Kiel, personal communication.

Clyne, M. A. A., and R. T. Watson. 1977. *J. Chem. Soc. Faraday I, 73*, 1169.

Cox, R. A. 1978. Paper presented at WMO Symposium, Toronto, Canada, June 26-30.

Cox, R. A., and K. Patrick. 1979. *Internat. J. Chem. Kinet. 11*, 635.

Davis, D. D., G. Machado, B. Conaway, Y. Oh, and R. T. Watson. 1976. *J. Chem. Phys. 65*, 1268.

DeMore, W. B. 1976. Paper presented at the International Conference on the Stratosphere and Related Problems, Logan, Utah, September.

Fairchild, C. E., E. J. Stone, and G. M. Lawrence. 1978. *J. Chem. Phys. 69*, 3632.

Golden, D. M. 1979. *J. Phys. Chem. 83*, 108.

Graham, R. A., and H. S. Johnston. 1978. *J. Phys. Chem. 82*, 254.

Graham, R. A., A. M. Winer, and J. N. Pitts, Jr. 1978. *Geophys. Res. Lett. 5*, 909.

Hamilton, E. J., Jr., and R. R. Lii. 1977. *Internat. J. Chem. Kinet. 9*, 875.

Horowitz, A., and J. G. Calvert. 1978. *Internat. J. Chem. Kinet. 10*, 713.

Howard, C. J., and K. M. Evenson. 1976. *J. Chem. Phys. 64*, 4303.

Howard, C. J., and K. M. Evenson. 1977. *Geophys. Res. Lett. 4*, 437.

Johnston, H. S., and J. Podolske. 1978. *Rev. Geophys. Space Phys. 16*, 491.

Knauth, H. D. 1978. *Ber. Bunsenges. Phys. Chem. 82*, 212.

Knauth, H. D., H. Alberti, and H. Clausen. 1979. *J. Phys. Chem. 83*, 1604.

Leu, M. T., and C. L. Lin. 1979. *Geophys. Res. Lett. 6*, 425.

Margitan, J. J. 1978. 13th Informal Conference on Photochemistry, Clearwater Beach, Florida, January 4-7.

Michael, J. V., D. F. Nava, W. A. Payne, and L. J. Stief. 1979. *J. Chem. Phys. 70*, 1147.

Molina; M. J., and L. T. Molina. 1978. *J. Phys. Chem. 82*, 2410.

Moortgat, G. K., and E. Kudszus. 1978. *Geophys. Res. Lett. 5*, 191.

Moortgat, C. K., K. Slemr, W. Seiler, and P. Warneck. 1978. *Chem. Phys. 54*, 444.

Perry, R. A., R. Atkinson, and J. N. Pitts, Jr. 1976. *J. Chem. Phys. 64*, 1618.

Perry, R. A., R. Atkinson, and J. N. Pitts, Jr. 1977. *J. Chem. Phys. 67*, 458.

Reimann, B., and F. Kaufman. 1978a. 13th Informal Conference on Photochemistry, Clearwater Beach, Florida, January 4-7.

Reimann, B., and F. Kaufman. 1978b. *J. Chem. Phys. 69*, 2925.

Smith, W. S., C. C. Chou, and F. S. Rowland. 1977. *Geophys. Res. Lett. 4*, 517.

Stief, L. J., J. V. Michael, W. A. Payne, D. F. Nava, D. M. Butler, and R. S. Stolarski. 1978. *Geophys. Res. Lett. 5*, 829.

Stimpfle, F., R. A. Perry, and C. J. Howard. 1979. *J. Chem. Phys.* in press.

Thrush, B. A. 1977. Cambridge University, private communication.

Timmons, R. B. 1977. MCA final report.

Watson, R. T., G. Machado, B. Conaway, S. Wagner, and D. D. Davis. 1977. *J. Phys. Chem. 81*, 256.

Zahniser, M. S., and C. J. Howard. 1979. NOAA Aeronomy Laboratory, Boulder, Colorado, private communication.

4 ATMOSPHERIC TRANSPORT

INTRODUCTION

Current concerns about the fate of the stratospheric ozone layer are based, primarily, on numerical predictions from one-dimensional, chemical-diffusion models. The preferred model for obtaining chemical transports would be a three-dimensional, dynamical model, but such a model is not available at present. The reduction from three to one spatial dimensions greatly simplifies the problem, but it involves several assumptions. In this chapter we are mainly concerned with the errors made if the long-term, average vertical atmospheric transport is approximated by a diffusion process. Are the required simplifying assumptions qualitatively and quantitatively justified? What degree of uncertainty is introduced in the predicted profiles of trace gases by the constraints imposed in simplifying the transport, and, in turn, what degree of uncertainty is introduced in the calculations of O_3 change by CFMs?

The three-dimensional motions of the atmosphere are strongly asymmetrical. On the average, horizontal speeds exceed vertical speeds by ratios of 500-1000 to 1. These ratios are consistent with the atmosphere being a very thin fluid surrounding a very large spheroid. Thus, to a first approximation, the flow is horizontal, resembling a shallow river undulating, meandering, and eddying as it circles the globe.

Despite the fact that the flow is predominantly horizontal, each meander and eddy has small vertical velocities associated with it. These vertical speeds of millimeters and centimeters per second are too small to be measured, but they contribute substantially to the transport and to the dispersion of a tracer. Trajectories computed on surfaces of constant entropy clearly indicate the importance of the small vertical velocities. Because velocity shears (changes in direction and speed of the wind) in the vertical are much larger than in the horizontal, the small vertical displacements increase the deformations in the fluid. Adjacent particles move away from each other faster, increasing the probability that they follow independent paths.

The tendency for each small parcel of air to generate its own trajectory makes it practically impossible to describe the observed motions in fine detail. Instead, one can, at most, analyze and predict larger-scale motions and the corresponding trajectories. The effects of the small air parcels, which contribute to the smaller-scale dispersion, must be described statistically.

Ozone itself is perhaps the most useful tracer of air transport from the stratosphere to the troposphere. The transport of ozone deduced from analyses of the large-scale flow patterns has certain well-defined features. From its source at mid levels of the tropical stratosphere, it spreads poleward and downward while making several undulating transits around the globe. When it reaches the lower stratosphere, the probability increases that it will be transported toward the equator and downward into the troposphere. When in the troposphere, convective motions, especially those associated with thunderstorms, disperse it rapidly. Other downward transported species, in particular the NO_y and ClO_y families, presumably follow similar routes.

In the one-dimensional chemical models, all of these meteorological details are ignored and vertical fluxes are assumed proportional to the gradient of the mixing ratio (or mole fractions) χ of a given species since mixing ratio is conserved following an individual parcel of fluid.

The flux of species i, therefore, is expressed by the triple product

$$F_i = -\bar{\rho} K(z) \frac{\partial \chi i}{\partial z} \qquad (4.1)$$

where the density of the standard atmosphere is used for $\bar{\rho}$ and $K(z)$ is specified as a function of height; if data are available to determine the other terms in Eq. (4.1), $K(z)$ can be estimated.

In our previous report, we estimated a variety of $K(z)$'s consistent with observed profiles of CH_4 and N_2O. Since then more data have become available on the distribution of these species, and especially their latitudinal variations.

However, use of these new data with the procedures of our previous report indicate the uncertainties in estimating transport rates from CH_4 and N_2O are as large as previously. This lack of improvement in the estimated $K(z)$ is, in part, due to an overoptimism in previous estimates and, in part, to remaining uncertainties in the chemical lifetimes of the tracer (especially CH_4) within the lower stratosphere.

Hence, to further sharpen our estimates of the likely time scales for tropospheric-stratospheric transport and the range of uncertainty, we have also carefully determined the $K(z)$ required to give an optimum fit to the observed profile of global ozone. This estimate also incorporates data from the numerical tracer studies of Mahlman and Moxim (1978). Our best estimate of vertical transports is obtained by combining the $K(z)$ estimates derived from methane, nitrous oxide, and ozone-numerical tracer estimates. The latter uses a somewhat different approach than applied in our previous report, whose details are therefore presented in Appendix B.

RATIONALE FOR THE DIFFUSION APPROXIMATION

If we ignore for the moment the zonal motions, the typical transport path is poleward and downward in the stratosphere and equatorward and downward in the troposphere. At no latitutde does it simply move downward. What, then, is the physical justification for the vertical diffusion in a one-dimensional model? If the model represents a global mean, the integration provides the justification. When the continuity equation for each species is summed or integrated over all latitudes and longitudes, direct reference to horizontal transport no longer appears. Only the mean vertical flux remains in the equation.

However, to evaluate this mean flux one must know the vertical velocity and the concentration of each species at thousands of horizontal grid points. Since these velocities are not observed, they must either be derived from the data with the aid of equations, or they must be predicted by a numerical model. The concentrations would also have to be predicted, so one would be forced back to a three-dimensional model. Hence, for simplicity, we forget about the point values and approximate the mean flux of all species by down-gradient diffusion. More realistic transport treatments would be preferable, but since the O_3 change calculations have been carried out with 1-D models, it is necessary to evaluate the merits and shortcomings of such an approach.

Once the horizontal fluxes have been eliminated by extending the integration over the complete globe, all effects of atmospheric transport are reduced to a mean vertical flux that varies with z and t. This mean flux for gas i, which is denoted by the symbol F_i, is given by

$$F_i = \overline{w'c'_i} \qquad (4.2)$$

where the overbar denotes the horizontal global mean; w' is the local vertical velocity ($\bar{w} = 0$), and $c'_i = c_i - \bar{c}_i$. It is understood that F can vary with z and t only, while w' and c' vary with x, y, z, and t. To determine exactly how they vary we would have to solve the complete set of hydrodynamic equations and would have gained little then by the horizontal integrations. We gain only if we can relate the flux to a predicted mean variable. Therefore, the basic simplifying assumption in 1-D modeling involves replacing the mean turbulent or deviation flux by Eq. (4.1).

It seems reasonable that the mean transport, or mean flux, produced by the large numbers of quasi-independent air parcels will be proportional to the vertical gradient of the species' mean mixing ratio. We must keep in mind that the zonal mean circulations associated with the Hadley and Ferrel cells are, themselves, small residuals between large, fluctuating velocities; but here, these residuals from the zonal means are part of the w's whose global mean is approximately zero. Thus, a Hadley circulation transports a trace gas upward at one latitude and downward at another latitude. A net transport occurs only if its mixing ratio is different on the up path and on the down path.

This condition is implicit in a nonzero $\overline{w'c'}$, i.e., in the average correlation between w' and c'. However, to justify the use of the diffusion approximation in a 1-D model, the mean correlation must not only be proportional to the negative gradient of the mean mixing ratio for all species, but the coefficient of proportionality, K, must also be independent of the species. It is not very probable that such stringent conditions can be met in view of the fact that photochemical sources and sinks, vertical fluxes, and chemical reactions all vary with latitude, longitude, and height for each gas, giving rise to many nonlinear effects. Despite this skepticism, the approximation would still be useful if the K profiles derived from both upward and downward fluxing trace gases were similar in shape and comparable in magnitude. We could then quantify the range of uncertainty in the approximation and estimate the resulting range in the trace gas profiles.

The basic problem in using Eq. (4.2) to evaluate transport is our inability to measure the vertical velocity w'. Vertical velocities associated with the large-scale wave cyclones are too small to be measured by any present-day sensors. Their magnitudes are ~1/1000 of the horizontal velocity components, but they are equally important because the depth of the atmosphere is also about 1/1000 of the horizontal dimensions. On the other hand, the vertical velocities associated with strong convective motions are comparable in magnitude with the horizontal velocities, but these are also difficult to sample because of their small horizontal scales.

Another problem is the nonrepresentative sampling of most of the trace gases. Only a few have been measured with sufficient accuracy at a sufficiently large number of sites to determine representative global means. It should be clear, therefore, that no direct evaluations of transport are currently possible. It does not follow, however, that we know nothing about the transport of trace gases. Many case studies, diagnostic and predictive numerical studies, and specially designed field and aircraft experiments have been made to determine which processes and which scales of motion control the transports in the troposphere and stratosphere.

On the basis of these studies we know (1) small-scale convective motions dominate the flux in the tropical troposphere; (2) large-scale, quasi-horizontal (but inclined) motions associated with wave cyclones dominate the transport in extratropical latitudes in the troposphere and lower stratosphere; and (3) radiatively forced mean circulations predominate in the upper stratosphere. Since (1) and (2) are large in the troposphere but decrease in the stratosphere, we expect the K values for a 1-D model to be large near the surface but to decrease with height. This decrease should continue until the effect of (3) becomes dominant. Thus, the K profile would have a minimum in the lower-mid stratosphere.

The magnitude of the minimum, acting as an increased resistance to the vertical flow, either increases the mixing ratio gradient or decreases the vertical flux, or both. Assuming it acts in the combined way, it functions as a control on the time necessary for an average trace-gas molecule to penetrate into the upper stratosphere from a ground-level source. In a 1-D model it controls the characteristic time for the fluorocarbons F-11 and F-12 to enter the region where the ultraviolet radiation will release their chlorine atoms, and it controls the atoms' average residence time in the chemically active region where they can destroy ozone.

DERIVATION OF *K* PROFILES

In order to derive a *K* profile from Eq. (4.1) and a given chemical tracer, we need the following information:

(i) Global average profiles of the given species including its time history if it is not in steady state,
(ii) Global average sources and sinks of the given species.

For a given species, both of these terms will be somewhat uncertain. The degree of uncertainty in these input parameters will determine the uncertainty in the *K* profile. This uncertainty may be reduced, if we infer *K*'s from a number of different species and obtain consistent results.

In particular, if we were to restrict our attention to N_2O data, the inferred *K* would be uncertain by at least a factor of 4. However, as we shall see, the N_2O inferred *K* profile is in close agreement with *K*'s inferred from two independent tracers. Consequently, our estimated uncertainty with regard to the *K*'s is much less than it would be in considering only N_2O.

We have used two drastically different procedures in deriving *K* profiles. The first approach is that used in the NAS, 1976 report. This approach involves adjusting the *K*, subject to constraints on its smoothness, so as to minimize the difference between the observations and the concentrations calculated by solving the diffusion equation. Chemical lifetimes are taken from the Lawrence Livermore Laboratory model (see Chapter 8). The second approach, developed by Danielsen, is to fit a smooth analytic function to the data and choose *K* so that the function is an exact solution to the diffusion equation. This approach is described in detail in Appendix B. In application, it differs further from the first approach in that a *K* is first derived without reference to sources and sinks and then corrected for sources and sinks by intuitive reasoning rather than reference to any model sources and sinks.

Although these two approaches seem radically different, we infer on the basis of comparison that, at least for N_2O, they provide remarkably similar *K* profiles. Consequently, we infer that the major sources of uncertainty in deriving

K lie in the uncertainty of the global average of species profiles and the degree to which the inferred *K*'s are species-dependent.

Method II, as detailed in Appendix B has been applied not only to the N_2O data but also to synthetic tracer data generated by the GFDL 3-D model and global average ozone. The 3-D model data have a known global average, and so are not subject to the sampling error of observationally measured species. They appear to simulate at least qualitatively the observed processes responsible for downward tracer transport. However, because of the limited number of layers in the stratosphere and presence of an artificial upper boundary near the region of interest, some numerical errors in the transport simulation would be expected. The profile of observed global ozone is much better known than that of other species, so a *K* derived from it is not subject to much uncertainty from possible observational error. Rather, it can only be significantly uncertain because of inadequate knowledge of source terms and basic defects in the concept of the *K* parameterization. Appendix B shows that the *K* profiles derived from the N_2O, synthetic tracer, and ozone global profiles all agree within better than a factor of 2 in the lower stratosphere, where *K* reaches minimum values and consequently largely determines the transports between troposphere and stratosphere.

Figure 4.1 shows the available N_2O with smooth analytic fits to the tropical, midlatitude, and polar data and a global mean profile. These fits use the functions described in Appendix B. There is obviously a wide spread in the data, but it is difficult to estimate precisely the uncertainty in the global average estimate. We assume that the smooth tropical versus the average of the polar and midlatitude profiles represent the extreme limits of the global average profile. We interpret "extreme" as meaning three standard deviations from the expected value.

CFM LIFETIMES

We use the approach of the NAS, 1976 report to measure differences in *K* profiles in terms of F-11 and F-12 lifetimes. Table 4.1 compares these lifetimes for *K*'s derived using method I, the expected and extreme smooth global average profiles inferred from Figure 4.1. Also shown are lifetimes for the preferred *K* derived from method II using a combination of ozone, GCM tracer, and the global

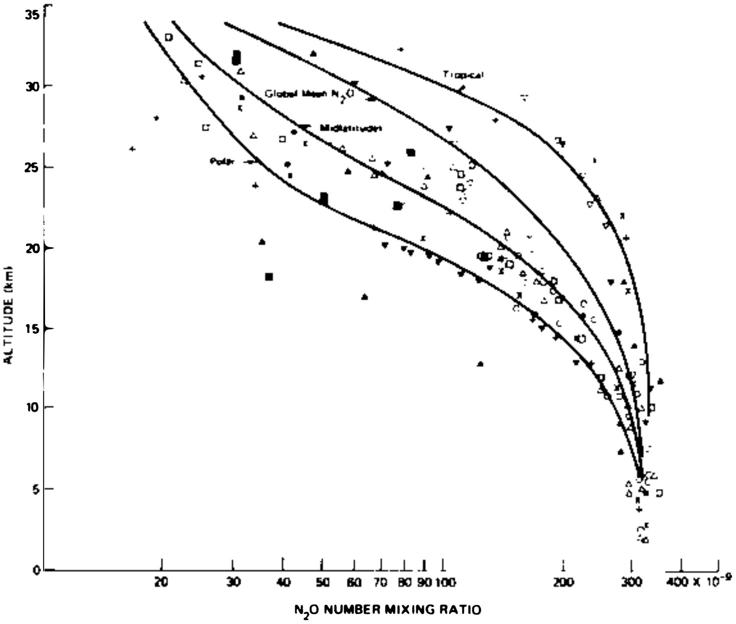

FIGURE 4.1 Averaged global profiles of N_2O mixing ratio used to derive $K(z)$. The data are taken from Chapter 7.

N_2O profile of Figure 4.1. We also show the results from method I, using an earlier, less careful, estimate of the global average N_2O profile, and results from method I, using an estimate of the global average CH_4 profile.

We infer from items 1 and 2 in Table 4.1 that the K derived by Danielsen in Appendix B is closely consistent with the K derived using the method of the NAS, 1976 report and Danielsen's analysis of the global average N_2O data as shown in Figure 4.1. Item 3, furthermore, confirms the insensitivity of the transport rates to the processing of the N_2O data to obtain a global average. The "global average" used for item 3 was much less carefully derived than that in Figure 4.1. Its most significant difference was a much steeper decrease of N_2O in the lower stratosphere than shown in Figure 4.1, which accounts for the 10 to 15 percent slower transport than obtained using the analysis of Figure 4.1.

Items 4 and 5 show that we can infer up to a range of 6 in transport by assuming an extreme range for the N_2O

TABLE 4.1 Characteristic Decay Time (Years) for an Instantaneous Source of CFM, Using Various Eddy-Mixing Coefficients Further Discussed in Text[a]

	e-fold Decay Time	
K derived from	F-11	F-12
1. Combining N_2O, O_3, synthetic tracer as described in Appendix B	70	110
2. N_2O global average of Figure 4.1; method from NAS, 1976 report	75	125
3. As in 2, except based on another independent analysis of the N_2O data	94	140
4. As in 2, but using the 3σ upper limit for N_2O	25	42
5. As in 2, but using the 3σ lower limit for N_2O	160	250
6. As in 2, except using an estimate of global average CH_4	36	56
7. As in 6, but estimating a lower limit to the global average CH_4	100	(not available)

[a] See the NAS, 1976 report for further details as to how these are calculated. The decay time corresponds to the lifetimes of the CFMs in steady state.

profile, e.g., between the tropical profile and the average midlatitude and polar profiles of Figure 4.1. Interpreting this as 3σ limits, we infer that the transport time scale derived from N_2O alone has a factor of 4 uncertainty at the 95 percent (2σ) confidence limits.

An indication that transport rates may be rather uncertain is obtained from item 6, in which the transport rate inferred from CH_4 is a factor of 2 faster than that inferred from N_2O. However, we give this result little weight because the CH_4-inferred *K* profile is sensitive to the poorly known CH_4 loss rates in the lower stratosphere (cf. NAS, 1976 report for further discussion) and the global average of CH_4 is more uncertain because of fewer data. Indeed, a plausible lower limit to the global average CH_4 profile implies a *K* that is significantly slower than that inferred from the preferred N_2O global average profile.

DISCUSSION AND CONCLUSIONS

In this chapter the diffusion approximation to the global mean vertical flux has been evaluated. It is this simplifying assumption that makes the 1-D, photochemical-diffusion models useful for numerical predictions of trace chemistry in the atmosphere. The degree to which they are useful depends on the generality of the diffusion coefficient *K*(z), and, in particular, whether it is independent of the trace gases being transported either upward or downward.

At present there is no set of data capable of determining the actual generality of the diffusion assumption. However, *K* profiles can be derived from independent sets of data and compared for similarities and differences. From such comparisons, estimates of the uncertainty in the diffusion approximation can be made.

Two widely different approaches were used in this chapter to infer *K*(z). The first approach was that used in the NAS, 1976 report but with updated estimates of the global average N_2O and CH_4 profiles and the latest lifetimes for these species as obtained from the LLL model. The second approach, developed for this study by Danielsen, involves approximating the global profiles with a few simple functions and furthermore neglecting any possible sources or sinks. Besides N_2O, this second approach was applied to the global average O_3 profile and an inert synthetic tracer generated from the GFDL 3-D model. These latter two tracers have well-known global average profiles.

The preferred *K*(z) obtained from the first approach is that inferred from the global average N_2O profile of Figure 4.1. This gives F-11 and F-12 lifetimes, respectively, of 75 and 125 years. Consideration of the variations in transport due to uncertainty in the N_2O profile and differences in the transport inferred from CH_4 suggest that the transport rates inferred from the N_2O and CH_4 data are probably uncertain at the 95 percent level by a factor of 2 in either direction.

Results obtained from the second approach apply only to heights below 30 km. The mean obtained from three independent data sets is a smoothly varying continuous *K* profile, which decreases from a maximum value at the surface to a minimum at approximately 21 km and then increases again above this level. The range in *K*(z) at any level obtained from the various data sets in the second approach was within ±33 percent of the mean at that level. In other words, the largest *K* was about 2 times the smallest *K* at the same height.

In summary, the analysis of Appendix B using the second approach suggests transport time scales to be known within a factor of 2. The preferred *K*'s derived by the two approaches were found to give remarkably similar estimates for the lifetimes of F-11 and F-12 (i.e., 70 and 110 years, respectively, for method II versus 75 and 125 years for method I). This agreement supports the contention that transport rates can be specified within a factor of 1.0 ± 0.3.

Within these uncertainty limits the analyses of this chapter indicate no apparent distinction between upward and downward transport rates. In other words, *K*(z) inferred from the downward-moving synthetic tracer and O_3 is practically indistinguishable from the upward moving N_2O.

In conclusion, we assign an uncertainty in the ozone destruction due to transport uncertainty of 1 ± 0.3. This conclusion requires that the assigned uncertainty be dominated by the uncertainty in the CFM lifetimes.

Uncertainty in the lifetimes of the CFMs will translate directly into uncertainty in the ozone destruction rates *only* if all other chemical concentrations in the stratosphere are assumed fixed. However, a change of transport in a 1-D model necessarily changes the distributions of other species as well. These further changes have been found generally to provide a negative feedback on the change in the ozone destruction, i.e., to reduce the effect of the uncertainty. In particular, it was found with the GSFC model that a variation in *K* produced either a negligible or a 30 percent as large variation in ozone change depending on whether the model held constant the fluxes or the mixing ratios of the species other than CFMs, which are long-lived in the troposphere.

It is also possible, however, if transport errors in different species were to add randomly rather than in the correlated fashion of the 1-D models, that the overall uncertainty of the ozone change could be somewhat larger than the uncertainty in the CFM lifetimes. We believe it likely, however, that the uncertainties due to transport are smaller than the uncertainty in the CFM lifetimes and that our error estimate is a conservative one.

REFERENCE

Mahlman, J. D., and W. J. Moxim. 1978. Tracer simulation using a global general circulation model: results from a mid-latitude instantaneous source experiment, *J. Atmos. Sci. 35*, 1340-1375.

5 INACTIVE SINKS AND THEIR ASSESSMENT

INTRODUCTION

It has been found useful in assessing the potential for various chemical and physical processes to destroy CFM's or otherwise remove them from the atmosphere to distinguish between active and inactive types of removal processes. The distinction concerns whether or not the process results in the ultimate destruction of ozone. Thus an inactive process, as exemplified by physical absorption on surfaces such as polar ice, removes the substance (CFM) from the atmosphere so that it can have no effect on ozone. However, an active process, such as photolysis in the stratosphere, destroys the substance, but its products undergo photochemical reactions that lead to the destruction of ozone.

Another useful concept in assessing removal of CFM's from the atmosphere is that of a lifetime or residence time that is characteristic of the particular process causing the removal. Since it will be used in this chapter, the description of the concept given earlier in the NAS, 1976 report is repeated here.

In order to assess the effect of halocarbon release on O_3 destruction, it is necessary to consider the ratio of inactive to active halocarbon removal. Let us consider the case of continuous release of a halocarbon at a constant rate. This constant release rate will, given enough time, be balanced by an equal removal rate--a condition referred to as a steady state. In this case, the maximum O_3 destruction will occur when a steady state has been achieved. At steady state, the input flux F of the halocarbon (molecules cm^{-2} sec^{-1}) must be balanced by all the removal processes for the halocarbons, i.e., $F = \Sigma\phi_i$, where ϕ_i is the removal flux for a particular process. We will assume, for simplicity, that halocarbons are mixed uniformly in latitude and longitude and consider globally averaged quantities.

The total removal flux ϕ can then be expressed as an integral with respect to altitude:

$$\Phi = \int_0^\infty Lxn\,dz \qquad (4.1)$$

where n is the total number of molecules cm^{-3} at altitude z, and x, the mixing ratio, is the fraction (by volume) of the molecules that are the halocarbon. L is the (first-order) local loss rate constant (sec^{-1}) for the halocarbon by all processes. The local removal time can then be defined as $t_c = 1/L$. (For example, a bimolecular chemical reaction between the halocarbon and species X would have $L = k_x[X]$, where k_i is the rate constant and $[X]$ is the concentration of X).* The tropospheric removal time for halocarbons is generally equal to or greater than the vertical tropospheric mixing time (which is the order of a week) except for some unsaturated halocarbons; therefore, to a good approximation, the halocarbons have a constant mixing ratio, x, in the troposphere. In some parts of the stratosphere the reverse is true. In this case, the mixing ratio decreases with altitude as the photolytic loss rate increases with altitude. The total number density of the atmosphere, n, decreases approximately exponentially with altitude.

The residence time for a halocarbon in the atmosphere can be defined as the average time its molecules reside there. If at any time the release of a particular CFM is suddenly terminated, the residence time, τ^0, is the time required for the concentration to drop to $1/e$ of its value at the time of termination.† Under steady-state conditions, the residence time, τ^0, equals the total column density divided by the input flux or by the total removal flux, i.e.,

---

*It is assumed that $[X]$ and k_i do not change with time. This assumption is equivalent to using globally averaged values of concentrations and temperatures at a given altitude z in the 1-D models (Chapter 8).

†If a particular CFM is released into the atmosphere at a constant rate (starting) at $t = 0$, the residence time, τ^0, is also the time required for the fractional difference between the steady-state amount and the amount actually present to reach $1/e$.

$$\tau_i = \frac{\text{total column density (molecules cm}^{-2})}{\text{input flux (molecules cm}^{-2}\text{ sec}^{-1})}$$

$$= \frac{\text{total column density}}{\text{removal flux}} \qquad (4.2)$$

The partial residence time for a particular removal process, τ_i, can then be defined as the time that would be required to remove the total column by that process alone:

$$\tau_i = \frac{\text{total column density}}{\phi_i} \qquad (4.3)$$

where ϕ is the removal flux for that particular process. If the total column density is N halocarbon molecules cm^{-2}, then

$$\tau_i = \frac{N}{\int_0^\infty L_i x n dz} \qquad (4.4)$$

Since most of the halocarbon will be located in the troposphere, where it has an approximately constant mixing ratio, the column density is, to a close approximation, given by c_0H_0, where c_0 is the number density of the halocarbon near the surface and H_0 is the scale height* near the surface = 8.4 m.

By definition, at steady state, the input flux, F, must be balanced by the sum of all removal fluxes ($F = \Sigma\phi_i$). It follows that the total residence time, τ^0, is related to the partial residence times for individual processes τ_i by the relation

$$1/\tau^0 = \sum_i 1/\tau_i \qquad (4.5)$$

The relative importance of any removal process is inversely proportional to its partial residence time, the fraction it removes being τ^0/τ_i. For example, an inactive removal process with a partial residence time that is 10 times τ^0 will remove 1/10 of the halocarbon, leaving 9/10 to affect the stratospheric ozone.

---

*The scale height, H, is the vertical distance over which the atmospheric pressure drops by a factor of e.

Because tropospheric removal is generally inactive, while stratospheric removal is generally active toward ozone removal, it is useful to compare loss processes in the troposphere with loss processes in the stratosphere. We may define the quantities

$$\tau_T = \frac{N}{\int_0^Z L_T x n \, dz} \tag{4.6}$$

$$\tau_S = \frac{N}{\int_Z^\infty L_S x n \, dz} \tag{4.7}$$

where L_T and L_S are the effective loss rate constants in the troposphere and stratosphere, respectively, and Z is the altitude of the tropopause. Comparison of Eqs. (4.5)-(4.7) shows that

$$\frac{1}{\tau^0} = \frac{1}{\tau_T} + \frac{1}{\tau_S} \tag{4.8}$$

In terms of removal rate constants R, this becomes

$$R^0 = R_T + R_S \tag{4.9}$$

and the ratio $R_S/R^0 = \tau^0/\tau_S$ is the fraction of a halocarbon that reaches the stratosphere. Table 4.1 of the NAS, 1976 report lists this ratio together with other quantities for some CFMs and for CH_3Cl and CCl_4, assuming that photolysis and reaction with HO are the only removal processes.

All the removal processes for CFMs that were suggested at the time were assessed in the NAS, 1976 report. There is no new information for most of these that would necessitate a re-evaluation of the associated lifetimes. For a few of the processes the advent of new information has led to new estimates of the lifetimes. In addition, since the previous report, two new processes have been proposed as a possible important tropospheric sink of CFMs, viz., photodecomposition and thermal decomposition of molecules adsorbed on desert sand. The present chapter is primarily devoted to re-estimation of lifetimes for the oceanic removal and estimation of lifetimes for the newly proposed processes. Table 5.1 lists all the processes considered here and in the previous report along with their respective estimated removal lifetimes and fractional contributions to their overall removal rates.

As in the previous report, removal of the major CFMs, F-11 and F-12, is estimated mainly to occur in the stratosphere by photolysis--the tropospheric removal processes generally having considerably longer lifetimes.

The problem of determining the composite atmospheric lifetimes of CFMs by observing trends in their atmospheric burdens is considered. This problem is similar in some respects to that of determining ozone trends discussed in Chapter 6. The problems differ in other respects because ozone has relatively large natural fluctuations.

TABLE 5.1 Removal Times and Removal Rates for F-11 and F-12

Process	Removal Time, τ (years)
Active Removal in Stratosphere	
Photolysis and $O(^1D)$ reaction	50; 90[a]
Surface Processes	
Removal by oceans	$>(600;\ 1.7 \times 10^3)$
Removal by soil and microbes	$>10^4$
Entrapment in polar ice	$>10^5$
Photodecomposition on desert soil	>500; 1800
Tropospheric Processes	
Photodissociation	$>5 \times 10^3$
Reactions with neutral molecules	$>10^4$
Direct ionization	$>10^6$
Ion-molecule reactions	$>10^3$
Heterogeneous process	$>6 \times 10^4$
Lightning	$>10^6$
Inactive Removal in Stratosphere	
Ionic processes	$>10^5$
Heterogeneous processes	$>10^8$

[a] Slightly different values of 54 and 80 years were obtained as most likely values in Table 4.2 of the NAS, 1976 report.

The most notable changes in the lifetimes listed in Table 5.1 are the increased values for removal in the oceans. The previous lower limits of the lifetimes for F-11 and F-12 of 70 and 200 years, respectively, listed in Table 4.2 of the NAS, 1976 report, were recognized as extreme limits and were not used in the evaluation of ozone reduction by CFMs. However, a lifetime of 270 years for F-11 was used for such purposes. This lifetime estimate was based on a calculation that took into account the measured concentrations of F-11 (in one experiment) in surface ocean waters. The re-evaluation of lifetimes based on more comprehensive measurements of greater than 600 years for F-11 and 2×10^4 years for F-12 greatly reduces the perceived importance of removal by the oceans so that its effects need not be specifically accounted for in calculations of ozone reductions.

SURFACE AND TROPOSPHERIC REMOVAL

In this category of inactive removal, new information has prompted a re-assessment of (a) the CFM removal processes by atmospheric reactions with OH and (b) the removal by unspecified processes in the oceans. Removal of various halocarbons, including CFMs, by reaction with OH radicals in the troposphere was discussed in Chapter 3 and needs no further amplification here.

Removal by the Oceans

In the NAS, 1976 report the removal by the oceans by an unspecified process (which might be microbiological) was considered in two different ways. Both ways used the same thin-film model of transport of gases across the air-sea interface. The first way calculated a limiting lifetime assuming that each molecule was destroyed upon penetrating the (hypothetical) thin film, thus not permitting a buildup of significant concentrations in the ocean surface waters. The lifetimes for F-11 and F-12 calculated in this manner were ~ 70 years and ≥ 200 years, respectively. These estimates would have been adopted as representing conservatively low minimum lifetimes if there had been no data showing that, in fact, the surface ocean waters contained important concentrations of the compounds. At the time of writing the previous report there were data from a study by Lovelock that indeed indicated that the surface waters of the oceans contained concentrations of F-11. However, they were lower than the concentration required for equilibrium with F-11 in the overlying air. By assuming that the lack of equilibrium was caused by an oceanic sink, an estimate of the lifetime of F-11 of ≥270 years was obtained. This estimate was used in arriving at a possible 1/5 diminution in the estimated ozone reduction due to CFMs. Recent studies by Rasmussen *et al.* (1976) and Singh *et al.* (1979) have shown that the surface ocean waters are essentially at equilibrium saturation with respect to the overlying atmospheric concentrations of F-11, indicating little or no biological or other removal by the oceans. New estimates of lower limits of the lifetimes were made using the second way of calculating based on an assumed finite gradient of CFM across the thin film. To arrive at a lower limit it was assumed that the oceans were 10 percent undersaturated with respect to the atmosphere--the amount of undersaturation corresponding to an assumed uncertainty in the measurements that determined that equilibrium saturation exists. The average concentrations of F-11 and F-12 were taken as 130 ppt and 210 ppt, respectively. The lifetimes so obtained are ≥600 years for F-11 and ≥2000 years for F-12. In view of the new values there is deemed to be no reason for including an effect due to ocean removal in calculating ozone reductions by CFMs.

CFM Destruction in the Desert

Two processes by which CFMs may be removed from the atmosphere have recently been suggested. Both processes concern molecules (of CFM) adsorbed in the surface of desert sands. The first process, and maybe the lesser in importance, is photodecomposition, and the second is thermally induced decomposition. Each process is discussed separately below. The following section examines the proposition that the presence of F-21 ($CHFCl_2$) in the atmosphere is indicative of a tropospheric sink of F-11, possibly the suggested thermal decomposition on desert sand.

Before beginning the discussion of decomposition on the surface of desert sands it should be noted that Alyea *et al.* (1978) have shown that atmospheric transport of the CFM or other trace substance such as N_2O to desert surfaces is not a rate-limiting process for tropospheric lifetimes greater than a few years.

Photodecomposition Ausloos *et al*. (1977), Rebbert and Ausloos (1978), and Gab *et al*. (1977; 1978) reported on the photodecomposition of certain compounds, including F-11, F-12, CCl_4, N_2O, and CH_3CCl_3, by visible and near-ultraviolet light when they are adsorbed on the surfaces of silicaceous materials such as desert sand, silica gel, ground quartz, and sea sand. The laboratory studies of Ausloos *et al*. (1977) were performed using closed Erlenmeyer flasks with the solid on the bottom in a thin layer (~5 mm) with an atmosphere of halocarbon plus 10 percent ethanol (no O_2 present). The decomposition product C_2H_5Cl was measured following photolysis. The experiments permitted the efficiencies of decomposition (adsorbed molecules reacted per incident photon) to be determined for F-11, F-12, and CCl_4. It is difficult to assess the lifetime of atmospheric halocarbons using such experimental results, mainly because knowledge of the details of adsorption of the halocarbons, surface reactions, and desorption of the products relevant to the real world is missing. Furthermore, attempts to calculate the lifetimes in the atmosphere involve extrapolation of the laboratory results over many orders of magnitude in concentration.

Nonetheless we have adduced lifetime estimates using a line of approach given by Kong and Sze (1978), which involves drastically simplifying assumptions about unknown processes of adsorption, reactions of the surface, and desorption of products and neglects any effects of soil composition and conditions of soil moisture and temperature on the processes. Leaving the details aside, the estimated lifetime lower limits are 540 years for F-11 and 1800 years for F-12. As will be seen in the following section, the discovery of a significant dark reaction in the presence of oxygen renders dubious the results that led to the idea that photodecomposition may be an important process in the atmosphere. At this juncture we judge this process to be quite insignificant for CFM removal from the atmosphere relative to stratospheric active sinks. However, we include the above estimated lifetime limits for the process in Table 5.1 as conservatively low values. We point out that the laboratory studies to date have not provided data on which more reliable estimates can be made.

Thermal Decomposition The same two research groups that investigated the photodecomposition of halocarbons on sand have recently reported the unexpected finding (arrived at independently) of a dark reaction of even greater magnitude than the photodecomposition (Bahadir *et al*., 1979; R. E.

Rebbert and P. Ausloos, National Bureau of Standards, private communication). This in itself casts doubt on the reality of *atmospheric* photodecomposition of adsorbed CFMs, though presumably the observations of Ausloos *et al.* (1977) with a gas phase that excluded oxygen are indicative of the existence of such a mechanism. Both experiments used isotopically labeled carbon in the halocarbons and showed that labeled CO_2 is produced. The partial pressures of halocarbon were of the order of 10^{-1} Torr and lower. R. E. Rebbert and P. Ausloos (National Bureau of Standards, private communication) report that the order of reactivity is $CH_3CCl_3 > CCl_4 > CH_3Cl > CFCl_3 > CF_2Cl_2$ and that 1,1-dichlorethylene is a decomposition product of CH_3CCl_3. Both research groups found that the reactions were slow under conditions of high relative humidity, and they were considerably faster in very dry air. The important variable was presumably soil moisture, which was regulated by the relative humidity in the experiments. In their brief report on F-12 degradation Bahadir *et al.* (1978) noted that beyond exposures time of about 72 hours no further thermal decomposition occurred; and then ensuing irradiation with UV light ($\lambda > 290$ nm) for a period of six days produced no observable degradation. Also they reported that with 200 g of sand present in their 6-liter reactor the ultimate portion of F-12 destroyed was 8.7%, but with 800 g of sand present the F-12 was 71 percent decomposed.

It may be concluded by some that these experimental results show that there could be a tropospheric sink of CFMs in desert sands. However, lack of knowledge to permit relating the experiments to actual atmospheric processes is even more acute than in the case of photodecomposition. Perhaps the most important observation is that of the apparent saturation effect mentioned above, wherein the F-12 destruction ceases after a period of time. This could indicate that the sand surfaces became saturated with adsorbed degradation products (CO_2 and HCl), which are only slowly desorbed if at all. Thus the sites for adsorption of CFM became blocked, thereby preventing further CFM degradation. Clearly, before any assessment of this process as a CFM tropospheric sink can be made, a considerable amount of carefully designed quantitative research must be done.

As a consequence of the above considerations we assign no lifetime to this process. Our assessment of CFM effects does not, therefore, account explicitly for any possible thermal decomposition sink because we consider it unlikely to be of consequence.

F-21 as a Product of F-11 Destruction

Fluorocarbon-21 ($CHCl_2F$ or F-21) has been detected in the atmosphere by several workers using gas chromatography, and at least one set of preliminary results have been reported by Singh *et al.* (1979). They found quite variable concentrations at several sites in California ranging from a few tenths of a part per trillion to about 20 ppt, with an average of 5 ppt for the nonurban marine site at Point Arena. R. A. Rasmussen and S. Penkett (Oregon Graduate Center, private communication, 1979) have used interfaced gas chromatography-mass spectrometry techniques to measure F-21 in numerous samples collected in pressurized cans taken from various places (at ground sites and aloft using aircraft) around the world. They find the concentrations to be quite variable, although not exceeding 3 ppt, and they estimate the global average concentration to be less than 1 ppt. They also report finding concentrations as high as 20 ppt in urban-industrial areas.

F. S. Rowland (University of California, Irvine, personal communication, 1979) has pointed out that F-21 may occur as an artifact in gas-chromatographic systems that employ Teflon fittings and tubing. Indeed Singh *et al.* (1979) note the possibility of F-21 as an artifact as a qualification of their reported concentrations. R. A. Rasmussen and S. Penkett (Oregon Graduate Center, private communication, 1979) believe that their measured concentrations are demonstrably real and not artifacts.

Assuming for the moment that the measured F-21 concentrations are not due to artifact contamination, we may examine the question as to whether or not it may be indicative of a significant tropospheric sink of F-11. A simple box-model approach representing F-11 as the sole source of F-21 and representing the F-21 sink as reactions with OH radicals in the troposphere (lifetime of a few years) leads to a likely lower limit of F-11 lifetime for conversion to F-21 of 300 years. A lifetime as low as 30 years can be obtained by assuming extreme global average values of OH and F-21 concentrations. These results are similar to those obtained using a 1-D numerical model with complex photochemistry (J. P. Jesson, E. I. du Pont de Nemours and Company, personal communication, 1979). On the basis of this caluclation and the attendant assumptions, it appears likely that conversion of F-11 to F-21 represents at best a minor sink of F-11. However, the possibility of it being more important cannot be ruled out.

The foregoing analysis assumed that F-21 is a product of F-11 degradation. This supposition appears to have arisen because of the findings that F-11 is degraded by thermal and photochemical processes when adsorbed on sand and that F-21 exists in the atmosphere. The following items are worthy of attention for the further assessment of this issue: F-21 has not been reported as a degradation product of F-11 by any of the investigators. (This does not mean that it was not present, however.) The major carbon-bearing product of F-11 degradation with O_2 present detected in the laboratory work (discussed above) was CO_2.

It has been pointed out by F. S. Rowland (University of California, Irvine, private communication, 1979) that under conditions of oxidative degradation and low relative humidities (such as those studied in the laboratory) the substitution of a hydrogen atom for a chlorine atom, which is required to convert F-11 to F-21, is a very unlikely chemical process. In fact, as indicated above, the principal degradation product appears to be CO_2.

When we consider the above discussion along with the report of R. A. Rasmussen and S. Penkett (Oregon Graduate Center, private communication, 1979) that the largest F-21 concentrations found were in urban-industrial areas, we find that there is little reason to credit the notion that F-21 in the atmosphere arises from F-11 destruction on desert surfaces.

LIFETIMES, MASS BALANCES, AND TRENDS IN CFM BURDENS

The NAS, 1976 report noted that lifetime estimates for CFMs could be made from comparisons of atmospheric burdens expected on the basis of amounts released to those based on measured concentrations. Using the concept of lifetime, the budget of a trace substance is expressible as a balance between sources and removals in which the net removal rate is the rate of change of burden characterized by a lifetime τ. Thus, if the appropriate information of release rates and atmospheric burdens (estimated from atmospheric concentrations) are available, the lifetime of a substance can, in principal, be obtained. Atmospheric burdens are determined from concentrations measured at various places and times and assumptions concerning their representativeness. Thus uncertainties is estimated lifetimes of CFMs are strongly related to uncertainties in

- Release rates of CFMs.
- Chemical analyses of CFMs in the atmosphere.

- Calculations of global average concentrations from a limited number of observations in space and time.

A study of the general problem of determining lifetimes using the budget modeling concepts outlined above has been presented by Cunnold *et al*. (1978). They recognize two different methods for using the same data. In the first method, the determined value of the lifetime is that which gives the best agreement between a series of predicted burdens and the series of observed burdens (based on measured concentrations). The second method derives a lifetime that produces the least differences between a series of predicted and observed relative rates of change of burden. In each method, a type of least-squares criterion is applied to arrive at objective values of the lifetimes. Since the second method relies on relative changes in burdens, it presumably would have an advantage over the first method in not requiring instruments at different stations to be continually intercalibrated. Cunnold *et al*. (1978) used a single-station time series of F-11 for Adrigole (Pack *et al*., 1977) to show that with 95 percent confidence the lifetime of F-11 is greater than 9 years when a conservatively estimated, overall systematic error of 30 percent (2σ) was used. The error figure represents roughly equal contributions from errors in release rate estimates, instrumental measurements, and representativeness of a single station.

The uncertainty limits on lifetimes due to representiveness can be reduced, in principle, by increasing the number of stations at which concentration measurements are made and by conducting the measurements over a long enough period of time. Cunnold *et al*. (1978) have shown, e.g., that with a network of four stations at remote sites around the world after 2 to 5 years of operation the 2σ (95 percent confidence) limits given in Table 5.2 might be expected for various actual lifetimes.

Thus, if Cunnold *et al*. (1978) are correct, after five years of operation the data from a four-station network should permit the recognition of atmospheric lifetimes of 30 years or less. Depending on the actual lifetime, operation periods longer than 5 years may be required to establish that the compound has longer lifetimes than 30 years. However, if the actual lifetime is substantially longer than 30 years (e.g., 50 years) a 5-year period or slightly longer should suffice to show that the lifetime is longer than 30 years.

TABLE 5.2 Four-Station Network,[a] 95 Percent Confidence Limits of Lifetimes

Years of Operation	Actual Lifetimes (Years) 10	15	20	50
2	5-30	>7	>8	>12
3	7-18	9-32	12-48	>21
4	8-14	11-22	14-33	>27
5	8.5-12	12-20	15-29	>33

[a] From Cunnold *et al*. (1978).

The Chemical Manufacturers Association (CMA) has undertaken a program for measuring CFMs continuously at four remote sites around the world in the hope that a trend (as described above) may be detected after a few years of operation. It is difficult now to predict what the systematic errors in representativeness of four stations will be. However, a few years of operation should make it possible to judge the effectiveness of the network in trend detection. We believe that the CMA experiment has the potential to provide useful data for lifetime estimation of CFMs.

RECOMMENDATIONS

1. Laboratory studies of the decomposition of CFMs on desert sand should be designed to provide data from which atmospheric lifetimes could be directly calculated. The fundamental physical-chemical understanding will derive from measurements of adsorption isotherms, decomposition rates, and product desorption rates, all under varying conditions of known relative humidity, CO_2 content of the gas phase, and temperature. Another type of experiment that readily permits calculations of lifetimes involves the use of chambers in which the rates of trace gas transfer to and from the soil can be measured and then scaled to the atmosphere. Also the products of decomposition should be definitively determined and checked by mass balance.

2. Surveys of various possible industrial sources of F-21 should be made. Further, the analytical methodology for F-21 should be carefully developed and standardized,

and data along with quality control information should be published in the open literature.

REFERENCES

Alyea, F. N., D. M. Cunnold, and R. G. Prinn. 1978. *Atmos. Environ. 12*, 1009.

Ausloos, P., R. E. Rebbert, and L. Glasgow. 1977. *J. Research Nat. Bur. Std. U.S. 82*, 1.

Bahadir, M., S. Gab, J. Schmitzer, and F. Korte. 1978. *Chemosphere 12*, 941.

Cunnold, D., F. Alyea, and R. Prinn. 1978. *J. Geophys. Res. 83*, 5493.

Gab, S., J. Schmitzer, H. W. Thamm, H. Parlar, and F. Korte. 1977. *Nature 270*, 331.

Gab, S., J. Schmitzer, H. W. Thamme, and F. Korte. 1978. *Angew. Chem. 90*, 398; Int. Ed. (Engl). *17*, 366.

Kong, T. Y., and N. D. Sze. 1978. Heterogeneous photodecomposition of halogenated compounds in the troposphere. Paper presented at Am. Geophys. Union April meeting, Washington, D.C.

Pack, D. M., J. E. Lovelock, G. Cotton, and C. Corthoys. 1977. *Atmos. Environ. 11*, 329.

Rasmussen, R. A., D. J. Pierotti, J. Krasnek, and B. Halter. 1976. Trip report on the cruise of the *Alpha Helix* research vessel from San Diego to San Martin, Peru, March 5-20, 1976. NSF report 75-04688.

Rebbert, R. E., and P. Ausloos. 1978. *Geophys. Res. Lett. 5*, 761.

Singh, H. B., L. J. Salas, H. Shigeishi, and E. Scribner. 1979. *Science 203*, 899.

6 GLOBAL OZONE OBSERVATIONS

It has been suggested that ozone measurements could be used directly as an "early-warning system" of any decrease due to human activity, thus, perhaps obviating the need for model predictions. The feasibility of this suggestion requires an assessment of all sources of errors in the available ozone data and an evaluation of the extent to which such errors are likely to be reduced in the near future.

In the next section, the measurement of ozone, its distribution and fluctuations in space and time, will be discussed. This is followed by a statistical analysis for detecting a trend from the data of the measurement network. The use of this network to represent global ozone amounts is subject to sources of error that cannot be entirely assessed from the data. These assessments are then made. The final section indicates the consequences of the results obtained for the early-warning problem.

The discussion of ozone measurements will show that they are difficult to make and subject to many uncertainties, including possibly long-term instrumental drift trends. Further, it is known that the column ozone amount varies greatly with longitude and latitude and with the season. The fluctuations due to these causes are of the order of 100 times the predicted annual rates of change. The reliable data extend only over some 20 years and come from about 70 Dobson stations* largely placed on continents in the northern hemisphere. No matter how this information is combined to estimate a global ozone trend, there is no way to obtain a standard error that reflects the uncertainties

---

*Stations employing the Dobson spectrophotometer to measure total ozone concentration at a given location.

due to station choice and position or to long-period variations due to instrumental or natural causes. However, for the task at hand, an assessment of the errors due to these causes must be provided. If we were to find a trend that was large in comparison with all the errors we know of, it could either be man-made or due to some unsuspected natural cause. There are many examples of empirical correlations of meteorological variables with sunspot activity that suddenly disappear for no apparent reason and of trends suddenly changing, see, e.g., Pittock (1978). If the observed trend of ozone changes follows predicted trends, the evidence in favor of its human origin would be very strong although not conclusive.

OZONE MEASUREMENTS

The average total amount of ozone in a 1-cm^2 column of the atmosphere is 8×10^{18} molecules (or 3 mm at standard temperature and pressure). The latitudinal variation is about ±20 percent of the yearly global average, as is the seasonal variation at subpolar latitudes. During a winter or a spring month, variations could amount to ±50 percent of the average value, and year-to-year variations, as observed at individual stations, could be as high as ±10 percent. For comparison, the model-predicted ozone changes that we would like to detect correspond to 0.1 to 0.2 percent per year (cf. Chapter 9).

At present, two ground-based methods are in use for measurement of total ozone in a vertical column. The first (Dobson spectrophotometer) is based on observation of the spectral radiance of the solar beam after is has been dispersed through a quartz prism. The second (designated M-83) involves observations of the solar radiance in a number of ultraviolet and visible ozone absorption bands after the radiation has been isolated through use of a set of interference filters. In both cases, the total ozone is determined as a result of measuring the ratio of the received radiance in two or more ozone absorbing bands after the solar beam has undergone atmospheric absorption.

The Dobson spectrophotometer is the standard instrument adopted by the World Meteorological Organization, and of the 70 stations using the Dobson about 55 are in the northern hemisphere. An instrument using a filter is the M-83, developed and used since 1957, principally in the Soviet Union and Eastern Europe. About 35 M-83's are now reporting observations.

Total ozone as determined by the methods described above is inversely proportional to the difference between absorption coefficients in the wavelength pairs (or double pairs) used in the measuring technique. Total ozone observations made before 1957 with the Dobson spectrophotometer were based on a single wavelength pair. Those made after July 1957 were based, generally, on a double wavelength pair (the so-called A/D wavelengths). Corrections to the assumed ozone absorption cross sections used for the Dobson spectrophotometer require significant adjustment to the reported total ozone values. These adjustments have been made for reported observed values prior to 1957. However, with the single exception of the Arosa station, no station data set has been made homogeneous for Dobson observations before and after July 1957. It should be noted that even in the case of Arosa the single pair (C) and the double pair (A/D) observations are still not compatible, although the discrepancy has been reduced since a new set of absorption coefficients for the C pair was recommended for international use in 1968. (See discussion by Birrer, 1974.) The result of these various adjustments could have introduced a set of nonrandom changes of reported ozone values where the observations were taken in the C pair. Because there probably is a nonrandom component of meteorologically introduced noise to the total ozone variations, these changes would be difficult to detect. For the foregoing reasons, long-period total ozone changes should not be based on station data obtained prior to July 1957.

Present efforts directed toward an international program of Dobson instrument intercomparison and the careful development of a set of standardized instructions for operation of the Dobson spectrophotometer can increase the achievable accuracy of the observations to ±3 percent, with a long-term precision of ±1.5 percent for the network global average.

Total ozone can be observed from satellites by use of either of two techniques, one involving observations of backscattered solar ultraviolet radiation (BUV), the other involving observations of upward emitted infrared (9.6-μm) radiation. Satellite infrared observations were made available for 10 months (April 1970 to January 1971) and from March 1977 onward. BUV observations have been available from April 1970 to late 1977 and since October 1978 on different satellite systems.

The accuracy of satellite measurements involves both instrumental errors and errors due to assumptions in the method of deriving total ozone information from the observations. Better precision can be attained if the instrument error is nonrandom, as may be the case, in part, for the BUV observations. This is not true, however, for the derived data, since they are based on assumptions involving the cloudiness distribution and the initial assumed vertical ozone distribution. In addition, satellite infrared observations are quite sensitive to the independently determined mean temperature of the lower and middle stratosphere.

The absolute accuracy of satellite observations of total ozone is not known. The mean (rms) difference between near simultaneous BUV and ground-based (both Dobson and M-83) observations is about ±5 percent. We will discuss these comparisons below.

VERTICAL OZONE DISTRIBUTION

The model results of Chapter 9 show that the effect of CFM release on the ozone concentration at 40 km is about twice as great as it is on the ozone column amount. Thus, measurement at this altitude region might provide a more sensitive indicator of ozone perturbations. Moreover, the ozone concentration in this altitude region is expected to be less variable than at lower altitudes.

Several methods have been used to measure vertical ozone distribution. The "Umkehr" method makes use of zenith sky observations with a Dobson spectrophotometer as the solar elevation decreases (i.e., early morning or late afternoon). A mathematical inversion technique is used to derive the mean ozone amount in nine layers (each approximately 4.5 km thick) from the surface to about 40 km. In the middle and upper stratosphere the accuracy is of the order of ±10 percent. In addition to the various errors inherent in all Dobson-type observations (haze, polarization effects, internal light scattering, etc.), Umkehr observations, as currently made, suffer from severe meteorological biases. As noted, Umkehr data are derived principally from low-sun observation when the signal-to-noise ratio is normally not very large. As a result, such observations are not normally taken during times of rain or thick cloudiness. Tropical stations with pronounced monsoonal effects, or higher-latitude stations with strong seasonal cloudiness variations, could show year-to-year or even longer-term ozone variations at different levels that result from climatic variations that are not well documented. Also, high-latitude stations cannot take Umkehr observations during the winter months.

At present there are about 15 stations taking "routine" Umkehr observations, about half of which have records for over 20 years. The observational frequency, however, is highly irregular. Most stations take observations only about 3 to 4 times per month (Arosa is an exception with an average of about 15 to 20 observations per month). For most stations considerable portions of the data record are completely missing. Only Arosa and Tateno have mean monthly values for at least 90 percent of the 20-year record. Low-latitude stations have very few observations during summer months, and, as indicated above, many high-latitude stations have a minimum number of observations during the winter months. The error introduced by this seasonal bias in the calculated average stratospheric ozone concentration has not been evaluated.

There is a network of *in situ* measurements of vertical ozone distribution using an electrochemical technique. Measurements are currently made at about 20 stations, all but one in the northern hemisphere, with a frequency of about 2 to 4 observations per month (3 European stations make several per week). The highest altitude of these measurements usually does not exceed 30 km, although W. Khomyr (NOAA, Boulder, Colorado, private communication) has recently flown an improved version to 40 km with good results.

Comparison between the two methods shows that the Umkehr method consistently underestimates the ozone concentration at and below the level of the ozone maximum and overestimates it above this altitude (London and Angell, 1979). The electrochemical measurements are believed to be more reliable up to 25 km, and the Umkehr values more reliable above that level.

In situ measurements are also made to altitudes of about 50 km by rocket ozonesondes using optical methods. Regular monthly flights, initiated in 1976 at Wallops Island, Virginia; Churchill, Manitoba; and Antigua, West Indies, have been curtailed recently. However, even observations once per month in polar latitudes are not sufficient to give representative mean monthly values, particularly during the winter season when the natural variations are large. The precision of the measurements is probably about ±10 to 20 percent.

SATELLITE OBSERVATIONS

Vertical ozone distributions in the stratosphere have been determined from satellite measurements on a piecewise routine basis since August 1967. Quasi-global observations, based on a technique analogous to that used in the Umkehr method, were made for a period of about 1½ years from OGO-4 (August 1967-January 1969) and for 7½ years from Nimbus-4 (from April 1970 to July 1977). The Nimbus-4 observing system was reactivated in the fall of 1978 to provide data from comparison with the observations from Nimbus-7 (launched October 1978). The BUV-type observations can provide mean ozone concentrations in about four layers in the interval 30 to 55 km over the sunlit part of the globe (i.e., where the solar zenith angle is ≤75°). Other satellite systems have been in operation for periods of less than one year or are planned for the future. These systems (limb observations using UV or IR methods or solar occultation) have the capability of higher vertical resolution than BUV techniques, but the data are not yet generally available, either for validation of the BUV observations or for direct use in determining long-term ozone variations. At present, only the data derived from Nimbus-4 observations are suitable for time series analyses.

It is difficult to put more than rough estimates on the accuracy of the BUV system. Comparison with near-simultaneous rocketsonde observations and with Umkehr observations indicate differences between satellite and other stratospheric observing techniques of the order of ±20 percent. Part of this difference, of course, is due to the errors involved in the nonsatellite systems.

A recent comparison of the contemporary monthly ozone data derived from Umkehr and satellite observations for the 11-month period May 1970-March 1971 (Mateer *et al.*, 1978) showed that there seems to be better agreement between the two measuring systems for levels between about 35 to 45 km than below, particularly at tropical and mid-latitudes, where the meteorological biases to the Umkehr observations are presumably reduced. It is not possible to place any error estimates on the compared data because of the small sample used. However, if the available raw satellite data were processed, further comparison could be used to establish estimates of the usefulness of the long series of Umkehr data to detect stratospheric ozone trends. In addition, the effects of aerosols and the meteorological (cloud) bias in the observations need to be known better than at present if these estimates are to be realistic. Proposed programs for satellite stratospheric ozone observations should be made overlapping among the different observing techniques, and the data base for each satellite system should be validated not only with rocketsonde and Umkehr ozonesonde observations but also intercompared among themselves.

OZONE VARIATIONS

The distribution of total ozone as related to photochemical and atmospheric dynamical processes and its day-to-day variance as functions of latitude and season are well documented and reasonably well understood. The observed average vertical distribution and its seasonal and latitudinal variation are also fairly well understood. In addition, progress has been made in documenting and explaining particular patterns of ozone variations associated with special meteorological events. An important case in point is that of the strong increase in total ozone and ozone concentrations in the lower stratosphere at the time and in the region of so-called "sudden warmings." However, strong evidence is lacking for other natural or man-induced perturbations to the ozone distribution. For instance, it is not known whether volcanic activity or nuclear explosions have caused ozone variations. There is some evidence for a quasi-biennial oscillation (QBO) in total ozone and in the ozone concentration in the middle stratosphere, but the hemispheric and latitudinal pattern is unclear, and there is no theory for the existence of a QBO in ozone at mid and high latitudes. There is no consistent evidence for a solar-induced perturbation to the total ozone variation, and the evidence for such a relation, involving stratospheric ozone, is rather weak. It should be noted that even in the most compelling case recorded to date--the apparent pronounced decrease of upper-stratospheric ozone in the polar zone following the strong proton event of August 4, 1972--the results of independent ozonesonde measurements up to a height of about 30 km are not consistent with this decrease. It has been suggested that the satellite observations may have been contaminated by a process analogous to that found when the satellite passes through a trapped-particle radiation belt such as the South Atlantic anomaly (Mateer *et al.*, 1978). There are observed station and hemispheric year-to-year ozone variations. Recent studies have shown that these hemispheric variations are quite likely related to observed year-to-year changes in the large-scale patterns of the general circulation of the atmosphere--particularly the strength of the tropical Hadley cell (Newell and Wu, 1978). However, we do not know what atmospheric parameters are related to the longer-period ozone changes, much less what causes them. Long-period ozone changes (trends) can be taken as variations over periods of about five years or more. The problems involved in understanding natural long-period ozone changes are, in principle, the same as those involved in understanding long-period changes of other atmospheric variables.

As discussed above, the sparseness of observing stations in the ozone network, the lack of sufficient precision in the measurements, and the inconsistency in the year-to-year changes among the few stations taking observations preclude any likelihood of detecting long-period ozone changes prior to 1957. The number of observing stations throughout the world significantly increased after that time, the measurement technique was greatly improved, and considerable effort went into global analysis of the network data. The number of stations reporting total ozone measurements (all methods) is given for each year 1958-1975 in Figure 6.1. However, during the entire 18-year period, about two thirds of the reporting stations in the northern hemisphere were located between 30 to 60° N.

Data from the global ozone network can be used to indicate large-scale geographic patterns of the ozone distribution, approximate zonal averages (where the data are sufficient), and hemispheric or global long-period variations. Hemispheric values, of course, must involve area weighted averages. Also, because there is a very large seasonal variation in ozone, that variation needs to be filtered for long-period changes unless the seasonal variations are desired.

Ground-based total ozone observations are not homogeneous in space or time. As a result, three different but related methods are used to derive zonal or hemispheric ozone values. One method is to draw mean monthly hemispheric ozone maps from all the observed station data and to use interpolated, geographic, grid-point values as the data base for the computed zonal and hemispheric averages. This process involves a certain amount of subjective extrapolation (London *et al.*, 1976). A second method is to average all mean monthly station data in a latitude belt (zonal average) and then to extrapolate the zonal data to those latitudes where occasionally no data are available, i.e., equatorial or high-polar-latitude regions, in order to derive the hemispheric values. This method is objective but may, in some cases, be unrepresentative, as in the case of the southern hemisphere, where the presence or absence of one or two stations, for particular

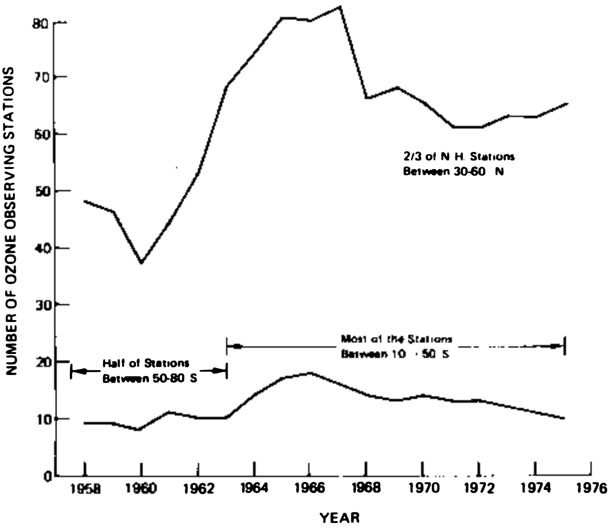

FIGURE 6.1 Number of total ozone observing stations in the northern (upper) and southern (lower) hemisphere during the period 1958-1975. About two thirds of all observing stations in the northern hemisphere during this period were at latitudes between 30 to 60° N. At these latitudes, about two thirds of the instruments used were Dobson type, one third were filter (M-83) type. In the southern hemisphere practically all stations used Dobson instruments.

years, can make a very large difference in the zonal average. A third method involves arranging the various stations into geographically contiguous groups and computing mean monthly values for each group. Broad latitudinal values are then derived by assigning, in a semiobjective way, a quality assessment to each group. Hemispheric data are then determined from suitable area weighting of the mean data groups (Angell and Korshover, 1976). Comparison of the results derived from these methods shows that they differ only in detail. We will therefore give only results obtained from the second method, that is, direct zonal averaging of the station data.

It was first suggested by Komhyr *et al*. (1971) from Dobson observations at a number of stations that there was an increase in total ozone during the 1960's. Many subsequent studies have since substantiated and extended the earlier results of Komhyr *et al*.

The annual variation of total ozone for the northern and southern hemisphere for the period 1958-1975 (extrapolated to 1976 on the basis of preliminary data) is shown in Figure 6.2. In addition to the year-to-year variations, the means values for each hemisphere are shown for the entire period, and, for the northern hemisphere, a smoothed average curve is drawn. It is obvious that during the 1960's there was a distinct increase in total ozone and that increase did not continue through the first half of the 1970's. Also indicated, but with some uncertainty because of the small number of observing stations, is that no such dramatic change took place in the southern hemisphere. There was a substantial decrease in the mean latitude of observing stations in the southern hemisphere after 1964, which was the principal reason for the indicated decrease after that time. If the two curves are reasonably representative of the hemispheric conditions, it is difficult to reconcile the differences in the long-period changes for each hemisphere with a direct solar-cycle influence on the ozone variation.

During the 18-year period, the ozone amounts seemed to have increased slightly more than 6 percent in the northern hemisphere and decreased slightly less than 2 percent in the southern hemisphere, if at all. For the northern hemisphere, the average change took place in 1961-1971.

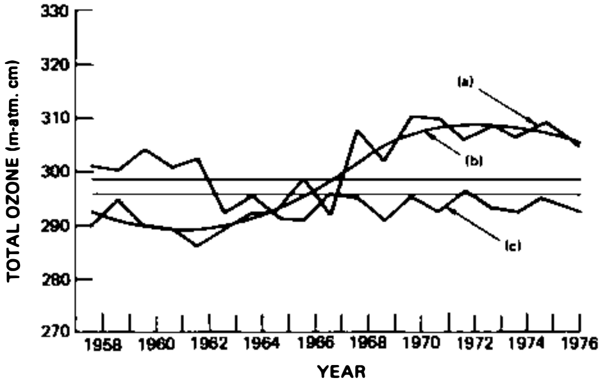

FIGURE 6.2 (a) Annual variation of total ozone, northern hemisphere; (b) smoothed curve of total ozone, northern hemisphere; (c) annual variation total ozone, southern hemisphere. Values given in Dobson units (m-atm cm). The straight horizontal lines represent the long-term (18-year) hemispheric averages.

Detailed analysis shows that this increase occurred at all latitudes but was of unequal strength in different geographic regions (London and Oltmans, 1978/79). The reason for the apparent increase of ozone in the northern hemisphere has, to our knowledge, not been explained. We suspect, from analysis of the adjusted data set for Arosa for the period 1932-1975 that this relatively short period (10-year) increase may be a transient phenomenon or one associated with long-period ozone variations.

One of the problems involved in the use of station observations in analysis of zonal or hemispheric average variations is that of the geographic representativeness of the data. It is well known that there is a meteorological association with total ozone and, indeed, an even stronger association with ozone in the lower stratosphere. The relationship is such that, on the average, total ozone is higher in the region of pressure troughs. This association is reasonably well understood and results from ozone transport processes involving the patterns of vertical and horizontal motions around pressure troughs and ridges and the characteristic vertical and latitudinal gradients of the ozone mixing ratio. Thus year-to-year or longer-period average zonal variations may simply be the reflection of a sampling bias resulting from changes of the position of large-scale planetary waves. A study of this possibility has recently been conducted by Miller *et al.* (1979), who concluded that the ozone trends determined from ground-based data are real and are not artifacts of the limited sampling of the ground-based observations. These studies were confined to midlatitudes of the northern hemisphere and may not be applicable to estimated averaged variations in the southern hemisphere.

As pointed out earlier, there is, in addition to the sampling bias, a meteorological bias, since it is often difficult to take ground-based total ozone observations in the presence of thick clouds or rain. In addition, when observations are taken during adverse meteorological conditions, the error limits of the observation are approximately doubled. It is, therefore, necessary to test both the sampling and meteorological biases by an independent observing system, if available. At present, there are two sets of satellite total ozone data, only one of which has sufficient available information to be useful for such a comparison. These two data sets are derived from the IRIS and BUV observations on Nimbus-4. They cover the period April 1970-January 1971 (IRIS) and April 1970-April 1972 (BUV). We show in Figures 6.3 and 6.4 the mean monthly

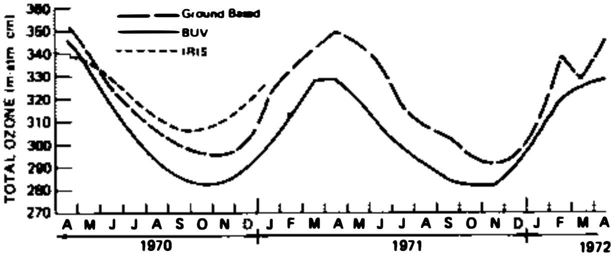

FIGURE 6.3 Monthly variation of total ozone (northern hemisphere) derived from three different methods as indicated. Values are in Dobson units (m-atm cm).

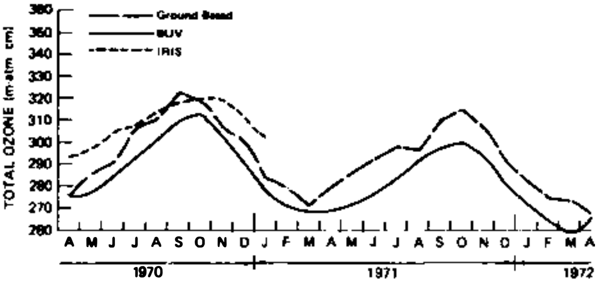

FIGURE 6.4 Same as Figure 6.3--southern hemisphere.

variation of IRIS, BUV, and ground-based total ozone as discussed above for each hemisphere. The dominant feature of each curve is the seasonal variation. For both hemispheres the IRIS and BUV curves (from data obtained from the same satellite) show higher and lower ozone values, respectively, than the ground-based derived ozone data. We are not concerned here with the absolute values, but rather with the relative variations as derived from each system. For this reason we compare the differences in mean annual ozone amount (April 1970 to March 1971; April 1971 to March 1972) for the BUV and the ground-based observations. In Dobson units (10^{-5} m at S.T.P.) the values are

	1970-1971	1971-1972	Difference
Northern hemisphere			
BUV	296.8	294.3	-2.5
Ground based	309.5	308.2	-1.3
Southern hemisphere			
BUV	288.7	280.2	-8.5
Ground based	295.8	291.8	-4.0

In both cases the changes have the same sign and are of approximately the same value. It is noteworthy that the discrepancy in the amount of change as indicated by the two observing systems is larger for the southern hemisphere, as could be expected because of the few observing sites in that hemisphere.

It is of interest to extend this comparison to a midlatitude region in the northern hemisphere, where there is a large number of ground-based stations but where ozone and meteorological variations are also quite large. In addition, BUV observations in midlatitudes do not suffer from the limitations of low sun or absence of observed sunlight. This comparison is shown in Figure 6.5. Again, the seasonal variation is quite pronounced, and the BUV values are lower than those derived from IRIS or, in general, ground-based observations. The annual difference for the two years for which data are available is, for 40-50° N:

	1970-1971	1971-1972	Difference
BUV	340.4	331.6	-8.8
Ground based	348.9	342.8	-6.1

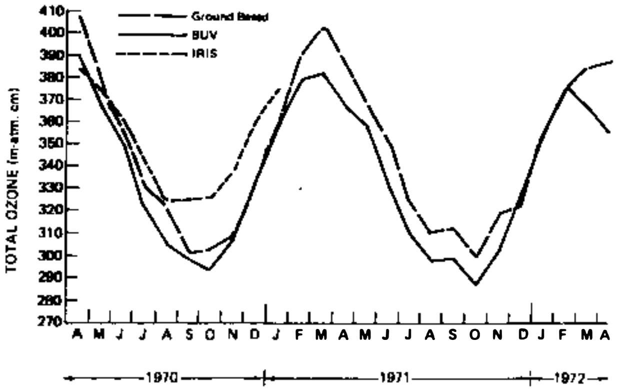

FIGURE 6.5 Same as Figure 6.3--40 to 50° N.

The results for 40 to 50° N are consistent with those derived from the hemispheric data. There is an ozone decrease shown in each case, and the amounts of the decreases are about the same. It is difficult to provide a statistical evaluation of these results, but we conclude that, at least for the northern hemisphere, the projected improved ground-based network, when combined with a monitoring system of satellite observations, could provide useful data in evaluating long-period ozone changes.

There are four current satellite systems from which total ozone is derived, as shown in the summary of satellite observations (Table 6.1). These are TOMS and SBUV ultraviolet observing techniques and DMSP and TIROS-N infrared techniques. The data from these satellites and the remaining data from Nimbus-4 need to be processed expeditiously to aid in extension of the comparison with ground-based observations and evaluation of the precision obtainable from these observations for long-term changes.

STATISTICAL METHODS FOR TREND ANALYSIS

Greatly improved methods for analyzing single-station data were introduced by Hill and Sheldon (1975), whose work was motivated by the CFM problem. Their initial paper applied to the full (monthly values from 1932 to 1974) Arosa series methods of Box and Jenkins (1970).

To remove the seasonal effects, deviations from monthly means were used. These deviations showed 25- and 133-month periodicities. To make such assertions, one needs valid standard errors. The technique used here is to search among statistical models in a class [denoted technically by an autoregressive moving average process (ARMA) and specified in Appendix C] to find one that fits the data better than others in this class. These models are a generalization of a least-squares fit of each deviation to a linear combination of its previous values at certain time lags. In this case, standard errors for the fitted coefficients may be computed in much the same way as they are in the linear least-squares method of elementary statistics, assuming that the general model is correct. They concluded that the ozone decline at Arosa in the early 1970's was a consequence of the 133-month cycle and would be reversed in the late 1970's. In fact, data from 1975, 1976, and 1977 show some signs of increasing.

Thus, their model, which contains only cyclical terms, seems capable of predicting several years ahead. Rather

TABLE 6.1 Summary of Satellite Observations of Ozone[a]

Satellite Name	O_3 Detection Method	Status of Available Data
OGO-4	BUV	August 1967-January 1969. Vertical distribution: 5 months of data available, the remaining data being processed
Nimbus-3	IR	April-July 1969. Total ozone: processed data are available
Nimbus-4	IR	April 1970-January 1971. Total ozone: processed data are available
	BUV	April 1970-July 1977; reactivated November 1978 with very limited observations. Total ozone: April 1970-April 1972 data processed and available; the remaining data being processed. Vertical distribution: limited data available, remaining data being processed
Atmospheric Explorer-5	BUV	November 1975-May 1977. Total and vertical distribution (tropical latitudes only): data still being processed
Nimbus-6	Limb IR	June 1975-January 1976. Vertical distribution: data have been processed but not yet generally available
DMSP (MFR)	IR	Since March 1977. Total ozone: ozone: data being process
DMSP (MFR)	IR	Since March 1977. Total ozone: data being processed
Tiros-N	IR	Since October 1978. Total ozone and vertical distribution: data being processed
Nimbus-7	SBUV/TOMS	Since October 1978. Total ozone and vertical distribution: data being processed

[a] Additional satellites with ozone observing capabilities are planned for the period 1984-1985.

than try to estimate a trend, it assumes that none is present and tries to show that this assumption is supported by the data. This methodological improvement prompted two later studies, using data from several stations. In these studies, the data are asked to disprove the same null hypothesis--no trend. Before describing them, another method of studying these series should be mentioned.

One may imagine a monthly data series as the summation of waves of various frequencies. Long-term trends, whatever their origin (natural, man-made, or instrumental) are then low frequency, daily weather changes are very high frequency, while the seasonal and biennial effects are intermediate. Then the numerical processes described in the last paragraph may be thought of as filtering out various frequencies. The variability in the data may be associated with different frequencies. The distribution of variance by frequency is called the spectrum of the data. A flat spectrum indicates "white noise," that is, no dependencies, as is required for the use of a least-squares analysis. When the spectrum was computed for the raw Arosa data, it was dominated by a large peak at one year. However, the series of residuals from the monthly means gave a much flatter spectrum than did the series of 12-month differences. Thus, though either of these two methods may be used to eliminate the seasonal variation, it seems that the former works better on this type of data. It also produced fewer very large residuals. In any case, the spectrum of the residuals changes with the fitting method, i.e., decreases occur where the fitted function has a frequency component. To give a valid standard error to a trend, one needs to know the true spectrum. This difficulty tends to be overlooked in parametric fitting procedures where the programs always produce output, but it corresponds to the assertion that the errors as seen through the residuals reflect the lack of fit.

To throw more light on the CFM problem, such methods need to be applied to a number of stations. To get global coverage and to avoid correlated stations, Hill chose those stations listed in Table 6.2. This led to the analyses of Tiede *et al*. (1977) and Parzen and Pagano (1978). These analyses were made to try to detect a noncyclical decrease in global ozone in the early 1970's. The papers cited above showed no signs of decreases before then, and Hill and Sheldon had dealt with the case of Arosa in the early 1970's. One may wonder why the analyses were done before and after 1970, when the injection of the CFMs into

TABLE 6.2 Stations Selected for Global Analysis of Total Ozone Data

Zone	Station	Location	Period	Mean Level	No. of Missing Values
North Temperate	Edmonton	54° N, 114° W	7/57-12/75	357	0
	Arosa	47° N, 10° E	1/57-12/75	333	2
	Tateno	36° N, 140° E	7/57-12/75	323	0
Tropics	Mauna Loa	20° N, 156° W	1/64-12/75	277	0
	Huancayo	12° S, 75° W	2/64-12/75	264	1
	Kodaikanal	10° N, 77° E	1/61-4/75	261	0
South Temperate	MacQuarie Isl.	54° S, 159° E	3/63-12/75	340	0
	Buenos Aires	35° S, 58° W	10/65-12/75	288	0
	Aspendale	38° S, 145° E	7/57-12/75	320	0

the atmosphere essentially began in 1950. However, the models show that the initial rate of decrease is very small. For example, Figure 9.1 suggests less than a 1 percent change to 1970, but from 1970 to 2010, the curve A proceeds roughly linearly at a rate of 0.1 percent per year. Thus, the depletion curve (zero to 1970, linear thereafter) is not a bad approximation over the first 50 years or so.

Parzen and Pagano, using methods described in Appendix C, found no reason to include an unsuspected trend in each of the stations except for Huancayo, where the result is attributed to instrument drift.

Tiede *et al*. studied the statistical structure of each of the station series to 1969 but then used a further method, due to Box and Tiao (1975), to test for a decrease in the 1970's. This latter method simply fits by least squares a trend shaped like a hockey stick to the post-1969 data, after making suitable adjustments for the serial dependencies in the data. They found the Huancayo data to be anomalous (Komhyr has informed us of troubles with the instrument there) and no evidence for significant decreases--although there are some negative slopes (e.g., Arosa), they are small compared with their standard errors. In this work, the seasonal variation is eliminated by differencing observations one year apart.

They go on to check that the slope estimates seem to be independent and then suggest that their average, which is slightly more accurate than the individual slopes, should be the basis for a decision on whether, in fact, there has been a decrease. Again, the trend does not depart significantly from zero, even when only the statistical standard error is used.

The method, which assumes a linear decrease starting in 1970 as well as seasonal variation, allows the cumulated ozone decrease by year 1970 + *y* to be estimated as *y* times the annual slope. This number may then be compared with predictions in Figure 9.1. While the statistical analysis provides a standard error for *y* times the slope, this standard error must be increased to account for error sources not represented in this standard error. These are discussed below.

This application of the Box-Tiao analysis may be criticized for the following reason. If the physical-chemical theory is correct, the average ozone over each station will be a different smoothly decreasing function of time. In this analysis, it is assumed that for every station a linear decrease begins at the *same* time, 1970, though possibly with a different slope. The curve in Figure 9.1 is not linear until approximately 1985, a decade after the release rate has been taken as constant. Therefore, the estimate obtained by multiplying the average annual slope by *y* will be misleading until *y* corresponds to 1990 or later. Thus the accuracy of an early warning system obtained by this method will be partly illusory, certainly in the near future. It will be important to find a method of trend analysis that meets this objection and, if possible, gives reasonably accurate predictions in the next 10 to 20 years.

For this report G. Watson of Princeton University carried out a further extensive analysis. The previous analyses mentioned above used actual Dobson values (cf. Appendix C). The present analysis used, in addition, logarithms of the Dobson values, which seemed appropriate since a monthly ozone value can be regarded as the product of factors associated with latitude, longitude, time trend, seasonal or monthly effects, and random effects. If the last three were not too variable, the "multiplicative" analysis would be roughly the same as the "additive" analysis. This is what was, in fact, found. Also, the analyses employed different methods for removing the seasonal variation and for filtering out the time correlation. The data are over too short a time to decide on the optimum methods. Thus, it is possible to get many different estimates of average station slope together with their standard errors. For this report, many further calculations were made, including starting the linear decrease not only at

1970 but at 1966 and 1960. The average slope was never found to be significantly different from zero, and its sign changed from case to case. Thus, the current methods for analyzing the observed trend show no significant changes in the total ozone, even when only the statistical error is used. It is very unlikely that the use of more than nine stations would change this judgment.

The standard errors of the estimates of the ozone change over a given period of time are more nearly constant than the slope estimates themselves. These standard errors may be calculated for future slope estimates found by one of the methods mentioned above. If the future time is year 1970 + y, the ranges of the standard errors obtained are

$$(0.07\%,\ 0.18\%) \text{ for } y = 6 \text{ years}$$
$$(0.05\%,\ 0.13\%) \text{ for } y = 10 \text{ years}$$
$$(0.02\%,\ 0.07\%) \text{ for } y = 15 \text{ years}$$

A simple summary of these results is that the statistical error of a slope estimate made with data to the year 1970 + y is $0.75/y\%$, approximately. This summary might be wrong by a factor of 2. Since the estimated cumulative ozone depletion is y times the slope estimate, the standard error of the estimated cumulative ozone depletion is $0.75\% \times y = 0.75\%$, to a factor of 2. Thus, on the basis of statistics alone, we would not expect to detect an ozone change less than 2 × 0.75% = 1.5%. From Figure 9.1 one would not have expected to see this until about now.

OTHER SOURCES OF UNCERTAINTY IN ESTIMATING AN OZONE TREND

Statistical trend analyses, such as those described in the previous section, provide, in principle, a powerful tool for estimating possible ozone change. They remove all variations in the data that are statistically predictable and reduce the time series to the minimum *white-noise* variance component and any possible trend. If the spectrum of ozone fluctuations were flat on time scales longer than those resolved by the available ozone record, the white-noise variance obtained by the time series analysis would determine the uncertainty of the ozone trend. For example, we could infer on the basis of the trend analysis that if there were no apparent trend in the data (as is currently the case) we could be 95 percent confident that ozone had not changed by more than ±1.5 percent over a period of 10 to 15 years because of man-made effects or, conversely, if we saw a 3 percent ozone change, that it had changed by between 1.5 and 4.5 percent. The longer the record, the smaller is the uncertainty of the trend.

Analysis of meteorological time series, however, generally shows also a strong *red-noise* component, i.e., additional fluctuations on time scales long compared with that resolved by a short meteorological record. For example, global surface temperatures warmed by 1°C between 1860 and 1940, a variation comparable or larger in magnitude than the observed year-to-year temperature fluctuations. Indeed, as discussed earlier, global average total ozone appears to have fluctuated by up to 5 percent in the last two decades, because of unknown but presumably natural causes. Thus, it is generally believed that the white-noise variance of the statistical analysis, as described above, severely underestimates the actual uncertainty of the trends of global ozone due to human activities.

The above assertion is all that we can say with confidence. However, to determine what level of ozone change can be detected by a trend analysis requires a quantitative estimate of the likely magnitude of variations in the inferred global ozone time series due to all possible reasons. These estimates can only be made by theoretical and analog reasoning, since, if they could be established from the ozone record, they could be made part of the statistical analysis variance.

We are primarily interested in fluctuations on time scales between 5 and 100 years. Longer-time-scale variations can be regarded for practical purposes as constant; shorter ones would be resolved by the existing data. We believe the following discussion is fairly complete with regard to likely sources of such long-period ozone variation. However, our estimates of the likely variation due to a given source could easily be in error by more than a factor of 2, and our total estimate of the variance in long-period variations should not be regarded as precise to better than a factor of 2. It is one of our major conclusions that these estimates should be refined through further research.

The low-frequency errors involved in the time-series analysis are summarized as follows. It should be emphasized again that the error estimates cannot, at present, be based on hard data but represent our best guesses based, in part, on the information discussed in this chapter.

1. Dobson instruments are not generally calibrated with periodic regularity. Thus, some nonrandom calibration

corrections, including nonrandom drift in the optical wedge characteristics and deterioration of the internal optics, will produce changes in the reported ozone amounts that, in general, will not be averaged out in the reported ozone amount--particularly where the A/D pair is not used exclusively. Long-term stratospheric temperature trends and variation in the extraterrestrial constant could also contribute to the low-frequency (red) portion of the instrument and observational standard error. We judge the standard error component to be about 0.5 to 1 percent.

2. Turbid sky conditions involving haze and aerosols introduce an error in the "observed" total amount of ozone that could be as large as a 0.2 to 0.5 percent long-period variation (i.e., 10 to 20 years or longer). Turbidity, both volcanic and nonvolcanic, could be responsible for an additional 0.3 to 0.5 percent error in observed ozone.

3. Variations in global average ozone are dependent on meteorological conditions in two ways:

(a) Meteorological variations in observing condition (i.e., cloudiness amount, etc.);

(b) Atmospheric dynamics responsible for ozone transport and photochemical interaction. These, of course, involve long-period meteorological changes that border on climatic variations. The year-to-year variations as shown by analysis of the average standard deviation of the mean monthly total ozone amounts taken over periods of 3 to 5 years are of the order of 3 to 5 percent. The variation for longer periods is probably about 1 to 2 percent.

4. The geographic distribution of observing stations introduces a fixed bias associated with known geographic patterns of total ozone. This bias introduces an error of the order of a few percent if the large-scale stratospheric circulation pattern were stationary. If, however, the large-scale planetary waves shift over long time periods, an error of the order of 0.5 percent in global average ozone could be introduced as a result of the present fixed position of the ozone observing stations in the northern and southern hemisphere. Polar night ozone is unobservable.

5. It is possible that variations in solar flux (both electromagnetic and particle) could introduce a significant variation in the observed values of total ozone. The major part of these variations could be suitably filtered. However, it is quite possible that a residual influence, solar or galactic, could be present, in the amount, we judge, of about 0.2 percent.

6. For a given observation period, the chemical composition of the stratosphere and troposphere need not remain fixed. Causes for such variations could be systematic over the duration of the observation period and could result in a nonrandom bias in the trend analysis. Extraterrestrial influences, such as flux variations in solar UV, cosmic rays, and man-made influence, such as the systematic deterioration of tropospheric environment through pollution (e.g., NO_x, CO, CO_2), could lead to low-frequency variations in global O_3. We estimate this could be a few percent but not less than 1 percent.

In Table 6.3 we summarize our conclusions as to the magnitude of the various contributions to error in ozone trend estimates. Where we had assumed a range in the error estimate, we take the midpoint of that range for the tabular value.

TABLE 6.3 Source of Variance in Estimates of Global Ozone on Time Scales Not Resolvable from the Available 20-Year Record[a]

	$\pm 1\sigma$	σ^2
1. Minimum white noise	0.75	0.56
2. Dobson calibration; instrument correction	0.75	0.56
3. Sky conditions (haze and aerosols)	0.75	0.56
4. Meteorology (observing conditions and transport variations)	1.5	2.25
5. Geographic distribution of stations	0.5	0.25
6. Solar variations	0.2	0.04
7. Chemistry and boundary condition	1.0	1.0
$\Sigma\sigma^2$		5.22
σ_T		±2.2%

[a] The values are assumed to represent standard error contributions for the purpose of inferring an ozone trend due to human activities.

TREND ANALYSIS

From Table 6.3 we see that the variance associated with a trend estimate of the percentage decrease in global ozone is 5.2 percent and has an estimated standard error, σ_T, of 2.2 percent. This value suggests that the threshold of detectability is about 5 percent, which is not very sensitive to the period over which this change occurs. *Total cessation of CFM release at that point will result in a decrease in total global ozone of about 7 percent some 15 years later and remaining over 5 percent for many decades thereafter.*

According to Figure 9.1, this detection threshold would correspond to the predicted most likely value, around 1988 to 1990. However, this detectability threshold may be overly optimistic because of the crude assumptions for the shape of the ozone change with time caused by CFM release. If the predicted values *are* correct, detection should be fairly certain by 1995.

It will be seen from our analysis that the uncertainty due to the inadequate sampling with only 9 Dobson stations contributes only about 12 percent to the total uncertainty. Hence, the elucidation and decrease of the other errors is seen to be more important than extending the Dobson network or refining its analysis, though not its maintenance. Maintaining the network and keeping its instruments in perfect condition is vital. The drift and calibration problem should be overcome. With more data, long-term variabilities will gradually be resolved. Dobson stations with longer records, combined with extensive satellite data, will reduce the uncertainty due to converting station to global average estimates. If these things come to pass, the detection problem can be solved.

Our analysis takes account of calibration problems and those trends whose causes have been identified. At present, however, we have a record of close to a 6 percent increase during the 1962-1973 period in ozone measured in the northern hemisphere (Figure 6.2) for which we have no explanation. This corresponds to a variance of about $\frac{1}{2}(3)^2 = 4.5$ (percent)^2. If we were to add this variance to the others in Table 6.3, the total variance increases from 5.2 to 9.7 for a standard error of 3.1 percent. This would delay the detectability of any trend due to human activity and increase the maximum ozone depletion correspondingly, following any control action.

Since the 6 percent increase was for the northern hemisphere while the southern hemisphere observations suggest a partial compensating effect, a much smaller adjustment in the standard error might actually obtain. We have, therefore, decided to use the unadjusted figure of 2.2 percent in this report with an understanding that it may be overoptimistic.

REFERENCES

Angell, J. K., and J. Korshover. 1976. Global analysis of recent total ozone fluctuations, *Mon. Weather Rev. 104*, 63-75.

Birrer, W. M. 1974. Some critical remarks on trend analysis of total ozone data, *Pure Appl. Geophys. 112*(3), 523-532.

Box, G. E. P., and G. M. Jenkins. 1970. *Time Series Analysis and Forecasting Control*. Holden Day, San Francisco.

Box, G. E. P., and G. C. Tiao. 1975. Intervention analysis with applications to economic and environmental problems, *J. Am. Statist. Assoc. 70*, 70-79.

Hill, W. J., and P. N. Sheldon. 1975. Statistical modeling of total ozone measurements with an example using data from Arosa, Switzerland, *Geophys. Res. Lett. 2*, 541-544.

Komhyr, W. D., E. W. Barrett, G. Slocum, and H. K. Weickmann. 1971. Atmospheric total ozone increase during the 1960's, *Nature 232*, 390-391.

London, J., and J. K. Angell. 1979. The observed distribution of ozone and its variations, Vol. I, *Ozone and Perturbation, Man and Stratospheric Ozone*, CRC Press, to be published.

London, J., and S. J. Oltmans. 1978/79. The global distribution of long-term total ozone variations during the period 1957-1975, *Pure Appl. Geophys. 117*, 346-354.

London, J., R. D. Bojkov, S. Oltmans, and J. I. Kelley. 1976. Atlas of the Global Distribution of Total Ozone July 1957-June 1967, NCAR/TN/113+STR.

Mateer, C. L., D. F. Heath, and J. J. DeLuisi. 1978. Seasonal variation of the vertical distribution of stratospheric ozone as observed with the Umkehr and BUV methods, WMO Symposium on the Geophysical Aspects and Consequences of Changes in the Composition of the Stratosphere, Toronto, WMO, No. 511, pp. 161-167.

Miller, A. J., R. M. Nagatani, J. D. Laver, and B. Korty. 1979. Utilization of 100 mb mid-latitude height fields as an indicator of sampling effects on total ozone variations, *Mon. Weather Rev.*, to be published.

Newell, R. E., and Mao-Fou Wu. 1978. A pilot study of concomitant changes in total ozone and atmospheric general circulation, *Quart. J. R. Meteorol. Soc. 104*, 999-1003.

Parzen, E., and M. Pagano. 1978. *Statistical Time Series Analysis of Worldwide Total Ozone for Trends*. Unpublished report prepared for Manufacturing Chemists Assoc.

Pittock, A. B. 1978. A critical look at long-term sun-weather relationships, *Rev. Geophys. Space Phys. 16*, 400-420.

Tiede, J. J., P. N. Sheldon, and W. J. Hill. 1977. A time series intervention analysis of stratospheric ozone data. Methodology paper submitted for NASA sponsored symposium, *Ozone, Trend Detectability Thresholds*, Boulder, Colorado, July 28-29, 1977.

7 ATMOSPHERIC MEASUREMENTS

INTRODUCTION

The measurement of trace chemical constituents of the atmosphere plays a critical role in atmospheric understanding and in the development and validation of the photochemical models used for predictions of the effect of emission of atmospheric pollutants on the stratospheric ozone concentration. Measurements are required to identify the trace species present in the atmosphere, concentration measurements of certain species are needed to provide the boundary conditions for the model calculations, and measurements of the temporal and spatial distributions of certain trace species are required to test the model predictions. In addition, vertical profiles of N_2O and CH_4 are used to evaluate vertical transport parameters for use in the models. A global coverage is required in order to obtain suitable global average transport parameters for use in the 1-D models. In some cases, for example species introduced by anthropogenic activity, there are both local and interhemispheric variations that complicate concentration determinations. In many cases, there are diurnal/ seasonal composition variations that add to the difficulty of obtaining a comprehensive picture of atmospheric composition, and there are changes with time, due to anthropogenic inputs of some species. Short-period fluctuations have been observed for many species, e.g., NO, NO_2, and HO, which further complicates the task of acquiring average composition data and testing model predictions. For this reason, simultaneous measurements of some sets of chemically related species are required in order to test models sufficiently.

In addition to chemical-composition determination, the solar ultraviolet flux is an essential input to the photochemical models, and its determination in the atmosphere is a difficult measurement problem. The solar UV in the 1700-2424 Å wavelength region determines the rate of production of O atoms in the 50- to 70-km altitude region. The solar flux in the 1700-2085 Å region is suspected of being variable with solar activity; this is a major measurement problem to be addressed.

In addition to the original NAS, 1976 report, there has been subsequently a detailed NASA report (RP1010, August 1977) developed from a workshop involving a large number of scientists active in the field. ICAS report 20a published in March 1977 was developed by a Subcommittee on Instrumentation and Measurement Systems (SIMS) of the Interdepartmental Committee for Atmospheric Sciences (ICAS). More recently, a World Meteorological Organization (WMO) Report resulted from a meeting of experts in the field held in Seattle in August 1977. These reports provide a nearly complete review of trace-constituent measurement technology, even with the very rapid development of the field. The actual measurements are being made at such a pace that no review can remain current for long. A very recent review, "The Solar Output and Its Variations," published in 1977, reviews that subject comprehensively. A COSPAR working group has prepared a report, "Intercomparison/Compilation of Relevant Solar Flux Data Related to Aeronomy." (For complete citations of the documents given in this paragraph, see the Bibliography.)

GENERAL METHODS

The requirements on the needed atmospheric measurements are highly variable and almost unique to the species in question. The requirements include precision and accuracy, sensitivity, capability for obtaining geographical and temporal coverage, and ability to measure vertical profiles. Many of the current measurements are operating at the limit of available technology, and most of them compromise desired measurement properties. Many desired measurements exceed currently available technology and have not yet been carried out. In several cases, simultaneous measurements of photochemically related species (and perhaps solar flux) are needed, so that a compatability question arises.

The measurement techniques divide basically into two categories, remote and *in situ* observations. *In situ* measurements often have an advantage in giving better spatial resolution and more accuracy then a remote measurement.

Remote measurements may have an advantage in capability for long-time-series observations. Some species have been measured both remotely and *in situ*, while others have been measured by only one method, and some are yet to be measured.

In situ measurements in the troposphere and stratosphere require a measurement platform; some remote measurements require a platform and others do not. The problem of positioning the platform can be a limitation even when the measurement technology is well in hand. Platforms, particularly balloons and aircraft, are limited in their altitude range and, as a matter of logistics and economy, somewhat limited in their geographical disposition.

The *in situ* measurements may involve actual *in situ* concentration determination, as in the case of O, HO, Cl, and ClO measurement by resonance fluorescence, or it may involve acquisition of grab samples for subsequent analysis in the laboratory, as for example in the measurement of N_2O, H_2, CH_4, $CFCl_3$, and CF_2Cl_2.

Remote measurements, such as optical absorption measurements using the sun as a light source, may yield only the integrated column abundance; alternatively, by obtaining the absorption as a function of solar zenith angle, altitude profiles may be obtained. The deconvolution of these twilight data introduces some uncertainty, and, if the species measured is rapidly changing in concentration at twilight, an additional difficulty is introduced into the analysis.

Precision describes the reproducibility of a measurement method. Precision is relatively easy to determine for stable species in which repeated measurement of standard samples can be carried out. Subtle or difficult problems may arise even here if the sensitivity of the measuring instrument depends on external parameters such as temperature or pressure in its field application. For measurements of unstable species under a variety of ambient conditions, the problem of determining precision may be greatly increased. It may be very difficult in some cases to generate a reproducible standard, for example.

Accuracy is more difficult than precision to determine. Accuracy is the possible deviation of the measurement from the true atmospheric concentration; the deviation includes the variation implied by the precision plus systematic errors. Systematic errors are almost inherently unknowable, and estimates of the accuracy are always somewhat subjective. There are cases of atmospheric measurement by different investigators in which the reported concentrations differ by more than the sum of the estimated error limits, illustrating the point that experimenters sometimes underestimate their errors. It is therefore important to have different techniques available for the measurement of critical species to determine systematic errors.

The WMO workshop report tabulated a list of techniques that have been used for stratospheric *in situ* measurements. It also provides a list of measurement techniques applied to individual species, with estimates of precision and accuracy for each species. These tables are current and represent the considered judgment of a recent panel, which included a large fraction of the active measurers in the field. The satellite Nimbus-7 was launched in November 1978, and SAGE (Stratospheric Aerosol and Gas Experiment) is scheduled for launch in 1979. Both satellites are primarily oriented toward stratospheric trace-gas-composition measurements. The Solar Mesosphere Explorer (SME) satellite, projected for launch in 1981, will simultaneously measure O_3 from 30 to 80 km, solar UV flux, temperature, pressure, NO_2, and H_2O. These data should increase our knowledge of atmospheric ozone photochemistry and dynamics in the stratosphere. The Halogen Occultation Experiment (HALOE) is designed to measure O_3, NO, HCl, HF, CH_4, H_2O, and CF_2Cl_2, first on the Space Shuttle in 1981 and then on a free-flying satellite in 1982. There is little doubt that eventually a major contribution to our understanding of global atmospheric composition will come from satellite observations. At present, only the O_3 distribution has been contributed to by satellite observation.

SOLAR FLUX

The photochemistry of the atmosphere, including ozone production, is initiated by solar flux, and the intensity and wavelength distribution of this flux are critical inputs for atmospheric model calculations. This subject was discussed in NASA 1010, and that review is still current. The solar flux from about 180 to 600 nm is the region of most stratospheric interest. A major concern, which is not adequately resolved, is whether the critical 200- to 300-nm solar flux varies with time, especially with the 11-year sunspot cycle. It is known that the short-wavelength flux, $\lambda < 130$ nm, does vary with solar activity, e.g., the strong Lyman-α line at 121.6 nm has been observed to vary by about 35 percent in intensity over the 27-day rotational period near solar maximum. It is also known that the longer-wavelength flux does not vary greatly, e.g., the total solar flux at ground level is constant over the solar cycle to within a few percent. There is an annual variation in solar flux of 6.6 percent with the maximum in January due to change in solar distance. NASA report 1010 plots the solar spectral radiance from 130 to 300 nm and gives a plot of the sparse data on solar-cycle variation of flux between 180 and 340 nm. Recently, a detailed reported entitled, *The Solar Output and Its Variation* (see Bibliography), which is the product of a Solar Output Workshop held in Boulder in April 1976, has appeared. A chapter by Heath and Thekaekara summarizes the solar spectrum between 120 and 300 nm.

A recent report to the COSPAR Working Group IV (see Bibliography) involving a large number of experts in the solar-flux field, concludes that variability with the 11-year solar cycle cannot unambiguously be derived from available data. Simon (1978) has reviewed the solar-flux measurements between 120 and 400 nm, arriving at the same conclusion. It is clear that more measurements on solar flux are needed. Experiments are now being undertaken to measure O_2, O_3, and NO photolysis directly in the atmosphere using balloonborne gas mixtures in quartz flasks. The photolysis rates will be determined by chemical actinometry at different altitudes and solar zenith angles. This should yield the relevant convolution of solar flux, atmospheric absorption, and photodissociation cross section, thereby eliminating uncertainties in the molecular parameters, as well as the incident solar flux. Bahe and Schurath (1978) have measured the rate of $O(^1D)$ production by ozone photolysis near the ground and at 26 km in some initial experiments of this type.

CHEMICAL COMPOSITION

Nitrous Oxide, N_2O

The quality of atmospheric N_2O measurements has significantly improved in the last several years. Measurements of high precision (±1 percent) are now being reported, mostly using the electron-capture detector gas-chromatographic technique. Detailed tropospheric measurements have been carried out by many groups. The N_2O tropospheric mixing ratio appears to be constant in time for the last several years and constant over the globe to within the ~1 percent precision of current measurements.

Several laboratories have carefully intercompared standards and appear to have established an accuracy better than 5 percent on repeated intercomparison and calibration tests. Most of the measurements appear to lead to tropospheric N_2O mixing ratios of 325 ± 5 ppbv. However, Singh *et al.* (1977a) find lower average concentrations, 311 ± 2.3 ppbv, where the 0.8 percent standard deviation is slightly larger than the measurement precision, 0.4 percent. Careful measurements carried out by R. Weiss at Scripps Institution of Oceanography, which do not involve an electron-capture detector, yield a lower volume mixing ratio of 299 ppbv. Probably one can only estimate that the tropospheric N_2O concentration is 315 ± 20 ppbv until this discrepancy is removed.

The stratospheric N_2O distribution is extremely important for two reasons. The stratospheric N_2O provides the major stratospheric source of NO by its reaction with $O(^1D)$, and the vertical profiles of N_2O are used to obtain vertical eddy-diffusion coefficient profiles, since the source and sink distribution of N_2O is relatively well known. The stratospheric mixing ratio falls off with altitude, in a manner that depends on latitude and that varies in time at a fixed latitude. The most detailed stratospheric measurements are those of Schmeltekopf *et al.* (1977) and Goldan *et al.* (1979), who have reported stratospheric profiles, up to 35 km altitude in some cases, with a geographical distribution including Alaska, Wyoming, Antarctica, Brazil, and Panama. Figure 7.1 shows 13 Wyoming profiles obtained by Schmeltekopf from 1976 to 1979. Four recent profiles obtained in Southern France at almost the same latitude by a German consortium (Ehhalt, Fabian, Seiler, *et al.*; P. Fabian, Max Planck Institut, Lindau, private communication) show excellent agreement. The variability from one profile to the next increases with altitude and reflects atmospheric variability and not experimental scatter.

It has been found by Goldan *et al.* that the variability in the stratospheric N_2O obtained at Wyoming (41° N) at different seasons over several years is reduced by plotting the profiles against altitude above the tropopause. It is not generally possible to determine objective tropopause altitudes for a given time, even when reliable temperature, ozone, or water-vapor profiles are obtained simultaneously. However, there is a fairly regular annual variation of tropopause height, from about 10 km in the winter to about 13 km in the summer. Reducing the data to altitude above the average seasonal tropopause height clearly compresses

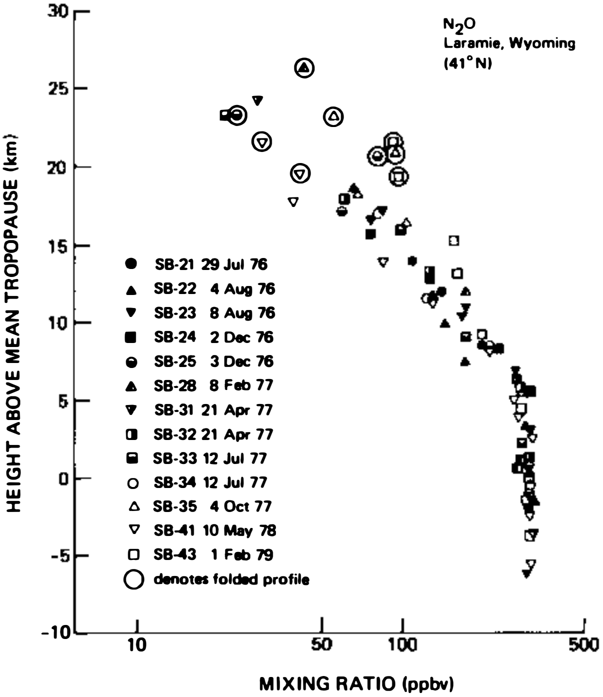

FIGURE 7.1 N_2O mixing ratio versus height above the mean tropopause at Laramie, Wyoming (41° N). The large circles identify portions of the individual profiles that were clearly irregular (Goldan *et al.*, 1979).

the spread of data and is therefore useful in generating an average stratospheric N_2O profile for any given season. The same is true for the F-11 and F-12 stratospheric profiles at Wyoming and presumably reflects the seasonal variation in the penetration of photodissociating UV transmission due to the varying ozone altitude distribution with season.

Above ~30 km, profiles are frequently observed that do not show smoothly decreasing N_2O mixing ratios with increasing altitude. Many examples have been observed, one of which is shown in Figure 7.2. Such behavior shows the strong role of the atmospheric motions in the stratospheric N_2O distribution and, of course, the inappropriateness of one-dimensional models to describe instantaneous profiles.

The same structure occurred also in the simultaneous F-12 profiles from these flights. This structure implies a need for better vertical resolution in sampling. Figure 7.3 shows the NOAA profiles divided into high, low, and middle latitude, plotted as a function of altitude above the tropopause. Reducing the profiles to a common tropopause height has greatly reduced their spread. However, a residual latitudinal dependence of the vertical falloff in concentration is evident. Krey *et al.* (1977) reported lower stratospheric distributions from 1 to 75° N for July 1979. Their 30 to 40° latitude data agree very well with the profiles of Figure 7.1 in the 14.5- to 19.5-km altitude range covered by these data. When reduced to altitude profiles by grouping in latitudinal range bins 0 to 10° N, 30 to 40° N, and 60 to 70° N, there is a significant latitudinal dependence to the vertical falloff rate. Plotting the data as a function of altitude above the tropopause would reduce this spread to well within the range of the data shown in Figure 7.3. There remains a need for somewhat broader geographical coverage with better altitude resolution, and such experiments are being carried out.

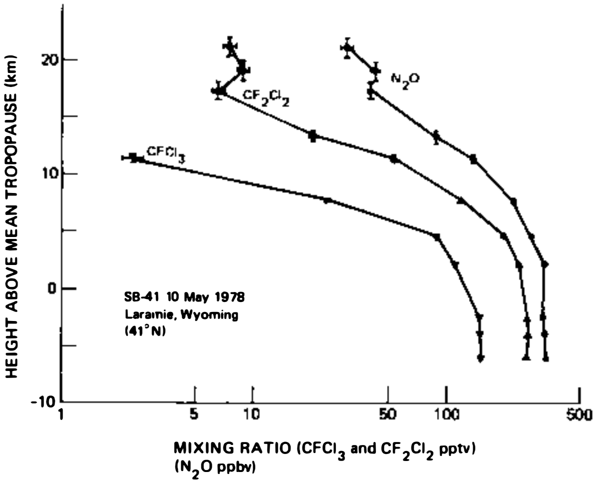

FIGURE 7.2 $CFCl_3$, CF_2Cl_2, and N_2O mixing ratio profiles showing the effects of mass-air motions at approximately 17 km above the tropopause (Goldan *et al.*, 1979).

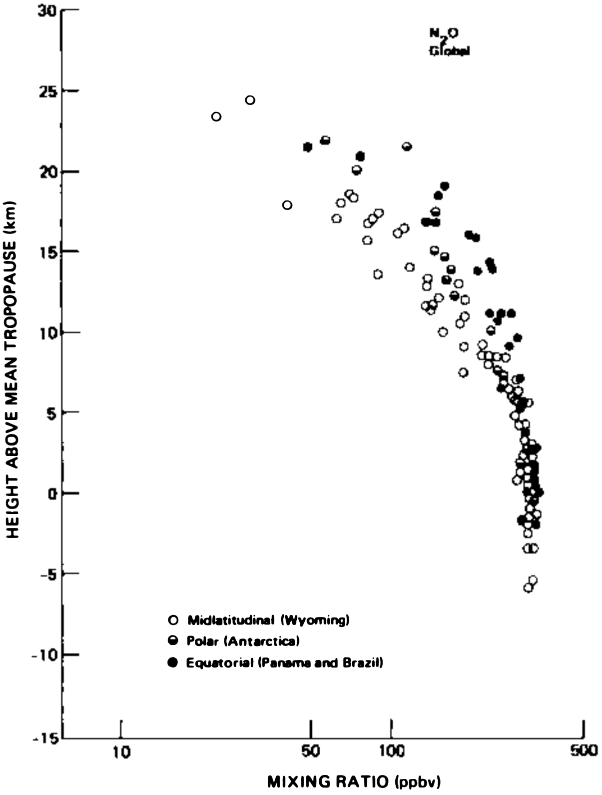

FIGURE 7.3 N_2O mixing ratio versus height above the mean tropopause from different latitudes (Goldan *et al.*, 1979).

Chlorocarbons

The tropospheric chlorocarbon concentrations are of concern as the source of stratospheric chlorine. The stratospheric profiles provide the altitude distribution of this source.

Tropospheric F-11 and F-12

A precise global tropospheric budget of F-11 and F-12 would allow an assessment of tropospheric lifetimes by comparison with known release rates. An accuracy better than that for the global release rates (~5 percent) would be required for this purpose. Such accuracy does not yet exist. In addition, determinations of global budget are complicated by the interhemispheric differences reflecting the predominantly northern hemisphere source, by the increasing concentrations of F-11 and F-12 with time, and the very nonuniform ground-level concentrations due to urban sources. For these reasons current plans to assess the atmospheric lifetimes are largely focused on the trend analysis at selected stations in which only relative concentration measurements are required.

A large number of measurements are now becoming available that appear to reflect the northern hemisphere nonurban background levels of F-11 and F-12. This is supported by the reasonable agreement of many investigators and by the consistency of the measurements, many of which are made far from pollution sources, including measurements in the upper troposphere. The mid-1977 F-11 background mixing ratios in the northern hemisphere seemed to largely fall within about 10 percent of 140 pptv, i.e., 140 ± 14 pptv, and for F-12 the measurements seem even better, 250 ± 12 pptv or about a 5 percent spread. Intercomparisons of measurements between several laboratories that have carefully worked on their absolute calibration are consistently better than 5 percent. It seems likely that calibration gases can be prepared to 5 percent by careful volumetric procedures, and the precision of the gas chromatograph certainly exceeds this.

Singh *et al.* (1977a) found very large enhancements at several urban sites, as much as a factor of 15 for F-12 and as much as a factor of 50 for F-11. J. E. Lovelock (private communication, 1978) has found monthly means as large as 290 pptv for F-11 at Adrigole in 1976, reflecting pollution from Europe and the United States, so that the areal extent of tropospheric pollution may be quite significant. He has also found monthly means at Adrigole as low as 138 pptv in 1977.

Measurements in 1977 by Singh *et al.* (1979) yield a 12 percent N/S hemispheric gradient for F-11, and a 9.5 percent N/S gradient for F-12. Upper-tropospheric measurements of Schmeltekopf in January 1977 gave similar results (12 percent and 8 percent). Measurements by Tyson *et al.* (1978) found only a 6 percent gradient for both F-11 and F-12 in 1976. Goldan *et al.* (1979) report 8 percent N/S gradients for both F-11 and F-12 for early 1978 on a limited southern hemisphere data set. Large N/S hemispheric ratios have been deduced earlier from data in which the northern hemisphere concentrations reflected pollution enhancement.

Determination of the temporal increase in F-11 and F-12 concentrations are generally consistent with the release rates to within the measurement error. Singh *et al.* (1979) report a 10 percent/year increase in F-12 and a 12 percent/year increase in F-11 for the years of 1976 and 1977. Goldan *et al.* found a northern hemisphere increase of 10.7 ± 1.9 percent/year for F-12 and 10.4 ± 3.9 percent/year for F-11 for mid-1976 to mid-1979, and Fraser and Pearman (1978a; 1978b; 1978c) found an F-11 increase of 14.5 ± 1.5 percent/year from April 1976 to April 1978 in Australia and Tasmania. Goldan *et al.* found a similar southern hemisphere F-11 increase, 14.8 ± 2.9 percent/year in mid-1977, from their limited data set.

Stratospheric F-11 and F-12

Goldan *et al.* (1979) have stratospheric data for F-11 and F-12 from balloon flights from Wyoming, Panama, Antarctica, Alaska, Brazil, and Saskatchewan. These data are shown

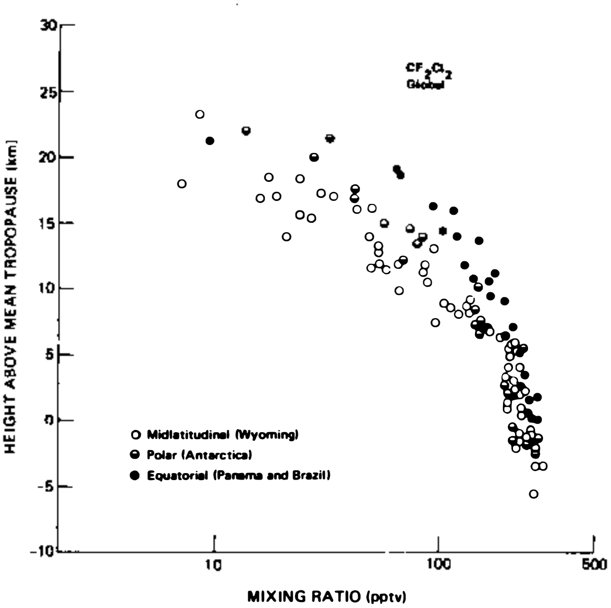

FIGURE 7.4 CF_2Cl_2 mixing ratio versus height above the mean tropopause from different latitudes from July 1976 to March 1979 (Goldan *et al.*, 1979).

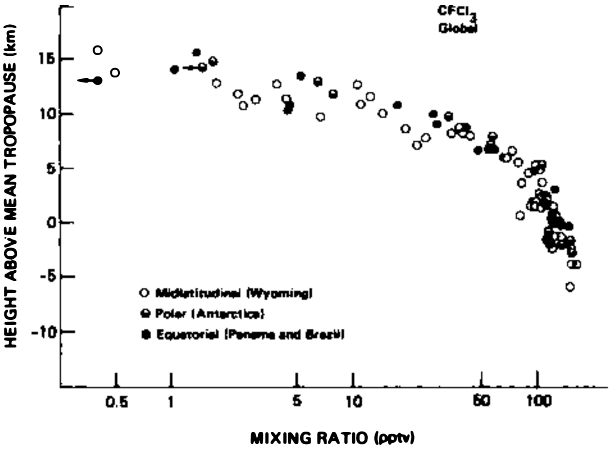

FIGURE 7.5 $CFCl_3$ mixing ratio versus height above the mean tropopause from different latitudes from July 1976 to March 1979. The arrows denote upper limits (Goldan *et al.*, 1979).

in Figures 7.4 and 7.5. The results of four flights in southern France in 1977 (P. Fabian *et al.*, Max Planck Institut, Lindau, private communication) agree extremely well with the Wyoming data. The data are plotted against altitude above the tropopause. This representation takes out much of the systematic latitudinal variation. In Figure 7.4 it is apparent that the low-latitude profiles for F-12 from Brazil and Panama fall off somewhat more slowly with altitude than the middle-latitude data from Wyoming. The high-latitude Antarctic profile lies in between. No systematic seasonal dependence has been detected in the several years of Wyoming observations. No residual latitudinal dependence is evident in the F-12 data of Figure 7.5. Vedder *et al.* (1978) have reported a latitudinal distribution of F-11 and F-12 profiles obtained from U-2 flights in the lower stratosphere. This more limited data set shows clear systematic latitudinal variations in the altitude profiles, much, but perhaps not all, of which would be removed by plotting the profiles as a function of altitude above the tropopause. A large fraction of the available stratospheric F-11 and F-12 profiles are compared by Volz *et al.* (1978). Individual profiles frequently show marked deviation from a monotone mixing ratio decrease with altitude, indicative of dominant transport effects. Figure 7.2 shows one of many examples that have been observed. The F-12 and N_2O behavior always parallel each other. The F-11 concentration usually was not detected at the altitudes at which these dynamic effects are pronounced. Further high-altitude stratospheric measurements with improved altitude resolution are needed to better define the frequency and extent of these kinds of dynamic perturbations to the altitude profile.

Methyl Chloride (CH_3Cl)

Methyl chloride is by far the most abundant tropospheric organic chlorine species. The NAS, 1976 report cited Rasmussen's 1975 measurement of 449 pptv and estimated a ±50 percent error in the CH_3Cl measurements. The electron-capture detector sensitivity for CH_3Cl is much lower than for F-11 and F-12, and surface adsorption and sampling stability problems are more severe with CH_3Cl. Far fewer measurements have been carried out. Grimsrud and Rasmussen (1975) reported 530 ± 40 pptv using gas chromatographic-mass spectrometric (GCMS) analysis. Cronn *et al.* (1977) report 569 ± 41.5 pptv for 34 measurements in the Pacific Northwest in March 1976. Singh *et al.* (1977a) report 713 ± 51 pptv at a background site in Yosemite, with an observed range of 655 to 999 pptv. Singh *et al.* (1977b) report 733 ± 134 pptv at Point Arena, in May 1977. Cronn *et al.* show an altitude profile for CH_3Cl (and several other species) from 6 km below to 4 km above the tropopause for March 11, 1976. The CH_3Cl concentration at the tropopause on that flight was 550 ppt, making CH_3Cl the most abundant chlorocarbon compound in the lower stratosphere. Robinson *et al.* (1977) reported a vertical profile in Alaska, showing scattered measurements between 650 and 800 pptv in the troposphere, falling off in the stratosphere. Recently, R. Rasmussen (Oregon Research Center, private communication, 1978) has obtained a number of measurements on the GAMETAG flights over the Pacific Ocean in August-September 1977. The data show no latitudinal dependence but do show a larger concentration of CH_3Cl in the boundary layer than above the boundary layer. North of the Intertropical Convergent Zone (ITCZ) the CH_3Cl concentration was 792 ± 39 pptv for 4 measurements in the boundary layer and 607 ± 42 pptv for 8 measurements above the boundary layer. South of the ITCZ, 12 boundary-layer measurements gave 822 ± 52 pptv and 8 measurements above the boundary gave 652 ± 45 pptv. Considering the relative number of chlorine atoms involved, CH_3Cl is competitive with F-11 and F-12 as a chlorine-atom source. There is clearly a need for more data on the global and vertical distribution of CH_3Cl and verification of the measurement reliability. Estimates of precision are about ±10 percent, and accuracy about ±50 percent from the WMO report (see Bibliography). An estimate of 620 ± 150 pptv fairly well covers the measurement range above the boundary layer in 1977.

Carbon Tetrachloride (CCl_4)

The situation with CCl_4 is similar to that with CH_3Cl. There are serious surface stability problems that thwart attempts to make precise measurements using grab samples. The NAS, 1976 report cited Rasmussen's value of 111 pptv and estimated a factor of 4 measurement uncertainty for CCl_4. An extensive data set is that of Cronn *et al.* (1977), in which 37 troposphere background samples yielded 122 ± 13 pptv. Singh *et al.* (1977a) report a May 1976 northern hemisphere continental United States background concentration of CCl_4 of 113.9 pptv, with no significant temporal or spatial variation. Singh *et al.* (1977b) report a May 1977 background at the relatively clean Point Arean coastal site of 123.5 ± 8.3 pptv. Pierotti *et al.* (1978) reported 134 ± 9 pptv for 68 measurements over North America. They found constant vertical CCl_4 profiles in the troposphere on two occasions. R. Rasmussen *et al.* (1975) found about 120 pptv at the South Pole in January 1975. There is no evidence for geographical variations in CCl_4 concentrations. R. Rasmussen (Oregon Research Center, private communication) found the CCl_4 mixing ratio to be 127 ± 2 pptv in 19 Antarctic samples in January 1977, 132 ± 5 pptv in 24 Idaho-Oregon samples in April 1977, and 136 ± 6 pptv in 50 Africa-Atlantic samples in July 1977. Cronn *et al.* show seven upper-troposphere, lower-stratosphere profiles in the Pacific Northwest in March 1976 that have a mean tropospheric mixing ratio of 122 pptv. The precision appears to be as good as ±15 percent. The accuracy may be as good as ±50 percent, but this remains to be demonstrated by more detailed calibrations and intercomparisons. The WMO report estimates are ±30 percent precision and ±100 percent accuracy. Fraser and Pearman (1978a) report CCl_4 concentrations of 159 ± 25 pptv in the southern hemisphere at the end of 1976. Tyson *et al.* (1978) report 167

± 10 pptv from almost a hundred upper-troposphere measurements, with no difference between the hemispheres.

Methyl Chloroform (CH_3CCl_3)

There is current concern about the increasing use of methyl chloroform as an industrial solvent. Methyl chloroform is relatively slowly removed by OH reactions so that a substantial fraction (~15 percent) may be transported into the stratosphere. There have been relatively few measurements. Lovelock first reported methyl chloroform measurements, and recently (Lovelock, 1977) he reported the trend in methyl chloroform concentrations in both the northern and southern hemisphere since 1971. The southern hemisphere abundance has increased from about 12 pptv, near the detection limit, in 1971 to 50 pptv in 1976. The northern hemisphere increase has paralleled this with about a factor of 2 greater mixing ratio. Lovelock deduces a relatively long atmospheric residence time of 5 to 10 years, which in turn suggests a low average HO concentration, $[HO] < 10^6$ cc^{-1}. Cronn *et al.* (1977) found 94.5 ± 8.2 pptv in 26 Pacific Northwest background samples in March 1976. They show seven upper-troposphere, lower-stratosphere profiles obtained in March 1976. Pierotti *et al.* (1978) report a value of 145 ± 25 pptv for 101 measurements made over North America from 18 to 65° N in October 1976. There was a wide scatter in measurements, from 110 to 170 pptv, much larger than the simultaneous F-11 and F-12 measurements. There was a lower average concentration below 30° N latitude. Within the large variability, the mixing ratio remained constant in the troposphere, falling sharply above the tropopause on a vertical profile. R. Rasmussen (Oregon Research Center, private communication, 1978) found the CH_3CCl_3 mixing ratio to be 72 ± 5 pptv for 36 samples obtained in Antarctica in January 1977, 115 ± 15 pptv for 25 Idaho-Oregon samples in April 1977, and 102 ± 14 pptv for 50 Africa-Atlantic samples in July 1977. Fraser and Pearman (1978a) report CH_3CCl_3 concentrations of 40 to 60 pptv in the southern hemisphere at the end of 1976.

Singh (1977b) reports an average northern hemisphere CH_3CCl_3 mixing ratio of 113 pptv and a southern hemisphere ratio of 75 pptv in 1977 and uses these concentrations to deduce low HO concentrations in the two hemispheres.

F. S. Rowland (University of California, Irvine, personal communication, 1978) found a North Temperate Zone average CH_3CCl_3 concentration of 94.8 ± 3.8 pptv and a South Temperate Zone average of 65.2 ± 1.2 corrected to January 1, 1978, giving good agreement with Singh's N/S hemispheric ratio. The concentration is increasing at about 1 pptv/month.

The spread of measurements by different workers reflects the difficulty in measuring CH_3CCl_3 well, and further work is necessary to develop a data set in which we can have complete confidence. Rasmussen has distributed intercalibration standards to a number of laboratories reporting measurements of CH_3CCl_3, and this should improve the measurement reliability in the coming years.

$CHCl_2F$ (F-21)

This compound has been observed by some workers. There has been a question as to whether the observed signals reflect atmospheric concentration or system contamination problems. S. A. Penkett and R. Rasmussen (Oregon Research Center, 1979, private communication) appear to have established the reality of trace tropospheric F-21 concentrations using GCMS analysis. The concentrations are less than 3 pptv, highly variable, with larger concentrations in the northern than in the southern hemisphere. A typical clean-air northern hemisphere value is ~1 pptv. At the South Pole and in Tasmania, concentrations as low as 0.5 pptv have been observed. Larger concentrations have been found in urban air.

Hydrogen Chloride and Hydrogen Fluoride (HCl and HF)

The stratospheric composition measurement status of HCl is substantially the same as reported in the earlier NAS, 1976 and NASA, 1977 reports. Raper *et al.* (1977) measured the vertical distribution of HCl with a balloonborne IR interferometer at Palestine, Texas, in September 1975 and May 1976. Their concentration profiles show an increase from 0.6 ppbv at 20 km to 1.7 ± 0.5 ppbv in the region of 37 km. The results from the two flights indicate no seasonal variation. The profile is consistent with the earlier Jet Propulsion Laboratory measurements from 14 to 21 km obtained with the U-2 (Farmer *et al.*, 1976) and generally agrees with spectroscopic measurements of Ackerman *et al.* (1976), Williams *et al.* (1976), and Eyre and Roscoe (1977). The only *in situ* measurements of HCl are those of

Lazrus *et al.* (1977), which detect acidic chlorine by means of base-impregnated filters. These filters sample HCl vapor with 100 percent efficiency and also sample $ClONO_2$ with 80 percent or more efficiency. The concentrations of acidic chlorine and HCl are comparable, at 25 km and below, suggesting that large $ClONO_2$/HCl ratios were not present. The variation observed with season is within the variance of the measurements and gives no evidence for a systematic seasonal variation. The filter profiles agree with the spectroscopic profiles below 25 km but show a minimum around 30 to 32 km not evidenced in the spectroscopic profiles. This discrepancy has not been resolved. Farmer and Raper (1977) have measured HF as well as HCl by means of near-IR absorption spectra. Within the error limits of 25 percent between 14 and 30 km and ±50 percent to 38 km, the HF/HCl ratio is constant with a mean value of 0.1. Zander *et al.* (1977) deduced an average HF mixing ratio of $(3.6 \pm 0.7) \times 10^{-10}$ above 27.9-km altitude by infrared absorption. This is substantially higher than the mixing ratio $(1.1 \pm 0.5) \times 10^{-10}$ found by Farmer and Raper.

Mroz *et al.* (1977) used an *in situ* filter-collection technique to measure stratospheric acid fluoride, which would collect COF_2 as well as HF, finding essentially constant mixing ratios in the range of 1×10^{-10} to 1.25×10^{-10} from 27 to 37 km. The Mroz *et al.* observations extend down to 15 km. No seasonal variability is apparent in their data.

A. L. Lazrus (NCAR, Boulder, Colorado, personal communication) has studied the acid fluoride variability with latitude, and no systematic variation has been observed.

Buijs (MCA Report May 31, 1978) has observed HCl and HF profiles in balloon flights in Alaska and New Mexico in 1977. The HCl profile, but not the HF profile, appears to show a maximum at 23 to 25 km, where the HCl volume mixing ratio was 8×10^{-10} and the HF ratio was 10^{-10}. In a May 1976 measurement from Fairbanks, Alaska, Buijs found an HF/HCl ratio varying from slightly greater than 0.2 at 15 km down to 0.13 near 23 km, then increasing at 0.27 near 28 km, then decreasing to 0.23 at 30 km.

Water (H_2O)

H_2O is one of the most abundant and most important trace gases in the stratosphere. Yet the measurement of stratospheric H_2O is still a somewhat controversial subject.

Large temporal and spatial variations have been observed, and it is still not clear how much of this variability has been due to instrumental scatter and how much represents true fluctuations in stratospheric water vapor. Part of the difficulty arises from the fact that a variety of techniques have been used to measure stratospheric water vapor, each one having its own distinct analytical and interpretational problems, so that systematic errors are likely to contribute to the observed scatter. Both *in situ* and remote-sensing techniques have been used. For most substances, *in situ* measurements have fewer sources of error, are easier to interpret, and give a better height resolution. However, in the case of stratospheric H_2O, where the sampling platform has to ascend through the "wet" troposphere, outgassing of H_2O from instrument, payload, and vehicle surface during the measurement do create severe contamination problems. Contamination is much reduced in the case of remote, infrared techniques, which observe the H_2O concentration along an extended light path, most of which is remote from the sampling vehicle.

In an excellent review, Harries (1976) has summarized the available data on the vertical distribution of H_2O in the stratosphere, excluding obviously contaminated older measurements. The average profile obtained from data with wide scatter shows an increase from about 3 ppmv at the tropopause to about 4.5 ppmv at 40-km altitude. Occasionally, individual H_2O profiles have indicated narrow layers of water vapor in the lower stratosphere (cf. Murcray *et al.*, 1974), which tend to be washed out in any average profile but might be a real and even persistent feature of the stratosphere.

McKinnon and Morewood (1970), using an aircraft, made H_2O observations between 17-19 km altitude covering the latitude range from 69° N to 40° S. Harries *et al.* (1973; 1974) measured H_2O at altitudes of 15 to 17 km between 70° N and 40° S. More recently, Kuhn (1975) reported measurements between 50° S to 60° N and 15 to 17 km. All of these measurements were made by infrared techniques and are summarized by Harries (1976). They clearly show strong latitudinal variations of H_2O in the lower stratosphere with a broad maximum mixing ratio around the equatorial zone, reflecting the influence of the high-lying tropical tropopause and the penetration of the mean Hadley motion into the stratosphere. The most recent measurements by Hilsenrath *et al.* (1977), who flew aluminum oxide hygrometers between 11-19 km altitude and 70° N to 50° S confirm the equatorial maximum of H_2O in the lower stratosphere, although it appears narrower than in the older measurements (cf. Figure 7.2). In addition, however, Hilsenrath *et al.* also observed further maxima at 40° S and especially at 40° N, which persist to 17-19 km altitude, well above the tropopause.

There are a number of observations, notably those of Mastenbrook (1971) that are made on a regular basis and permit deduction of temporal variations. Mastenbrook (1971) found a prominent annual cycle at all levels up to 28 km over Washington, D.C., which decreases with height. He also found a secular increase. From microwave measurements, Waters *et al.* (1978) inferred the average H_2O volume mixing ratio in the 40 to 70 km region to be 5 ± 1 ppmv with a decrease above 75 km. Little variation with latitude from 75° N to 60° S was found in November 1976.

Hyson (1978) measured stratospheric water over Mildura, Australia, since 1972 using a broadband radiometer. The average mixing ratio between 15 and 21 km was found to be 2.7 ppmv. Fairly large variabilities were found at all altitudes between 11 and 20 km.

Kley *et al.* (1979) are using a balloonborne instrument that photodissociates H_2O to an excited HO radical, which is detected in emission. In two flights in Wyoming (42° N) in July and September in 1978 they found a minimum water-vapor concentration of 3.5 ppmv at 17-18 km with a gradual increase up to ~8 ppmv at 30 km. In late January 1979 in Wyoming the mixing ratio from the tropopause to 30 km was constant at 4 ppmv. In a flight from Brazil (5° S) a minimum of ~3 ppmv was observed at about 20 km, substantially above the tropopause, with a slight increase to ~4 ppmv at 23 km, the highest altitude measured on the flight.

Methane (CH_4)

Tropospheric Measurements Apart from local sources, the troposphere shows a relatively uniform CH_4 mixing ratio. Vertical gradients are virtually zero. There are, however, measurements that tend to indicate horizontal and temporal variations. Measurements over the Pacific Ocean showed a slight latitudinal variation with a decrease of about 0.1 ppmv in the tropics and a relatively constant mixing ratio in the southern hemisphere. That interhemispheric gradient, based on a published data set from a cruise of the U.S.C.G.C. *Glacier* from Long Beach, California, to the McMurdo Station, Antarctica (Lamontagne *et al.*, 1974;

Ehhalt, 1978) has been supported by recent GAMETAG measurements. An interhemispheric difference would not be unexpected because biogenic and anthropogenic CH_4 production is concentrated in the northern hemisphere.

Ehhalt and Heidt (1973a; 1973b) reported an average CH_4 mixing ratio over the North American continent of 1.41 ppmv based on aircraft sampling from 1965-1967. Balloon-borne measurements in the upper troposphere over eastern Texas also yielded 1.4 ppmv during that period. The measurements of Swinnerton *et al*. (1969), Lamontagne *et al*. (1974), and Larson *et al*. (1972) over the North Atlantic gave about 1.35 ppmv. More recent flights during 1974-1976 over eastern Texas by the National Center for Atmospheric Research (NCAR) gave a higher tropospheric average of 1.63 ppmv. A similar value of 1.65 ppmv was found during aircraft flights over southern France in 1977 (Fabian *et al*., 1977, 1978; Ehhalt *et al*., 1977). Bush *et al*. (1978) find a tropospheric mixing ratio of 1.64 ± 0.1 ppmv. NOAA, NCAR, and Jülich intercalibrations agree to within a few percent.

The early low NCAR values have been found to be in error because of a problem in data analysis (D. Ehhalt, Jülich, private communication), and there is no strong reason to believe that the tropospheric CH_4 concentration is changing with time.

Any seasonal variation of the tropospheric CH_4 mixing ratio has to be smaller than 10 percent, an upper limit based on NCAR's aircraft flights in 1965-1967 (Ehhalt and Heidt, 1973a; 1973b).

Stratospheric Measurements Since the NAS, 1976 report, the number of measured CH_4 profiles has nearly doubled--mostly obtained by *in situ* sampling and later analysis by gas chromatography in the laboratory. Fortunately, profiles have been measured over the tropics as well as over higher latitudes so that a reasonable latitudinal data coverage is becoming available. The data are summarized in Figure 7.6, showing the individual data plotted against true altitude. The NOAA 41° N profiles (Bush *et al*. 1978) are in excellent agreement with the Jülich 43° N profiles (Ehhalt *et al*., 1977). The data at higher latitudes show less variability than the profiles at lower latitudes mostly collected over Palestine, Texas, 32° N. This may have meteorological reasons: (1) For logistical reasons the flights at high latitudes have been flown during late spring or late summer, during the period of the so-called "turn around," with weak upper winds. Thus, they have

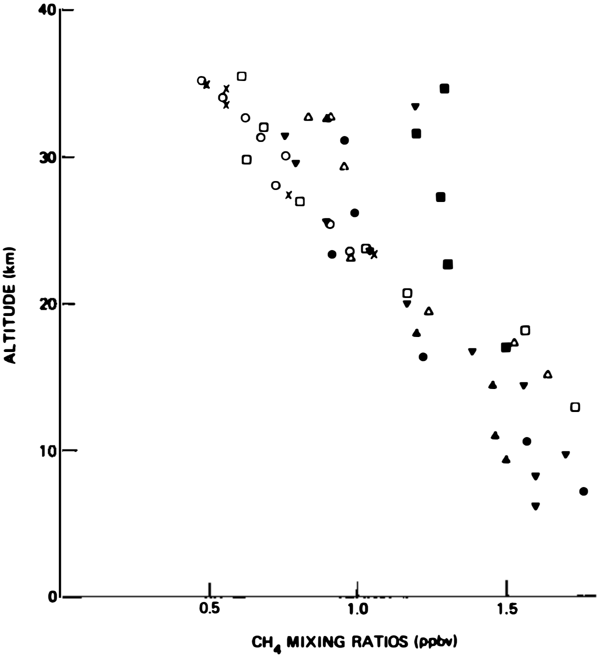

FIGURE 7.6 Stratospheric methane profiles:

O, June 7, 1977; tropopause	12.0 km	44° N 2° E
X, June 16, 1977	12.2 km	44° N 2° E
□, September 12, 1977	13.2 km	43°40' N 15' W
Δ, September 26, 1977	12.2 km	44° N 0° W

Balloon flights in southern France, D. H. Ehhalt, V. Schmidt, A. Volz, A. Khedim, F. J. Johnen, P. Fabian, R. Borchers, K. H. Weiler, W. Seiler, and F. Müller (private communication).

●, January 14, 1978 tropopause	8.5 km	78° S Antartica
■, March 6, 8, 1978	17.1 km	4° S Brazil
▲, February 14, 1978	10.4 km	41° N Wyoming
▼, May 10, 1978	11.3 km	41° N Wyoming

Y. A. Bush *et al*. (1978).

been collected during similar and rather weak upper wind fields, and variability introduced by horizontal advection should be smaller than for the present and older Palestine data, which were collected in all seasons. (2) The latitude at 32° N is located within the region of the downward branch of the stratospheric Hadley circulation, which introduces occasional compression of the vertical gradients and enhances variability. Still, apart from the values in the lower stratosphere, the profiles between 40 and 55° N agree rather well with the data from 32° N, indicating little variation between 32° N and higher latitudes during summertime. Of particular interest are the CH_4 measurements by Bush *et al.* (1978) over the tropics. Like those for N_2O, they show a rather weak vertical gradient, much smaller than that at higher latitudes, indicating the action of mean upward motions. The Wyoming data of May 10, 1978, are from the same grab sample for which F-11, F-12, and N_2O data are shown in Figure 7.2. The same anomalous vertical profile occurs, i.e., an increase in concentration above ~32 km. This must be a consequence of the atmospheric dynamics. Such findings are common.

Hydrogen (H_2)

Atmospheric H_2 measurements have been made by essentially two techniques: *in situ* grab or cryogenic sampling and subsequent analysis with a gas chromatograph equipped with an He ionization detector (Heidt and Ehhalt, 1972) and the HgO method (Schmidt, 1974). The latter, in which the Hg liberated by the reduction of HgO with atmospheric H_2 is measured, has been applied mostly to the troposphere. Both techniques have shown rather uniform vertical and horizontal mixing of H_2 in tropospheric background air with an average mixing ratio of 0.50 ppmv (Ehhalt *et al.*, 1977). Because of a 10 percent difference in absolute calibration, the data obtained by the HgO method averaged 0.55 ppmv. The latter measurements also showed a small interhemispheric difference, the southern hemisphere showing an average H_2 concentration 0.01 ppmv lower. No seasonal variation or secular variation has been observed so far.

The stratospheric measurements of H_2 prior to 1975 have been summarized in the NAS, 1976 report as an average profile. It showed a more or less constant mixing ratio of 0.55 ppmv up to 30 km and a more or less linear decrease above that altitude to 0.40 ppmv at 50-km altitude. The data since 1975 obtained by the same method, cryogenic whole-air sampling and GC analysis, are consistent with this picture. The data between 40° and 55° show less scatter than the data at lower latitudes possibly for the same meteorological reasons as given above for CH_4. They also show a slight but continuous decrease beginning at the tropopause, which is not apparent from NCAR's data over Palestine.

Hydrogen Dioxide (HO_2)

There are now two techniques available to measure stratospheric HO_2: cryogenic *in situ* collection by matrix isolation and subsequent analysis in the laboratory by electron paramagnetic resonance (Mihelcic *et al.*, 1978b), and *in situ* resonance fluorescence after conversion to HO (Anderson *et al.*, 1979). The former method yielded two data points. A sample collected between 6:40 and 9:00 a.m. (solar zenith angle 75°-50°) over northern Germany, 53° N, on August 8, 1976, yielded 3×10^7 HO_2/cm^3 (~0.8 ppbv) at 30-km altitude. The other measurement gave 8.5×10^6 HO_2 at 29.8-km altitude. This sample was collected between 10:45 and 17:48 (solar zenith angle 76°-89°) over Holloman

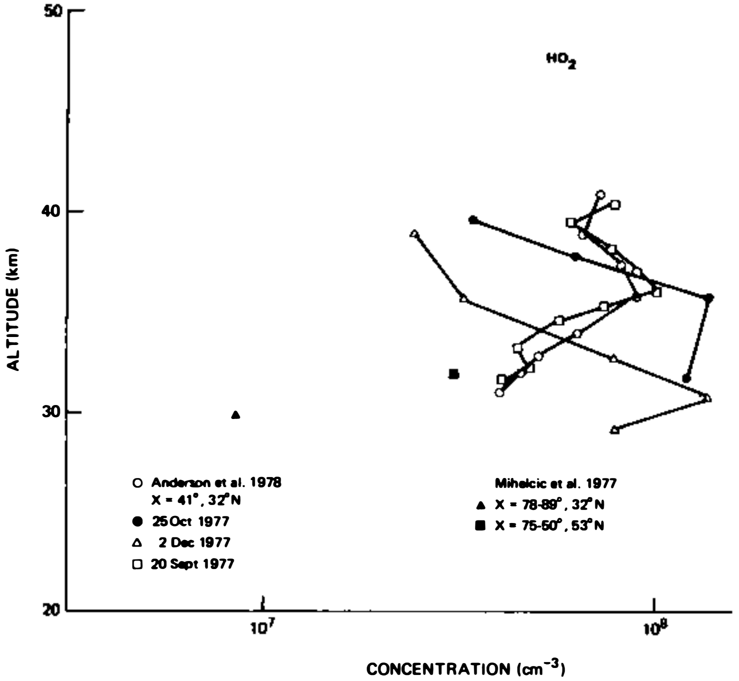

FIGURE 7.7 Stratospheric HO_2 measurements. Vertical profiles obtained by J. G. Anderson (personal communication) by resonance fluorescence techniques. Two isolated points obtained by Mihelcic *et al.* (1978a; 1978b) by matrix isolation techniques.

Air Force Base, New Mexico, 32° N, on March 4, 1977. Both measurements have an error of about a factor 3. The resonance fluorescence measurement has yielded the three HO_2 profiles between 30- and 40-km altitude shown in Figure 7.7.

Hydrogen Peroxide (H_2O_2)

Murcray *et al*. (1978) established upper limits on the H_2O_2 mixing ratio of 10^{-9} at 20 km on March 4, 1977, using solar sunset spectra in the 1215-1315 cm^{-1} region.

Stratospheric HO

J. G. Anderson (private communication, 1978) has extended his earlier resonance fluorescence measurements (J. Anderson, Harvard University, 1976) of HO by additional balloon flights, yielding the data shown in Figure 7.8. Figure 7.9 shows the average (and spread) and these four flights joined onto Anderson's (1971) earlier mesospheric HO measurements, all corrected to midday. This profile yields an integrated HO column density between 20 and 70 km equal to 7×10^{13} molecules cm^{-2}.

Ground-based spectroscopic absorption observations of the column abundance of HO have been made with a Pepsios spectrometer at Fritz Peak Observatory by Burnett (1979). The initial Pepsios observations in 1975 (Burnett, 1976) were followed by measurements in October and December 1976 at Fritz Peak and measurements at Boca Raton, Florida, in March 1977 (Speranga, 1977). The HO vertical column abundances in 1976 and early 1977 averaged 2.2×10^{13} cm^{-2}, with no significant difference between Colorado and Florida results. In July 1977, observations with the Pepsios were resumed at Fritz Peak Observatory in order to obtain further data on seasonal and short-term variations. Approximately 500 hours of observations have been taken on 185 sunny days about equally distributed over summer, fall, and winter. Observations are limited to solar zenith angles less than 70° by the ultraviolet absorption due to ozone. The slant column detection limit at midday is about 2×10^{13} cm^{-2}. The average noontime abundance for this period was 5.7×10^{13} cm^{-2}. Seasonal and diurnal variations are present, caused by the slant-path dependence of the solar UV, which initiates the HO production. An additional seasonal change of 1.6×10^{13} cm^{-2}, with a maximum in spring, closely follows total ozone abundance.

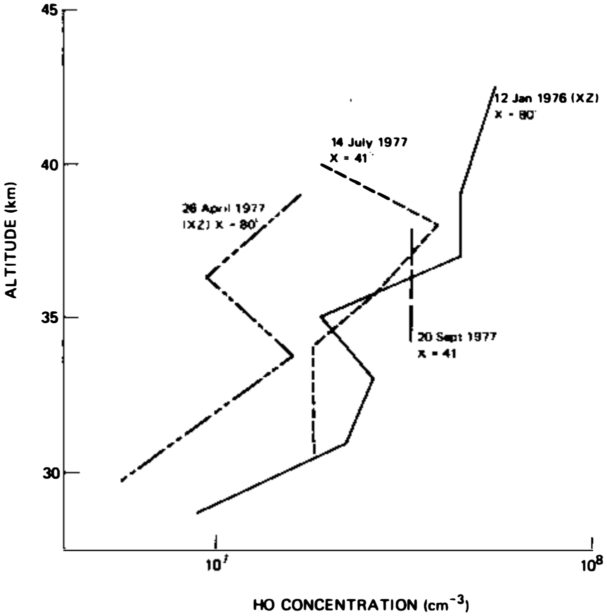

FIGURE 7.8 Stratospheric HO measurements obtained by resonance fluorescence. (J. G. Anderson, private communication.)

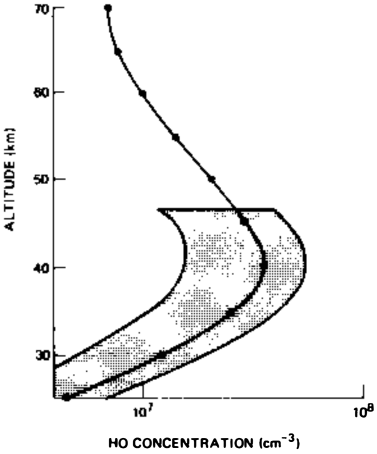

FIGURE 7.9 Average and spread of four flights of Figure 7.8 joined onto earlier flight of J. G. Anderson, Harvard University, all corrected to midday.

Tropospheric HO

The concentration and global distribution of tropospheric HO is very poorly determined. This is a critical problem since the concentrations of species such as CH_3CCl_3 and $CHClF_2$ reaching the stratosphere are determined by their tropospheric loss in reactions with HO.

Philen *et al*. (1978) report average midday HO concentrations of 1.5×10^7 cm^{-3} in the tropical and subtropical marine boundary layer and an order-of-magnitude lower concentration, 1.4×10^6 cm^{-3}, above the boundary layer, with a major discontinuity in HO concentration passing through the boundary layer. This leads to a model in which ~60 percent of the tropical tropospheric HO is within the first 1.4 km from the sea surface. Somewhat larger HO concentrations were found in the southern hemisphere, both in the boundary layer and in the free troposphere.

Carbon Monoxide (CO)

CO is an intermediate product of the CH_4 oxidation, and its atmospheric measurement provides a sensitive test of our understanding of the chemistry of CH_4 destruction. Its lifetime in the troposphere is relatively short, a few months, and it shows strong horizontal and vertical gradients in the troposphere. An idealized meridional cross section of tropospheric CO has been presented by Seiler and Schmidt (1974). Systematic temporal variations have been reported for a station in Hawaii. Aside from the stratospheric CO profiles reported in the NAS, 1976 report there are now a number more profiles obtained by cryogenic *in situ* collection and subsequent analysis by gas chromatography in the laboratory. Unfortunately, there is a large scatter in the data above 20-km altitude (between 10 and 250 ppb), which points to instrumental contamination during sampling. Below 20 km there is better agreement. The data decrease from a tropopause value around 100 ppb to 20-30 ppb at 19 km, with a general increase and large scatter of data above that altitude (Fabian *et al*., 1977, 1978; L. E. Heidt, NCAR, private communication 1978).

An interhemispheric difference in CO concentration of nearly a factor of 3 reported by Seiler has been supported by the 1977 and 1978 GAMETAG results (R. Rasmussen, Oregon Research Center, private communication), which suggests a northern hemispheric mean of 150 ± 15 ppbv and a southern hemispheric mean of ~50 ppbv. The mean CO level over the Pacific Ocean in the northern hemisphere is only 100 ± 27 ppbv. If only the free troposphere over the North American continent from 50 to 70° N is considered, the mean is 146 ± 17 ppbv.

Odd Chlorine (Cl and ClO)

The measurement of the ClO_x species is of primary importance because its concentration allows an immediate empirical estimate of the strength of the catalytic destruction of O_3, as well as an experimental test of the model calculations. By the time of the NAS, 1976 report, just one technique, resonance fluorescence, had been developed far enough to give first measurements of Cl and ClO. By this time, this technique has provided a number of profiles of ClO and Cl (Anderson *et al.*, 1977; 1979). Some ClO profiles are shown in Figure 7.10. All the measurements were obtained over Palestine, Texas, 32° N. Anderson's measurements reveal ClO profiles with a strong

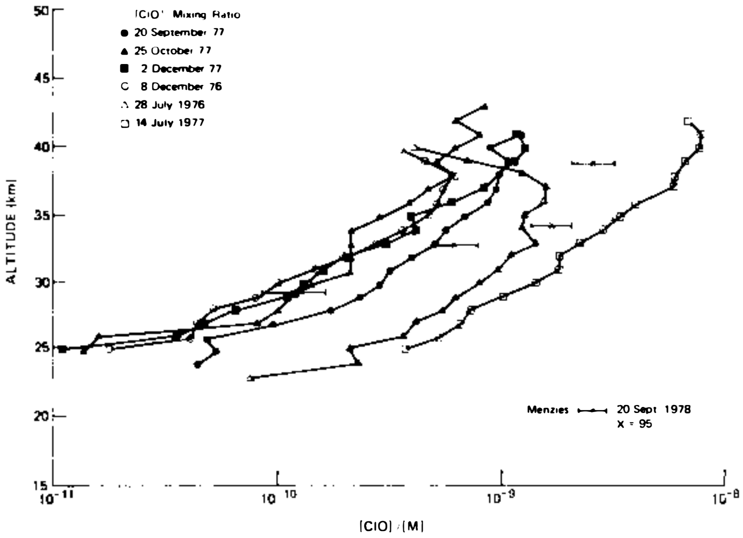

FIGURE 7.10 Stratospheric ClO profiles (Anderson *et al.*, 1979).

increase in mixing ratio in the lower and middle stratosphere, sometimes reaching a maximum between 30 and 40 km, sometimes showing a continued increase to maximum altitude reached by the balloon. Large fluctuations in the absolute concentration are observed with an indication of a seasonal variation with higher values in summer. The high values in summer, especially the profile from July 1977, which reached 8 ppbv peak concentration, are difficult to reconcile with the present consensus on total stratospheric Cl concentration, about 2 ppbv, and the observed stratospheric HCl mixing ratio, which averages around 1 ppbv. Menzies (1979) has also measured ClO concentrations substantially larger than those resulting from model calculations by means of solar infrared absorption spectra from a balloon platform launched at Palestine, Texas, September 20, 1978.

Besides these techniques, an aircraftborne microwave spectrometer has been used to search for millimeter wavelength emission from stratospheric ClO (Waters *et al.*, 1978). The measurements detected a significant amount of ClO, and comparison of theoretically calculated line shapes to the observed ones suggest that ClO should be present with peak concentrations between 0.5 and 1 ppbv. Although these measurements, which were made in June and August 1977, do not permit one to derive vertical mixing ratio profiles, they indicate lower average ClO abundances during summer than obtained by the resonance fluorescence technique and are more in line with the theoretical predictions.

The scarcity of ClO data from the infrared and microwave measurements and the large variability of the ClO concentration during summer observed by resonance fluorescence make it difficult to arrive at a firm conclusion on the stratospheric ClO concentration, or the reasons for its variation. More and preferably simultaneous measurements by the different techniques would help to solve the experimental uncertainty, and measurements of total chlorine would clarify the extent of natural variability.

Chlorine Nitrate ($ClONO_2$)

Murcray *et al*. (1978) suggest an upper limit for $ClONO_2$ at 20 km of 3×10^{-10} from a March 4, 1977, solar sunset spectrum at various zenith angles in which they failed to detect infrared absorption at 1292.5 cm^{-1}.

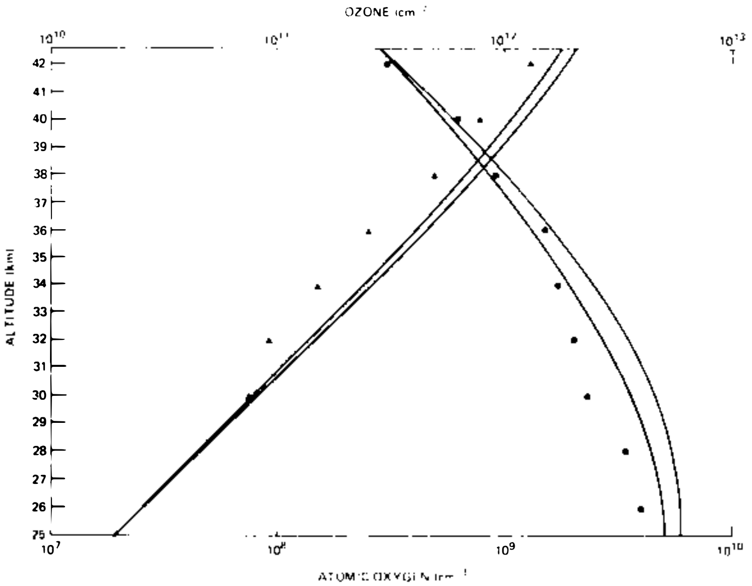

FIGURE 7.11 Simultaneous atomic oxygen and ozone measurements, December 2, 1977, 32° N solar zenith angle = 50° (Anderson, private communication).

Atomic Oxygen

J. G. Anderson (Harvard University, private communication, 1978) has extended his earlier stratospheric measurements using resonance fluorescence (Anderson, 1975) obtaining the simultaneous O and O_3 profile shown in Figure 7.11.

Stratospheric Odd Nitrogen

HNO_3 Few new measurements on stratospheric HNO_3 have been obtained since the NASA, 1977 report. Evans and co-workers (1978) have measured HNO_3 profiles for late summer at 50 to 55° N from several balloon flights. Their averaged HNO_3 profile is shown in Figure 7.12 with the standard deviation of four flights included as the upper and lower curves. Comparison with previous data, such as those in the NASA, 1977 report, show these to be representative profiles. Measurements of Murcray *et al.* (1975) showed a minimum HNO_3 column density at the equator above 18 km. Murcray

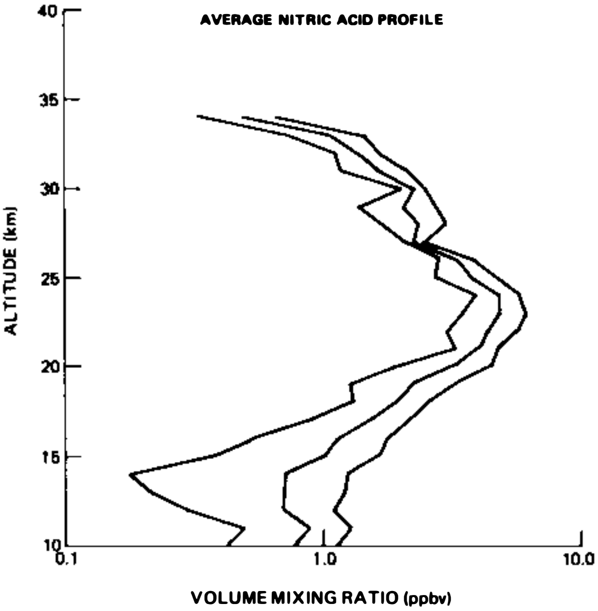

FIGURE 7.12 Average nitric acid profiles for late summer at 50 to 55° N latitude. Standard deviation from four stratoprobe flights shown as upper and lower bound curves (Evans, Kerr, McElroy, and O'Brien, personal communication), W. F. J. Evans, Atmospheric Environmental Service, Toronto, Canada.

et al. (1978) have extended the data analysis of the 1975 paper with the conclusion that the amount of HNO_3 above 18 km increases up to about 70° N, but from 70 to 75° N there is a significant drop in column density in the April 29, 1975, stratosphere. They find variability of the order of 50 percent in the atmospheric column content over a few days.

N_2O_5 Murcray *et al*. (1978) analyzed atmospheric emission spectra taken from 18.3 km during a U-2 flight of February 17, 1978, between 50 and 55° N to yield an upper limit on N_2O_5 of 0.1 ppbv at sunrise. Evans *et al*. (1978) on the other hand deduce a mixing ratio of 3 ppbv above 30 km in an August 20 predawn flight in 1977. This was deduced from a very weak and uncertain 8.1-μm feature. The large difference between the Murcray and Evans results, in addition to reflecting the altitude difference, 18 km as compared with 30 km, also is consistent with Noxon's finding of no diurnal variation of NO_2 at high latitudes in the winter, which implies a large decrease in winter stratospheric N_2O_5 in this region.

NO_3 Stratospheric NO_3 has recently been detected by Noxon *et al.* (1978). The column abundance was measured by its absorption near 6600 Å using the moon as a light source. Noxon *et al.* (1978) observed a stratospheric column abundance of $(1 \pm 0.2) \times 10^{14}$ molecules/cm^2 at Fritz Peak (40° N) just before dawn in April 1978. There is a seasonal variation in the NO_3, with a maximum in April and May.

HO_2NO_2 Murcray *et al.* (1978) established an upper limit on the HO_2NO_2 column density at zenith angles from 45 to 93.5° of 10 percent of the HNO_3 column density.

NO_2 Recent measurement of stratospheric NO_2 profiles by infrared techniques are reported by Evans *et al.* (1978). They have measured NO_2 profiles for late summer at 50 to 55° N. Their result (referring to a zenith angle of 90°) is shown in Figure 7.13. Large differences between morning and evening are observed, indicating a significant formation rate from N_2O_5 photolysis. Solar UV absorption was also used by Goldman *et al.* (1978) to derive NO_2 profiles. The authors point out that at present the errors from this method are significantly larger than those obtained for NO_2 profiles by the infrared technique.

Noxon has now collected a large body of data on the seasonal and global behavior of the stratospheric NO_2 column density (Noxon *et al.*, 1979; Noxon 1979). He uses ground-based UV absorption spectroscopy. His data were compared with those obtained by IR absorption (i.e., Murcray, Mankin) with good agreement. However, his results sometimes do not agree well with data taken with a Brewer-type instrument (see later).

The equatorial NO_2 is about one half of the midlatitude values. The southern midlatitude shows similar column densities to the northern midlatitude. The summer midlatitude shows about twice as much NO_2 as in the winter. Also, the center of gravity of the vertical concentration occurs at lower altitude in the summer.

The mean daytime stratospheric NO_2 column drops by a factor of 2 over 5 degrees of latitude at 40 to 50° N in winter under normal conditions when there is no stratospheric

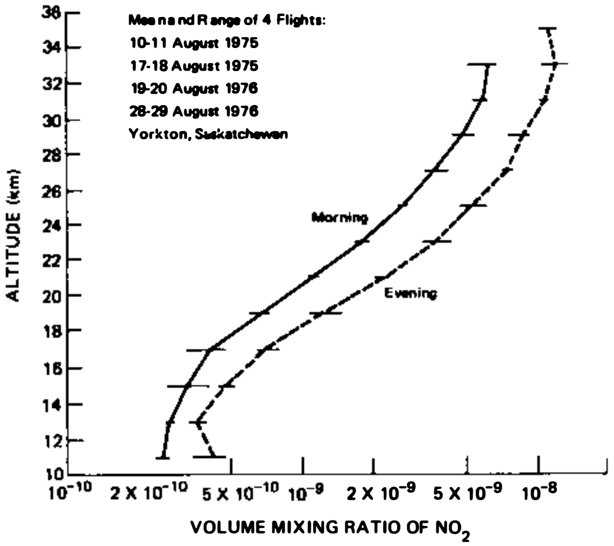

FIGURE 7.13 Stratospheric NO_2 measurements, 50-55° N latitude. Solar zenith angle 90°, standard deviations shown as error bars. Stratoprobe data, W. F. I. Evans, J. B. Kerr, C. T. McElroy, and R. S. O'Brien, Atmospheric Environmental Service, Toronto, Canada, personal communication.

warming. This cliff has now been observed by Noxon (1978) in the winter southern hemisphere as well.

Figure 7.14 shows Noxon's NO_2 column density as a function of latitude for different seasons. The existence of the cliff for the winter stratosphere is pronounced. Figure 7.15 shows the seasonal variation in stratospheric column of NO_2 over a 15-month period at Pt. Barrow, Alaska (~71° N).

At the Atmospheric Environment Service of Canada, J. B. Kerr (private communication) has used ground-based techniques for the measurement of stratospheric NO_2 for some years. At low absorption (evening at Cold Lake, both researchers doing simultaneous measurements), the absorption due to stratospheric NO_2 as measured by Kerr was about a factor of 2 larger than the value measured by Noxon. However, at large absorption (evening at Yorkton) both measured about the same absorption. The cause of the deviation at low absorption has not yet been resolved.

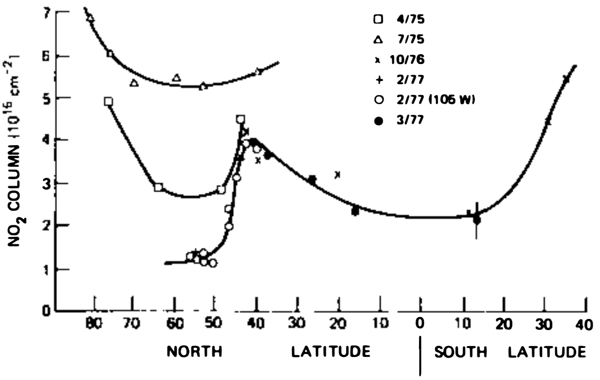

FIGURE 7.14 Stratospheric NO_2 column density versus latitude for several seasons (Noxon, 1979).

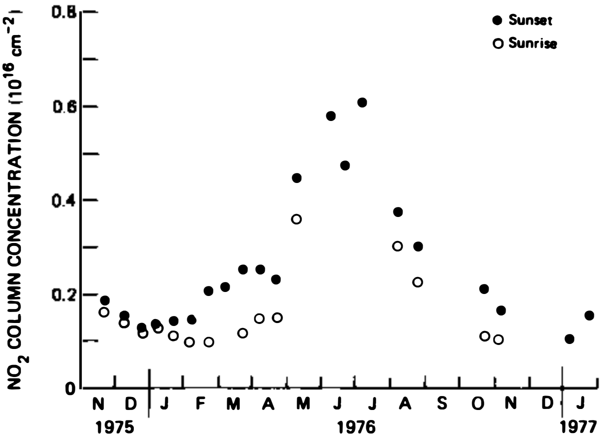

FIGURE 7.15 Stratospheric NO_2 column density versus time at Pt. Barrow, Alaska (71° N) J. F. Noxon (NOAA, personal communication).

Noxon has verified the calibration of his instrument using the sky as light source (when the NO_2 column is low) by varying the NO_2 in an absorber cell from large to low values.

W. Mankin of NCAR (private communication, 1978) has made measurements of the stratospheric NO_2 column using infrared absorption from a high-flying aircraft. His results are in excellent agreement with Noxon's ground-based observations. On a day-to-day basis, Mankin also finds substantial differences in the NO_2 column. A correlation between the height of the troposphere and the NO_2 column was found such that if the tropopause was high the NO_2 tended to be large, and vice versa.

NO The situation on stratospheric NO concentration measurements has not changed substantially since the NAS, 1976 and NASA, 1977 reports. Numerous balloonborne ozone chemiluminescence measurements of NO have been obtained, mostly by Ridley *et al*. (1973; 1974; 1975; 1976; 1977). The measurement uncertainty is in the range of 25 to 60 percent, and the natural variability exceeds this.

Lowenstein and co-workers (1974; 1975a; 1975b; 1978a; 1978b) have used a chemiluminescent detector to collect NO data as a function of latitude, longitude, and season in the northern hemisphere between 18- and 21-km altitude. The results show no longitudinal variation. At 18 km, there is very little variation in NO concentration south of 60° N, spring through fall; north of 60° N, the summer NO concentrations are higher than those measured in the fall. At 21 km, no significant NO concentration variations are seen south of 45° N during spring through fall, but there is a winter minimum at 40° N. North of 50° N, the summer NO concentrations are higher than those in the spring or fall. There are simultaneous NO, O_3, and HNO_3 measurements for several of the flights. They have estimated their uncertainty to be ±25 percent.

The highest balloonborne chemiluminescent NO measurement was made by Drummond *et al*. (1977) to an altitude of 45 km from Sioux Falls, South Dakota (43.4° N), on June 27, 1976. A previous measurement for NO to 30 km was made from Laramie, Wyoming (41.3° N), on November 1, 1975. The instrument was zeroed every minute and calibrated in flight every 5 minutes by adding calibration gas to the glass sample inlet tube. Their uncertainties are estimated to be from 25 to 50 percent, depending on altitude.

Recently, J. G. Anderson (Harvard University, private communication, 1978) has obtained an NO profile from 30 to 40 km using the resonance fluorescence technique. His results are in reasonable agreement with the overlapping altitude measurements of Drummond *et al.*

Nitric oxide has been measured *in situ* by Maier *et al*. (1978), using photoionization mass spectrometry between 38 and 30 km on April 26, 1977, from Palestine, Texas (31.8° N).

Sample gas was drawn through a glass-line inlet tube and flushed past an inlet leak valve to an ionization chamber of a quadrupole mass spectrometer. The low-pressure gas was then selectively ionized by a krypton lamp (123.6 and 116.5 nm), which was energetic enough to ionize NO but not N_2, O_2, and CO. The sensitivity to NO was then proportional to the photon flux, ionization cross sections, and concentration of NO in the ionization chamber and thus cryogenic pump flow rate. No inflight calibration was attempted, but background count rates were taken for each data point. Their measurements show a dramatic increase in NO concentration between 33 and 34 km that cannot be explained by the ozone profile, which was measured concurrently. Their uncertainties were estimated to be 10 percent at the higher altitudes and 100 percent at the lower altitudes.

At present, further isolated measurements of NO alone are of little interest. Either measurements of related families of species, e.g., NO, NO_2, HNO_3, N_2O_5, and O_3, are required as a test of photochemical theory or temporal or spatial distribution measurements are required to define further the variability of species concentrations.

RECOMMENDATIONS

As far as local measurements are concerned, we need measurements of related species in order to test photochemical theory. Generally, *isolated* measurements of a single short-lived species are no longer useful because the natural variability makes the measurements difficult to interpret.

Much of the natural variability of stratospheric species is due to dynamical and meteorological influences rather than photochemical ones. Time series of measurements of individual compounds are important to understand diurnal, seasonal, and solar-cycle variations, as well as the irregular variations whose causes need to be sought out.

In the same way, global distributions of individual species, particularly long-lived species, are still of great importance. Tropospheric global distributions provide needed data on interhemispheric mixing and source and sink distributions. Stratospheric distributions help in understanding the role of global circulation patterns, such as Hadley cell circulation, in determining species distributions. This requires better and more extensive measurements of stratospheric vertical profiles. In particular, in the case of the anthropogenic halocarbon compounds, the global spatial concentration distribution and the temporal increase need to be better determined. F-11, F-12, and CH_3CCl_3 are especially important. More F-21 measurements should be carried out.

The photoactive UV solar flux in the stratosphere needs to be more precisely measured and particularly its solar cycle variation, which is now in doubt. Direct *in situ* measurements of atmospheric photolysis rates would be valuable.

Certain critical minor stratospheric species are as yet unmeasured or only poorly measured. Measurements of HO_2NO_2, $ClONO_2$, HOCl, N_2O_5, NO_3, HO_2, H_2O_2, and OH are quite inadequate to date.

Tropospheric altitude profiles of certain groups of species, e.g., NO, NO_2, O_3, and also solar flux measured simultaneously, are needed to improve our understanding of the tropospheric ozone cycle, which is important to our understanding of the stratospheric ozone cycle because of their coupling. Boundary-layer effects on tropospheric concentrations of NO_x, ozone, and other species appear to be important and not well studied.

Further measurements of stratospheric Cl, ClO, and HCl are important to clear up the uncertainty associated with the large reported concentration and concentration variations.

A total chlorine concentration measurement would be of great value.

Tropospheric OH concentrations are needed to understand the CO cycle and methyl chloroform and other CFM loss rates.

Better information on washout of soluble atmospheric species such as NH_3, SO_2, HCl, and HNO_3 is needed. New experimental measurements strategies are required for this.

REFERENCES AND BIBLIOGRAPHY

Ackerman, M., D. Frimout, C. Lippens, et C. Muller. 1972. Determination de la distribution verticale du méthane stratosphérique par spectrométrie infrarouge en balloon, *Bull. Acad. R. Belgique, Cl. Sc. 55*, 493-501.

Ackerman, M., D. Frimout, A. Girard, M. Gottignies, and C. Muller. 1976. Stratospheric HCl from infrared spectra, *Geophys. Res. Lett. 3*, 81-83.

Ackerman, M., D. Frimout, and C. Muller. 1977. Stratospheric CH_4, HCl and ClO and the chlorine-ozone cycle, *Nature 269*, 226-227.

Anderson, J. G., J. J. Margitan, and D. H. Stedman. 1977. Cl and ClO in the stratosphere, three *in situ* observations, *Science 198*, 501-503.

Anderson, J. G. 1976. The absolute concentration of $OH(X^2\Pi)$ in the earth's stratosphere, *Geophys. Res. Lett. 3*, 165.

Anderson, J. G. 1971. Rocket-borne ultraviolet spectrometer measurement of OH resonance fluorescence with diffusive transport model for mesospheric photochemistry, *J. Geophys. Res. 76*, 4634.

Anderson, J. G. 1975. The absolute concentration of $O(^3P)$ in the earth's stratosphere, *Geophys. Res. Lett. 2*, 231-234.

Anderson, J. G., H. J. Grassl, R. E. Shetter, and J. J. Margitan. 1979. Stratospheric free chlorine measured by balloonborne *in situ* resonance fluorescence, *J. Geophys. Res.*, in press.

Bahe, F., and V. Schurath. 1978. Measurement of $O(^1D)$ formation by ozone photolysis in the troposphere, *Pure Appl. Geophys. 116*, 537-544.

Burkhardt, E. G., C. A. Lambert, and C. K. N. Patel. 1975. Stratospheric nitric oxide: measurements during daytime and sunset, *Science 188*, 1111-1113.

Burnett, C. R. 1976. Terrestrial OH abundance measurement by spectroscopic observation of resonance absorption of sunlight, *Geophys. Res. Lett. 3*, 319.

Burnett, C. R., and E. B. Burnett. 1979. Spectroscopic measurements of the vertical abundance of hydroxyl (OH) in the earth's atmosphere, *EOS 60*, 336.

Bush, J. A., A. L. Schmeltekopf, F. C. Fehsenfeld, D. L. Albritton, P. D. Goldan, and E. E. Ferguson. 1978. Stratospheric measurements of methane at several latitudes, *Geophys. Res. Lett. 5*, 1027.

Chaloner, C. P., J. R. Drummond, J. T. Houghton, R. F. Jarnot, and H. K. Roscoe. 1975. Stratospheric measurements of H_2O and the diurnal change of NO and NO_2, *Nature 258*, 696-697.

Cronn, D. R., R. A. Rasmussen, E. Robinson, and D. E. Harsch. 1977. Halogenated compound identification and measurements in the troposphere and lower stratosphere, *J. Geophys. Res. 82*, 5935-5947.

Cumming, C., and R. P. Lowe. 1973. Balloon-borne spectroscopic measurement of stratospheric methane, *J. Geophys. Res. 78*, 5259-5264.

Drummond, J. W., J. M. Rosen, and D. J. Hofmann. 1977. Balloon-borne chemiluminescent measurement of NO to 45 km, *Nature 265*, 319.

Ehhalt, D. H., and L. E. Heidt. 1973a. Vertical profiles of CH_4 in the troposphere and stratosphere, *J. Geophys. Res. 78*, 5265-5271.

Ehhalt, D. H., and L. E. Heidt. 1973. The concentration of molecular H_2 and CH_4 in the stratosphere, *Pure Appl. Geophys. 106-108*, 1351-1360.

Ehhalt, D. H., U. Schmidt, A. Volz, A. Khedim, F. J. Johnen, P. Fabian, R. Borchers, K. H. Weiler, W. Seiler, F. Müller, and X. Oeser. 1977. The vertical distribution of H_2, CH_4, H_2O, $CFCl_3$ and CF_2Cl_2 in the troposphere and stratosphere at midlatitudes, in *Proceedings of the 1st Meeting of the Coordination and Study Groups on the Ozone Shield Depletion Problem*, Brussels, October 24-25.

Ehhalt, D. H. 1978. The CH_4 concentration over the ocean and its possible variation with latitude, *Tellus*, in press.

Eyre, J. R., and H. K. Roscoe. 1977. Radiometric measurements of HCl, *Nature 226*, 243-244.

Evans, W. F. J., H. Fast, J. B. Kerr, C. T. McElroy, R. S. O'Brien, D. I. Wardle, J. C. McConnell, and B. A. Ridley. 1978. Stratospheric constituent measurements from project stratoprobe, WMO Symposium Proceedings, Toronto, June 26-30.

Fabian, P., R. Borchers, K. H. Wiler, U. Schmidt, A. Volz, D. H. Ehhalt, W. Siler, and X. Oeser. 1977. Simultaneously measured vertical profiles of H_2, CH_4, CO, N_2O, F-11, F-12, NO and O_3 in the midlatitude stratosphere, paper presented at the IAGA-IAMAP General Assembly, Seattle, Washington, September.

Fabian, P., R. Borchers, K. H. Weiler, U. Schmidt, A. Volz, D. H. Ehhalt, W. Siler, and X. Oeser. 1978. Simultaneously measured vertical profiles of H_2, CH_4, CO, N_2O, F-11, F-12, NO and O_3 in the midlatitude stratosphere, to be published.

Farmer, C. B., O. F. Raper, and R. H. Norton. 1976. Spectroscopic detection and vertical distribution of HCl in the troposphere and stratosphere, *Geophys. Res. Lett. 3*, 13-16.

Farmer, C. B., and O. F. Raper. 1977. the HF:HCl ratio in the 14-38 km region of the stratosphere, *Geophys. Res. Lett. 4*, 527-529.

Fraser, P. J. B., and G. I. Pearman. 1978a. Atmospheric halocarbons in the southern hemisphere, *Atmos. Environ. 12*.

Fraser, P. J. B., and G. I. Pearman. 1978b. The fluorocarbon-ozone theory - II. Tropospheric lifetimes--an estimate of the tropospheric lifetime of CCl_3F, *Atmos. Environ. 12*.

Fraser, P. J. B., and G. I. Pearman. 1978c. Atmospheric - halocarbons - The CSIRO southern hemisphere programme, Int. Clean Air Conf., Brisbane, May.

Goldman, A., F. G. Fernald, W. J. Williams, and D. G. Murcray. 1978. Vertical distribution of NO_2 in the stratosphere as determined from balloon measurements of solar spectra in the 4500 Å region, *Geophys. Res. Lett. 5*, 257.

Goldan, P. D., W. C. Koster, D. L. Albritton, and A. L. Schmeltekopf. 1979. Stratospheric $CFCl_3$, CF_2Cl_2 and N_2O height-profile measurements at several latitudes, submitted to *J. Geophys. Res.*

Graham, R. A., and H. S. Johnston. 1978. The photochemistry of NO_3 and the kinetics of the N_2O_5-O_3 system, *J. Phys. Chem. 82*, 254-268.

Grimsrud, E. P., and R. A. Rasmussen. 1975. Survey and analysis of halocarbons in the atmosphere by gas chromatography-mass spectrometry, *Atmos. Environ. 9*, 1014-1017.

Harries, J. E. 1976. The distribution of water vapor in the stratosphere, *Rev. Geophys. Space Phys. 14*, 565-575.

Harries, J.E. 1973. Measurements of stratospheric water vapour using far-infrared techniques, *J. Atmos. Sci. 30*, 1691-1698.

Harries, J. E., N. R. Swann, and D. G. Moss. 1974. H_2O, O_3, N_2O and HNO_3 in the arctic stratosphere, *Nature 250*, 475-476.

Heidt, L. E., and D. H. Ehhalt. 1972. Gas chromatographic measurement of hydrogen, methane and neon in air, *J. Chromatog. 69*, 103-113.

Hilsenrath, E., B. Guenther, and P. Dunn. 1977. Water vapour in the lower stratosphere measured from aircraft flight, *J. Geophys. Res. 82*, 5453-5457.

Hyson, P. 1978. Stratospheric water vapour measurements over Australia 1973-1976, *Q. J. R. Meteorol. Soc.*, p. 225, Jan.

Instrumentation and Measuring Systems for Stratospheric Research. 1977. Subcommittee of Instrumentation and Measuring Systems, Interdepartmental Committee for Atmospheric Sciences, ICAS 20a-FY 77. March.

Intercomparison/Compilation of Relevant Solar Flux Data. 1977. Related to Aeronomy, Report to the Working Group IV of COSPAR. J. P. Delaboudiniere, R. F. Donnelly, H. E. Hinteregger, G. Schmidtke, and P. C. Simon. June.

Jesson, J. P., P. Meakin, and L. C. Glasgow. 1977. The fluorocarbon-ozone theory II. Tropospheric lifetimes--an estimate of tropospheric lifetime of CCl_3F, *Atmos. Environ. 11*, 449.

King, P., I. R. McKinnon, J. G. Mathieson, and I. R. Wilson. 1976. Upper limit to stratospheric N_2O_5 abundance, *J. Atmos. Sci. 33*, 1657-1659.

Krey, P. W., R. J. Lagomarsino, and M. Schonberg. 1977. Stratospheric concentrations of N_2O in July 1975, *Geophys. Res. Lett. 4*, 271-274.

Kuhn, P. M., L. P. Sterns, and M. S. Lojko. 1975. Latitudinal profiles of stratospheric water vapour, *Geophys. Res. Lett. 2(6)*, 227-230.

Kyle, T. G., D. G. Murcray, F. H. Murcray, and W. J. Williams. 1969. Abundance of methane in the atmosphere above 20 kilometers, *J. Geophys. Res. 74*, 3421-3425.

Kley, D., E. J. Stone, W. R. Henderson, and A. L. Schmeltekopf. 1978. Altitude profile of water vapor by photodissociation: $H_2O + h\nu \rightarrow OH(A^2\varepsilon) + H$, *EOS 59*, 1089.

Kley, D., E. J. Stone, W. R. Henderson, J. W. Drummond, W. J. Harrup, A. L. Schmeltekopf, and T. L. Thompson. 1979. *In situ* measurements of water vapor in the stratosphere, *J. Atmos. Sci.*

Lamontagne, R. A., J. Swinnerton, and V. J. Linnenbom. 1974. C_1-C_4 hydrocarbons in the north and south Pacific, *Tellus 26*, 71-77.

Larson, R. E., R. A. Lamontagne, P. A. Wilkins, and P. E. Whittman. 1972. Radon-222, CO, CH_4 and continental dust over the Greenland and Norwegian Seas, *Nature 240*, 345-347.

Lazrus, A. L., B. W. Gandrud, J. Greenberg, and J. Bonnelli. 1977. Direct measurement of stratospheric fluoride, *Geophys. Res. Lett. 4*, 149-150.

Lovelock, J. E. 1977. Methyl chloroform in the troposphere as an indicator of OH radical abundance, *Nature 267*, 32.

Lovelock, J. E., R. J. Maggs, and R. J. Wade. 1973. Halogenated hydrocarbons in and over the Atlantic, *Nature 241*, 194-196.

Lowenstein, M., J. P. Paddock, I. G. Poppoff, and H. F. Savage. 1974. NO and O_3 measurements in the lower stratosphere from U-2 aircraft, *Nature 249*, 817.

Lowenstein, M., and H. F. Savage. 1975a. Latitudinal measurement of NO and O_3 in the lower stratosphere from 5° to 82° North, *Geophys. Res. Lett. 2*, 448.

Lowenstein, M., H. F. Savage, and R. C. Whitten. 1975b. Seasonal variations of NO and O_3 at altitudes of 18.3 and 21.3 km, *J. Atmos. Sci. 32*, 2185.

Lowenstein, J., H. F. Savage, and J. G. Borucki. 1978a. Geographical variations of NO and O_3 in the lower stratosphere, *J. Geophys. Res. 83*, 1975.

Lowenstein, M., W. L. Starr, and D. G. Murcray. 1978b. Stratospheric NO and HNO_3 observations in the northern hemisphere for three seasons, *Geophys. Res. Lett. 5*, 531-534.

Maier, E. J., A. C. Aikin, and J. E. Ainsworth. 1978. Stratospheric nitric oxide and ozone measurements using photoionization mass spectrometry and UV absorption, *Geophys. Res. Lett. 5*, 37-40.

Mason, C. J., and J. J. Horvath. 1976. The direct measurement of nitric oxide concentration in the upper atmosphere by a rocket-borne chemiluminescent detector, *Geophys. Res. Lett. 3*, 391-394.

Mastenbrook, H. J. 1971. The variability of water vapour in the stratosphere, *J. Atmos. Sci. 28*, 1495-1501.

McKinnon, D., and H. W. Morewood. 1970. Water vapour distribution in the lower stratosphere over North and South America, *J. Atmos. Sci. 27*, 483-493.

Menzies, R. T. 1979. Remote measurements of ClO in the stratosphere, *Geophys. Res. Lett.*, in press.

Mihelcic, D., D. H. Ehhalt, J. Klomfab, G. F. Kulessa, U. Schmidt, and M. Trainer. 1978a. Measurements of free radicals in the atmosphere by matrix isolation and electron paramagnetic resonance, *Ber. Bunsenges. Phys. Chem. 82*, 16-19.

Mihelcic, D., D. H. Ehhalt, G. F. Kulessa, J. Klomfab, M. Trainer, U. Schmidt, and H. Röhrs. 1978b. Measurements of free radicals in the atmosphere by matrix isolation and electronc paramagnetic resonance. *Pure Appl. Geophys. 116*, 530-536.

Mroz, E. J., A. L. Lazrus, and J. E. Bonnelli. 1977. Direct measurement of stratospheric fluoride, *Geophys. Res. Lett. 4*, 149-150.

Murcray, D. G., *et al.* 1974. Stratospheric mixing ratio profiles of several trace gases as determined from balloon-borne infrared spectrometers, in IAMAP, pp. 292-303, International Association of Atmospheric Physics, Melbourne, Australia.

Murcray, D. G., D. B. Barker, J. N. Brooks, A. Goldman, and W. J. Williams. 1975. Seasonal and latitudinal variation of the stratospheric concentration of HNO_3, *Geophys. Res. Lett. 2*, 223-225.

Murcray, D. G., J. W. Williams, D. B. Barker, A. Goldman, C. Bradford, and G. Cook. 1978. Measurements of constituents of interest in the photochemistry of the ozone layer using infrared techniques, p. 61, WMO Symposium Proceedings, Toronto, June 26-30.

Noxon, J. F. 1978. Stratospheric NO_2 in the Antarctic winter, *Geophys. Res. Lett. 5*, 1021.

Noxon, J. F. 1979. Stratospheric NO_2 in the Antarctic winter, *Geophys. Res. Lett.*

Noxon, J. F., R. B. Norton, and W. Henderson. 1978. Observations of atmospheric NO_3, *Geophys. Res. Lett. 5*, 675.

Noxon, J. F., E. C. Whipple, and R. S. Hyde. 1979. Stratospheric NO_2: observational method and behavior at mid-latitude, submitted to *J. Geophys. Res.*

Pack, D. H., J. E. Lovelock, G. Cotton, and C. Curthoys. 1977. *Atmos. Environ. 11*, 329-349.

Patel, C. K. N., E. G. Burkhardt, and C. A. Lambert. 1974. Spectroscopic measurements of stratospheric nitric oxide and water vapor, *Science 184*, 1173-1176.

Penkett, S. A., and R. A. Rasmussen. 1979. Troposphere $CHCl_2F$ measurements, *Nature*.

Philen, D., W. Hoops, and D. D. Davis. 1978. Boundary layer and free tropospheric OH measurements at tropical and sub-tropical latitudes in the northern and southern hemispheres, *EOS 59*, 1079.

Pierotti, D., R. A. Rasmussen, and R. Dalluge. 1978. Measurements of N_2O, CF_2Cl_2, $CFCl_3$, CH_3CCl_3, and CH_3Cl in the troposphere and lower stratosphere over North America, *J. Geomag. Geoelec.*

Raper, O. F., C. B. Farmer, R. A. Toth, and D. B. Robbins. 1977. The vertical distribution of HCl in the stratosphere, *Geophys. Res. Lett. 4*, 531-534.

Rasmussen, R. A., K. J. Allwine, and W. U. Zoller. 1975. Analysis of halocarbons in Antarctica, *Ant. J.* 321-324, Sept./Oct.

Rasmussen, R. A. 1978. Trans Pacific CO and CH_4 measurements, *EOS 59*, 1082.

Report of the Meeting of Experts on Measurements of Rare Species Relevant to the Ozone Budget, Seattle, August 18-21, 1977, World Meteorological Organization, Global Ozone Research and Monitoring Project.

Ridley, B. A., H. I. Schiff, A. W. Shaw, L. Bates, C. Howlet, H. Levaux, L. R. Megill, and T. E. Ashenfelter. 1973. *In-situ* measurements of nitric oxide in the stratosphere, *Nature 245*, 310.

Ridley, B. A., H. I. Schiff, A. W. Shaw, L. R. Megill, L. Bates, C. Howlett, H. LeVaux, and T. E. Ashenfelter.

1974. Measurement of nitric oxide in the stratosphere between 17.4 and 22.9 km, *Planet. Space Sci. 22*, 19-24.

Ridley, B. A., *et al.* 1975. *In situ* measurements of nitric oxide using a balloon-borne chemiluminescent instrument, *J. Geophys. Res. 80.*

Ridley, B. A., J. T. Bruin, H. I. Schiff, and J. C. McConnell. 1976. Measurement of NO between 17 and 34.5 km from Churchill, Manitoba, in *Proc. Fourth Conf. on the CIAP*, U.S. Department of Transportation, DOT-TSC-OST-75-38, pp. 417-421.

Ridley, B. A., M. McFarland, J. T. Bruin, H. I. Schiff, and J. C. McConnell. 1977. Sunrise measurements of stratospheric nitric oxide, *Can. J. Phys. 55*, 212-221.

Robinson, E., R. A. Rasmussen, J. Krasnec, D. Pierotti, and M. Jakubovic. 1977. Halocarbon measurements in the Alaskan troposphere and lower stratosphere, *Atmos. Environ. 11*, 213-215.

Schmeltekopf, A. L., D. L. Albritton, P. J. Crutzen, P. D. Goldan, W. J. Harrop, W. R. Henderson, T. L. Thompson, D. J. Hofmann, and N. T. Kjome. 1977. Stratospheric nitrous oxide altitude profiles at various latitudes, *J. Atmos. Sci. 34*, 729-736.

Schmidt, U. 1974. Molecular hydrogen in the atmosphere, *Tellus XXVI*, 78-90.

Seiler, W., and U. Schmidt. 1974. New aspects on CO and H_2 cycles in the atmosphere, in IAMAP, pp. 192-222, International Association of Atmospheric Physics, Melbourne, Australia.

Simon, P. C. 1978. Irradiation solar flux measurements between 120 and 400 mm. Current position and future needs, *Planet. Space Sci. 26*, 355-365.

Singh, H. B., L. J. Salas, and A. Crawford. 1977a. Urban-nonurban relationships of halocarbons, SF_6, N_2O and other atmospheric trace constituents, *Atmos. Environ. 11*, 819-828.

Singh, H. B., L. J. Salas, H. Shigeishi, and A. H. Smith. 1977b. Atmospheric fates of halogenated compounds: Second year (Phase I) Summary Report, SRI, August.

Singh, H. B., L. J. Salas, H. Shigeishi, and E. Scribner. 1979. Atmospheric halocarbons, hydrocarbons, and SF_6; global distributions, sources and sinks, *Science 203*, 899.

The Solar Output and Its Variation. 1977. O. R. White, Ed., Colorado Associated University Press, Boulder, Colorado.

Speranga, P. D. 1977. Measurements of terrestrial OH abundances by spectroscopic observation of resonance absorption of sunlight, MS Thesis, Florida Atlantic University.

Swinnerton, J. W., V. J. Linnenbom, and C. H. Cheek. 1969. Distribution of methane and carbon monoxide between the atmosphere and natural water, *Environ. Sci. Technol. 3*, 58-70.

Tyson, B. J., J. C. Arvesen, and D. O'Hara. 1978. Interhemispheric gradients of CF_2Cl_2, $CFCl_3$, CCl_4, and N_2O, *Geophys. Res. Lett. 5*, 535-538.

Vedder, J. F., B. J. Tyson, R. B. Brewer, C. A. Boitnott, and E. C. Y. Inn. 1978. Lower stratosphere measurements of variation with latitude of CF_2Cl_2, $CFCl_3$, CCl_4 and N_2O profiles in the northern hemisphere, *Geophys. Res. Lett. 5*, 33.

Volz, A., D. H. Ehhalt, and H. Cosatto. 1978. The vertical distribution of CFM and related species in the stratosphere, *Pure Appl. Geophys. 116*, 545-553.

Waters, *et al.* 1978. Mircowave measurement of upper atmospheric gases, p. 79 in *Proceedings of WMO Conference*, Toronto, June 26-30.

Williams, W. J., J. J. Coster, H. Goldman, and D. G. Murcray. 1976. Measurement of the stratospheric mixing ratio of HCl using infrared absorption technique, *Geophys. Res. Lett. 3*, 383-385.

Zander, R., G. Roland, and L. Delboville. 1977. Confirming the presence of hydrofluoric acid in the upper stratosphere, *Geophys. Res. Lett. 4*, 117-120.

8 THEORETICAL MODELS OF THE STRATOSPHERE

INTRODUCTION

Because of the complexity of our present description of physical and chemical processes in the stratosphere, theoretical models of atmospheric trace-species distributions have become essential diagnostic and prognostic tools. Such models are based on a set of conservation equations describing the effect on individual trace species of atmospheric transport, chemical and photochemical kinetics, and various natural and anthropogenic sources. The current status of the most important classes of physical processes has been reviewed individually in the preceding chapters. In this chapter we examine the status of research on stratospheric models and their application to problems in atmospheric pollution. The scope of the present discussion has been expanded beyond the NAS, 1976 report to include models both less and more complex than the one-dimensional models. This serves not only to present the bulk of results derived from one-dimensional models in the proper context but also as a reference point for future revisions. Various models are discussed according to the extent to which they have been developed.

The following section is a brief description of the different classes of models, including their characteristics. The next section on the modeling of trace species concentrations in the stratosphere begins with a definition of chemical and transport lifetimes. Stratospheric trace species are classified into long (years), intermediate (months and days), and short (less than a day) chemical lifetimes. The diagnostic capability of stratospheric models for each of these classes of trace species is then discussed. Finally, the nature of prognostic applications of theoretical models is discussed.

GENERAL CLASSIFICATION OF STRATOSPHERIC MODELS

Depending on the problems to be studied, models differ in the level of detail in which they represent the spatial variation of trace-species distributions. These differences in spatial resolution serve as a useful and convenient basis for model classification.

(a) *Box models*: These assume the total spatial homogeneity (complete uniform mixing) of individual trace species. Consequently, such models are represented by a set of ordinary differential equations describing the time evolution of individual trace species controlled by chemical interactions only. Such models have been very useful in the diagnosis of experiments in laboratory kinetics and in the analysis of global mass balance or long-lived trace species. Under limited and well-controlled circumstances they are useful even in the diagnosis of atmospheric measurement data.

(b) *One-dimensional models (1-D models)*: These simulate the vertical distribution of atmospheric trace species. They include a detailed description of chemical interactions. They also describe in a simplified way the effect of atmospheric transport. Net vertical transport is represented by a phenomenologically constructed transport parameter, given the dimension and form of a diffusion coefficient (cf. Chapter 4). Horizontal variations in composition can at best be inferred only indirectly. The models are thought to represent either global or midlatitude averages. One-dimensional models describe the main features of atmospheric chemistry without excessive demands on computer time.

(c) *Two-dimensional models (2-D models)*: These have spatial resolution in the vertical and meridional directions and, consequently, improved representation of transport. Such models may simulate seasonal and meridional variations of trace-species distributions but require considerable increase in computing and input data. Unfortunately, the transport representations remain mostly parameterized even for these complex models. There is still a lack of feedback from atmospheric chemistry to the dynamics. This feedback can only be included in a realistic sense in the three-dimensional models.

(d) *Three-dimensional models (3-D models)*: These, in principle, give the closest simulation of the real atmosphere. Through the solution in all three dimensions of the appropriate equations of continuity in momentum, energy, and the mass of each species, such models can include many of the feedbacks that are lacking in the simpler models. Computationally, however, they are very time-consuming, and, so far, the chemistry has been simplified to such a degree that important details may have been lost. Three-dimensional models with considerably more detail in chemistry are currently being developed, but their exact role in atmospheric trace-species studies is yet to be determined.

Since the detailed modeling of atmospheric chemistry is a relatively young science with overall information somewhat limited, most models have been diagnostic in their application and validation. The distribution and variabilities of most of the trace species have been modeled reasonably well (see next section), the most notable exceptions being the high ClO measurements of Anderson, which have already been discussed in Chapter 7.

The question of anthropogenic influences on the ozone layer requires the use of models for prediction. The capability of the models for making predictions over decades or centuries has never been adequately demonstrated and in all likelihood never will be without a well-developed long-term atmospheric monitoring program of nearly comparable duration. Limited validations such as the model predictions of the effects of PCA (polar cap absorption) events on polar stratospheric ozone and of the current stratospheric chlorofluoromethane distribution are reassuring but not conclusive. The study on PCA events, in particular, needs to be re-examined because of the strong coupling of NO_x, ClO_x, and HO_x cycles in the current chemistry, which was not accounted for in the original study. Furthermore, in a sensitivity study with 1-D models, Duewer *et al.* (1977) demonstrated that, under limited circumstances, diagnostically similar 1-D models of the stratosphere can indeed yield very different predictions for the effect of NO_x effluents from SST's on ozone. Consequently, it is necessary to recognize the distinction between prognostic and diagnostic applications of the same model and establish their individual limitations and uncertainties.

Box models can provide only limited information, especially with regard to predictions. However, because of their simple structure, in certain applications they are highly sensitive to uncertainties in input variables. For example, analysis of the atmospheric lifetime of long-lived halocarbons with box models has shown the lifetime to be highly sensitive to uncertainties in the ratio of measured global abundance to the total amount released. For F-11 and F-12, an uncertainty of 5 to 10 percent in this ratio would lead to an uncertainty of 25 to 50 percent in the deduced atmospheric lifetime (Chang and Penner, 1978). More sophisticated analyses involving trends in global abundance and amount released have similar uncertainties (cf. Chapter 5 and Cunnold *et al.*, 1978). Understanding this type of uncertainty is of particular importance in the search for tropospheric sinks. Similar uncertainties are present in the more complex models but are not so simply analyzed. Box models, with or without associated sensitivity analysis, help to establish the relative importance of physical processes (such as stratospheric sinks, tropospheric sinks, interhemispheric mixing rate, and nonuniform source rates) and suggest those problems that are most worthy of detailed examination with more complex models.

The structure of 1-D models has been described in detail in the NAS, 1976 and the NASA, 1977 reports. The vertical transport parameterization is mainly based on globally averaged values of vertical distributions of tracers such as N_2O and CH_4. Consequently, for other predominantly upward moving tracers, the 1-D model should be considered to be a globally averaged model. This is probably true also for the net downward moving tracers with long local chemical lifetimes in the altitude range of the tropopause. But in the stratosphere the detailed representation of the photochemical interactions is such that only local variables such as temperature and solar-flux intensity (both in space and time) can be used. This local dependence significantly complicates the interpretation of model results. The local chemical lifetime of all stratospheric chemical trace species depends on the local concentrations of O_3 and of $O(^3P)$ and $O(^1D)$, which are directly proportional to the local solar flux. Hence the self-consistently derived, odd-oxygen concentration profile in the 1-D model is positively correlated with the seasonal solar-flux intensity, contrary to observation of the seasonal variation of hemispherical and global ozone contents. In the absence of detailed information on the spatial and temporal variations of all the trace species either from measurement or more complex models, it is not possible to derive the proper averaging (weighting) factors for the nonlinear photochemical and chemical interaction processes in the 1-D model. Because of the essential role of odd oxygen [$O(^1D)$, O, O_3] in the life cycles of almost all other trace species in the stratosphere, all 1-D models are limited to representing local stratospheric conditions, in particular, that latitudinal region and season where the model-derived ozone profile closely represents the local measurements. Typically, 1-D models best represent the photochemistry of about 30° N latitude at about the fall equinox. However, this is also the region where there is considerable stratospheric and tropospheric exchange; hence we expect the actual local concentrations of trace species in the altitude range of 10-30 km to be strongly affected by fluctuations in atmospheric transport processes. Because of this mix of partially local and global representations, both the diagnostic and prognostic applications of the 1-D model must be applied and analyzed with great care with regard to the intrinsic compatibility of the model and its intended use.

The inclusion of the latitudinal dimension in 2-D models considerably reduces the above-mentioned difficulty of the 1-D model. These models are capable of representing the gross seasonal and latitudinal variations of odd-oxygen and other trace species. However, in considering the chemical and photochemical processes with greater resolution, we see the need to better resolve the relative role of chemistry and transport on yet finer scales. For example, Noxon (1978) has shown that, in order to understand the latitudinal distribution of column measurements of NO_2, an analysis of three-dimensional air-mass trajectory is a necessary step. The natural question as to the exact time and spatial scale that the 2-D model is capable of resolving is yet to be answered. The available results in both diagnostic and prognostic applications are encouraging, and in future years the 2-D models may prove to be the most useful models in understanding stratospheric chemistry.

Three-dimensional models are simply too time-consuming to be used widely in prognostic studies of the effect of anthropogenic influences on ozone. They are most valuable in examining the effect of coupling processes incompletely represented in the simpler models. Examples of such processes are three-dimensional transport, radiative-transport coupling, chemical-radiation-transport coupling, and accuracy of spatial and time-averaging techniques in simpler models. Three-dimensional models with up-to-date chemistry are still being developed, and the currently available results from 3-D models all deal with transport as the controlling process. Although the detailed representations of stratospheric chemistry are continuously being improved in 3-D models, it will be several years before they are comparable with that of the 1-D or even 2-D model. In summary, 3-D models with photochemistry will probably remain for the most part a research tool in the near future.

MODELING TRACE-SPECIES CONCENTRATIONS IN THE STRATOSPHERE

The results of a model calculation can be evaluated by comparison with suitably obtained atmospheric measurements. Several basic types of information have proven to be useful, in particular, the height and latitudinal distributions of individual species and groups of species, the partitioning of related species, and the local diurnal and seasonal variations of individual species. Comparisons with these data help to test the diagnostic and to a certain extent also the prognostic adequacy of the model. For the reasons outlined in the previous sections, interpretation of the results from such tests are not always simple and must be accepted with various degrees of qualification. The demonstration of the general, overall agreement of the models with observations, however, provides a level of confidence in their basic reasonableness. Of course, such judgment has a large subjective component.

The measured atmospheric trace-species concentrations have shown a significant degree of local variability (see Chapter 7), which makes comparisons between measurement data and modeling results somewhat subjective and, at times, somewhat inconclusive. As the data base and theoretical models continue to improve, the nature of atmospheric variability should be better understood, and its influence on data interpretation must be dealt with.

The following formulation will provide the theoretical framework for the discussions in the rest of the chapter. The total rate of change in a volume, V, of any given trace species or sum of trace species in the atmosphere X is given by

$$\frac{dX}{dT} = F_i - F_o + P - L$$

where F_i and F_o are the net transport flux of X into and out of the volume V, respectively; P and L are, respectively, the total chemical production and loss of X in the volume V. Since the mathematical signs associated with gain and loss are included in this equation all quantities F_i, F_o, P, and L are positive. The usual definition of lifetime due to a particular process, i.e., the ratio of local concentration, X, divided by the given loss rate, then simply defines the transport and chemical lifetimes, respectively, as

$$\tau_T = \frac{X}{F_O} \text{ and } \tau_C = \frac{X}{L}$$

At a given time and location, whether the concentration of a variable X is more influenced by transport and by chemistry can be determined according to the relative magnitude of τ_T and τ_C. If τ_T is greater than τ_C then local chemistry is a more dominant factor in determining the species concentrations that one measures. If τ_T is less than τ_C then transport is more dominant. Although these lifetimes have not yet been obtained from field measurements, they may be estimated from other data or theoretical models. Such estimates are very useful in interpreting modeling results and measurement data. For example, F-12 has practically infinite chemical lifetime in the troposphere, hence its distribution and total content are completely due to transport processes and distribution of release rates. If a model uses the correct source function, then any disagreement in tropospheric content of F-12 between model and atmospheric data would be due to the error in the net upward transport flux of F-12 in the model. On the other hand, almost all F-12 is destroyed in the stratosphere, resulting in no net outgoing flux. Hence any differences between theory and data on the total content of stratospheric F-12 would indicate an error in the stratospheric destruction rate of F-12. Furthermore since the local (at any given altitude) chemical lifetime of F-12 below 25 km is longer than one year, the variability in local F-12 data should be consistent with the fluctuations in atmospheric transport at those altitudes. Unless a theoretical model can represent such variability below 25 km, detailed comparison with F-12 data gathered at different times and places would not be instructive. Gaining the ability to model the stratosphere well enough to be able to make such comparisons is one of the critical advances in stratospheric studies needed in the future.

The basic model used in the following discussion and for the predictions of the next chapter is the model developed at Lawrence Livermore Laboratory (LLL) by Change and coworkers. Most of the details have been discussed in Appendix D of the NAS, 1976 report. Since 1976, several significant improvements have been made in this model, as in other models at Goddard Space Flight Center (GSFC), National Oceanic and Atmospheric Administration (NOAA), National Center for Atmospheric Research (NCAR), Harvard, Dupont, and other institutions. The most significant change is the formulation of a totally self-consistent diurnal averaging procedure for the nonlinear chemical reaction terms. Consequently, a major difficulty of the 1-D model pointed out in the previous report has been solved. Furthermore, the current model contains a radiative-transfer submodel, which can provide temperature profiles consistent with natural or perturbed O_3, H_2O, CO_2, and NO_2 vertical profiles, thereby allowing an analysis of the temperature-chemistry feedback process. The only fixed trace species in the model are N_2, O_2, H_2, CO, and H_2O below 12 km. The model can either be run as a fully diurnal model (following the sunrise and sunset exactly) or as a diurnally averaged model using the proper averaging procedure provided by fully diurnal calculations. Overall, this model is more complex and more detailed than many other models except for the parameterization of methane oxidation in the lower stratosphere. After a detailed comparison with the Harvard, GSFC/NASA, and NOAA models, it was concluded that this reference model (LLL model) is representative of the current generation of 1-D models. Although among these 1-D models there are still many differences in the basic model structure, such as the type of boundary conditions, solution techniques, the model vertical resolution, and details in radiative transfer submodel, the agreements among model results are within the natural variations in the measured data. Unfortunately, at present, there is no such cross-verification and communication in 2-D model development. In fact, most 2-D models are rather incomplete in the representation of current stratospheric chemistry. Consequently, only limited qualitative results can be derived from such models. It is expected that in another two years many more results will be derived from 2-D models. As was mentioned before, 3-D models are still under development, and the limited results are not directly applicable to the analysis of trace-species distributions.

In order to establish a theoretical model for the current stratosphere so that comparison with the atmospheric measurement data of recent years might be made, a time-dependent calculation was carried out with the reference model using the published CFM release rates as source functions. This was necessary, because the chlorine content of the stratosphere is not constant in time. Current estimates indicate that CFMs are a principal source of atmospheric chlorine, which they have been releasing into the atmosphere for about 30 years, and that the process is still continuing. Consequently, the chlorine budget of the stratosphere is continuously increasing. This time-dependent calculation not only provides a current stratosphere for diagnostic purposes but also provides a test for the model in predicting the accumulation of CFMs in the troposphere and their vertical distributions in the stratosphere. In this calculation, it is assumed that currently observed tropospheric concentrations of CCl_4 and CH_3Cl are the source for background chlorine. CH_3CCl_3 is not used mainly because of the apparent conflict between the CH_3CCl_3 budget and the measured HO concentrations in the lower troposphere; there is at present no way of reconciling this conflict within a totally self-consistent model. With or without CH_3CCl_3 as a source of present stratospheric chlorine, the analysis of the following sections are the same, except where noted. Starting with this background chlorine, CFMs are released according to the time history. The vertical profiles of minor trace species, established by the model for January 1978 is shown in Figures 8.1-8.6. These are all diurnally (24-h) averaged quantities. The relevant noontime and nighttime values are discussed in individual sections. The performance of stratospheric models in predicting the vertical distribution of known trace species that are believed to be important to ozone chemistry is discussed in the following sections (with the data base from Chapter 7).

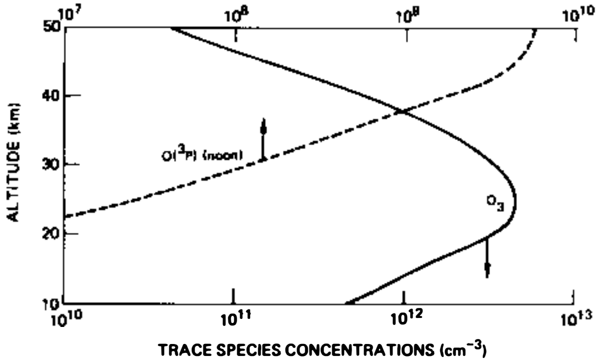

FIGURE 8.1 Vertical profile of oxygen atoms and O_3 concentration.

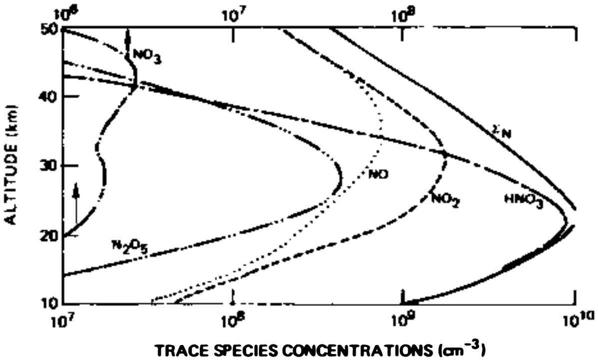

FIGURE 8.2 Concentrations of odd-nitrogen species.

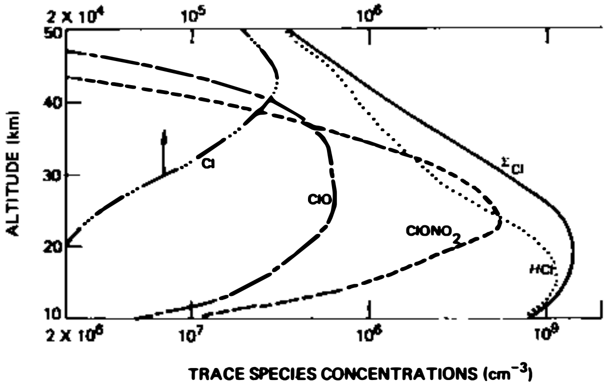

FIGURE 8.3 Concentrations of odd-chlorine species

TRACE SPECIES WITH LONG STRATOSPHERIC CHEMICAL LIFETIME

The trace species N_2O, CF_2Cl_2, $CFCl_3$, CCl_4, CH_3CCl_3, CH_4, CH_3Cl, and H_2O all have stratospheric chemical lifetimes of at least a year or more. Consequently, their stratospheric abundance is totally determined by fluxes from the troposphere (strictly speaking this is not true for H_2O, as will be explained below). In fact these species are the sources for all the minor trace species in the stratosphere that are known to be essential in ozone chemistry.

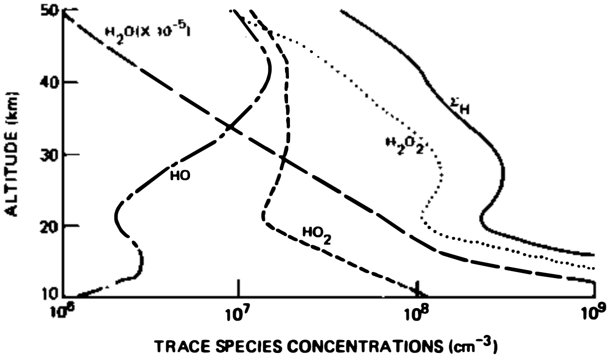

FIGURE 8.4 Concentrations of odd-hydrogen species.

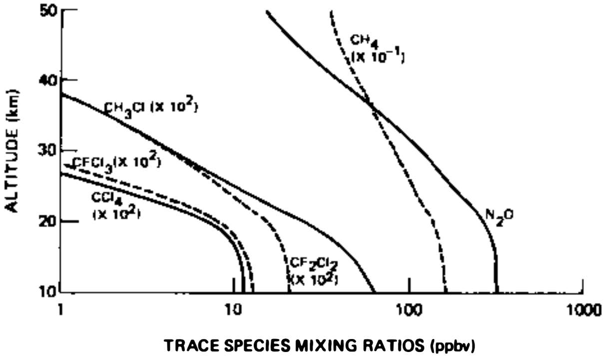

FIGURE 8.5 Long-lived trace species mixing ratios versus altitude.

Nitrous Oxide (N_2O)

The basic input variable for modeling N_2O is its observed tropospheric mixing ratio. Models can either use this number directly or convert it to a source flux derived from the measured mixing ratio and an assumed atmospheric lifetime. The reference model uses 320 ppbv at the surface as an input parameter; current measurements give 319 ± 10 ppbv in the troposphere. In the stratosphere, N_2O local chemical lifetime increases from 6 months at 35 km to thousands of years near the tropopause. In fact, one may

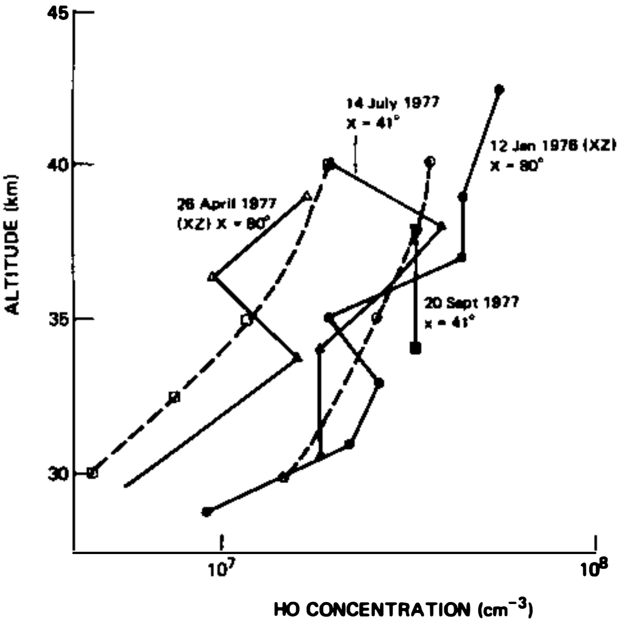

FIGURE 8.6 Comparison of measured and calculated HO profiles (measurements by J. G. Anderson, Harvard University).

⊙ January 2, 1976 Solar zenith angle, $x = 80°$
□ September 20, 1977 Solar zenith angle, $x = 41°$
Δ July 14, 1977 Solar zenith angle, $x = 41°$
● April 26, 1977 Solar zenith angle, $x = 80°$

Values at $x = 80°$ have been multiplied by a factor of 2. Theoretical values at $x = 41°$ and 80° are shown as dashed curves.

state that the variability of its vertical concentration profiles in the lower and middle stratosphere is strictly due to atmospheric transport process. One-dimensional and even 2-D models can at best provide a global qualitative picture, but no exact quantitative agreement, locally. The 1-D models can indeed simulate the average vertical distribution of N_2O. Both N_2O and CH_4 have been used as tracers for deriving the effective net vertical diffusion coefficient in 1-D models, although their estimated chemical lifetimes are directly dependent on the detailed results from the model. Therefore, such agreement between data and model results is a necessary condition. This self-consistency confirms that the model is functioning as expected, i.e., the more complex full model does not change the expected chemical cycles of N_2O and CH_4; hence no re-evaluation of the effective diffusion coefficient is necessary.

Methane (CH_4)

Methane behaves much the same as N_2O in the atmosphere, except that it has a comparatively short lifetime of approximately 10 years in the troposphere, as a result of reaction with HO. Differences between northern and southern hemisphere data may be detectable and used to estimate average HO concentrations in the troposphere (Ehhalt, 1978). The reference model uses 1.64 ppmv (cf. Chapter 7) of CH_4. Since the local chemical lifetime of CH_4 increases from 6 months at 40 km to more than 10 years at the tropopause, its stratospheric variability is also controlled by transport processes. In particular, the qualitative latitudinal similarity in the vertical profiles of N_2O and CH_4 from 5° S and 40° N confirms this view (Chapter 7).

Carbon Tetrachloride (CCl_4) and Methyl Chloride (CH_3Cl)

As input parameters, the reference model uses 112 pptv of CCl_4 in the troposphere, which is at least 10 percent lower than the currently available averages but certainly within the limits of data uncertainty. CCl_4 is virtually indestructible in the troposphere but photodissociates in the stratosphere. Its local chemical lifetime is of the order of 6 months at about 24 km. Therefore, in addition to the instrumentation difficulties associated with grab sampling (Chapter 7) there should be large variability due to transport, making interpretation of stratospheric measurements of CCl_4 a rather difficult task. Measured concentrations of CH_3Cl have shown so wide a spread that it is difficult to assess the adequacy of model results. Nevertheless, with an input of 746 pptv at the surface (which is approximately in the middle of the range for Rasmussen's data in 1977), the model estimates 580 pptv at the tropopause, which seems to be consistent with the 550 pptv reported by Cronn *et al.* (1977). The estimated local chemical lifetime is approximately 1 year up to 26 km. This again makes transport variability an important factor in the interpretation of CH_3Cl data.

F-11 ($CFCl_3$) and F-12 (CF_2Cl_2)

F-11 and F-12 are the focal point of this study, and their atmospheric abundance serves as a true test of the ability of simple 1-D models to represent the average net vertical transport of trace species. The release rates of these chemicals and of CH_3CCl_3 are well documented (Chapter 2). Since the model uses only the time-dependent source rate (release rate) in computing its atmospheric distribution, a comparison of both the model-derived tropospheric and stratospheric burdens with measurement data would be a stringent test of the adequacy of the model. As reported in Chapter 7, global averages of F-11 and F-12 in the troposphere are not readily obtainable. If the northern hemisphere averages as reported in Chapter 7 are used to estimate the global average in January 1978, the reference model is at most 10 percent lower than the tropospheric burdens of F-11 and F-12. About 5 to 8 percent of this is attributable to the accuracy of the approximate source function used in the model. Hence the averaged net vertical transport in the model is at most 10 percent off (at least as far as F-11 and F-12 are concerned). This near agreement then provides a partial (but important) confirmation that the transport approximations based primarily on N_2O and CH_4 indeed have a more general validity and applicability. Similar to other trace species with long local chemical lifetimes, both F-11 and F-12 are sensitive to variations in local transport processes at altitudes up to 30 km for F-11 and 40 km for F-12. This is again consistent with observation. In general, the model-predicted stratospheric vertical profiles of $CFCl_3$ and CF_2Cl_2 are both slightly on the high side of the data averages (taking the model tropopause to be at 12 km). The model seems to show slightly more destruction in the lower stratosphere (5 to 10 km above tropopause) for $CFCl_3$ than the data suggest. On the other hand, this could be due to weaker net upward transport in the model. Fortunately, in the maximum destruction altitude of $CFCl_3$ and CF_2Cl_2 (20 to 30 km and 25 to 40 km, respectively), the model-predicted profiles are in reasonable agreement with available data.

Methyl Chloroform (CH_3CCl_3)

At this time there is considerable uncertainty in the interpretation of measurement data and the modeling of atmospheric concentrations of CH_3CCl_3. A simple box-model analysis based on measurement data would yield a CH_3CCl_3 atmospheric lifetime of 5 to 12 years. This, in turn, would imply an average tropospheric HO concentration of less than 10^6 molecules/cm^3. However, most stratospheric-tropospheric coupled models have more HO than this estimate, which then leads to a much lower CH_3CCl_3 concentration in the atmosphere if the well-known release rates are used (Neely and Plonka, 1978). Although CH_3CCl_3 is estimated to be a major source of stratospheric chlorine and could provide another direct test on the adequacy of models, it is not practical to include it in the 1-D model at this time in the same manner as the other sources of stratospheric chlorine. The reference model used in this report has temporarily omitted this source, which could contribute from 0.2 to 0.3 ppbv of chlorine to the stratosphere. This omission is of no practical consequence to the present report as far as the effect of F-11 and F-12 on ozone is concerned.

Water (H_2O)

Methane is a principal source of water in the stratosphere. At the tropopause, H_2O concentration is maintained both by a downward flux from the stratosphere and an upward flux from the troposphere. It is believed the tropospheric-stratospheric exchange process helps to maintain H_2O at the saturation level at the tropical tropopause and, hence, in the rest of the stratosphere. 1-D models generate reasonable H_2O vertical profiles well within the uncertainty of the data, starting with 3 ppmv at the tropopause and slowly increasing to 5 ppmv at 50 km. Again, since stratospheric water has only weak chemical sinks and sources, its variability is mostly due to transport fluctuations (see also the discussion in Chapter 7).

Hydrofluoric Acid (HF)

Unlike other species in this class, HF is produced in the stratosphere (as the principal end product of F-11 and F-12 destruction in the stratosphere). Its local chemical lifetime is more than a year, even at the height of 50 km. Consequently, the stratospheric distribution of HF is very much influenced by atmospheric transport. The measured mixing ratios in the range of 1×10^{-10} to 3.6×10^{-10} at about 30 km (Chapter 7) are consistent with the model predictions of approximately 2.4×10^{-10} at 30 km.

Analysis of the latitudinal variations in HO and, hence, HCl concentrations, demonstrates that, in order to simulate the HF/HCl ratios, local conditions must be used. The data of C. B. Farmer and O. F. Raper (Jet Propulsion Laboratory, 1977) at 33° N latitude cannot be simulated in the absence of appropriate, local O_3 data. The data of Buijs *et al.* (1978) at 65° N are consistent with model calculations at this latitude. The observational data on HF and HF/HCl ratios have a range of uncertainty of a factor of 3. Until this uncertainty range is narrowed, the lower values of HF cannot be taken as conclusive evidence for incomplete chemistry in the models.

Total Chlorine

Table 8.1 summarizes the sources of chlorine in the model and compares them with the estimates from tropospheric data. As was pointed out before, the reference model probably underestimates the total budget by not including the uncertain contributions of methyl chloroform. This total tropospheric source of 2 ppbv of odd chlorine results in a 1.7 ppbv of ClO_x at 40 km because of the photochemical destruction at lower altitudes of the source molecules. By comparison, the total NO_x mixing ratio at 40 km is 15.9 ppbv and the total HO_x mixing ratio at 40 km is 3.2 ppbv.

TABLE 8.1 Concentrations of Stratospheric Chlorine from Various Sources as Estimated from Tropospheric Data and Calculated in the Reference Model

	Estimate from Tropospheric Data (ppbv)	Reference Model (ppbv)
CH_3Cl	0.47-0.77	0.75
CH_3CCl_3	0.12-0.27	0.00
CF_2Cl_2	0.48	0.42
$CFCl_3$	0.42	0.38
CCl_4	0.49	0.45
TOTAL	1.98-2.43	2.00

TRACE SPECIES WITH INTERMEDIATE STRATOSPHERIC CHEMICAL LIFETIME

Trace species such as HNO_3 and HCl have chemical lifetimes of about a week in the stratosphere. Similarly the well-known trace-species families O_x $[O(^1D) + O(^3P) + O_3]$ and NO_y $(N + NO + NO_2 + NO_3 + HNO_3 + 2N_2O_5)$ also have net chemical lifetimes of about a week. The chlorine family, ClO_x (Cl + ClO + HCl), has a somewhat shorter stratospheric chemical lifetime on the order of ½ to 1 day. This is due to the strength of the coupling reaction $ClO + NO_2 + M \rightarrow ClONO_2 + M$, since neither of the above (usual) definitions include $ClONO_2$. If we consider the broader family ClO_y $(ClO_x + ClONO_2)$, then it becomes a pure tracer with no chemical loss, except possibly through the incompletely quantified reactions involving HOCl. This arbitrariness in defining the family of trace species illustrates clearly the point that if complete simultaneous measurements of all the members of a family were obtained, for example the ClO_y, then all variability in the data would be due to processes other than photochemistry. On the other hand if only part of the family members are measured simultaneously (in the present example ClO_x, i.e., without $ClONO_2$), then the variations due to chemical reactions involving the missing members, i.e., $ClONO_2$, must be considered.

Together with the HO_x family $(H + HO + HO_2 + 2H_2O_2)$ (to be discussed later), the O_x, NO_y, and ClO_y families include almost all the trace species that are of major interest in stratospheric chemistry. The O_3, HNO_3, and HCl downward fluxes from the stratosphere represent almost all of the transport loss of the trace species in their respective families, and the transport time scales are all of the order of a year or more. Because of these similarities and relations, it is appropriate to discuss these families here and leave the partitioning of individual families to the next section.

Odd Oxygen (O_x, O_3)

In the stratosphere the dominant O_x species is O_3. $O(^3P)$ begins to contribute more than a few percent only about altitudes of approximately 45 km. A comparison of the model-derived O_3 distribution with atmospheric data therefore represents an evaluation of the whole O_x family in the stratosphere. The reference model vertical profile of O_3 (Figure 8.1) compares well with the average profile obtained by Watanabe and Tohmatsu (1976) at 30° N. Below 25 km it is less than the midlatitude profile of Krueger and Minzner (1976). This is expected, since this midlatitude profile is a geometric average of data at given heights from all latitudes, including the downward displaced ozone peaks at high latitudes, which are the result of meridional transport. Because of the ambiguity about whether a 1-D model is truly global, the present study will use the local ozone vertical distribution for comparison with the reference model but include the uncertainty in transport as a separate uncertainty factor in the final analysis (Chapter 9).

Odd Nitrogen (NO_y, HNO_3)

The principal source of odd nitrogen in the stratosphere is N_2O through reaction with $O(^1D)$. There is also a small amount of ion-molecule reactions initiated by cosmic rays. Since most of the production occurs below 35 km, with a small net loss from the N + NO reaction above 45 km, total NO_y in the model is fairly uniformly distributed between 30-45 km, with a mixing ratio of 19 ppb at 40 km. The corresponding NO_x mixing ratio of 10.4 ppbv at 25 km compares well with the range of measured values (Chapter 7), while at 35 km the NO_x mixing ratio from the model (15.4 ppbv) is at the high end of the stratospheric data range. This is considered to be reasonably good agreement, since this data range is composed of many individual, totally independent measurements. The HNO_3 vertical profiles from the reference 1-D model is still on the high side of the measured data range. This is typical of all 1-D models. The peak of the HNO_3 mixing ratio is about 23-25 km and, in general, is consistent with all the available data. Although total NO_y has a fairly uniform average source function and is probably uniform latitudinally, HNO_3 has a local chemical lifetime of 10 to 20 days throughout the altitudes where HNO_3 is most abundant and can vary significantly over a few days as was found by Murcray *et al.* (1978). The increase toward the pole in HNO_3 above 18 km found by Murcray *et al.* (1978) appears qualitatively consistent with the latitudinal changes in the solar-flux intensity and temperature.

HNO_4 plays a relatively minor role in stratospheric chemistry. Models that include it find HNO_4 to amount to about 15 percent of HNO_4 and to have a height profile similar to HNO_3.

Odd Chlorine (ClO_y, HCl)

Since the total stratospheric chlorine in the model can only be removed as HCl through the downward transport into the troposphere, its stratospheric mixing ratio can be estimated from the source species mixing ratios in the troposphere. If we disregard, for the moment, the two high values of ClO vertical profiles by Anderson (Chapter 7), then the total ClO_y mixing ratio at 20 km is approximately 0.5 to 1.0 ppbv (all HCl), and at 35 km it is 1.6 to 2.3 ppbv. The reference model gives 0.75 ppbv at 20 km and 1.65 ppbv at 35 km, which agree reasonably with the experimental values. The two high ClO profiles of Anderson by themselves would indicate a ClO mixing ratio of 1.4 and 3.3 ppbv of chlorine at about 35 km. Together with the estimated 1.7 ppbv of HCl this would require a source of at least 3 to 5 ppbv of chlorine. Such large values are simply not accountable by current understanding of the sources and sinks of chlorine in the atmosphere. Although Waters *et al*. (1978) provided some data that disagree with one of the high profiles, a more definitive explanation of the discrepancies between the photochemical theory and the high measurements by Anderson is still required.

In the lower stratosphere, HCl is the predominant form of ClO_y. The model gives mixing ratios of 0.28 ppbv at 15 km and 0.55 ppbv at 20 km, which can be compared with the measured values of 0.2 ppbv and 0.3 to 0.7 ppbv at these altitudes, respectively. If these observed values are used to estimate the downward flux of odd chlorine, then theory and experiment agree within factors of 2 to 3. This near agreement provides another independent estimate of the degree of uncertainty due to transport. The dip in the HCl vertical profile at 30 km as reported by Lazrus *et al*. (1977) and Williams *et al*. (1976) is not explicable within the context of 1-D models. But a preliminary 2-D calculation by Pyle (1978) suggests that HCl has local maxima and minima in the vertical direction, extending from near the equator to the polar region. A balloon experiment around 32° N would be quite likely to sample through this region and observe a dip in the vertical profile. This result coupled with the ClO result (see next section) further demonstrates the limitations of a 1-D model and at the same time suggests the potential usefulness of the ability of 2-D models for taking into account the effect of horizontal transport and the representation of local chemistry at individual latitudes and seasons.

With the current photolysis rate coefficients, HOCl is a minor chlorine component; its concentration is calculated to be similar to ClO. Its presence decreases the calculated ClO concentration by about 15 percent (Figure 8.3) in the altitude region between 25 and 35 km. HOCl has a very small effect on the efficiency of the chlorine catalytic cycles in destroying ozone.

TRACE SPECIES WITH SHORT STRATOSPHERIC CHEMICAL LIFETIME

Individual trace species NO, NO_2, NO_3, N_2O_5, $O(^3P)$, Cl, ClO, $ClONO_2$, HO, HO_2, and H_2O_2 all have much shorter chemical lifetimes than the previously discussed species. As a result, their individual local concentrations are quite variable, usually on a time scale of hours to seconds. They all vary diurnally (except H_2O_2) and seasonally and probably even vary on the time scale of changing albedos because of the presence of aerosols and clouds at lower altitudes. It is usually impossible to obtain local conditions such as solar flux, temperature, and local concentrations of several related trace species in a single measurement experiment. Hence, it is rarely possible to compare quantitatively the available data on these trace species with theoretical models. However, if individual collections of data are used as a group, then the total local variability in the data is often a good guide for testing the theory. For example, the range of variations in data should be within the limit of model predictions; otherwise the model must be considered inadequate in representing this set of data. Furthermore, variability in the shape of individual vertical profiles is also a useful indicator of the acceptable domain of model results.

Odd Nitrogen (NO, NO_2, NO_3, N_2O_5)

Since 1972, there has been a considerable number of NO measurements in the stratosphere. By now its stratospheric variability is well established, and any attempt to model a particular set of data of NO alone has long been deemed as not very useful, except for the diurnal cycle of NO. As was pointed out in the NAS, 1976 report, the successful modeling of the NO diurnal cycle confirmed locally the accuracy of the NO_x catalytical cycle. The reference 1-D model yields an NO mixing ratio of 0.1 ppbv at 20 km gradually increasing to 9.0 ppbv at 50 km. This theoretical profile is practically in the middle of the available data. Without, at least, a simultaneous measurement of NO_2, individual NO data will be of steadily declining usefulness in the future.

Modeling of stratospheric NO_2 distributions suffers from the same difficulty as that of NO because of their coupling through the NO_x catalytic cycle. Although through the use of the appropriate solar flux, temperature, and ozone a 1-D model can approximate the low NO_2 column measurement at latitudes above 50° N (Noxon, 1978), a full explanation involves the coupling of three-dimensional transport and photochemistry (Noxon *et al.*, 1978a). Nevertheless, on the average, simple 1-D models do produce NO and NO_2 distributions that are consistent with stratospheric data.

Stratospheric NO_3 abundance as estimated by photochemical models falls far short of the observed amount (Noxon *et al.*, 1978a). This could be due to errors in the accepted rate coefficients as suggested by Noxon *et al.* (1978a). This suggestion is still tentative since it is based on a single set of data without much corroborating data on local temperature and ozone concentrations. Fortunately, this unsettled state of affairs is of minimal importance to this study, since NO_3 does not play a significant part in determining the concentrations of ClO_x.

The current estimates of stratospheric N_2O_5 concentrations are all consistent with the model. The upper limit of 0.1 ppbv at 18.3 km by Murcray *et al.* (1978) and the 3 ppbv at 30 km deduced by Evans *et al.* (1978) agree with the results from diurnal calculations under comparable conditions of 0.06 ppbv and 2.1 ppbv, respectively.

$O(^3P)$

The local concentrations of $O(^3P)$ are directly proportional to the local ozone concentrations and solar-flux intensity. The agreement between theory and experiment data is good; the small differences in detail reflects similar differences in O_3.

Cl, ClO, and $ClONO_2$

Most of the available data on Cl and ClO are from Anderson *et al.* (1977; in press). The two measured high values of ClO are not reconcilable with current theoretical understanding and suggests that there may be major weaknesses in the current theory. The other four ClO profiles, on the other hand, are in reasonable agreement with theoretical models. A major discrepancy is the rate of decrease in ClO concentrations with decreasing altitude; one-dimensional models yield a much more gradual decrease. The 2-D calculations by Pyle (1978) show that near 30° N (where Anderson *et al*. collected their data) there is indeed a much sharper vertical gradient between 20 and 35 km than that derived from 1-D models; apparently a result of transport processes in this region.

These 2-D model results are, of course, preliminary, but highly encouraging.

Although $ClONO_2$ was shown to be a critical species in the assessment of CFM impact on stratospheric ozone, up to now only an upper limit on stratospheric abundance has been suggested. The limit of 0.3 ppbv at 20 km is at least a factor of 2 higher than the model indicates. The measurement is therefore inconclusive, although somewhat reassuring.

Odd Hydrogen (HO, HO_2, H_2O_2)

The calculated concentrations of HO_x shown in Figure 8.4 are all diurnally averaged values. Both HO and HO_2 undergo gradual changes throughout the daylight hours. For both HO and HO_2, the ratio of noon values to the diurnally averaged values could be as much as 5 in the winter hemisphere high latitudes and in the present case (30° N, fall equinox) is approximately 2.5 in the altitude range of 10 to 20 km, and slightly greater than 3 between 20 to 30 km; it then gradually decreases to around 2 at 45 km. Because of this large averaging factor and the gradual diurnal changes, only diurnal models should be used for comparison with experimental data. Between 30 to 40 km the model-estimated HO_2 profile at comparable times of the day during the fall season lies on the low side of the data of Anderson *et al*. (1978), approximately $4.6 \times 10^7/cm^3$ as compared with an average of $7 \times 10^7/cm^3$ (Figure 7.7). At 30 km the local value near sunset is also about a factor of 2 less than the data by Mihelcic *et al*. (1978). Considering the rate of change of local HO_2 concentrations near sunset and the uncertainty in the exact time when the data were collected, this disagreement is not significant.

The HO diurnal profiles compare very well with the available data between 30 to 40 km (Figure 7.8). At the corresponding time the theoretical profiles both ($\chi = 41°$ and

χ = 80°) fall in the middle of the data range (Figure 8.6). This agreement is probably fortuitous since there are no corroborating data on CH_4, H_2O, and ozone, which are essential in determining the local concentrations of HO. Unfortunately, in the critical region (Chapter 9) of 10 to 30 km there are no data on HO and HO_2.

The only estimated value of H_2O_2 at 20 km is an upper limit too far above the model concentrations to be of real use. Because of the central role played by HO_x in determining the effect of changes in NO_y concentrations on ozone, lower stratospheric measurements of HO, HO_2, and H_2O_2 have become more important than ever.

Overall, the data on HO_x seem to support the adequacy of the theory for the present application to potential chlorine perturbations, but for other prognostic applications such as NO_x perturbations, refinement of HO_x budget and chemical cycles must be carried out.

PROGNOSTIC APPLICATIONS OF MODELS

In prognostic applications, the models are used to evaluate the response of the chemical system to changes in certain parameters. In choosing a model for this purpose we ask, "Can the model predict the effects of interest?" and "To what extent should the predictions be accepted?" If the changes lead to a steady state (this is usually easily established) and we are interested only in the final state, then the prognosis required is nothing more than the diagnosis of this future state. Therefore, all the model techniques developed for present diagnostic applications can be used, except that no data are available for verification, and the constrained variables used are themselves predictions. If the actual path to the final state is also of interest, then a time-dependent model is necessary. The time-dependent solution can also provide the final state, but only at considerably higher cost than the steady-state solution techniques used in the first type of analysis. Thus, the sophistication of the model used should be commensurate with the detail of the output desired.

For predictions of events on the time scale of decades to centuries, testing and verification through new field measurement programs are not always feasible. *A priori* estimates of the reliability of such model predictions are necessary. This is especially so if current predictions are to be used as a basis for policy decisions. There are at least four ways of assessing the quality of model predictions. These are (a) comparing observed and computed concentrations in the present ambient atmosphere, (b) comparing the predictions of various modeling efforts with each other, (c) analyzing model response to known uncertainties in input parameters, (d) comparing model predicted response to perturbation with the observed response to perturbations. All of these approaches, for one reason or another, are currently of limited value and can only become more useful through a vigorous research program.

Comparison of observed and calculated ambient atmospheres provides a necessary condition for model acceptance (at least as far as properties that affect the matters of primary interest are compared). However, different models with radically different perturbational sensitivities can yield predicted ambient atmospheres (i.e., diagnostics) that differ by less from one another than do various atmospheric measurements (Duewer *et al.*, 1977; Stolarski *et al.*, 1978). Thus, reasonable agreement between model and observed ambient atmospheres does not imply that the perturbational sensitivity of the model will be correct. As more data become available for comparison with models, and the relationships between observation and model output are better understood, models will become increasingly constrained and the latitude for error correspondingly reduced.

Because various modeling groups differ somewhat in their interpretation of available data and in their choice of approximations, model predictions do differ. However, at any period of time, most models used very nearly the same data bases, made similar interpretations of most of the data, and used approximations that yielded rather similar results. For example, in studying the potential effects of SST operations at 20 km, most models predicted ozone changes at steady state of roughly -10 to -18 percent in 1975 (Grobecker *et al.*, 1974) and +2 to -1 percent in 1978 (Broderick, 1978; Popoff *et al.*, 1978). The change in predictions over the three-year time period reflects both new measurements of reaction-rate coefficients and the recognition of the importance of including chlorine chemistry. Thus, degree of agreement of the predictions of different models is (excluding speculations and obvious errors) likely to lead to an overoptimistic interpretation of the uncertainty in the prognosis.

The analysis of model response to uncertainty in input parameters might be carried out by a variety of techniques. Monte Carlo-type numerical experiments (Chapter 9; Stolarski *et al.*, 1978; Rundel *et al.*, 1978) have been used to estimate the uncertainty in predictions of the impact of CFMs on stratospheric ozone due to uncertainties in the chemical-rate constants employed in the model. Study of the sensitivity of model predictions to variations in individual parameters or groups of input parameters can yield essentially the same type of information. One obtains a distribution of calculated effects with some expected error (1σ or 2σ error) and some skewness. Unfortunately, these parameters are likely to provide only a lower bound to the expected error in model predictions. This is the case because such experiments do not include potential errors introduced by the basic model structure, unknown or omitted processes, or any of a myriad of other potentially severe sources or error in addition to the estimated errors in measured chemical rate coefficients.

The fourth method of assessing the reliability of model predictions is to compare model predictions of the atmospheric response to actual perturbations with the observed response. Unfortunately, for such comparisons to be convincing, the real observed perturbation must be fairly close to the perturbation of interest. If the models predict a severe, persistent response to a perturbation (as is the case for a large increase in CFMs) the potential environmental cost of carrying out the experiment (or permitting it to proceed) may more than outweigh one's desire to have more confidence in model predictions before acting on them. In any case, the magnitudes of the perturbations required for the models to predict an observable response similar to those of current concern are typically quite large and beyond direct experimentation (see Chapter 9).

This leaves us with the possibility of examining the ozone record for effects of past events. A list of potentially interesting events has been prepared by Bauer (1978). There are no well-characterized past events that provide large-scale injections of chlorine, although volcanic eruptions, especially the 1963 Agung eruption, may have done so. There are two types of past events that may have increased stratospheric NO_x sufficiently to have affected ozone during the period for which ozone measurements exist. These are the large atmospheric nuclear tests of the 1950's and 1960's (Foley and Ruderman, 1973; Chang *et al*., 1979) and large polar-cap absorption events (Heath *et al*., 1977). At present, the model-predicted response of the ozone column to the nuclear tests is smaller than the unexplained variability in the ozone record (Chang *et al*., 1979). Thus comparison of the ozone record with the computed effects of the nuclear tests on total ozone provides only an upper limit to the sensitivity of stratospheric ozone to such an injection of NO_x. Larger local perturbations in ozone are predicted in the upper stratosphere from the nuclear tests. However, the measurements of ozone at the altitudes most likely to have been affected are of dubious quality.

The large polar-cap absorption event of August 1972 was accompanied by apparent decreases in upper-stratospheric ozone at high latitudes. The observed changes in ozone were in close agreement with the response calculated using a two-dimensional model with chemistry current at that time (Heath *et al.*, 1977). Since 1976, the representations of the chemistry have changed in ways that have greatly altered their perturbational response to lower-stratospheric injections of NO_x. However, the calculated response of the upper stratosphere to NO_x increases has been relatively unchanged. Thus, it is likely that the models would continue to represent this perturbation reasonably well, although no new calculations have been made.

Another type of prognostic application has been the prediction of the atmospheric response to variations in solar flux. Short-term predictions of the effects of such events as solar eclipses (Wuebbles and Chang, 1979) or diurnal variability (Kurzeja, 1975) are mainly of diagnostic interest. Longer-term predictions of response to the 11-year solar variability (Callis and Nealy, 1978; Penner and Chang, 1978) are of little use in testing model predictions for other phenomena since the nature of the perturbation itself is poorly established.

Consequently, in assessing the reliability of model predictions in the absence of opportunities for direct test, we must take into account the full range of uncertainties and obtain a "best" answer with a "most likely" confidence level, as is done in Chapter 9.

SUMMARY

Since the predictive powers of stratospheric (particularly 1-D) models cannot be tested directly, the accuracy of individual components of the models must be assessed separately and the results integrated somewhat subjectively. Upward transport of source species (F-11 and F-12), photolysis of source molecules, interaction of the photofragments with ozone and other trace species, and the downward transport of sink species (HCl) are the principal components of the model used to predict the effect of CFMs on stratospheric ozone.

In this chapter we have demonstrated that the model can successfully simulate the accumulation of CFMs in the troposphere and stratosphere resulting from releases during the past 30 years. We therefore also expect the model to be able to simulate the upward transport of CFMs for future releases, at least in the time scale of 30 years.

Given the present amounts of the CFMs in the stratosphere, we have obtained basic agreement between observed and model predicted amounts of chlorine and related species. There are some important disagreements (e.g., the high ClO observations) that have yet to be resolved. If all evidence is given equal weight we are led to an acceptance of the basic adequacy of the model chemistry. The observations yet to be explained can be represented in the uncertainty range applied to the model predictions (Chapter 9). Since the relative amounts of the trace species in the stratosphere are reasonably well represented by the model, this condition is expected to obtain also for a new level of total chlorine (from increases in CFMs).

The treatment of the downward transport of HCl and O_3 and other species in the model is validated from comparison with measured height profiles. We therefore expect it to be applicable to future scenarios. Consequently, we expect the model to be reasonably accurate in describing the major physical and chemical processes in assessing the potential impact of CFMs on ozone. Uncertainty ranges expressing our judgment on the confidence level of each component of the model can be combined to obtain overall confidence limits (Chapter 9). Reduction of these ranges of uncertainty will require more sophisticated and carefully analyzed 2-D and, ideally, 3-D models. Interaction between different groups developing these multidimensional models should be encouraged. Atmospheric measurement groups should be encouraged to publish full details of their measurments along with their final results, including time, location, and meteorological information. Such information will greatly assist modelers in the use of the observational data to check their model outputs.

REFERENCES

Anderson, J. G., J. J. Margitan, and D. H. Stedman. 1977. Cl and ClO in the stratosphere, three *in situ* observations, *Science 198*, 501-503.

Anderson, J. G., H. J. Grassl, R. E. Shetter, and J. J. Margitan. In press. Stratospheric free chlorine measured by balloon borne *in situ* resonance fluroescence, *J. Geophys. Res.*

Bauer, E. 1978. A catalog of perturbing influences on stratospheric ozone 1955-1975, Rep. FAA-EQ-78-20, Dept. Transportation, Fed. Aviat. Admin., Off. Environ. Quality, Washington, D.C.

Broderick, A. J. 1978. *J. AIAA 65*, 643-653.

Buijs, H. L., G. Vail, and G. Tremblay. 1977. Simultaneous measurement of volume mixing ratios for HCl and HF in the stratosphere, preprint.

Callis, L. B., and J. E. Nealy. 1978. *Geophys. Res. Lett. 5*, 249-252.

Chang, J. S., and J. E. Penner. 1978. Analysis of global budgets of halocarbons, *Atmos. Environ. 12*, 1867-1873.

Chang, J. S., W. H. Duewer, and D. J. Wuebbles. 1979. *J. Geophys. Res. 84*, 1755-1765.

Cronn, D. R., R. A. Rasmussen, E. Robinson, and D. E. Harsch. 1977. Halogenated compound identification and measurements in the troposphere and lower stratosphere, *J. Geophys. Res. 82*, 5935-5947.

Cunnold, D., F. Alyea, and R. Prinn. 1978. *J. Geophys. Res. 83*, 5493-5500.

Duewer, W. H., P. J. Wuebbles, H. W. Alselalsesser, and J. S. Chang. 1977. *J. Geophys. Res. 82*, 935-942.

Ehhalt, D. H. 1978. The CH_4 concentration over the ocean and its possible variation with latitude, *Tellus 30*, 169-176.

Evans, W. F. J., H. Fast, J. B. Kerr, C. T. McElroy, R. S. O'Brien, D. I. Wardle, J. C. McConnell, and B. A. Ridley. 1978. Stratospheric constituent measurements from Project Stratoprobe, WMO Symposium on the Geophysical Aspects and Consequences of Changes in the Composition of the Stratosphere, WMO 511, pp. 55-59.

Farmer, C. B., and O. F. Raper. 1977. *Geophys. Res. Lett. 4*, 527-529.

Foley, H. M., and M. A. Ruderman. 1973. *J. Geophys. Res. 78*, 4441-4450.

Grobecker, A. J., S. C. Coroniti, and R. H. Cannon, Jr. 1974. *Facts of Stratospheric Pollution by Aircraft.* CIAP Report DOT-TST-75-50.

Heath, D. M., A. J. Krueger, and P. J. Crutzen. 1977. *Science 197*, 886-889.

Hudson, R. D., ed. 1977. *Chlorofluoromethane and the Stratosphere*, Ref. Publ. 1010, NASA Goddard Space Flight Center, Greenbelt, Md.

Krueger, A. J., and R. A. Minzner. 1976. A mid-latitude ozone model for the 1976 U.S. Standard Atmosphere, *J. Geophys. Res. 81*, 4477-4481.

Kurzeja, R. J. 1975. *J. Atmos. Sci. 32*, 899-909.

Lazrus, A. L., B. W. Gandrud, J. Greenberg, J. Bonelli, E. Mroz, and W. A. Sedlacek. 1977. Midlatitude seasonal measurements of stratospheric acidic chlorine vapor, *Geophys. Res. Lett. 4*, 587-589.

Mihelcic, D., D. H. Ehhalt, G. F. Kulessa, J. Klomfab, M. Trainer, U. Schmidt, and H. Rohrs. 1978. Measurements of free radicals in the atmosphere by matrix isolation and electronc paramagnetic resonance, *Pure Appl. Geophys. 116*, 530-536.

Murcray, D. G., J. W. Williams, D. B. Barker, A. Golden, C. Bradford, and G. Cook. 1978. Measurements of constituents of interest in the photochemistry of the ozone layer using infrared techniques. WHO Symposium on the Geophysical Aspects and Consequences of Changes in the Composition of the Stratosphere, WMO 511, pp. 61-68.

Neely, W. B., and J. H. Plonka. 1978. *Environ. Sci. Technol. 12*, 317.

Noxon, J. F. 1978. Stratospheric NO_2 II. Global behavior, preprint.

Noxon, J. E., E. C. Whipple, Jr., and R. S. Hyde. 1978a. Stratospheric NO_2: I. Observational model and behavior at mid-latitude, preprint.

Noxon, J. F., R. B. Norton, and W. R. Henderson. 1978b. Observation of atmospheric NO_3, *Geophys. Res. Lett. 5*, 675-678.

Penner, J. E., and J. S. Chang. 1978. Possible variations in atmospheric ozone related to the 11 year solar cycle, *Geophys. Res. Lett. 5*, 817-820.

Popoff, I. G., R. C. Whitten, R. P. Turco, and L. A. Caponi. 1978. *An Assessment of the Effect of Supersonic Aircraft Operations on Stratospheric Ozone Content*. NASA Ref. Publ. NTIS.

Pyle, J. A. 1978. A zonal mean model of the stratosphere including feedback between chemistry, radiation and dynamics, WMO Symposium on the Geophysical Aspects and Consequences of Changes in the Composition of the Stratosphere, WMO 511, pp. 240-245.

Rundel, R. D., D. M. Butler, and R. S. Stolarski. 1978. *J. Geophys. Res. 83*, 3063-3073.

Stolarski, R. S., D. M. Butler, and R. D. Rundel. 1978. *J. Geophys. Res. 83*, 3074.

Watanabe, T., and T. Tohmatsu. 1976. An observational evidence for the seasonal variation of ozone concentration in the upper stratosphere and the mesosphere, *Report of Ionosphere and Space Research in Japan, 30*, 47.50.

Waters, J. W., J. J. Gustincic, R. K. Kokan, H. K. Koscoe, P. N. Swanson, T. de Graauv, A. R. Kern, T. G. Phillips, and W. J. Wilson. 1978. Microwave Measurements of Upper Atmospheric Gases: H_2O, O_3, CO, ClO, N_2O, WMO Symposium on the Geophysical Aspects and Consequences of Changes in the Composition of the Stratosphere, p. 79.

Williams, W. J., J. J. Coster, H. Goldman, and D. G. Murcray. 1976. Measurement of the stratospheric mixing ratio of HCl using infrared absorption technique, *Geophys. Res. Lett. 3*, 383-385.

Wuebbles, D. J., and J. S. Chang. 1979. *Geophys. Res. Lett. 6*, 179-182.

9 OZONE CHANGE PROJECTIONS

INTRODUCTION

Earlier chapters have summarized the present state of our knowledge of the processes responsible for the generation and destruction of ozone. The general concepts regarding the intervention of stratospheric chlorine in ozone photochemistry have changed little since the NAS, 1976 report. However, our perceptions of the problem have changed somewhat; also there have been significant changes in the current best estimate of ozone decrease, and there is now available more detail regarding the spatial structure of the most likely change. Now that control to limit the releases of F-11 and F-12 is perhaps inevitable, and indeed already in effect to some degree, their possible substitutes and other likely sources of stratospheric chlorine must receive increased scrutiny.

We have become increasingly aware that the effect of chlorine compounds on the ozone cycle is strongly coupled to the actions of other trace species whose concentrations are also likely to change significantly over the next several decades or more because of human activities. For example, it now appears that if the concentrations of stratospheric odd-nitrogen compounds were to increase, the net decrease of total column ozone due to halocarbons would be less than its value if nitrogen compounds were to remain fixed. On the other hand, a reduction in stratospheric nitrogen would amplify the impact of chlorine increases on stratospheric ozone. Changes in CO, CO_2, and H_2O may also have some impact. We shall return later to this question of the impact of possible changes of other species on the chlorine-ozone catalytic cycles.

There have been substantial improvements in the laboratory measurements of the rate constants of relevant stratospheric chemical processes (cf. Chapter 3). Updated rate constants, as incorporated into computer models such as described in Chapter 8, have more than doubled the projected future ozone change because of continued release of chlorine to the stratosphere from that estimated in the NAS, 1976 report. Much of this revision is the result of measurement of the rate constant of the reaction

$$NO + HO_2 \rightarrow NO_2 + HO \qquad (9.1)$$

A larger value for this rate constant accentuates the perceived impact of chlorine species and reduces the impact of nitrogen species on ozone. This reaction appeared to have only a minor influence on ozone chemistry when models used previously severely underestimated values for its rate. We shall see that more than half of the uncertainty in estimating future ozone change is still a consequence of uncertainties in chemical reaction rates, despite the fact that the chemical processes are perhaps the best-understood component of the system. The large cumulative sum of known errors is a consequence of the large number of reactions involved. It is also difficult to quantify errors due to possible omissions in the current chemical schemes and systematic errors in the current estimates of some of the rate coefficients.

Other sources of uncertainty include possible tropospheric sinks, uncertainties in transport rates, future changes in atmospheric composition, and all the errors inherent in approximating the 3-D stratosphere with various meteorological feedbacks by a 1-D transport-chemistry model. These factors now contribute somewhat less than half of the estimated overall uncertainty in predicting *global average* ozone column change. However, uncertainties in transport may be a major limiting factor in estimating the *latitudinal and seasonal variations of ozone change*.

SCENARIOS FOR FUTURE RELEASE RATES OF CHLORINE SPECIES THAT REACH THE STRATOSPHERE

The CFMs F-11 and F-12 still appear to present the most serious future threat to the ozone layer and so are given the greatest attention here. Of the other anthropogenic sources, two further components apparently are likely to contribute enough additional chlorine to the stratosphere to cause significant reductions of ozone in the next few decades. These are F-22 and CH_3CCl_3 (methyl chloroform).

F-11 and F-12, Release and Effect

It is not the role of this report to judge what would be an acceptable level of ozone reduction, so we must consider a reasonably wide range of future options with regard to addition of chlorine to the stratosphere. However, because of the remaining large uncertainties in the estimates of ozone change and lack of information regarding global capabilities for regulation, a large number of highly detailed scenarios seems unwarranted. Thus, we have selected four scenarios that seem to us to span the range of release rates likely for F-11 and F-12 for the next decade.

The NAS, 1976 and the NASA, 1977 reports used scenarios in which the release rates of F-11 and F-12 remained constant at their 1973 and 1975 levels, respectively. For comparison purposes our Case A maintains constant release rates at the 1977 level. (The actual release rates in 1973, 1975, and 1977 were all within 5 percent of one another.) Case B and Case C assume the same release rates as Case A until 1983. Case B and Case C assume that release rates are reduced by 25 percent in 1983, and Case B then assumes that release is continued indefinately. Case C assumes a further curtailment of release rates in 1988 to 50 percent of the 1977 release rates, and constant release after that point. There should be enough information contained in these three scenarios to allow interpolation to other possibilities within their range or extrapolation to smaller release rates, if even Case C is found to be environmentally unacceptable. Although the release rate in the United States is unlikely to increase because of, at least in part, existing regulations, it continues to increase elsewhere, particularly in Europe. The Committee on Alternatives for the Reduction of Chlorofluorocarbon Emissions (CARCE) has suggested that a likely scenario for global release rates is constant release rate at the 1977 level until 1980, a 7 percent per annum growth rate until 2000, and a continuing constant release rate at the year 2000 level beyond that date. This is our Case D.

Figure 9.1 summarizes the expected global average column reductions for the assumed three scenarios. These are calculated with the time-dependent fully diurnally averaged model of the stratosphere described in Chapter 8; the integrations all start in 1950, with F-11 and F-12 added at their actual release rates for the 1950-1977 period.

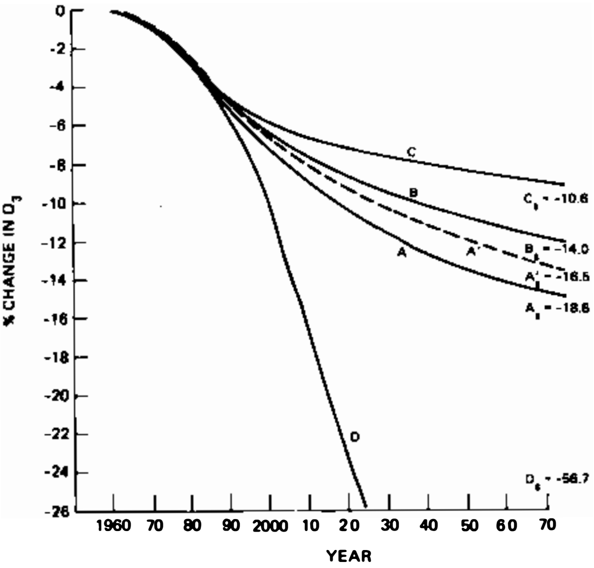

FIGURE 9.1 Ozone reduction for various scenarios: A, constant release rate at the 1977 value; A_S, steady-state value = -18.6%; A', constant release rate at the 1977 value, same as A but multiplied by a factor of 0.89 to correct for feedback effects and the possible existence of a tropospheric sink; B, 1977 release rates until 1983, from then on reduced by 25%; B_S, steady-state value = -14.9%; C, 1977 release rates until 1983, reduced by 25% until 1988, reduced an additional 25% after 1988; C_S, steady-state value = -10.6%; D, 1977 release rates until 1980, increasing by 7% per year until 2000, then constant release rate at the year 2000 value; D_S, steady-state value = -56.7%.

The dashed line (denoted A') shows our final estimates for Case A, which consists of multiplying the model results by 0.89. The basis for this correction factor is described later. Cases B, C, and D should be similarly corrected to obtain our final best estimates for these scenarios.

The following model estimates, inferred from Figure 9.1, are particularly notable: (a) a 2 percent change of ozone has already occurred due to F-11 and F-12, half of this during the last decade; (b) the ozone change by the year 1990 due to F-11 and F-12 is near 5 percent, almost independent of the assumed scenario; (c) the final steady states range from 18.6 percent to 10.6 percent between Cases A and C (or 16.5 percent to 9.4 percent after adjustment), i.e., a 50 percent reduction in release implies a somewhat less (43 percent) decrease in the ozone change; (d) half the steady-state values would be reached in 15 to 30 years, depending on the scenario.

For steady release rates less than that of Scenario C, linear scaling should be adequate, considering the uncertainties of the estimate, i.e., 10 percent of 1977 release rates will still imply a 1.9 percent ozone reduction at steady state.

Case D, which includes an exponential growth between 1980 and 2000, leads to a 25 percent decrease in ozone by the year 2023 and a steady-state decrease of 56.7 percent. At very high values of ozone depletion there would be large changes in the dynamics and temperature structure of the stratosphere, which would invalidate the transport parameterization of the 1-D model. Therefore no great reliance can be placed on the steady-state prediction, although it can be concluded to be at least 30 percent.

As we shall discuss, there are uncertainties in various aspects of our ozone change estimate. Some of these, such as that due to the cumulative errors resulting from known uncertainties in the model reaction rate coefficients, can be estimated quantitatively. The contributions of other error sources can only be guessed subjectively. Combining all calculated or guessed error sources, we obtain Figure 9.2, which shows our estimate of the probability of occurrence of various ranges of steady-state ozone change (for Case A'). This figure indicates, in particular, that there is a three out of four chance that the ozone decrease would

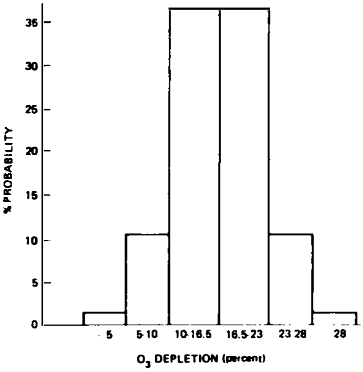

FIGURE 9.2 Probability estimates of ozone depletion for Case A', constant release rate at 1977 value.

lie between 10 and 24 percent, and less than one chance in 20 that it exceeds 28 percent or is less than 5 percent. All the above numbers can be divided by approximately 9 to obtain the estimated current (1979) ozone change due to CFMs and its uncertainty range.

B. Other Chlorine Compounds

The chlorocarbons now of greatest concern for the ozone layer besides F-11 and F-12 are methyl chloride (CH_3Cl), carbon tetrachloride (CCl_4), methyl chloroform (CH_3CCl_3), and F-22 (CHF_2Cl).

Methyl chloride is a major natural source of stratospheric chlorine (cf. Chapter 2), maintaining up to 0.8 ppbv of total chlorine in the ozone layer, in spite of its short tropospheric lifetime. At present, there is no basis for expecting any future changes in its tropospheric generation rate.

Carbon tetrachloride is as long-lived as F-11 and F-12, and since it currently has comparable tropospheric concentrations, it now provides comparable amounts of Cl atoms to the stratosphere. The relative lack of concern for its future effect on the ozone layer derives entirely from its current apparently small anthropogenic release rates (estimated at less than 5 percent of the release rates of F-11 or F-12). Hence, although the current CCl_4 atmospheric burden is believed to be mostly of anthropogenic origin, it is believed not likely to increase significantly in the future.

Methyl chloroform and F-22 will require increased future attention as significant sources of stratospheric chlorine that are potentially controllable but the releases of which now appear likely to increase rapidly in the near future. The major sink for both these species is reaction in the troposphere with HO. Unfortunately, the concentrations of tropospheric HO are rather uncertain and introduce the largest uncertainty in estimating the effects of CH_3CCl_3 and F-22 relative to that of F-11 and F-12. Current theoretical models and measurements (Chapters 7 and 8) suggest an average tropospheric HO concentration of between 0.2×10^6 and $1.5 \times 10^6/cm^3$. Earlier models used higher average concentrations (the NAS, 1976 report used $2 \times 10^6/cm^3$), and consequently shorter lifetimes for HO reactive halocarbon species were inferred.

The NAS, 1976 report gave a tropospheric lifetime for CH_3CCl_3 of one year. More recent estimates are essentially of the form, 4 years × $10^6/n(\mathrm{HO})$ (McConnell and Schiff, 1978; Crutzen and Fishman, 1977). The doubling of the lifetime, for a given HO concentration, relative to the NAS, 1976 report, allows for the temperature dependence of the rate of the reaction of HO with CH_3CCl_3. In summary, according to current best estimates, the tropospheric lifetimes of CH_3CCl_3 lies between 3 and 20 years and probably between 4 and 12 years. The range of measured interhemispheric ratios of CH_3CCl_3 is consistent with its lifetime lying in this range. The tropospheric lifetime of F-22 is similarly poorly known but likely to be in the range of 10 to 50 years. Translating these lifetimes into contributions of Cl atoms to the stratosphere, we infer that between 0.1 and 0.2 of the CH_3CCl_3 molecules produced and between 0.2 and 0.5 of the F-22 molecules produced will reach the stratosphere.

The 1976 release rate for CH_3CCl_3 of 4 × 10^5 metric tons is comparable with the individual release rates of F-11 and F-12, and, correspondingly, CH_3CCl_3 should, in steady state at the 1976 rates, destroy between about 8 and 15 percent as much O_3 as the sum of F-11 and F-12. However, McConnell and Schiff (1978) infer from current increases in production of CH_3CCl_3 a release rate by 1982 of 16 × 10^5 metric tons and a corresponding 20 percent increase of O_3 destruction over that due to F-11 and F-12 (assuming an 8-year tropospheric lifetime for CH_3CCl_3). In summary, if the release of CH_3CCl_3 were to continue to grow, and if, as appears likely, its tropospheric lifetime is as long as 10 years or so, it may begin to provide more Cl atoms to the stratosphere than either F-11 or F-12. In any case, it appears that its contribution of Cl is large enough to warrant serious consideration of controlling its release rate.

The compound F-22 is now a relatively small source of stratospheric Cl, primarily because of its relatively small release rate of 0.6 × 10^5 metric tons/year. Per molecule, it releases between 4 and 10 times less Cl to the stratosphere than do F-11 and F-12, because of its tropospheric losses and its single chlorine atom. Thus, its substitution for current usage of F-11 and F-12 should greatly reduce the Cl released to the stratosphere. However, its substitution for growth of F-11 and F-12 usage may still need to be carefully considered, especially if its release rates are to become comparable with the current release rates of F-11 and F-12.

All the other anthropogenic chlorocarbon species of which we are aware either have release rates much smaller than that of F-11 and F-12 or tropospheric lifetimes significantly less than a year, or both. However, any other chlorine-containing substitutes proposed in the future as substitutes for F-11 and F-12 should be carefully considered as to likely tropospheric lifetimes before their use is implemented.

INTERACTION WITH OTHER SPECIES

It has been argued by several authors (most forcibly by McElroy, 1976) that agricultural usage of chemical fertilizers may in the future tend to produce more N_2O than now is generated by natural biological processes. For example, Logan *et al.* (1978) anticipate a twofold to threefold increase in the surface release of N_2O in the next century due to increased use of chemical fertilizers. On the other hand, it may also be argued (Ellsaesser, 1978) that other aspects of agricultural modification of the earth such as changes of soil pH, drainage, and oxygenation may be more important than addition of fixed nitrogen in modifying N_2O production, and indeed may lead to a net decrease of total N_2O release from the soil. Liu *et al.* (1976) and Johnston (1977) have suggested increases of N_2O but smaller than those asserted by Logan *et al.* It is beyond the scope of the present report to sort out the current conflicting claims regarding future changes in the sources of stratospheric nitrogen. Rather, we wish merely to point out that the uncertainty of the magnitude of future changes introduces a large uncertainty in estimating the future impact of chlorocarbon releases on stratospheric ozone.

Table 9.1, obtained by use of the GSFC model, shows the percent variation of stratospheric O_3 with joint variations of N_2O and Cl_x. These results differ somewhat from those of Logan *et al.* (1978), especially in the range of low Cl_x and high N_2O. Whereas in Table 9.1 there is a small increase in total ozone for present Cl_x but increasing NO_x, Logan *et al.* predict a small decrease in ozone. This difference in model sensitivity to N_2O (i.e., odd nitrogen) increase is also observed in other models (J. Chang and S. C. Liu, NCAR, private communication, 1978). It appears to be due primarily to the differences between different models in HO_x concentrations in the lower stratosphere (10-20 km), which in turn are due to differences in the treatment of CH_4 oxidation. The strong dependence on HO of the ozone change due to NO_x results from the strong coupling of HO_x and NO_x cycles through the reaction of HO_2 with NO. Models

TABLE 9.1 Percentage Change of the O_3 Column for Joint Changes in N_2O Release and CFM Release[a]

N_2O Increase (Factors)	CFM Addition (Steady State at Factor Times 1975 Rates)					
	0	0.2	0.4	0.6	0.8	1.0
1/2	-3.7	-10.7	-16.8	-22.2	-27.0	-31.6
1	0[b]	-5.3	-9.9	-14.1	-17.9	-21.5
2	+3.5	+0.2	-2.8	-5.7	-8.4	-10.9
3	+4.2	+2.1	+0.1	-1.8	-3.7	-5.5
4	+3.2	+1.8	+0.5	-0.8	-2.0	-3.2

[a] N_2O factors are based on a reference model that requires a flux of 1.4×10^9 molecules cm^{-2} sec^{-1} to maintain a ground-level mixing ratio of 330 ppbv. The reference model has ~1.2 ppbv Cl_x from 1.0 ppbv CH_3Cl and 0.1 ppbv CCl_4 at the ground. The CFM additions are in multiples of the fluxes of 9.92×10^6 molecules cm^{-2} sec^{-1} for F-11 and 1.37×10^7 molecules cm^{-2} sec^{-1} for F-12.

[b] Reference model.

with low HO_x concentrations (e.g., Harvard and NOAA) suggest that O_3 would decrease a small amount with an increase in NO_x at altitudes above 15 km. But models with factors of 2-3 times more HO_x (GSFC and LLL) suggest that O_3 could increase somewhat because of an increase in NO_x for altitudes up to approximately 23 km. These ozone increases below 23 km due to addition of N_2O in these models are sufficient to nearly cancel the corresponding O_3 decreases at higher levels, so that there would be only small net decreases or even net increases. Fortunately, at the currently estimated stratospheric NO_x concentrations of 12-17 ppbv (of Chapter 8), the ozone change due to addition of Cl_x is relatively insensitive to the amount of HO_x present in the lower stratosphere, so this uncertainty in HO_x does not dominate the estimate of uncertainty in ozone change, and all the current models give similar predictions.

Another major anthropogenic perturbation of atmospheric composition occurs because of the burning of fossil fuels. Fossil-fuel combustion has contributed around 20 percent of atmospheric CO_2 up to now and up to half of the global CO. Such a large fossil-fuel contribution to CO is inferred in part from the observed factor of 3 greater northern than southern hemisphere CO concentrations. (See Chapter 7 for further discussion of observed CO concentrations.) Future scenarios for fossil-fuel burning (Baes *et al.*, 1977) suggest a fivefold to tenfold increase in the next century. Carbon dioxide acts to warm the troposphere but cool the stratosphere. The photochemistry of a colder stratosphere would generate larger O_3 concentrations than now present. With the atmospheric temperature structure calculated for double the current CO_2, stratospheric ozone would increase by about 2 percent (Boughner, 1978). Carbon monoxide increases may also significantly modify atmospheric ozone concentrations. The percentage increases in CO may be even larger than the CO_2 increases. Concentrations of CO, NO_x, and O_3 in the troposphere are major factors limiting the tropospheric concentrations of HO. Fishman and Crutzen (1978) infer that the net effect of interhemispheric differences between these species is to provide roughly comparable HO concentrations in the two hemispheres. A decrease of HO with increase of CO would increase the Cl available to the stratosphere from natural and anthropogenic chlorine-containing compounds whose lifetimes are controlled by tropospheric HO. It appears, however (at least from the calculations of Logan *et al.*), that the dominant effect of an increased removal of HO by increased CO is to increase ozone in the troposphere. In converting CO to CO_2, the H atom in HO is released and forms HO_2, which reacts with NO to form NO_2, whose photodissociation makes odd oxygen. They estimate an order of 5 percent increase of global O_3 due to increasing CO (and H_2) from combustion of fossil fuel in the next century. The estimated ozone changes due to these sources depend on tropospheric NO concentrations, which are poorly known and currently measured to be much lower than assumed in their calculations. Hence, their ozone change estimates are probably high and certainly much more speculative than estimates of ozone change due to Cl_x. Since the time history of likely changes of atmospheric composition by the buildup of fossil-fuel burning and application of fertilizers are expected to be rather dissimilar to CFMs, it is not feasible to combine their effects with CFM-ozone change estimates.

Besides changes of atmospheric composition, changes of stratospheric temperature structure will modify ozone photochemistry, as already mentioned in the context of CO_2. Also notable are the temperature changes due to changes in ozone itself. In the upper stratosphere, ozone modulates temperature primarily through its absorption of solar radiation; whereas in the lower stratosphere, the absorption of tropospheric thermal radiation by the 9.6-μm band of ozone is more important. The vertical profiles of ozone and temperature change for such a chemical-radiative equilibrium calculation are shown in Figure 9.3 for steady-state CFM released at 1977 rates, for comparison with the calculation without feedback. With the feedback, the calculated ozone change is reduced from 18.6 percent to 16.8 percent.

The concentration of water vapor in the stratosphere may also undergo significant future change as a consequence of other modifications in atmospheric climate indirectly resulting from CFM changes. Stratospheric H_2O is believed to be particularly susceptible to changes in the temperature of the tropical tropopause, since much of the upward transport of water into the stratosphere is thought to occur there, and the mixing ratios of water so transported could

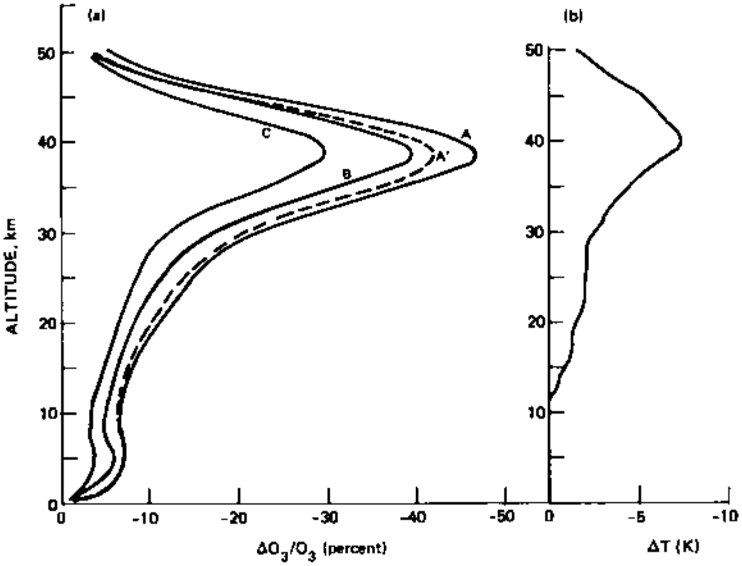

FIGURE 9.3 (a) The fractional change in ozone, $\Delta O_3/O_3$ (%) as a function of altitude for Cases A, B, and C (solid curves). The dotted curve gives the result for Case A, including the effect of temperature feedback. (b) Calculated temperature change at steady state for Case A as a function of altitude.

not exceed the saturation mixing ratio at those (cold) temperatures. The temperature change shown in Figure 9.3 suggests that CFM ozone change would probably at most decrease the tropical tropopause temperatures by 1 to 2 K. The thermal-infrared radiative effects of CFMs themselves would be expected to have a somewhat larger effect and increase the tropopause temperature by 2 to 3 K (Dickinson *et al.*, 1978). Depending on the details of the interactions between these processes, we would expect that future change of stratospheric water vapor due to CFMs directly and indirectly would be between +60 percent and -20 percent, and correspondingly to change the projected ozone depletion of Case A by an amount of between +4 percent and -1 percent, at most. The temperature of the tropical tropopause is also, in turn, somewhat sensitive to the water-vapor concentrations there. More water would lead to more infrared cooling, so this feedback would tend to reduce excursions in water concentrations. Taking this into account, we estimate the most probable net correction to the ozone depletion due to water vapor feedback as 0.9 percent.

VERTICAL AND HORIZONTAL PROFILES

The emphasis of this and past studies has been to describe the global average change of ozone within a total column. This is the quantity that 1-D models are believed to provide most reliably (or at least with the most quantifiable uncertainties). However, as a by-product of the derivation of total column change, the 1-D models also predict the change of ozone as a function of altitude. This vertical structure of the ozone change is required for climate modelers to determine the effect of the ozone change on the global thermal balance. (Fractional ozone change uniform with altitude has little effect on the global thermal budget because of cancellation between the solar and thermal infrared changes.)

Figure 9.3(a) shows the fractional change of ozone for the three scenarios, as well for Case A', including temperature feedback. As already noted in the previous section, the calculated temperature change [Figure 9.3(b)] has no drastic impact on the ozone change profile. The fractional change of the ozone profile is qualitatively similar to that given in our previous report, with maximum change around 40 km. The peak change for Cases A, B, and C is 45 percent, 38 percent, and 29 percent, respectively. In addition, the location of the maximum ozone concentration remains the same for all cases. We are not able to attach any meaningful uncertainty range to this profile change but expect its qualitative structure to be but little modified with future refinements of the chemical model, providing these changes lie within the current 2σ uncertainty range of the model chemistry.

Two-dimensional models of ozone change due to CFMs are now being developed. Their chemistry has not yet been sufficiently validated for the panel to use them to estimate the effects of two-dimensionality on estimates of global ozone change. However, they are already useful in suggesting the latitudinal variation of the ozone change, which is needed for estimating possible local increases of ultraviolet radiation and hence regional biological impacts of ozone change. It would be useful also for estimating climate change using multidimensional climate models.

At the 1978 WMO stratospheric chemistry meeting in Toronto, Pyle (1978) and Vupputuri (1978) presented preliminary 2-D results for the ozone change due to CFMs. We do not know whether, in principle, a 2-D eddy-transport parameterization is capable of providing an accurate description of the effects of transport on the latitudinal variations of ozone change. However, it is evident that photochemical processes can be calculated more satisfactorily in a 2-D model than a 1-D one, provided it is comparable in all other aspects.

The most useful result of the 2-D models with regard to the present report is their predicted relative latitudinal and seasonal variation of ozone change. Table 9.2 summarizes this information. Both models indicate qualitatively

TABLE 9.2 Latitudinal and Midlatitude Seasonal Relative Variations of Percentage Ozone Change Due to CFM, According to the Pyle and Vupputuri Models, and Expressed in Terms of Ratios

Ratio	Pyle Model	Vupputuri Model
Annual 50°/equatorial[a] change ratio	1.6	1.15
Winter/summer change ratio at 50°	1.8	1.2

[a] This states, e.g., that the percentage ozone change (in Pyle's model) is 1.6 times as large at 50° as at the equator.

that these variations should follow the latitudinal and seasonal variations of natural ozone. That is, they predict larger relative changes of ozone in middle and high latitudes than in the tropics, and that in middle to high latitudes, the relative changes would be largest in late winter and smallest in late summer. Quantitatively, the variations shown by Pyle are about four times as large as those shown by Vupputuri and, combined with the poleward increases of natural ozone, suggest a factor of 2 to 3 more change of ozone column (in absolute units) in middle latitudes than in the tropics. It is tempting, but not justifiable, to argue that the actual latitudinal-seasonal variations should lie within the range suggested by these two models. Procedures for validating the transport parameterizations of 2-D models are still in too primitive a state to make quantitative statements regarding the likely range of errors due to uncertainties in these parameterizations. The predicted relative latitudinal-seasonal structure of ozone change is probably relatively insensitive to errors in the chemical modeling and is primarily dependent on the model transport. Until some degree of confidence is developed in the transport parameterizations of the 2-D models, results such as given in Table 9.2 can only be used for a suggestion, not a definitive statement, as to the likely latitudinal-seasonal distribution of the ozone change.

ANALYSIS OF MODEL UNCERTAINTIES DUE TO INPUT UNCERTAINTIES

The chemistry of stratospheric ozone has now been extensively studied for nearly a decade. There has been a continuing effort to evaluate all the laboratory studies of reaction rates to determine the most likely values for rates and the range of uncertainty to be attached to them. The most recent analyses have provided the input to the chemical model calculations used for this report. We discuss here the determination of the uncertainty of our ozone-change estimates due to the known uncertainties in the model input.

In the NAS, 1976 report a limited error analysis was made by calculating the sensitivity of the ozone-change estimate to errors in seven reaction rates believed to be most critical in determining ozone uncertainty. The sensitivity factor r for a rate k was defined as given in Chapter 3. The total error due to uncertainties in the seven rate coefficients considered was then combined by assuming that the probability distributions of the rates and the ozone-change distribution were "log normal." These sensitivity factors *r* are model and problem dependent. For example, the *r*'s for steady-state ozone change at current emission rates are somewhat different than those for steady state at one half of the current emission rate. In this instance, the differences of *r* between scenarios is perhaps less than that which might be obtained in comparing different chemical models. An examination of the variations of the *r*'s with model and scenario leads to the conclusion that these differences are probably small enough within a small range of scenarios that we can use one set of *r*'s for our discussion of the relative contributions of various reaction uncertainties to the overall uncertainty. Table 3.2 summarizes the *r*'s obtained (from the GSFC model and 1978 CFM emission to steady state) for the reactions contributing most significantly to the ozone change error. For example, considering ClO + O in Table 3.2, we see that it has a sensitivity factor of 0.44. That is, if the rate constant for this reaction alone were increased by 10 percent in the model, the model estimate of ozone depletion would increase by 4.4 percent of the ozone depletion. The error analysis defined in Chapter 3 shows that, if all other rate coefficients were known precisely, we would be 95 percent certain that the ozone change was between a factor of 0.85 and 1.17 of the calculated best values.

To determine the total uncertainties due to reaction-rate coefficients, the individual uncertainties must somehow be combined. In our previous report, we used a log normal distribution and estimated a total error by the exponential of the square root of the sum of u_i^2. This approach has defects that led to it being abandoned in the present report for obtaining a final error estimate. The major criticism of our previous error-estimate procedure was that it was likely to overestimate the lowest probable ozone change. The more elaborate Monte Carlo error analysis that has been carried out for this report and discussed below gives somewhat smaller values for both the upper and lower limits than does the previous procedure.

By definition, the total error due to uncertainties in all the rate constants is that obtained by allowing all rate constants to have their likely error simultaneously. More specifically, the model's probability distribution of ozone change is that which would result when all the individual uncertain rate constants vary within their given individual probability distributions. The numerical procedure necessary to evaluate the ozone-change probability distribution is referred to as the Monte-Carlo technique.

This analysis was carried out for the panel by scientists at GSFC for Scenario A and is described further in Appendix D. For such a calculation, it is necessary to know the probability distribution of errors for each rate entering the model. Since such information was not available, the distribution of the logarithm of the rate errors was assumed to be "normal," i.e., "Gaussian." Further calculations showed the 95 percent probability limits to depend somewhat on the assumed probability distribution.

In a number of cases, such as the reaction of HO_2 with NO, a new measurement has been accepted, which would be considered improbable on the basis of the previously assumed distribution. The new value is accepted because of the higher perceived accuracy in the method of measurement and the tacit belief that the previous measurements had large but unrecognized systematic errors. Such large errors are becoming more unlikely since most of the significant reactions are now measured by direct methods and several different techniques (Chapter 3).

In order to combine sources of error, we shall assume that the different error sources are uncorrelated and each normally distributed. The above described Monte Carlo analysis gives an uncertainty factor of 1.00 ± 0.52 for the known rate uncertainties and a factor of (1.0 ± 0.2) due to the ignorance of the probability distribution for random rate errors. By uncertainty factor, we mean that the predicted ozone change is multiplied by this factor to give the 95 percent uncertainty limits. The variable part of all uncertainty factors are combined by root-mean-square sums; we have a total uncertainty factor due to errors in reaction rates of (1.0 ± 0.56), i.e., $(0.56)^2 = (0.52)^2 + (0.2)^2$.

In the NAS, 1976 report no attempt was made to estimate the systematic errors in evaluating rates or omission of chemical processes. Without such estimates, decision makers are free to make their own judgments ranging from uncritical acceptance of the current models to complete skepticism as to their having any likelihood of being correct. The panel has had considerable experience with this problem and is familiar with several such instances of large changes of the predicted ozone depletion due to correction of such errors in the past.

Several reactions have recently been suggested to have possible significance in the halocarbon-ozone problem. These include the reaction of Cl atoms with formaldehyde (CH_2O), the reaction of ClO with BrO, and the reaction of ClO with HO to form HCl. Since these reactions are still somewhat speculative they have not been included in the model calculations. Since they operate in different directions with respect to the effect of halocarbon releases on ozone, we do not believe that their inclusion will have a large affect on the predicted values of ozone depletion. We have, however, made an "educated guess" on the uncertainty introduced by the omission of these, and other unrecognized, reactions. This uncertainty has the effect of increasing the range of the bar graph (Figure 9.2) to a 3 out of 4 chance that the ozone decrease would lie between 9 or 24 percent and less than 1 chance in 20 that it is outside the range of 3 to 30 percent.

ERRORS IN THE ONE-DIMENSIONAL TRANSPORT PARAMETERIZATION

One-dimensional models for ozone change due to CFMs appear rather insensitive to the transport parameterization. Variations of the eddy-mixing coefficient profile over as wide a range of values as possible permitted by observed chemical profiles (O_3, N_2O, CH_4, for example) gives but a small change in the calculated ozone depletion. This result appears to be a consequence of many compensating transport-controlled processes in the model. For example, a slower transport would permit larger Cl_x concentrations to build up in the stratosphere, but also larger NO_x concentrations. The first of these would enhance the ozone depletion, and the second reduce it. On the other hand, if the transport errors made for each species were independent of each other, then they would be expected to be additive, at least in a mean-square sense. In the 3-D atmosphere, it is unlikely that the errors made in transport for individual species are either uncorrelated or completely correlated. Hence, we adopt the position of the NAS, 1976 report that a fair estimate of the uncertainty in ozone change due to CFMs can be made by considering the uncertainty in the CFM lifetimes in the atmosphere due to transport uncertainty. The NAS, 1976 report showed by extensive numerical examples that it was extremely unlikely that an acceptable 1-D profile for the eddy-mixing coefficient could be found that would change the CFM lifetimes from their best values by more than a factor of 1.4 in either direction.

A further thorough study of the derivation of transport in 1-D models has been made for the present study, as reported in Chapter 4. Two independent approaches were used. The first approach, that of the NAS, 1976 report, repeated the calculations of the previous report in deriving transport parameterizations from estimates of the global average profiles of N_2O and CH_4 species. Current estimates of the lifetimes of these species were obtained from the LLL model, and latest data were used to estimate the global profiles. The transport rates inferred from our current best estimates of the global averages of these species was within 10 to 20 percent of those inferred in the NAS, 1976 report.

The transport rate estimated from CH_4 is a factor of 2 faster than that from N_2O. Also, the transport rate inferred from N_2O was estimated to be uncertain by a factor of 2 in either direction because of uncertainty in the global average N_2O profile. The increased data on N_2O suggest a somewhat wider possible variability than inferred in the NAS, 1976 report.

The second approach, described in detail in the Appendix B, involves fitting simple analytical functions to the species data to provide smooth global averages. As applied, it did not require information on sources. Its application to N_2O yielded similar results to that of the first method, increasing our confidence in the insensitivity of the transport estimates to the methodology used. It helped to sharpen considerably our estimates of the rate of vertical transport by considering two further sources of data. These were the global averages of O_3 and a synthetic tracer generated in a 3-D model simulation. Both of these species have well-defined global averages. The preferred transport parameterization inferred by method II using these data and a global N_2O profile was in close agreement with the transport parameterization inferred using method I and the global average N_2O profile. Hence our uncertainty range for 1-D transport parameterization is now estimated to be a factor of 1.0 ± 0.3. This error estimate does not include the uncertainty due to the inherent inadequacy of 1-D models for describing 3-D processes, which is treated in the next section.

ERRORS DUE TO THE INADEQUACY OF THE ONE-DIMENSIONAL ASSUMPTION

There are uncertainties in our ozone-change estimates due to the errors necessarily made in a 1-D model in calculating various kinds of averages. These errors result from the use of average values for species concentrations in the nonlinear expressions describing their chemistry. Large diurnal variations in species concentrations have been approximately allowed for in the current models by carrying out diurnal integrations. Additional errors still remain because of latitudinal and seasonal variations of solar radiation and of concentrations due to transport. For example, transport in the lower stratosphere acts on species with stratospheric sources (i.e., O_3, NO_y, ClO_y) to increase their concentrations in high latitudes, especially when solar fluxes are low or nonexistent. None of the 2-D modeling studies have yet suggested any drastic modifications of the calculated ozone change due to such effects. Additional analysis of this error would require comparison of 2-D and 1-D model predictions using the same photochemical schemes, and this has not been done. Besides latitudinal-seasonal effects, there are errors due to the neglect of longitudinal and day-to-day fluctuations in various parameters, which would require a realistic 3-D model to evaluate. The overall uncertainty in global average change due to approximating the 3-D chemistry with 1-D model expressions is estimated to be about a factor of 2, i.e., an error factor of 1.0 ± 0.3.

There are additional errors due to feedbacks between ozone, stratospheric temperature, water vapor, and other meteorological processes and to those aspects of the 3-D transport processes that are inherently incapable of representation by a 1-D model. These features, all told, are believed to introduce another factor of 2 uncertainty, such that the overall uncertainty in global-average ozone change in approximating the 3-D stratosphere with feedbacks by a 1-D model is given by the factor 0.95 ± 0.4. Uncertainties in the current concentrations of specified tropospheric substances were considered in the Monte Carlo calculations and found to have a negligible effect on the predicted ozone changes. As discussed above, substances other than halocarbons may also change in the future as a result of human activity. Such changes will not significantly broaden the uncertainties in predicted ozone changes due to halocarbons over the next 20 to 50 years but may do so over a longer period, from 50 to 100 years. Information regarding latitudinal and seasonal variations in the ozone change will require multidimensional models.

ERROR DUE TO TROPOSPHERIC SINKS

Besides the previously discussed error sources, the predicted ozone change is uncertain because of possible tropospheric sinks for the CFMs. As discussed in Chapter 5, there is only one sink that may remove CFMs on a time scale less than several hundred years. This is photodecomposition on desert soil to which we assign a nominal removal rate of 1.0×10^{-3} year^{-1} or, for an average CFM lifetime of 70 years, a correction factor of 0.9 to the otherwise predicted ozone change. The error range of this correction factor estimate is taken to be 0.07 percent, i.e., tropospheric sinks are believed to remove somewhere between 0 and 14 percent of the CFMs produced.

SUMMARY AND CONCLUDING REMARKS

The considerations of the above section are combined with the previously discussed factors determining ozone change and its uncertainty. The result of combining all these terms is given in Table 9.3. Our best estimate of ozone depletion at steady state and for sustained 1977 emission rates is 16.5 percent. There is a quantifiable uncertainty due to known uncertainties in reaction rates of about ±8 percent. We obtain a total uncertainty of ±11.5 percent.

The NAS, 1976 report gave an expected value for steady-state ozone change for continuing F-11 and F-12 emissions of 7.5 percent and a 95 percent certainty range of 2 to 20 percent. The present analysis gives an estimated steady-state change of 16.5 percent for sustained 1977 emission rates with a 95 percent certainty range of 5 percent to 28 percent. There have been small changes in the CFM emissions between 1976 and 1977, but the major reason for the increase in the expected ozone reduction has been previous systematic errors in values assigned to the chemical rate coefficients used in the models, especially that for HO_2 + NO.

It is paradoxical that the assigned uncertainty range has not decreased appreciably despite the significant improvements in the understanding of stratospheric chemistry over the last two years. This has occurred for several reasons. First, the previous analysis underestimated the effect of reaction rate uncertainty by considering only the seven reactions at that time believed to be most crucial to the error analysis. Second, the previous analysis added errors assuming a log-normal distribution, whereas here we have assumed a normal distribution for each of the factors in Table 9.3. This approach tends to lower the lower limit for ozone reduction and even allows for the possibility of negative values (not possible with the analysis in the NAS, 1976 report). For the above two reasons, the previous "factor of 5" estimate of the uncertainty due to known errors in the reaction rate coefficients has only shrunk to a factor of 4. Further reductions in this uncertainty factor can be expected, but it appears extremely unlikely

TABLE 9.3 Summary of Various Contributions to Predicted Global Mean Ozone Change and Error Estimate for 1978 Emission of F-11 and F-12 (Scenario A) until Steady State is Reached

(a) *Expected Ozone Reduction*

	NAS 1976	Present
LLL 1-D model	7.5%	18.6%
Temperature feedback (LLL model)	Not included	-1.8%
Water-vapor feedback	Not included	0.9%
Tropospheric sinks	-1.5%	-1.2%
TOTAL	6.0%	16.5%

(b) ± *Error Contributions (2 standard deviations)*

Source	Error Normalized to Apply for an Ozone Reduction of 1.0	Percentage Error for Expected Ozone Reduction of 16.5%
Known rate-contant errors	0.56	9.2%
Effects of 3-D chemistry and feedbacks to meteorology	0.4	6.6%
Transport	0.3	5.0%
Tropospheric sinks	0.1	1.5%
ROOT-MEAN-SQUARE SUM	0.7	11.5%

(c) From (a) and (b), *Predicted Ozone Change* is 16.5 ± 11.5%

it can ever be reduced by more than half of its current value (Chapter 3). The uncertainty due to errors in selecting an optimum 1-D transport parameterization has been somewhat reduced from that previously assigned.

We have taken into account some of the errors inherent in the 1-D models. These include 3-D effects of chemical rates, transport, and feedbacks with meteorological processes due to spatial and time variations. Finally, we have included an educated guess as to the likely net uncertainty due to chemical rates that are systematically in error or omitted.

Most of the prior discussion has applied to the steady-state results for Case A, emission continuing at 1977 rates. Applying corrections corresponding to those shown in Table 9.3 for Cases B and C, we infer:

Case B (3/4 of 1977 rates)
decrease of O_3 (steady state) = 13.3 ± 9.3%
Case C (1/2 of 1977 rates)
decrease of O_3 (steady state) = 9.4 ± 6.8%

Since more than 100 years would be required for the ozone change to nearly achieve the steady-state values, it is also important to consider the likely ozone change in the nearer future. For example, our best estimates are:

In 50 years (year 2028)
Case A, decrease of O_3 = 10 ± 7%
Case B, decrease of O_3 = 8 ± 6%
Case C, decrease of O_3 = 6 ± 4%
And in 20 years
Case A, decrease of O_3 = 6.1 ± 4.2%
Case B, decrease of O_3 = 5.6 ± 3.9%
Case C, decrease of O_3 = 5.2 ± 3.5%

The estimated current ozone decrease due to known past releases of CFMs is 2.1 ± 1.5 percent.

It is evident that future restrictions on CFM releases will have little effect on the ozone changes over the next 20 years because of the long atmospheric lifetimes of the CFMs and the release that has already occurred over the past 15 years.

All the above ozone change estimates are made independently of the ozone trend estimates as discussed in Chapter 6. It is, however, possible to improve our estimates by making use of the information given by the observed ozone change. The observed ozone change in 1978 is 0.0 percent with a variance* of $(1.75 \text{ percent})^2$; this may be combined with the model estimate of a 2.1 percent decrease with a $(0.7 \text{ percent})^2$ variance, to give a combined estimate of

---

*The variance is defined as the square of the standard deviation.

1.8 percent. This number represents the best estimate of the 1978 ozone change based on both the trend analysis and the model prediction. All the other estimates of ozone decrease given in this chapter could likewise be multiplied by 0.86 (= 1.8/2.1) to account for the current information given by trend analyses; however, such a correction is rather speculative because of the large uncertainty now attached to the trend analysis variance estimates. In the future, as the predicted ozone depletion increases, the trend estimates should give relatively more information, particularly if the trend analysis is further refined. For example, 20 years hence, the variance of the theoretical estimates and trend analysis estimates may both be about $(0.5\%)^2$, in which case both estimates would have to be given equal weight in determining the ozone decrease due to CFMs that had occurred up to that time. Furthermore, if the trend analysis and theoretical ozone change estimates for 20 years hence were to remain at 0 to 5 percent, it could be judged highly likely (95 percent probable) that one or the other were seriously in error. It should also be obvious that such a judgment is not possible now; perhaps with rapid enough improvements in both the theory and trend analyses it could be made as soon as a decade from now, but 20 years seems more likely to be the time required.

Again, as discussed earlier, the total ozone percent changes are not expected to be distributed uniformly in an ozone column. The largest percent changes are likely to occur in the upper stratosphere and, in percentage, exceed the column change by approximately a factor of 2. Furthermore the ozone changes are likely to have seasonal and latitudinal variations. Some preliminary 2-D model results indicate largest changes in high latitudes and in the winter hemisphere.

In interpreting the predicted ozone reduction, it is important to keep several aspects in mind:

1. Case D, considered likely in the absence of further regulation, leads to an expected ozone depletion of ozone in 30 years exceeding 30 percent, which would clearly have serious consequences.
2. The upper limit of the ultimate steady state for Case A (28 percent) is as likely (or unlikely) as the lower limit (5 percent) and would also have serious consequences.
3. Neither the upper nor lower limits are very probable (less than a chance in 40 that one would be exceeded).

There is a good chance (better than 3 out of 4) that the steady-state, Case A ozone reduction is within 6.5 percent of the expected value of 16.5 percent, i.e., between 10 and 23 percent.

4. For every year that CFM emissions continue at the present rate, it is likely that ozone will be reduced by additional 0.1 to 0.2 percent and that this reduction would persist nearly unabated for several decades or more after the emissions were halted.

5. The reduction of ozone by other chlorocarbons, especially CH_3CCl_3 and F-22, has not been included in the numbers given in this report. However, if the releases of these compounds are in amounts comparable with the amounts of F-11 and F-12 released to the atmosphere, the total reduction of stratospheric ozone due to all chlorocarbons will be significantly greater (up to several percent more) than the estimates of this report.

6. In estimating the uncertainty in ozone reduction for various CFM emission scenarios, we have not included in the error estimates the possible effects of human intervention in the nitrogen and carbon global cycles. These effects are expected to introduce negligible error in the ozone change estimates for the next 20 to 50 years, but they significantly broaden the uncertainty in the ozone change that may occur 100 to 200 years from now in response to CFM emissions.

REFERENCES

Baes, C. F. 1977. Carbon dioxide and climate: The uncontrolled experiment, *Am. Sci. 65*, 310-320.

Boughner, R. E. 1978. The effect of increased carbon dioxide concentrations on stratospheric ozone, *J. Geophys. Res. 83*, 1326-1332.

Crutzen, P. J., and J. Fishman. 1977. Average concentrations of OH in the troposphere, and the budgets of CH_4, CO, H_2 and CH_3CCl_3, *Geophys. Res. Lett. 4*, 321-324.

Dickinson, R. E., S. C. Lui, and T. M. Donahue. 1978. Effect of chlorofluoromethane infrared radiation on zonal atmospheric temperatures, *J. Atmos. Sci. 35*, 2142-2152.

Ellsaesser, H. W. 1978. Has man increased stratospheric ozone? *Science 199*, 173.

Fishman, J., and P. J. Crutzen. 1978. The origin of ozone in the troposphere, *Nature 274*, 855-857.

Johnston, H. S. 1977. Analysis of the independent variables in the perturbation of stratospheric ozone by nitrogen fertilizers, *J. Geophys. Res. 82*, 1767-1772.

Liu, S. C., R. J. Cicerone, T. M. Donahue, and W. L. Chameides. 1977. Sources and sinks of atmospheric N_2O and the ozone reduction due to industrial fixed nitrogen fertilizers, *Tellus 29*, 251-263.

Logan, J. A., M. J. Prather, S. C. Wofsy, and M. B. McElroy. 1978. Atmospheric chemistry: response to human influence, *Phil. Trans. R. Soc. London 290*, 187-234.

McConnell, J. C., and H. I. Schiff. 1978. Methyl chloroform: impact on stratospheric ozone, *Science 199*, 175.

McElroy, M. B. 1976. Chemical processes in the solar systems: a kinetic perspective. *M.T.P. Int. Rev. Sci. 9*, D. Herschbach, ed., Butterworths, London.

Pyle, J. A. 1978. A zonal mean model of the stratosphere including feedback between chemistry, radiation and dynamics, WMO Symposium on Geophysical Aspects and Consequences of Changes in the Composition of the Stratosphere, WMO No. 511, Toronto, Canada, pp. 240-245.

Stief, J. J., J. V. Michael, W. A. Payne, D. F. Nava, D. M. Butler, and R. S. Stolarski. 1978. The reaction of $Cl + H_2CO \rightarrow HCl + HCO$ decreased sensitivity of stratospheric ozone to chlorine perturbations, *Geophys. Res. Lett. 5*, 829-831.

Vupputuri, R. K. R. 1978. The possible impact of past and projected future atmospheric release of CFMs on stratospheric ozone and its climate investigated in a 2-D time dependent model, WMO Symposium on Geophysical Aspects and Consequences of Changes in the Composition of the Stratosphere, WMO No. 511, Toronto, Canada, pp. 263-267.

APPENDIX A THE TREATMENT OF UNCERTAINTIES (cf. Chapter 3)

PRECISION AND ACCURACY

All through this report a consistent effort has been made to assess the accuracy or uncertainty of all numbers given. Particular attention has been paid to the estimates that will be used to predict global ozone because their uncertainties will generate uncertainty for the prediction.

In the simplest situation, a parameter can be estimated by n repetitions of the same experiment. Then if $x_1,\ldots,x_n$ are the n determinations, an estimate s of the measurement standard deviation σ is found from the sample variance

$$s^2 = \frac{\sum_{1}^{n}(x_i - \bar{x})^2}{n - 1}$$

The estimate from the n observations is $\bar{x}$, and the analysis is often summarized by $\bar{x} \pm s$. This analysis typically is used when x is affected additively by various sources of variation. If the observations $x_1,\ldots,x_n$ are drawn from a Gaussian or normal population $(2\pi)^{\frac{1}{2}}\sigma^{-1}\exp[-(x - \mu)^2/2\sigma^2]$ with mean μ and standard deviation σ, then $\bar{x}$ and s estimate μ and σ. Then $\bar{x}$ is Gaussian with mean μ and standard deviation (or, synonymously, standard error) $s/\sqrt{n}$. Then the assertion that μ is in the interval $(\bar{x} - 2s/\sqrt{n}, \bar{x} + 2s/\sqrt{n})$ will be true about 95 percent of the time. Statisticians call this a 95 percent confidence interval. More casually, the ends of the interval are often called "2σ limits," "95% error limits," and "error bars" and perhaps written $x \pm 2s/\sqrt{n}$. If just numbers are given, these limits could be confused with $\bar{x} \pm s$.

In other situations, the logarithm of x is Gaussian with mean μ, variance σ^2. Then the distribution of x has a longer tail to the right than to the left and so is not symmetric. The 95 percent limits are usually taken as exp$(\bar{y} \pm 2s'/\sqrt{n}$, where $\bar{y}$ and s'^2 are the mean and variance of log x_1,..., log x_n. The log-normal distribution occurs typically when x is affected multiplicatively by various sources of error.

In the last two paragraphs we have been discussing what is usually called the *precision* of a determination. There also may occur systematic errors, which lead to the estimate being biased. The systematic errors tend to remain fixed from one observation to the next, whereas the precision is controlled by errors that vary from one observation to the next. The latter often are called random errors. Systematic errors are usually revealed by intercomparisons of methods. By definition, they are unknowable. Hence, their assessment is always done by appeal to expert judgment. The combination of random and systematic errors determines the *accuracy* of the method.

The accuracy of an estimate is often expressed by the same devices as the precision, despite the fact that part of the accuracy rests on opinion rather than measurement. For example, it is common for an expert, say, to assess accuracy by saying something (e.g., m) is correct to a factor f, meaning that the true value should be in the interval $(m/f, mf)$. In these cases it is sometimes reasonable to assume a log-normal distribution. In this scale, the interval is (log m - log t, log m + log t). If the expert is asked further to give an f so that this is a 95 percent interval, one may identify log f with 2σ.

We always want to get a feeling for the probability or confidence that the interval given includes the true value. Thus, an effort always must be made to give a specific probability curve to the accuracy--usually normal or log normal.

In situations where a system evolving with time is measured at successive times, one often imagines that the measurements are the sum of a smooth function of time plus random error. By thinking of the measurements as the summation of sine waves of different frequencies and phases (just as one thinks of sound), one is led to think of components of the error with different frequencies. In our case the system is the atmosphere. The systematic errors might be the inadequacies of the model. This vocabulary is used in Chapters 6 and 9.

SENSITIVITY ANALYSES

Propagation of the errors in the parameters $\theta_1,\ldots,\theta_n$ of the numerical model of Chapter 8 leads to a probability distribution for the global ozone, or for R, the percentage reduction in global ozone. Here $R = f(\theta_1, \theta_2, \ldots; t)$ where $f(\cdot)$ is a function that the computer takes a lot of time to evaluate. If, again and again, a computer experiment is conducted in which θ_1, θ_2, • are chosen from their presumed distributions (as discussed in the previous section) and then $R = f(\theta_1, \theta_2, \ldots; t)$ calculated, we can gradually build up knowledge of the distribution of R. This is the so-called Monte Carlo method used in Chapter 9.

This simulation method, however, does not give an estimate of the error contribution from the uncertainty of individual rate coefficients. Suppose that the central or most likely values of the θ's are $\theta_1{}^0$, $\theta_2{}^0$, ..., and that t corresponds to the steady state, i.e., $t \to \infty$. Then, approximately,

$$R = R_0 + \sum \left(\frac{\partial R}{\partial O_i}\right)_{\theta^0} (\theta_i - \theta_i{}^0)$$

if all the $\theta_i - \theta_i{}^0$ are small. To determine $(\partial R/\partial\theta_i)\theta^0$, one could compute $R_0 = f(\theta_1{}^0, \theta_2{}^0, \ldots; \infty)$ and $R_0 + \Delta R_1 = f(\Theta_1{}^0 + \Delta\theta_1, \ldots)$. Then $\Delta R_1/\Delta\theta_1$ is approximat-ly $(\partial R/\partial\theta_i)_{\theta}0$. This may be repeated for θ_2, etc. If we write

$$\frac{\Delta R}{\Delta\theta_i} = r_i \frac{R_0}{\theta_i{}^0} \qquad\qquad i = 1, 2, \ldots$$

then

$$\frac{R - R_0}{R_0} \approx \sum r_i \frac{\theta_i - \theta_i{}^0}{\theta_i{}^0} \tag{A}$$

and

$$r_i \approx \frac{\Delta \log R}{\Delta \log \theta_i}$$

Thus r_i indicates the contribution to the percentage change in R due to a percentage change in θ_i. Hence r_i is a measure of the sensitivity of the system to changes in the ith parameter θ_i. This is clearly an *approximate* argument.

If the θ's stand for chemical reaction rate constants k, one may argue that their estimates are log-normally distributed. If the chemists have provided an uncertainty factor f_i so that

$$\frac{1}{f_i} k_i^0 \leq k_i \leq f_i k_i^0 \qquad (i = 1,2, \ldots)$$

is a 95 percent range for k, then it is asserted that $\log(k_i/k_i^0)$ is Gaussian, mean zero, and standard deviation, $\frac{1}{2} \log f_i$.

If (A) is written

$$\Delta \log R = \sum r_i \, \Delta \log(k_i/k_i^0)$$

then $\Delta \log R$ is Gaussian, mean zero, and standard deviation

$$\left[\sum r_i^2 \left(\frac{\log f_i}{2}\right)^2\right]^{\frac{1}{2}}$$

This approximate method was used in the NAS, 1976 report to provide 95 percent limits

$$R_0 \exp \left\{ \pm \left[\sum \left(r_i \log f_i \right)^2\right]^{\frac{1}{2}} \right\}$$

While this method is now thought to be too crude, it does lead to a helpful method for evaluating the relative importance of different reactions, namely $(r_i \log f_i)^2$ with $\sum(r_i \log f_i)^2$, and has been used in Chapter 3.

APPENDIX B DERIVATION OF $K(z)$ PROFILES (cf. Chapter 4)

This appendix reports the results of a study by E. F. Danielsen to determine eddy-diffusion coefficient profiles from globally averaged chemical tracer data. Three independent sets of data are considered.

The first is based on grid-point data obtained from a numerical tracer experiment designed by J. Mahlman for the Fluid Dynamics Laboratory's general circulation model. The second is based on a first approximation to the observed mean ozone profile, below the ozone maximum. The third is based on the observed mean nitrous oxide, N_2O, profile. The second and third methods provide an opportunity to test profiles derived from a downward fluxing gas, O_3, and an upward fluxing gas, N_2O.

This study produced the remarkable result that the observed profiles can be adequately represented by a constant and, at most, two hyperbolic (transition) functions defined as

$$T_k = \frac{\exp\,[m_k(Z - Z_k)]}{1 + \exp\,[m_k(Z - Z_k)]} \tag{B.1}$$

$$\frac{1}{m}\frac{dT_k}{dZ} = S_k = \frac{\exp\,[m_k(Z - Z_k)]}{\{1 + \exp\,[m_k(Z - Z_k)]\}^2} \tag{B.2}$$

These functions are shown in Figure B.1. The *K* profiles inferred from these expressions are desirably smooth but otherwise closely similar to the profiles derived from fitting procedures with more degrees of freedom.

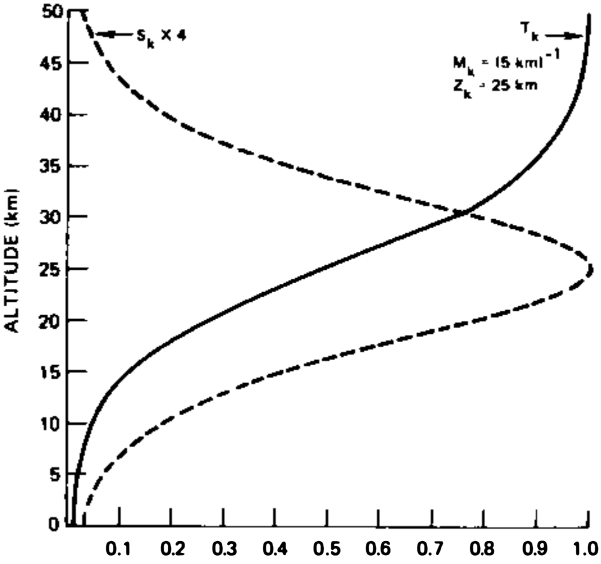

FIGURE B.1 Hyperbolic transition functions, T_k and S_k versus altitude.

NUMERICALLY DERIVED TRACER DATA

The main advantages of the numerically derived tracer data are that the flux $\overline{w'c'}$ has been evaluated directly from millions of grid-point values and all mean values are representative. To those who distrust numerical models, these advantages may not compensate for the lack of real measurements, but this model does simulate rather closely the zonal mean statistics of the atmosphere (Mahlman and Manabe, 1972), and Mahlman has taken great care to remove the diffusive effects of truncation errors in the finite differencing approximations. In particular, the model develops the observed correlation between conservative tracers (like radioactivity from nuclear explosions) and potential vorticity (Danielsen, 1968; Mahlman and Moxim, 1978), a correlation that permits one to relate extratropical transport to large-scale wave cyclones. The model does not resolve small-scale convective motions but includes their effects by a convective adjustment and a simulated precipitation removal. In general, the three transport mechanisms of the last section are simulated in the model.

In deriving each *K* profile we will first use a vertically integrated form of the continuity equation to determine the mean flux as a function of z, then we will solve Eq. (B.1) for *K*(z). The equation determining the flux at level z is

$$F(z) = F(0) - \partial\Psi/\partial t + \phi \qquad (B.3)$$

where *F*(0) is the surface flux, Ψ is the number or mass of the *i* molecules per unit area in the column from the surface to height z, and ϕ is the net source (if positive) or sink (if negative) of *i* molecules in the same column.

Our first case, the tracer experiment, has no internal chemical-photochemical sources or sinks. Following an initial injection at midlatitudes in the stratosphere, the tracer spreads in three dimensions because of transport only. When it reaches the middle and lower troposphere, a percentage is removed to simulate wet and dry removal processes. In the 3-D model these are internal physical sinks. Because present 1-D models do not simulate such sinks explicitly, they must be implicitly incorporated

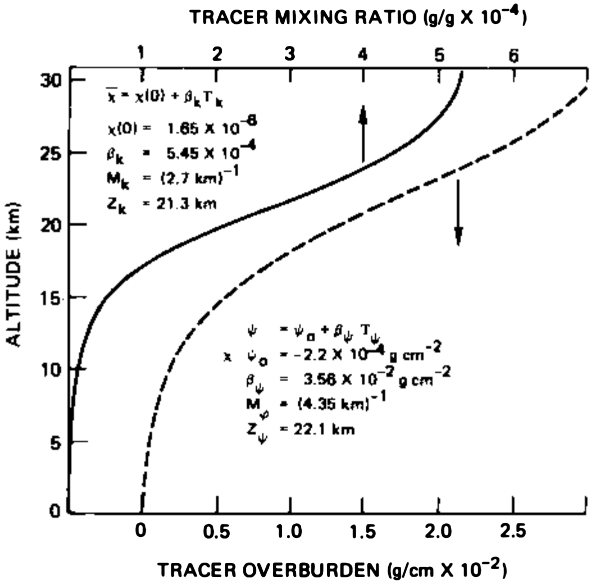

FIGURE B.2 Tracer mixing ratio and tracer overburden versus altitude.

into the K profile. We are obliged to set $\phi = 0$ at all levels and augment the surface flux. As $F(0)$, we use the mean of the four fluxes between 4 and 13.6 km, with the last two levels being close to the top of the wet removal in the 3-D model.

Knowing $F(0)$ and setting $\phi = 0$ in Eq. (B.3) we can determine $F(z)$ by evaluating $\partial\Psi/\partial t$. To determine Ψ we first compute the annual average of χ at each level. These values appear in Figure B.2 as crosses. Next, these data are fitted with a constant plus a transition function, as shown by the continuous line in Figure B.2. The fit is tested in both linear and logarithmic coordinates. Values of the four constants determining the fit are listed also in Figure B.2. When χ is multiplied by $\bar{\rho}$ and integrated vertically, we obtain the Ψ profile shown by the dashed line. Finally, using the change in Ψ over the year, we obtain $\partial\Psi/\partial t$ and use Eq. (B.3) to evaluate $F(z)$.

Once we establish representative flux values as continuous functions of z, we then use Eq. (B.1) to compute

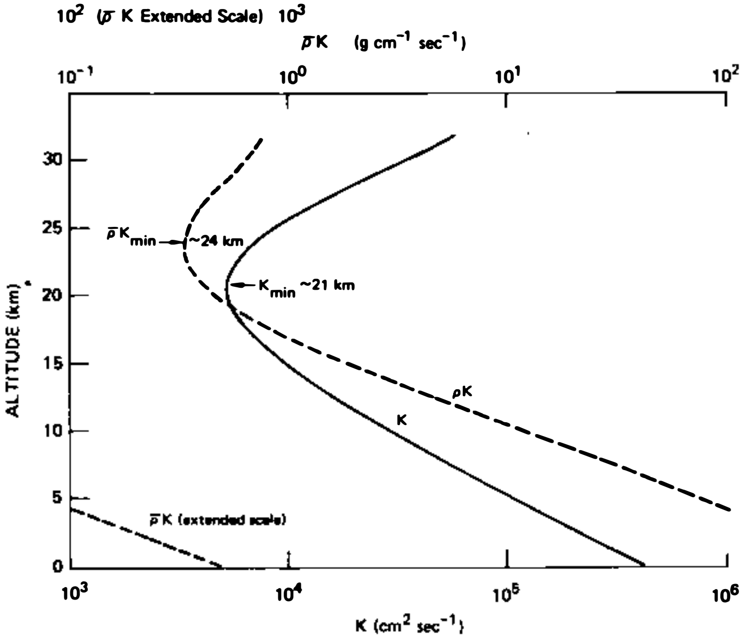

FIGURE B.3 K and $\bar{\rho}K$ profiles.

the K profile. For $\bar{\rho}$ we use the density in a standard atmosphere. The K and $\bar{\rho}K$ profiles derived by this method from the tracer data are plotted in Figure B.3. Note that K varies smoothly to a distinct minimum at ~21 km and then increases above. Such a profile agrees with our expectations, but now we have numerical values as well as the expected shape.

OZONE DATA

Because ρ decreases rapidly with height, the minimum in $\bar{\rho}K$ is about 3 km higher than the minimum in K. It is this $\bar{\rho}K$ minimum at 24 km that acts to restrict the vertical flux and to increase the vertical gradient of χ_i. Therefore, if the K profile is generally valid and the flux of any gas is approximately constant in the vicinity of 24 km, the magnitude of the gradient $|\partial\bar{\chi}_i/\partial z|$ will be a maximum at that level.

These conditions appear to be met by the mean ozone profile [Figure B.4(a) and B.4(b)]. From the surface to 30 km it is based on the ozonesonde data of Hering and Borden (1964a; 1964b; 1965). For each of the four seasons, zonal mean profiles are first computed by averaging all data for stations within five separate latitude bands. These zonal means are then weighted by the percentage of the earth's surface area appropriate to the band in order to obtain global-seasonal means; and, finally, all the seasonal means are averaged to obtain a global means. The extension to 70 km is an educated guess based on a variety of sources, including rocket and sounding data.

Deriving a K profile from the mean ozone profile at first appears to be simpler than it was for the tracer data because the ozone profile is close to steady state. However, the appearance is an illusion because the internal sources and sinks are not zero, therefore, the ϕ in Eq. (B.3) is not zero. If we based the $\phi(z)$ profile on 1-D model computations, the solution would be model-dependent, which we would prefer to avoid. The functional fit to the ozone data suggests an alternative approach. The partial fit, $\bar{\chi}_{O_3} \simeq \chi(0) + \beta_k T_k$, shown as the dashed line in Figure B.4(b), rather closely approximates $\bar{\chi}_{O_3}$ up to 24 km, and its implied source is at $+\infty$. Therefore, if we restrict our derivation to the partial fit, we only neglect the secondary sources by assuming $\phi = 0$. The reason is implicit in Figure B.4(b). It is the $-\gamma_s T_s$ functions that generate the maximum in $\bar{\chi}_{O_3}$ at 32 km, lowering the primary source

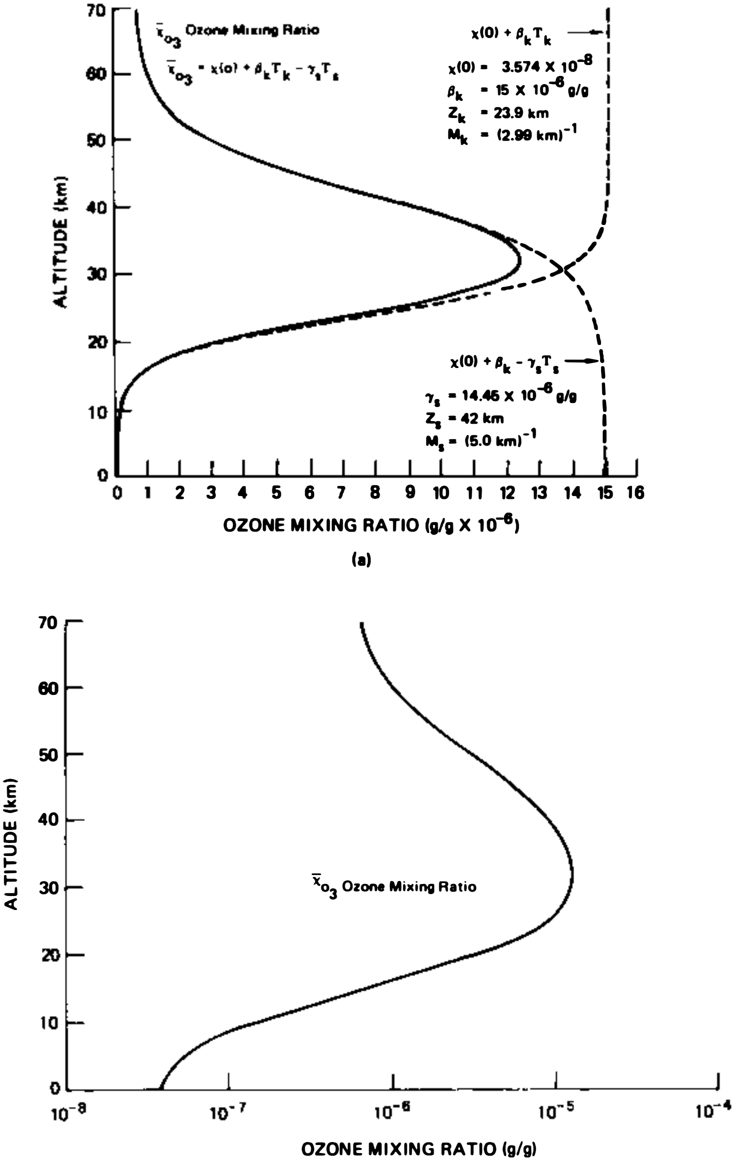

(a)

(b)

FIGURE B.4 (a) Ozone mixing ratio, based on ozonesonde data, (b) ozone mixing ratio, partial fit to function $\chi(0) + B_k T_k$ and $\chi(0) + B_k - \partial_s T_s$.

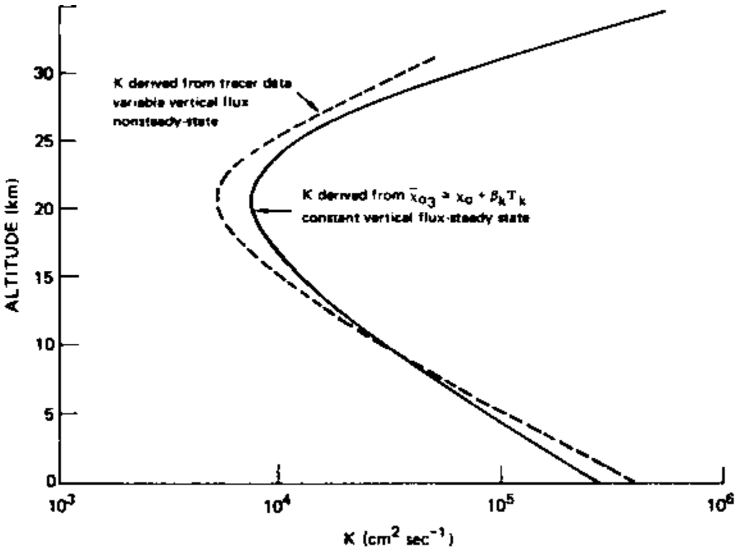

FIGURE B.5 *K* profiles derived from $\bar{\chi}_{O_3} \sim \chi_O + B_k T_k$ and from tracer data.

from +∞ to ~32 km. Thus $-\gamma_S T_S$ controls the primary source and the upward flux above the primary source.

By neglecting $\gamma_S T_S$, setting $\phi = 0$, assuming steady state and a surface flux of 7×10^{10} molecules $cm^{-2}\ sec^{-1}$, we obtain the *K* profile shown in Figure B.5 as the continuous line. Indeed, the new *K* profile has a shape similar to the former, and from the surface to 24 km, it differs in magnitude by <1.5. One possible interpretation to be drawn from this comparison is that our assumption is reasonable, and that the secondary sources are not large from the surface to 25 km.

NITROUS OXIDE DATA

The third *K* profile is derived from the global-mean nitrous oxide mixing ratio, $\bar{\chi}_{N_2O}$. This gas is selected because its primary source is at the earth's surface, and its primary sink is photolysis in the stratosphere. The *K* derived from it will provide a direct evaluation of the generality of the diffusion approximation for downward and upward moving gases. Figure B.6 shows the global mean profile that we derive from measurements made between 1975 and 1977 (Schmeltekopf *et al.*, 1977; and Chapter 6). After all data are plotted versus height above sea level, three zonal mean profiles are drawn from the data at tropical, midlatitude, and polar stations. Again, as with the ozone, these profiles are weighted by their percentage surface area and then summed to produce the global mean. In contrast with $\bar{\chi}_{O_3}$, the global mean of $\bar{\chi}_{N_2O}$ is strongly influenced by the tropics.

Note that the tropospheric gradient, 0 to 13 km, is extremely small but finite. It is small enough to be overlooked. Indeed, the statement is often made that, "the troposphere is completely mixed," implying a zero gradient. If this statement were true, the K would have to be infinite, but, as we shall see, the tropospheric K's derived from this N_2O profile are actually smaller than those derived previously, despite the very small mean gradient.

In contrast to the $\bar{\chi}_{O_3}$ profile, the best fit is obtained by a transition and a symmetric function, but, again, only seven constants are required. Here we cannot use a partial fit because both functions describe the major sink. For what it may be worth, the approximation $\bar{\chi}_{N_2O} \approx \bar{\chi}_O - \beta_k T_k$ resembles quite closely a mean for mid-high latitudes, so the $+\gamma_s S_s$ describes the tropical influence. Again, to

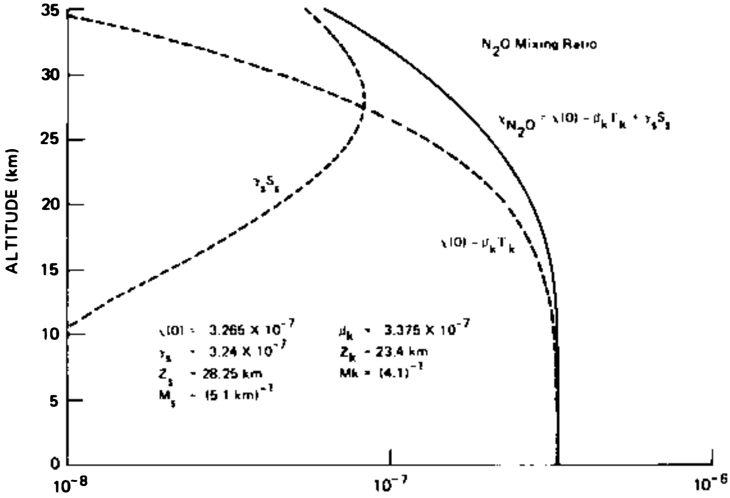

FIGURE B.6 Global mean profile--N_2O mixing ratio.

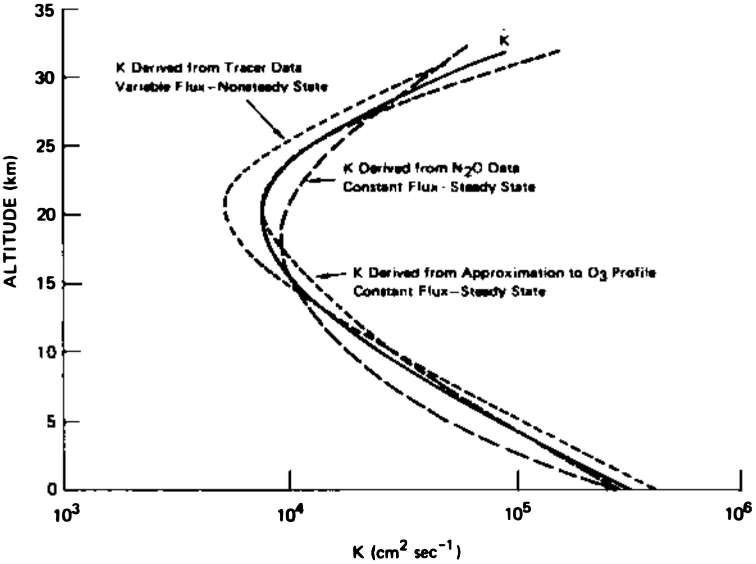

FIGURE B.7 *K* profile computed from $\bar{\chi}_{N_2O}$ profile.

avoid dependence on a model, we neglect the destruction by photolysis and chemistry, and assume $\phi = 0$ and $\partial\Psi/\partial t = 0$ to compute a K profile. Later we will discuss the profile resulting from $\phi \neq 0$, where ϕ is determined from a 1-D model.

The K profile computed from the $\bar{\chi}_{N_2O}$ profile, under the above assumptions with $F(0) = 2 \times 10^9$ molecules cm^{-2} sec^{-1} (Schmeltekopf *et al.*, 1977) is presented in Figure B.7 as a dashed line. Included for comparisons are the two previously derived K profiles as dotted lines and a simple mean of the three profiles as a continuous line. The latter, labeled $\bar{K}$, is included for those who would consider each of the three profiles equally possible.

We notice that all profiles have similar shapes and that the range at any level is less than a factor of 2, i.e., $K = \bar{K}(1 \pm 0.33)$ includes all profiles. However, the tracer data yield the smallest and sharpest minimum, the N_2O data the largest and broadest minimum. Within the ±33 percent range there seems to be no inherent problem produced by the sign of the mean transport.

PROPOSED PROFILES FOR 1-D MODELS

Each of the three profiles previously derived from independent data has an increasing trend near the upper limit of its applicability. Such a trend is anticipated because the adiabatic heating and cooling rates increase in magnitude in the upper stratosphere, as do the zonal mean vertical motions. Although the latter must be specified explicitly in a 2-D model, their effects are implicit in a 1-D model, where they contribute to an increase in the magnitude of K.

Ascending and horizontally diverging mean motions produced by heating in the upper, sunlit stratosphere produce a stable, anticyclonic flow, but converging and descending motions in the cooling hemisphere generate a less stable cyclonic flow, which is usually referred to as a polar vortex. Occasionally this vortex becomes unstable with an associated increase in the horizontal and vertical transports. The K in a 1-D model must include the mean effects of these intermittent instabilities and other turbulent transports as well as those of the zonal mean circulations. Assuming that the turbulent transports and the zonal mean transports increase with the adiabatic rates, we increase the K's by a factor of 10 between 30 and 70 km and maintain a factor of 2 uncertainty.

The $\bar{K}$ profile shown in Figure B.8 is a slightly modified version of that in Figure B.7 extended to 70 km in accordance with the above reasoning. Modifications between 20 and 30 km involve a slight reduction in $\bar{K}$ to account for the expected decrease in the magnitude of both the N_2O and O_3 flux due to internal sinks and sources, respectively.

Figure B.9 depicts two additional K profiles, labeled K_1 and K_2, which bracket the uncertainty range in the stratosphere but which converge to the upper limit in the lower troposphere. Adopting larger tropospheric K values is equivalent to assigning a low probability to those tropospheric K's derived from N_2O data.

We assign a low probability to the tropospheric K's because

1. They are extremely sensitive to small changes in the N_2O profile;
2. The global mean N_2O profile is not known with sufficient accuracy to overcome this sensitivity;
3. The global mean O_3 flux and mixing ratio profile are much less sensitive and much better known.

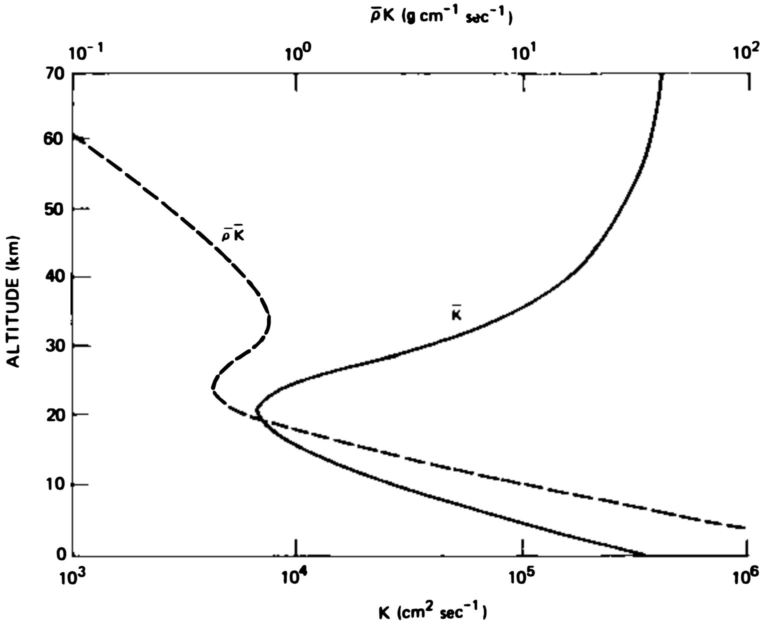

FIGURE B.8 $\bar{K}$ profile extended to 70-km altitude.

We mentioned earlier when discussing the $\bar{\chi}_{N_2O}$ profile that, although the tropospheric gradient was very small, the *K*'s derived from it were smaller in the troposphere than the *K*'s derived from the tracer and ozone data. However, if the mean gradient of $\bar{\chi}_{N_2O}$ from the surface to 12 km is reduced by 40 percent, the *K*'s would be increased to equal those derived from the tracer data. A 40 percent reduction is produced by increasing the $\bar{\chi}_{N_2O}$ at 12 km by 3 ppbv, i.e., by a 1 percent change in the mean mixing ratio at 12 km, or a +0.5 percent change at 12 km, and a -0.5 percent change at the surface. With no fear of contradiction, we can state here that the mean N_2O profile is not known to this required accuracy.

On the other hand, the mean tropospheric ozone flux is 30 to 40 times greater than the nitrous oxide flux, so for the same *K* profile, the $\bar{\chi}_{O_2}$ gradient should be ~35 times the $\bar{\chi}_{N_2O}$ gradient. Of course, the signs are reversed, and here we refer only to their magnitudes. The ratio obtained from the mean data in this report [see Figures B.4(b) and B.6] is 21/1, where the $\bar{\chi}_{O_3}$ values have been

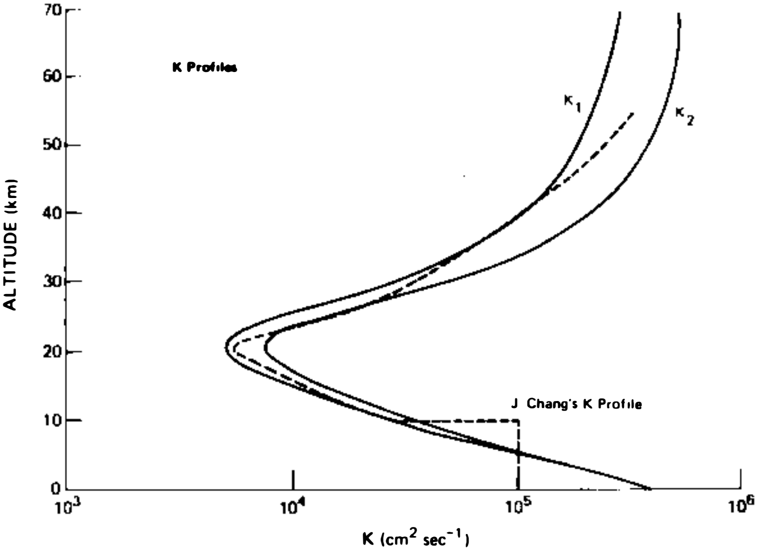

FIGURE B.9 *K* profiles that bracket the uncertainty range in the stratosphere.

divided by 1.66 to convert from mass to number mixing ratio. Again, an increase of 1 percent in $\bar{\chi}_{N_2O}$ at 12 km will increase the mean gradient ratio to 35/1. Therefore, the larger tropospheric *K*'s are consistent with the tracer data and the ozone data, and are not inconsistent with the present nitrous oxide data.

EFFECTS PRODUCED BY DIFFERENT *K* PROFILES

If we accept the $\bar{K}$, K_1, K_2 profiles as reasonable in form and magnitude, we can evaluate their effects on the mean ozone profile by comparing the results obtained by a 1-D model for each *K* profile. In one test to date with a stratospheric model* the average difference in $\bar{\chi}_{O_3}$ was only 2 percent, and above 50 km it was reduced to 0.3 percent. The maximum difference was 8 percent at any one

---

*Recent tests run with the NASA-Ames Research Center's one-dimensional stratospheric model. Special thanks to R. Turco and R. Whitten.

level. In these computations the flux at ~10 km was held fixed as a boundary condition.

It is simpler for us to make an alternative test, i.e., to fix the $\bar{\chi}_{O_3}$ profile and then to determine how the flux and sources vary with the K profiles. In these tests all chemical processes are included implicitly in the results. Again, we will use K_1 and K_2, but we will compare these K's, the fluxes, and the sources to those derived by J. Chang from his chemical-diffusion model.

Before discussing the results, we should indicate that Chang does not consider his model to be representative of a global mean. Rather, because of the specification of the solar flux, he considers the model to represent conditions at about 30° of latitude. We have included the K profile used in his model as the dashed line in Figure B.9. Note that above 10 km his K profile undulates between the limits of K_1 and K_2. Below 10 km his constant K value is approximately the mean of the decreasing K profiles. Despite these differences, the model's $\bar{\chi}_{O_3}$ profile is very similar to the global mean shown in Figure B.4. The differences are mostly confined to the value of the maximum. The model has a maximum of 17.4×10^{-6} g of O_3/g of air, while the global mean has a maximum of 12.4×10^{-6} g/g. This maximum difference of 40 percent decreases to 5 percent at 10 km and at 50 km, i.e., at about ±20 km from the height of the maximum.

The vertical fluxes computed from the K_1 and K_2 profiles of Figure B.1 and the $\bar{\chi}_{O_3}$ profile of Figure B.4 are presented in Figure B.10. Note that the vertical flux is negative below 32 km, but positive above. For the K_2 diffusion coefficient profile, the downward flux oscillates at about -7×10^{10} molecules cm^{-2} sec^{-1} from the surface to 25 km. This represents a reasonable annual mean value based on the deposition of strontium-90 and the positive correlation between ^{90}Sr and $\bar{\chi}_{O_3}$ (Danielsen, 1968; Danielsen and Mohnen, 1977).

In contrast, the K_1 flux generally increases (becomes less negative) below 25 km and the model's flux decreases. Thus, the K_1 profile implies a net source, the model a net sink below the 25-km level. The positive flux in the model lies midway between the limiting fluxes of profiles K_1 and K_2, i.e., it will be consistent with $\bar{K}$ at these altitudes.

The corresponding distributions of the apparent sources and sinks obtained from differentiating the inferred fluxes are plotted in Figure B.11 and confirmed with the sources and sinks in Chang's model. Generally, the profiles are similar in phase, differing mostly in magnitude. The major

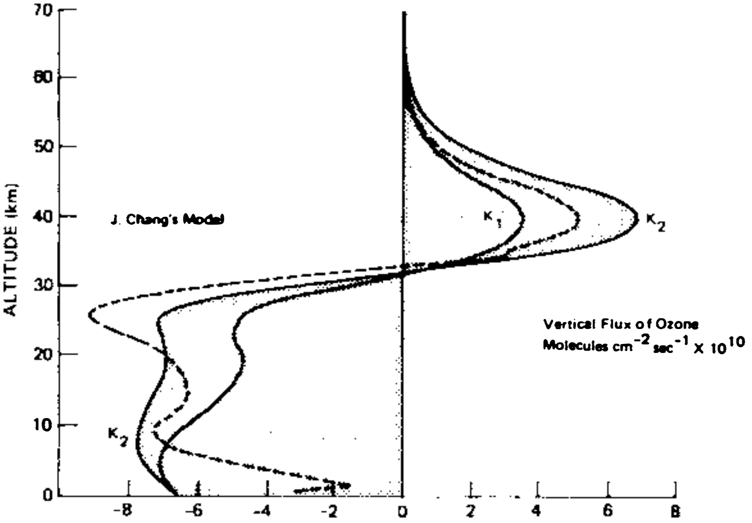

FIGURE B.10 Vertical flux of ozone computed from *K* profiles and $\bar{\chi}_{O_3}$ profile.

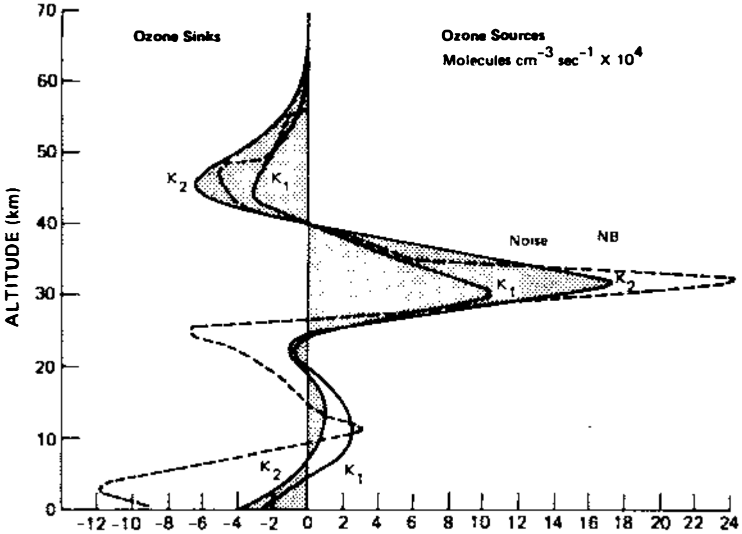

FIGURE B.11 Distribution of apparent ozone sources and sinks.

source is in the stratosphere near 32 km. Ozone molecules diffusing upward from this source are destroyed above the 40-km level. The ozone molecules diffusing downward are destroyed mainly at the ground according to the K_1 and K_2 profiles but are destroyed both in the mid stratosphere and in the troposphere according to the model. The differences in strength of the apparent and model source at 32 km and of the apparent versus model sinks at 25 and 3 km are significantly larger than that due to differences in the diffusion coefficient and are presumably caused by differences in solar production or chemical rates and by the neglect of nonlinear terms in the production or chemical-reaction terms.

Noting that the K profiles were derived without reference to sources and sinks of O_3, it is perhaps surprising how well the model sinks can be inferred from the profiles and the observed O_3 profiles.

CONCLUSIONS

Three diffusion-coefficient K profiles are derived from independent sets of data, including an upward and downward moving trace gas, and an inert tracer from a three-dimensional numerical experiment. Based on the general similarity in magnitude and shape of these K profiles, we conclude that the diffusion approximation is valid within a factor of 2 uncertainty, i.e., the differences are included in $K(z) = \bar{K}(z)\ (1 \pm 0.33)$. Here $\bar{K}(z)$ is a smoothly varying function of height, decreasing approximately exponentially in the troposphere from a surface value of 3.3×10^5 cm^2 sec^{-1} to a minimum of 7×10^3 cm^2 sec^{-1} at 21 km, then increasing again to a maximum of 4.1×10^5 cm^2 sec^{-1} at 70 km. The mesospheric maximum is an untested extrapolation because no appropriate data are available.

Whether the factor of 2 uncertainty is an actual limitation of the diffusion approximation or just an apparent limitation caused by our inability to resolve $\partial\bar{\chi}_i/\partial z$ with sufficient accuracy cannot be decided at present.

The critical factor for the troposphere is the percentage change in $\bar{\chi}_i$ over the mean depth of the troposphere. Since ozone has a large flux, ~10^{11} molecules cm^{-2} sec^{-1}, and a relatively small mean tropospheric number mixing ratio, the percentage change is ~100. These large percentage changes are measurable. By contrast, nitrous oxide has a much smaller flux, ~10^9 molecules cm^{-2} sec^{-1} and a relatively large tropospheric mixing ratio, so the percentage change is ~0.3. Such small percentage changes are well within the error limits of measurement and nonrepresentative sampling. The percentage changes for F-11 and F-12 are also small, as are those of most trace gases with a surface or near-surface source.

At present, only the O_3 flux and $\bar{\chi}_{O_3}$ gradients are large enough in the troposphere to be unambiguous. Therefore, it is worth noting that the tropospheric K's derived from the approximation to the $\bar{\chi}_{O_3}$ profile differed from those derived from the tracer data by less than a factor of 1.5, i.e., $K(1 \pm 0.20)$ would span the uncertainty. With use of the complete $\bar{\chi}_{O_3}$ profile, the K's equaled those derived from the tracer data near the surface. The K_1 and K_2 profiles discussed above are consistent with these results.

The existence of one minimum in the K, K_1, and K_2 profiles at approximately 21 km, which yields a minimum in ρK at 24-25 km, is consistent with our knowledge of three-dimensional transport and also consistent with the general trend in χ_i profiles. Many mean profiles have only one major maximum in the magnitude of their vertical gradients, and they are located close to 24 km. Individual profiles at one place and time will contain more than one maximum, caused by the large-scale, wave-dominated transports, but these will not survive the global averaging of many, many such local profiles. Also, if the "maximum" gradient is a few kilometers above or below 24 km, there is usually evidence for significant sources or sinks in the vicinity--F-11 and CO profiles are good examples.

Finally, a factor of 2 uncertainty in the K profile does not imply a factor of 2 uncertainty in the $\bar{\chi}_i$ profiles. For example, only slight changes in the $\bar{\chi}_{N_2O}$ profile, changes barely detectable in current data, can maintain a certain vertical flux against a factor of 2 change in K. In addition, there are many possible negative feedbacks in a complex chemical 1-D model that dampen the effects of changes in K's. Since the $\bar{\chi}_i$ profiles will adjust to maintain a flux compatible with the sources for species i, uncertainties in the source functions of current 1-D models, such as the neglect of nonlinear terms, are probably more serious than a factor of 2 uncertainty in K profiles.

REFERENCES

Danielsen, E. F. 1968. Stratospheric-tropospheric exchange based on radioactivity, ozone and potential vorticity, *J. Atmos. Sci. 25*, 602-518.

Danielsen, E. F., and V. A. Mohnen. 1977. Project Dustorm report: ozone transport, *in situ* measurements and meteorological analyses of tropopause folding, *J. Geophys. Res. 82*, 5867-5877.

Hering, W. S., and T. R. Borden, Jr. 1964a. *Ozonesonde Observations Over North America*, Vol. I., AFCRL-64-30(I), Air Force Cambridge Research Laboratories, Office of Aerospace Research, USAF, L. G. Hanscom Field, Mass., 512 pp.

Hering, W. S., and T. R. Borden, Jr. 1964b. *Ozonesonde Observations Over North America*, Vol. II., AFCRL-64-30(II), Air Force Cambridge Research Laboratories, Office of Aerospace Research, USAF, L. G. Hanscom Field, Mass., 280 pp.

Hering, W. S., and T. R. Borden, Jr. 1965a. *Ozonesonde Observations Over North America*, Vol. III., AFCRL-64-30(III), Air Force Cambridge Research Laboratories, Office of Aerosapce Research, USAF, L. G. Hanscom Field, Mass., 265 pp.

Hering, W. S., and T. R. Borden, Jr. 1965b. "Mean Distributions of Ozone Density Over North America, 1963-1964," AFCRL-65-913, Air Force Cambridge Research Laboratories, Office of Aerospace Research, USAF, L. G. Hanscom Field, Mass., 19 pp.

Mahlman, J. D., and S. Manabe. 1972. Numerical simulation of the stratosphere: implications for related climiate change problems, in *Proceedings of the Survey Conference* (Cambridge, Mass.), Climatic Impact Assessment Program, U.S. Dept. of Transportation, DOT-TSC-OST-72-13, pp. 186-193.

Mahlman, J. D., and W. J. Moxim. 1978. Tracer simulation using a global general circulation model: results from a mid-latitude instantaneous source experiment, *J. Atmos. Sci. 35*, 1340-1375.

Schmeltekopf, A. L., D. L. Albritton, P. J. Crutzen, P. D. Goldan, W. J. Harrop, W. R. Henderson, J. R. McAfee, M. McFarland, H. I. Schiff, and T. L. Thompson. 1977. Stratospheric nitrous oxide altitude profiles at various latitudes, *J. Atmos. Sci. 34*, 729-736.

APPENDIX C

STATISTICAL MODELS FOR DOBSON STATION OZONE READINGS (cf. Chapter 6)

The empirical approach depends on finding statistical regularities in the data. For the series of monthly Dobson readings from a particular station, $\{y_1, y_2, \ldots, y_T\}$, say, the most obvious feature is the seasonal variation. There are several ways that this may be reduced. The simplest is to consider the series of differences $y_{13} - y_1$, $y_{14} - y_2$, ... If B is the backshift operator, so that $Bt_t = y_{t-1}$, the new series is $(1 - B^{12})\, y_t$ for $t = 13, \ldots, T$. This technique is used by Tiede *et al.* (1977). As will be seen below, they then seek a model for the series $(1 - B^{12})y_t$, $t = 13, \ldots, T$. Alternatively, one may find the means of all Januarys, Februarys, etc. and subtract from each y_t, the mean of the month corresponding to t, $\bar{y}_{\cdot m}$, say. The series $y_t - \bar{y}_{\cdot m}$ will thus be free of seasonal changes of level if there is no long-term trend and is said to be the result of applying the Buys-Ballot filter to the series y_t. By contrast, $(1 - B^{12})y_t$ is free of seasonal changes even if the seasonal pattern gradually changes. This distinction will be important later. For many of the series, the variability of $y_t - \bar{y}_{\cdot m}$, as measured by the monthly standard deviation $s_{\cdot m}$, changes from month to month. This suggests that the statistical analysis of the series,

$$z_t = \frac{y_t - \bar{y}_{\cdot m}}{s_{\cdot m}} \qquad t = 1, \ldots, T$$

since it is varying around zero with a standard deviation of unity, should only involve the serial dependence of its elements. Parzen and Pagano (1978) have used this method.

It is reasonable to hope that a sequence from which the seasonal variation has been removed might have a simple structure, e.g., approximate linear dependence on its past. In this case,

$$z_t = \phi_1 z_{t-1} + \dots + \phi_p z_{t-p} + u_t \tag{C.1}$$

where the residuals u_t show no time dependence and are uncorrelated. If this is so, the coefficients $\phi_1, \dots, \phi_p$ may be estimated by applying least squares to the data. In practice, p has also to be found so that the residuals have the desired properties. Parzen and Pagano (1978) use one of several methods to do just this. The stochastic difference equation model (C.1) defines an autoregressive (AR) process. A wide class of processes may be approximated this way by allowing p to be large. Note that Eq. (C.1) may be written

$$\phi(B) z_t = u_t \tag{C.2}$$

where

$$\phi(B) = 1 - \phi_1 B - \dots - \phi_p B^p$$

There are situations in which Eq. (C.1) might be a discrete approximation to a theoretical model (though in our case, this does not seem to be so).

If z_t were observed subject to independent measurement errors, as $Z_t = z_t + e_t$, then putting $z_t = Z_t - e_t$ in Eq. (C.2), we find

$$\phi(B) Z_t = u_t + \phi(B) e_t \tag{C.3}$$

Equation (C.3) suggests a generalization of Eq. (C.2), namely,

$$\phi(B) Z_t = \phi(B) a_t \tag{C.4}$$

where $\theta(B) = 1 - \theta_1 B - \dots - \theta_q B^q$ and $\{a_t\}$ is a sequence of independent disturbances. If $\theta(B) = 1$, Eq. (C.4) reduces to Eq. (C.2). This equation generates an autoregressive moving average process (ARMA) and is the model assumed for $(1 - B^{12}) y_t$ by Tiede *et al*. (1977). The ARMA process for large enough p and q can model essentially any stationary process. It should not be thought of only as related to an AR via measurement error. Naturally, it will fit a stationary series better than an AR process, but usually it will do so with fewer parameters. Model (C.4) is much harder to fit than is Eq. (C.2), but programs and experience have made its use very popular [see, e.g., Box and Jenkins (1970)]. Specifically, Tiede *et al.* use, where y_t is the monthly ozone series,

$$\phi(B)(1 - B^{12})y_t = \theta(B)a_t \qquad \text{(C.5)}$$

and demand that B^{12} appear in $\theta(B)$. At this stage, they do not take account of the seasonal changes in variability so one could expect them to get a_t's with differing variances--not quite what the model presupposes. To find p and q and the coefficients in $\phi(B)$ and $\theta(B)$ some experience in examining graphical output is required in the effort to get independent stable residuals. By contrast, Parzen and Pagano use a more objective method to determine p; however, they do less-detailed study of the residuals than do Tiede *et al.*

These authors had in mind additive models of the form

$$\left.\begin{aligned} y_t &= M_m + \text{error} && \text{(before CFMs)} \\ y_t &= M_m + \text{trend} + \text{error} && \text{(after CFMs)} \end{aligned}\right\} \qquad \text{(C.6)}$$

where the M_m are the true monthly means. The differences are (i) methods of eliminating M_m's, (ii) taking or not taking the differing monthly variances into account, (iii) the different stationary processes fitted. However, if it is more reasonable to assume a multiplicative model, we would have on taking logarithms,

$$\left.\begin{aligned} \log y_t &= \log F_m + \text{error} \\ \log y_t &= \log F_m + \log\ (\text{trend}) + \text{error} \end{aligned}\right\} \qquad \text{(C.7)}$$

Since $\log F_m$ are monthly constants and log (trend) is a function of time, the same methods may be applied to the multiplicative as to the additive models.

There is an inevitable problem in subdividing the variation in y_t or $\log y_t$ into these three parts: monthly, trend, and error. The error gets what is not fitted.

Tiede *et al.* and Parzen and Pagano both fit, without trend, to pre-1970 data and then use 1970-1975 data to check for trend. This is somewhat arbitrary. The model calculations begin their depletion curves in 1950.

Tiede *et al*. justified their procedure by actually depleting their series with a published depletion curve and showing that their procedure found that the linear slope was to a close approximation now reduced by the average slope of the curve in the 1970-1975 period. This is only a justification if all stations deplete with the same curve. They then applied to each station their estimated filter from Eq. (C.5) to the Eq. (C.6) in the form $y_t = M_m + \omega\{t\}$ + error, where $\{t\}$ is zero for all of 1970, unity for 1971, etc. Writing

$$y_t'' = \frac{\hat{\phi}(B)(1 - B^{12})}{\hat{\theta}(B)} y_t, \quad x_t'' = \frac{\hat{\phi}(B)(1 - B^{12})}{\hat{\theta}(B)} \{t\} \qquad \text{(C.8)}$$

they have for 1970 onwards

$$y_t'' = \omega x_t'' + (\text{error})'' \qquad \text{(C.9)}$$

where (error)" is assumed to have the white-noise character of the $\{a_t\}$ in Eq. (C.5). They then estimate the "staircase" slope ω from Eq. (C.9) by a weighted least squares. The weights are monthly standard deviations, which they did not introduce in fitting the process. The slopes for the nine stations are averaged, and this average is compared with its computed standard error. The average slope is not significantly different from zero.

Parzen and Pagano do not look for slopes: they argue that if trends are present the observations for each station will deviate systematically from the model predictions. They first check this, station by station, by comparing mean squares before and after 1970. They then give another test that will reflect an unequal number of positive and negative signs in the deviations of the observations from the predictions. These tests have much less power than the slope tests. They, like Tiede *et al*., decide there are no indications of a trend during 1970-1975 except in Huancayo, which both suggest may be due to other causes.

For this report more calculations were done. The Tiede *et al*., technique of estimating a slope for each station and averaging the slopes was carried out with the Parzen and Pagano method of seasonal elimination and AR fitting. The same methods were applied to the multiplicative model (C.7). Limitations of computing prevented the Box-Jenkins method from being applied to data corrected by monthly means and to the multiplicative models. The combination of $1 - B^{12}$ seasonal elimination and AR process fitting was tried. A spectral analysis of the largest series, that from Arosa, suggested that the Buys-Ballot filter was superior here to the $1 - B^{12}$ filter because it produced smaller residuals and a flatter spectrum. In all these calculations various simultaneous fitting programs were used. In particular, all the data were used for all fittings, in contrast to the procedures used by Tiede *et al*. This technique becomes more valuable when there is an increasing amount of data after the time when a trend begins. In different analyses, a linear trend was assumed to start in 1960, 1966, and 1970. Each time the program produced an estimated slope using the data to the end of 1976 and standard errors for this estimate and those that might be expected if the same analysis were made of all the data that will be available in years into the future from 1976. If the multiplicative model standard errors are multiplied by 300, they agree very well with those from the additive model. This is to be expected if

$$\left.\begin{aligned} \log y &= \log M_m + \log \text{trend} + \text{error} \\ \log \text{trend} &= \beta(t) \end{aligned}\right\}$$

for then

$$\frac{d}{dt} \log y = \frac{1}{y}\frac{dy}{dt} = \beta$$

Roughly $y = 300$ D.U. so $dy/dt \approx 300\ \beta$. We may therefore continue with either model. The three slope estimates are much less than their standard errors, which were 0.1, 0.16, and 0.25 D.U., compared with the Tiede *et al*. standard error of about 0.5 D.U. for 1970. The twofold increase apparently comes from the use of the $1 - B^{12}$ seasonal filter not from the different error processes involved. The use of the $1 - B^{12}$ with an AR process led to a threefold increase. Thus none of these methods revealed a general decrease, but they were tried for reasons to be explained.

A further calculation was performed to test a prediction by Penner and Chang (1978). They gave a predicted amount of ozone, since 1950, that showed a solar effect. This variable was inserted into almost all of the above calculations, instead of the "hockey-stick" depletion starting in 1970. No relationship could be found with observed station ozone. This may partly be due to the fact that individual stations will not be expected to follow the Penner and Chang curve.

The main purpose of trying out almost every permutation and combination of known models and methods was to see if any particular model plus method stood out as giving a superior fit. Had we found one, then it would be of use in attacking the question--when could one expect to detect predicted trends?

The calculations mentioned above enable us to give a standard error to a slope estimated from these nine Dobson stations in the future. The figure depends on when the trend is assumed to begin, the error model, and the statistical methods. The computed standard errors fall in the D.U. ranges (0.15, 0.40) for 1980, (0.06, 0.22) for 1985, and (0.05, 0.20) for 1990.

REFERENCES

Box, G. E. P., and G. M. Jenkins. 1970. *Time Series Analysis and Forecasting Control*. Holden Day, San Francisco.

Parzen, E., and M. Pagano. 1978. *Statistical Time Series Analysis of Worldwide Total Ozone for Trends*. Unpublished report prepared for Manufacturing Chemists Assoc.

Penner, J. E., and J. S. Chang. 1978. Possible variations in atmospheric ozone related to the 11 year solar cycle, *Geophys. Res. Lett.* 5, 817-820.

Tiede, J. J., P. N. Sheldon, and W. J. Hill. 1977. A time series intervention analysis of stratospheric ozone data. Methodology paper submitted for NASA-sponsored symposium, Ozone Trend Detectability Thresholds, Boulder, Colorado, July 28-29.

APPENDIX D

DETAILED ANALYSIS OF UNCERTAINTY IN STEADY-STATE OZONE CHANGE (cf. Chapter 9)

This appendix describes the detailed formal analysis of the uncertainty in steady-state ozone change due to F-11 and F-12. Two independent approaches were used as a check on the results, i.e., the uncertainty was estimated by a Monte Carlo simulation and by combining the sensitivities due to individual reaction rates. Several further tests were made of crucial assumptions of the analysis.

In the Monte Carlo simulations, a large number of individual model simulations are carried out with different rates used for each one, a value for each rate selected randomly according to its assumed probability distribution. Thus, with enough such model runs, the ozone-change probability distribution implied by the joint uncertainties in all the rates is established by a "brute-force" calculation. One difficulty in applying this procedure is that the probability distributions of reaction-rate constants are largely unknown, since evaluations of chemical rates generally give at most an uncertainty range. The sensitivity of the Monte Carlo simulations of the ozone-change uncertainty to the assumed probability distribution was estimated by examining the differences in the ozone-change statistics when a square-hat rather than a Gaussian distribution was assumed for the logarithms of the reaction-rate constants.

The probability distributions of ozone change obtained by the Monte Carlo calculations are much closer to a normal than a log-normal distribution. Thus, the grouping of the Monte Carlo statistics ("binning") suitable for determining a normal distribution should give a better estimate of the ±95 percent confidence limits than would grouping suitable for determining a log-normal distribution. Also, the square-hat distribution should give a lower limit to the possible variation of the 95 percent confidence limits with reaction-rate probability distribution. The numerical results tabulated in Table D.4 indicate that the best estimate of the 95 percent ozone uncertainty limits is the range between 0.42 and 1.58 of the ozone change calculated using the preferred (expected) rate constants. This range could be as little as 0.6 to 1.4 (or as large as 0.2 to 1.8) if the probability distributions of all the reaction rates were to be extremely different from log normal.

In principle, our knowledge of stratospheric chemistry should be increased, and hence the errors in ozone-change estimates reduced, by our knowledge of the observed distributions of stratospheric species. It was not possible to incorporate in detail our knowledge of stratospheric observations in our error analysis. However, some tests were made on the Monte Carlo simulations by discarding individual runs that were regarded as inconsistent with the observed stratosphere according to criteria given later. The remarkable result obtained as indicated in Table D.4 is that this discarding made only a negligible reduction in the ozone-change uncertainty.

MODEL USED FOR THE MONTE CARLO UNCERTAINTY ANALYSIS

The model used for the Monte Carlo simulation was the GSFC steady-state stratospheric photochemistry model as described by Rundel *et al.* (1978) and Stolarski *et al.* (1978); the height resolution of the model was refined from 5 km to 1.25 km, the lower boundary set at 12.5 km, and the eddy-mixing coefficient used was that of Chang and co-workers. Also flux lower-boundary conditions were used for many of the diffused species instead of fixed mixing ratios. The values used for these are given in Table D.1. The fluxes used for F-11 and F-12 in Table D.1 are such as to give an increase in the Cl_x mixing ratio above 35 km of approximately 5 ppbv (actually 4.93 ppbv). This change permits the amount of CFM in the stratosphere to respond to changes in the lifetimes of F-11 and F-12 as input parameters are varied. A two-stream multiple-scattering calculation has also been added to the model for the calculation of radiative fluxes at wavelengths longer than 285 nm. The effective ground-level albedo at the lower boundary of the model was set to 0.25. The chemical and photochemical kinetics data used for the simulations are listed in Table D.2.

TABLE D.1 Lower Boundary Conditions Derived from the LLL Time-Dependent Model and Used in the GSFC Steady-State Model for the Monte Carlo Error Analysis of this Report

Species	Type	Value	
Odd oxygen	Velocity	-0.04	cm sec^{-1}
CO	Flux	1.23×10^{10}	cm^{-2} sec^{-1}
CH_4	Flux	1.23×10^{10}	cm^{-2} sec^{-1}
H_2	Flux	2.15×10^{9}	cm^{-2} sec^{-1}
H_2O	Mixing Ratio	3.00	ppmv
CH_3Cl	Flux	5.50×10^{7}	cm^{-2} sec^{-1}
CCl_4	Flux	1.05×10^{6}	cm^{-2} sec^{-1}
Odd Cl	Velocity	-0.07	cm sec^{-1}
N_2O	Flux	1.40×10^{9}	cm^{-2} sec^{-1}
Odd nitrogen	Velocity	-0.06	cm sec^{-1}
$CFCl_3$	Flux	7.35×10^{6}	cm^{-2} sec^{-1}
CF_2Cl_2	Flux	1.03×10^{7}	cm^{-2} sec^{-1}

TABLE D.2 Chemical Equations--Thermal Reactions ($k = Ae^{B/T}$, where A is in molecules/cm^3 and sec units and B is in Kelvins)

	A	B
$O + O_2 + M = O_3 + M$	1.1×10^{-34}	510
$O + O_3 = 2O_2$	1.9×10^{-11}	-2300
$O_3 + NO = NO_2 + O_2$	2.1×10^{-12}	-1450
$O + NO_2 = NO + O_2$	9.1×10^{-12}	0
$N_2O + O(^1D) = N_2 + O_2$	5.5×10^{-11}	0
$N_2O + O(^1D) = 2NO$	5.5×10^{-11}	0
$N + O_2 = NO + O$	5.5×10^{-12}	-3220

TABLE D.2 (Continued)

	A	*B*
$N + NO = N_2 + O$	8.2×10^{-11}	-410
$O(^1D) + H_2O = 2OH$	2.3×10^{-10}	0
$O(^1D) + CH_4 = OH + 2HO_2 + CO$	1.3×10^{-10}	0
$O_3 + OH = HO_2 + O_2$	1.5×10^{-12}	-1000
$O + OH = O_2 + H$	4.2×10^{-11}	0
$O_3 + HO_2 = OH + 2O_2$	1.4×10^{-14}	-590
$O + HO_2 = OH + O_2$	3.5×10^{-11}	0
$H + O_2 + M = HO_2 + M$	2.08×10^{-32}	290
$O_3 + H = OH + O_2$	1.42×10^{-10}	-478
$HO_2 + HO_2 = H_2O_2 + O_2$	Note 1	
$HO_2 + OH = H_2O + O_2$	3.0×10^{-11}	0
$OH + NO_2 + M = HNO_3 + M$	Note 2	
$OH + HNO_3 = H_2O + NO_3$	8.9×10^{-14}	0
$H_2O_2 + OH = H_2O + HO_2$	1.0×10^{-11}	-750
$N_2 + O(^1D) + M = N_2O + M$	3.5×10^{-37}	0
$N + NO_2 = N_2O + O$	2.0×10^{-11}	-800
$NO + O + M = NO_2 + M$	1.6×10^{-32}	584
$NO + HO_2 = NO_2 + OH$	3.3×10^{-12}	254
$H_2 + O(^1D) = OH + H$	9.9×10^{-11}	0
$CH + OH = H_2O + O$	1.0×10^{-11}	-550
$N + O_3 = NO + O_2$	2.0×10^{-11}	-1070
$NO_2 + O_3 = NO_3 + O_2$	1.2×10^{-13}	-2450
$OH + CH_4 = H_2O + 2HO_2 + CO$	2.36×10^{-12}	-1710
$OH + OH + M = H_2O_2 + M$	1.2×10^{-32}	900
$H_2O_2 + O = OH + HO_2$	2.75×10^{-12}	-2125
$O + CH_4 = OH + 2HO_2 + CO$	3.5×10^{-11}	-4550
$CO + OH = H + CO_2$	Note 3	
$O(^1D) + M = O + M$	2.2×10^{-11}	99

TABLE D.2 (Continued)

	A	*B*
$Cl + O_3 = ClO + O_2$	2.7×10^{-11}	-257
$Cl + OClO = 2ClO$	5.9×10^{-11}	0
$Cl + CH_4 = HCl + 2HO_2 + CO$	7.3×10^{-12}	-1260
$Cl + NO_2 + M = ClNO_2 + M$	6.9×10^{-34}	2115
$Cl + ClNO_2 = 2Cl + NO_2$	3.0×10^{-12}	0
$ClO + O = Cl + O_2$	7.7×10^{-11}	-130
$NO + ClO = NO_2 + Cl$	1.0×10^{-11}	200
$ClO + O_3 = Cl + O_2 + O_2$	1.0×10^{-12}	-4000
$ClO + O_3 = OClO + O_2$	1.0×10^{-12}	-4000
$ClO + NO_2 + M = ClONO_2 + M$	Note 4	
$ClO + ClO = Cl + OClO$	2.1×10^{-12}	-2200
$ClO + ClO = 2Cl + O_2$	1.5×10^{-12}	-1238
$HCl + O(^1D) = Cl + OH$	1.4×10^{-10}	0
$OH + HCl = H_2O + Cl$	3.0×10^{-12}	-425
$O + HCl = OH + Cl$	1.14×10^{-11}	-3370
$O + OClO = ClO + O_2$	2.0×10^{-11}	-1100
$NO + OClO = NO_2 + ClO$	3.4×10^{-13}	0
$N + OClO = NO + ClO$	6.0×10^{-13}	0
$H + OClO = OH + ClO$	5.7×10^{-11}	0
$Cl + OH = HCl + O$	1.0×10^{-11}	-2970
$Cl + HO_2 = HCl + O_2$	4.1×10^{-11}	0
$Cl + HNO_3 = HCl + NO_3$	1.0×10^{-11}	-2170
$^*CFCl_3 + O(^1D) = 2Cl$	2.3×10^{-10}	0
$^*CF_2Cl_2 + O(^1D) = 2Cl$	2.0×10^{-10}	0
$Cl + H_2 = HCl + H$	4.7×10^{-11}	-2340
$Cl + H_2O_2 = HCl + HO_2$	1.6×10^{-12}	-384
$ClNO_2 + O = ClO + NO_3$	3.0×10^{-12}	-808
$^*CH_3Cl + OH = Cl + H_2O + HO_2$	2.2×10^{-12}	-1142

TABLE D.2 (Continued)

	A	*B*
$NO + NO_3 = 2NO_2$	8.7×10^{-12}	0
$NO_2 + O + M = NO_3 + M$	1.0×10^{-31}	0
$NO_2 + NO_3 = NO + O_2 + NO_2$	2.0×10^{-13}	0
$NO_2 + NO_3 + M = N_2O_5 + M$	Note 5	
$N_2O_5 + M = NO_2 + NO_3 + M$	Note 6	
$N_2O_5 + O = 2NO_2 + O_2$	1.0×10^{-14}	0
$N_2O_5 + H_2O = 2HNO_3$	1.0×10^{-20}	0
$O(^1D) + O_3 = 2O_2$	1.2×10^{-10}	0
$HO_2 + HO_2 + H_2O = H_2O_2 + O_2 + H_2O$	Note 7	

Chemical Equations for Photolysis Reactions

$O_2 = O + O$

$O_3 = O + O_2$

$O_3 = O(^1D) + O_2$

$NO_2 = NO + O$

$N_2O = N_2 + O(^1D)$

$NO = N + O$

$HNO_3 = OH + NO_2$

$H_2O_2 = 2OH$

$HO_2 = OH + O$

$ClONO_2 = ClO + NO_2$

$HCl = H + Cl$

$ClO = Cl + O$

$ClO = Cl + O(^1D)$

$ClNO_2 = Cl + NO_2$

$OClO = ClO + O$

TABLE D.2 (Continued)

---

*$CF_2Cl_2 = 2Cl$

*$CFCl_3 = 3Cl$

*$CCl_4 = 4Cl$

*$CH_3Cl = 2HO_2 + CO + Cl$

$N_2O_5 = 2NO_2 + O$

$NO_3 = NO + O_2$

$NO_3 = NO_2 + O$

$H_2O = H + OH$

NOTE 1: $$\frac{3.25 \times 10^{8} + M \times 4 \times 10^{-10}}{(1 + 3.5 \times 10^{-16} \times M \times e^{-2060T})\ (8M + 4 \times 10^{+20})}$$

NOTE 2: Tsang (1977) as given by Hudson (1977).

NOTE 3: $1.4 \times 10^{-13} + M \times 7.3 \times 10^{-33}$

NOTE 4: $$\frac{3.3 \times 10^{-23}\ T^{-3.34}}{1. + 8.7 \times 10^{-9}\ T^{-0.6} \times (M)^{1/2}}$$

NOTE 5: $$\frac{2.9 \times 10^{-12}}{7.0 \times 10^{+21}\ e^{-2670/T} + M}$$

NOTE 6: $$\frac{6 \times 10^{+14}\ e^{-10970/T}}{7.0 \times 10^{21}\ e^{-2670/T} + M}$$

NOTE 7: $$\frac{1.1 \times 10^{-34}\ e^{+3730/T}}{1 + M \times 3.5 \times 10^{-16}\ e^{-2060/T}}$$

*Products such as F, H_2, CO, and COF_2 are not followed when produced from halocarbons.

ASSUMPTIONS REGARDING THE ERROR DISTRIBUTION OF MEASURED RATE COEFFICIENTS

In making the Monte Carlo uncertainty calculations, a log-normal distribution of error in the individual rate coefficients was assumed. The most appropriate probability distribution to assume for rate coefficients is unknown. A log-normal distribution is a more convenient method of representing the distribution of error in a necessarily positive parameter when the error is comparable to the central value of the parameter than is a normal distribution. Possibly, many of the more directly and currently measured rate coefficients may have error distributions closer to normal and log normal. However, when the error is small relative to the central value, the differences between normal and log-normal distributions of error are not large, but when the error is large, a normal distribution would lead to unphysical negative values.

In the uncertainty calculations, it has been assumed that the error estimates cited in the NASA, 1977 report correspond to 1σ in a log-normal distribution of true error in the rate coefficients. An examination of recent attempts to evaluate chemical reaction-rate coefficients (Smith, 1978) suggests that rate coefficients were often less accurately known than was estimated by the evaluators, especially for the indirectly determined rate coefficients. If there were, in fact, a tendency to underestimate the uncertainty in indirectly determined rate constants or if some broader than normal distribution function, say a "Witch of Agnesi," should have been used, then the uncertainty analysis would tend to underestimate the true error in calculations. At this time there is not clear justification for using distributions other than log normal or for altering the interpretation of the error estimates given in the NASA, 1977 report. Although it is perhaps true that previous estimates of rate-constant uncertainty systematically underestimated the error (Smith, 1978), no alternative treatment is available at this time. The uncertainties in photodissociation rate coefficients were estimated by M. Molina (University of California, Irvine, private communication). Table D.2 lists the reactions considered and their uncertainties.

MODEL DEPENDENCE OF SENSITIVITY OF OZONE CHANGE TO INDIVIDUAL RATE CONSTANTS

Since the model used for the Monte Carlo uncertainty analysis is a steady-state model with very different model structure and computational detail than the time-dependent model used in the previous sections, it is necessary to compare these models in detail. For all the results discussed, the boundary conditions (as listed in Table D.1) for the GSFC model were obtained from the time-dependent model. On the average, all the trace-species concentrations as derived from these models are very comparable except for HO and HO_2. The GSFC model had a different diurnal averaging weighting factor for most species than the LLL model, and the difference is most noticable in HO and HO_2. Nevertheless, the overall uncertainty of model response to Cl_x changes should only be weakly affected by

TABLE D.3 Comparison between Sensitivities of LLL and GSFC Models for Some Selected Rates[a]

	LLL	GSFC
$N_2O + O(^1D)$	-0.508	-0.488^+ (one path only)
$HO + O_3$	-0.220	-0.372^+
$NO_2 + HO + M$	+0.331	-0.228^+
$Cl + CH_4$	-0.153	-0.117^+
$ClO + NO_2 + M$	-0.265	-0.193^+
$HO + HO_2$	-0.232	-0.126^- (-0.252^+)
$HO + HCl$	+0.277	$+0.233^+$
$ClO + O$	+0.414	$+0.405^+$
$ClO + NO$	-0.126	-0.119^+
$HO_2 + NO$	+0.218	$+0.175^+$
$HO_2 + O_3$	+0.166	$+0.085^+$

[a] The LLL results are obtained by assuming +2σ change of the rate, whereas the GSFC model values are for a 2σ perturbation of the sign indicated by the superscript.

this difference. However, the models would have somewhat different sensitivities to changes in NO_x sources.

The sensitivity of these models in response to uncertainties in individual chemical kinetics rate coefficients is another parameter for ascertaining the sensitivity in the chemical coupling of the GSFC (steady-state) and LLL (time-dependent) models. The comparison in Table D.3 of the most important reaction rates suggests that the agreement between these models is very good, except for the HO and HO_2 rates with O_3. These discrepancies occur for the reasons given above.

SUMMARY OF ERROR ANALYSES

Monte Carlo Results

Three differing cases of input parameter distributions were run. These were

1. Log-normal distributions for the reaction-rate constants and the photolysis parameters (approximately 1900 Monte Carlo trials);
2. Constant distributions in log space from $+1\sigma$ to -1σ for the reaction-rate constants plus photolysis parameters ($\simeq$600 trials);
3. Log-normal distributions on the reaction-rate constants only ($\simeq$700 trials).

Case 1 is considered to be the best current estimate for the overall uncertainty propagation as discussed above. This case was tested for its statistical adequacy in several ways. The 1895 cases consisted of 10 runs of approximately 200 cases each. A detailed examination of the ozone perturbation uncertainties for the individual 200 trial samples shows some variability in high- and low-side 2σ factors and in the means. The correlation coefficients with 200 cases and with a linear normal distribution are generally around 0.8. The progressive runs of the 200 case samples indicate a tendency of the 1σ points to move somewhat closer to the centerline case as more trials are considered and for the correlation coefficient of the fit to a linear normal distribution to improve to 96 to 97 percent when all cases are used.

Figure D.1 shows the histograms obtained for column ozone change above 12.5 km for a steady-state Cl_x perturbation. The upper figure shows the 1895 cases distributed

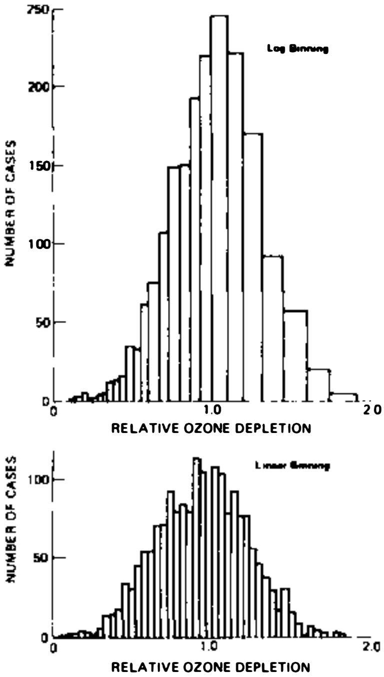

FIGURE D.1 Relative ozone depletions (1.0 corresponds to 19.8 percent).

according to a linear bin procedure, and the lower figure shows the same data distributed in equal logarithmic bins. The bins are defined by the ratio of the ozone depletion to the centerline case (using expected values of all the parameters) of 19.8 percent. (Note that this value corresponds to the column ozone about 12.5 km only and is higher by 2.5 percent than numbers from the time-dependent model.) The expected value for ozone depletion is 0.945 of the centerline, while the mean logarithm of the ozone depletion corresponds to 0.897 of the centerline.

These results were used to obtain a standard deviation for the ozone change estimate from the well-known formula

$$\sigma^2 = \frac{\Sigma(x_i - \bar{x}_o)^2}{n}$$

For the linearly binned case, the 1σ and 2σ factors were obtained simply from the mean by

$$f_{j\sigma} = \bar{x}_o \pm j\sigma, \quad j = 1 \text{ or } 2$$

The values obtained are given in Table D.4. These factors, *f*, are to be applied to the centerline case. For the logarithmically binned case, the standard deviation was obtained from

$$\sigma^2 = \frac{\Sigma(\ln x_i - \ln x)^2}{n}$$

The factors to be applied to the centerline are obtained from

$$f_{j\sigma} = \exp(\ln \bar{x}) \exp(j\sigma)^{\pm 1}, \; j = 1 \text{ or } 2$$

These are also shown in Table D.4 under the label "log output." These are further compared with 1σ and 2σ values obtained by counting to 2.5 percent and 16 percent of the cases from each end of the distribution. If the distribution were exactly normal, then these would correspond to the 2σ and the 1σ points. As can be seen from the table, the 1σ factors do not vary with the analysis technique. The 2σ factors are somewhat different depending on whether the log or linear binning is used. As expected, the counting yields factors corresponding more closely to the linear output.

Results for Case 2, constant distribution in log space from +1σ to -1σ, are also given in Table D.4. A total of 600 cases were run. The results, as expected, show a much smaller deviation from the centerline. This results from the absence of input values beyond the 1σ on either side of the center.

The results for log-normal distributions on reaction rates only are not shown in Table D.4 but differ only slightly in the third significant figure from the 1895 case reaction rates plus photolysis parameter run.

The final result given in Table D.4 is for 1213 cases out of 1895 that were obtained by discarding all cases in which computed concentrations of well-measured quantities such as HNO_3, N_2O, CH_4, O_3, and NO_y were more than ≃ a factor of 2.1 from the model centerline values, and in which the ozone column was more than a factor of 1.5 from the centerline. The discarded cases contain ozone

TABLE D.4 One- and Two-Standard-Deviation Ozone Change from Monte Carlo Calculations with Various Assumptions, Normalized to 0.95, i.e., Multiply by Ozone Change/0.95 to Obtain Error Estimates of Ozone Change

	Low	High
1 Sigma		
Log-normal input *1895 cases*		
Linear output	0.66	1.23
Log output	0.64	1.23
Counting	0.65	1.23
Square-distribution input in log space *599 cases*		
Linear output	0.79	1.15
Log output	0.79	1.15
Counting	0.80	1.14
Total input minus rejected cases *1213 cases*		
Linear output	0.68	1.21
Log output	--	--
Counting	0.66	1.22
2 Sigma		
Log-normal input *1895 cases*		
Linear output	0.38	1.51
Log output	0.46	1.77
Counting	0.41	1.50
Square distribution input in log space *599 cases*		
Linear output	0.61	1.33
Log output	0.65	1.39
Counting	0.59	1.30
Total input minus rejected cases *1213 cases*		
Linear output	0.41	1.48
Log output	--	--
Counting	0.45	1.50
Sensitivity	0.50	1.70

perturbations spanning the entire spectrum, with an emphasis on values in the tail on either side of the distribution. The subtractions of these cases from the overall distribution only slightly narrowed the distribution as indicated by the values in Table D.4.

REFERENCES

Hudson, R. D., ed. 1977. *Chlorofluoromethane and the Stratosphere*, Ref. Publ. 1010, NASA Goddard Space Flight Center, Greenbelt, Md.

Rundel, R. D., D. M. Butler, and R. S. Stolarski. 1971. Uncertainty propagation in a stratospheric model. 1. Development of a concise stratospheric model, *J. Geophys. Res. 83*, 3063.

Smith, W. S. 1978. Uncertainties in evaluated atmospheric rate constants, WMO Symposium on Geophysical Aspects and Consequences of Changes in the Composition of the Stratosphere, WMO No. 511, Toronto, Canada, pp. 37-46.

Stolarski, R. S., D. M. Butler, and R. D. Rundel. 1978. Uncertainty propagation in a stratospheric model. 2. Monte Carlo analysis of imprecisions due to reaction rates, *J. Geophys. Res. 83*, 3074.